Mechanisms of *Salmonella* Typhi Persistence

Taylor A. Stepien

A dissertation

submitted in partial fulfillment of the

requirements for the degree of

Doctor of Philosophy

University of Washington

2020

Reading Committee:

Ferric Fang, Chair

Lakshmi Rajagopal

Kelly Smith

Program Authorized to Offer Degree:

Pathobiology

University of Washington

Abstract

Mechanisms of *Salmonella* Typhi Persistence

Taylor A. Stepien

Chair of the Supervisory Committee:
Ferric C. Fang, M.D.
Professor of Laboratory Medicine and Microbiology
Adjunct Professor of Medicine
Professor, Pathobiology Program

Although human *Salmonella* infections are caused by a single species, *Salmonella enterica,* different *Salmonella* serovars cause distinctive clinical syndromes. Whereas non-typhoidal *Salmonella* (NTS) serovars typically cause self-limiting acute gastroenteritis, typhoidal serovars cause enteric fever, a severe protracted illness with systemic symptoms that can become chronic. Enteric fever accounts for a significant global burden of disease, with nearly 15 million infections and approximately 136,000 deaths annually. Currently the genetic basis for the distinct clinical outcomes caused by NTS and typhoidal *Salmonella* is not known. Enteric fever includes typhoid and paratyphoid fevers which are caused by *S.* Typhi and *S.* Paratyphi A, respectively; both are human host-restricted and unable to infect mice or other small animal models. Most *Salmonella* research has been conducted using the NTS serovar *S.* Typhimurium in murine models, which fail to recapitulate certain important aspects of human typhoid. The epidemiological features

of acute versus persistent *Salmonella* infection are distinctive; inherited or acquired deficiencies in cellular immunity lead to increased susceptibility to NTS infection, but not to enteric fever. Additionally, *S.* Typhi and *S.* Paratyphi A share significant genomic differences from *S.* Typhimurium in the form of genomic decay and novel virulence factors. This dissertation aims to understand the underlying mechanisms that lead to the distinct clinical syndromes caused by NTS and typhoidal *Salmonella* infection. First, we conducted a genome-wide screen for *S.* Typhi virulence determinants by infecting susceptible humanized mice with a high-complexity transposon mutant library of *S.* Typhi. The screen identified known virulence determinants such as the Vi capsular polysaccharide and iron acquisition genes. Interestingly, certain some predicted virulence determinants were shown to be dispensible for virulence, including the typhoid toxin and *Salmonella* Pathogenicity Island 2 (SPI2). Given that human immune cells are required for *S.* Typhi infection, we next explored the interactions of both *S.* Typhi and *S.* Typhimurium with human macrophages. *S.* Typhi persists within human macrophages by causing minimal apoptosis unlike *S.* Typhimurium, which induces apoptosis in a SPI2-dependent manner. These results are consistent with our observation that typhoidal serovars *S.* Typhi and *S.* Paratyphi A have lost a significant portion of SPI2-secreted effector proteins, especially those that inhibit the NF-κB pathway. Further, inhibition of NF-κB was sufficient to cause macrophage apoptosis and may present a new strategy for treatment of persistent *S.* Typhi infection. *S.* Typhi also avoids inflammatory macrophage polarization and fails to induce a T_H1 response in infected humanized mice. Such a response is required for NTS clearance in humans and represents another important difference between these serovars. Finally, due to the identification of iron acquisition genes as essential for *S.* Typhi virulence, we explored differences in iron acquisition capabilities between *S.* Typhi and *S.* Typhimurium. We found that *S.* Typhi is more sensitive to iron limitation,

indicating adaptation to a macrophage niche that is not iron-restricted. Taken together, these chapters demonstrate the importance of employing models using typhoidal *Salmonella* to understand mechanisms of persistent human *Salmonella* infection rather than reliance on murine-NTS models.

TABLE OF CONTENTS

LIST OF FIGURES

LIST OF TABLES

ACKNOWLEDGMENTS

I would like to express my sincere gratitude to the many people who supported me both professionally and personally in achieving this goal.

First, I thank my advisor, Dr. Ferric Fang, a uniquely brilliant individual with whom it has been an honor to work. Your dedication to rigorous and exciting scientific inquiry demonstrates how priviledged it is to be in the business of generating new knowledge. Thank you for recognizing my potential and for challenging me to continually improve.

I'm grateful for the help of every member of the lab, but especially for the mentorship and support of Dr. Stephen Libby, Joyce Karlinsey, Dr. Larissa Singletary, and Dr. Elaine Frawley.

Thank you to my committee members, Drs. Lakshmi Rajagopal, David Sherman, Nina Salama, and Kelly Smith, for patiently watching this project evolve and for contributing their expertise along the way.

The friends I made in the Pathobiology Program will be cherished not only for their scientific prowess, but also their generous offerings of advice, assistance, and love. Thank you especially to Jay Vornhagen, Justine Levan, Blair Armistead, and Chris Whidbey. Thank you also for the teachings and support of the Pathobiology faculty and to the program director Dr. Lee Ann Campbell.

I would also like to recognize the generous mentorship I've received throughout my life that led me down this path of continuing education. Thank you to Dr. Jo Handelsman, Dr. Jonathan Holt, Dr. Courtney Robinson, Dr. Justin Donato, Dr. Heather Allen, Dr. Katie (Mason) Summers, Dr. Jessamina Blum, Patricia Badger, Dr. Jean Weaver, Everett McKinney, Bonnie Benes, and many others who believed in my potential.

Finally, thank you to my family for their love and encouragement, including my in-laws Margaret Lewis and Todd Berry, my sisters Emma, Ali, and Kate, my besties Myla and Amanda, my parents, Bob and Dawn Stepien, and my husband, Andrew Berry. Mom and Dad, I'm grateful for the sacrifices you made to give me the best education possible, for instilling in me the importance of curiosity and hard work, and for fostering an appreciation of nature, the sciences, and the arts. Andrew, I'm so grateful to have experienced this journey together, and could not have made it to the end without your unending support, listening, encouragement, and love.

DEDICATION

To my parents.

Chapter 1. INTRODUCTION

1.1 EPIDEMIOLOGY OF ENTERIC FEVER

Enteric fever, comprising both typhoid and paratyphoid fever, is a systemic, life-threatening illness resulting from infection with *Salmonella enterica* belonging to serovars Typhi or Paratyphi A, B, or C[1]. These *Salmonella enterica* serovars are transmitted by contaminated food or water and pose a particular challenge in developing regions with limited access to water sanitation systems. South and Southeast Asia currently experience the highest incidence of enteric fever, with the greatest impact on children living in poverty (**Figure 1-1**)[2,3]. The estimated global burden of enteric fever is over 27 million infections and 200,000 deaths each year[4,5], although an updated meta-analysis estimates a significant decline in incidence in recent years[3]. Available data are likely to be underestimates due to misdiagnosis and under-reporting of typhoid and paratyphoid fever. Global incidence is difficult to estimate because the gold standard for diagnosis is a positive culture of *S.* Typhi or *S.* Paratyphi from a clinical sample[6]. Many hospitals in heavily afflicted areas lack facilities for blood culture and treat presumptive typhoid cases in the outpatient setting[7]. While multidrug-resistant *S.* Typhi has been responsible for enteric fever in most areas of Asia, infections with drug-resistant *S.* Paratyphi A are on the rise[8]. As recently as 2010, typhoid and paratyphoid fevers accounted for 1% of total worldwide mortality[9]. Reduction in the incidence of enteric fever will rely on 1) continued improvements to water sanitation systems worldwide, 2) increased use of vaccines, including newer conjugate vaccines that are effective in young children[3], and 3) the development of new and improved therapies.

1.2 *SALMONELLA* DIVERSITY AND HOST SPECIFICITY

1.2.1 Classification

Although enteric fever is the most prominent form of *Salmonella* infection in many developing regions, non-typhoidal *Salmonella* serovars are ubiquitous intestinal pathogens in all parts of the world. *Salmonellae* are gram-negative, rod-shaped, facultative anaerobic bacteria belonging to the family Enterobacteriaceae, most closely related to *Escherichia coli, Shigella,* and *Citrobacter*[10]. Current taxonomic classification recognizes only two species: *S. enterica* and *S. bongori; S. enterica* is further divided into seven subspecies I, II, IIIa, IIIb, IV, VI, and VII [11,12]. *S. enterica* subspecies I (*enterica)* includes 99% of the serovars that infect warm-blooded animals, while the remaining subspecies and *S. bongori* infect cold-blooded animals[11]. Subspecies *enterica* is further divided into over 2,500 serovars based on the White-Kauffman-Le Minor scheme[13]. This scheme takes into account the unique cell surface "O" antigens and flagellar "H" antigens of different serovars, as well as other rare antigens in some cases.

1.2.2 Host Adaptation

Most *Salmonella enterica* subspecies I serovars are "generalists" that can cause disease in a number of different hosts, usually causing gastroenteritis in humans with maintenance in other animal species as a reservoir. The generalist *Salmonella enterica* serovar Typhimurium is the leading cause of foodborne gastroenteritis in humans[14]. Some *Salmonella* serovars are host-adapted to better infect certain hosts, such as Dublin (cattle) and Choleraesuis (pigs). Other serovars are "specialists" or restricted to infection in a single host, including all typhoidal *Salmonella* serovars. The typhoidal serovar *Salmonella enterica* serovar Typhi formed its own clonal lineage approximately 10,000 to 71,000 years ago[15], while *Salmonella enterica* serovars

Paratyphi B and C each form their own lineage, and *Salmonella enterica* serovars Paratyphi A and Sendai form a fourth lineage[12].

The process by which *Salmonella* serovars have adapted to their hosts and the ways in which these adaptations affect their virulence and transmission are areas of intensive study. Host-restricted organisms may demonstrate a number of genetic signatures, including genomic rearrangements, horizontally-acquired traits, genomic decay and pseudogene formation. Indeed, human-restricted *S.* Typhi displays all of these features in its genome.

1.2.2.1 Gene Acquisition

Salmonella is distinguished from other enteric pathogens by horizontally-acquired genetic elements, including pathogenicity islands and islets, plasmids, and bacteriophages. The acquisition of *Salmonella* pathogenicity island 1 (SPI1) corresponds with the initial divergence of *Salmonella* from its last common ancestor with *E. coli* and allows *Salmonella* to invade the intestinal epithelium[16]. The acquisition of SPI2 occurred after *S. enterica* split from *S. bongori* and is required for survival within macrophages[16,17]. In total there are 21 known pathogenicity islands in *Salmonella,* with 11 carried in common by *S.* Typhimurium and *S.* Typhi[18]. Even SPIs that are present in both typhoidal and non-typhoidal *Salmonella* (NTS) serovars may have important differences, sometimes due to gene loss, which is discussed below.

The acquisition of two clusters of genes in particular is thought to have influenced the adaptation of *S.* Typhi to the human host: SPI7 and genes encoding the typhoid toxin[19]. SPI7 contains genes required for synthesis of a capsular polysaccharide known as Vi, and is present in two other host-restricted serovars, *S.* Dublin and *S.* Paratyphi C. The Vi antigen was originally identified as a virulence factor that enables *S.* Typhi to evade phagocytosis and serum complement deposition through inhibition of C3 component binding[20,21]. Vi was also found to modulate early

inflammatory responses by interfering with the detection of LPS by toll-like receptor 4 (Tlr4) receptors on epithelial cells, thereby inhibiting the production of IL-8[22,23] and interfering with neutrophil chemotaxis [24].

The typhoid toxin is a cytolethal distending toxin with a unique A_2B_5 structure. The toxin is encoded on a pathogenicity islet and causes cell cycle arrest via DNA damage[25,26]. Administration of purified typhoid toxin to mice is sufficient to induce malaise, weight loss, and a reduction in circulating immune cells including neutrophils, although it does not induce fever [26]. The toxin binds to surface glycoproteins that are unique to humans due to the lack of cytidine monophospho-N-acetylneuraminic acid hydroxylase (CMAH), leaving a unique terminus to which the toxin can bind[27]. Typhoid toxin has also been shown to reduce neutrophil influx in the intestine[28]. However, the importance of the typhoid toxin for virulence in human typhoid is controversial and will be subsequently discussed in further detail.

1.2.2.2 Gene Loss

Genomic decay leading to the loss of gene function (pseudogenes) can be seen in a number of host-restricted bacterial pathogens such as *Shigella flexneri* and *Yersinia pestis*[29]. When comparing *Salmonella* serovars, the generalist *S.* Typhimurium contains only 25 pseudogenes, corresponding to about 0.9% of its gene complement, while specialists *S.* Typhi (204 pseudogenes) and *S.* Paratyphi A (173 pseudogenes) have lost approximately 5% of their genes[30]. *S.* Typhi and *S.* Paratyphi A cause similar systemic diseases and share overlapping pseudogene complements; comparison of the pseudogenes shared between them reveals that a large proportion of these losses were caused by different inactivating mutations, suggesting convergent evolution towards a similar adaptive niche[31]. A comparison of the shared inactivated genes between these two typhoidal

serovars provides unique insight into how these pathogens have successfully adapted to their host-restricted lifestyles.

1.2.2.3 Mechanisms of Host Restriction

Although there are significant genomic differences between NTS and typhoidal *Salmonella,* no single virulence factor is absent in all NTS and present in all typhoidal serovars, or vice versa, as an explanation for their different host specificities[32]. Additionally, while some mutations affect virulence in both serovars, others that attenuate virulence in NTS have no effect on typhoidal *Salmonella*[33]. It has been postulated that the typhoid toxin is a major factor contributing to *S.* Typhi human restriction, due to the unique human glycoprotein to which it binds. Mice expressing some of the Neu5Gc-terminated sialoglycans are susceptible to the typhoid toxin. However, the role of the toxin in pathogenesis is uncertain[34]. Another proposed mechanism of *S.* Typhi human restriction is the loss of an effector protein, GtgE, a cysteine protease secreted by the type-3 secretion system (T3SS) encoded on SPI2. Secretion of GtgE by *S.* Typhimurium leads to cleavage of host GTPases Rab29, Rab32, and Rab38. Without GtgE, *S.* Typhi recruits these proteases to the *Salmonella*-containing vacuole of infected human cells. Expression of GtgE is sufficient to promote *S.* Typhi survival in murine macrophages [35]. Whatever the mechanisms of restriction, the ability of *S.* Typhi to endure as a pathogen in human populations relies on successful person-to-person spread, due to a limited ability to survive in the environment[36]. Therefore, it is advantageous for typhoidal *Salmonella* serovars like *S.* Typhi to persist within a human host until successful transmition to the next host.

1.3 *SALMONELLA* INFECTION IN THE HUMAN HOST

1.3.1 Human Salmonellosis

In immunocompetent individuals, NTS infection, most commonly caused by *S.* Typhimurium, typically results in gastroenteritis (inflammatory diarrhea) with nausea and vomiting[37,38]. Sources of transmission include contaminated animal-derived food products, produce, person-to-person contact and pets[1]. The incubation period following exposure is brief, typically 24-72 hours. Once ingested, NTS invades the intestinal epithelium, where a rapid inflammatory response is induced, triggering an influx of neutrophils. The presence of neutrophils in the stool is a hallmark of *S.* Typhimurium-induced diarrhea[37,39]. The infection is typically acute and self-limiting, and rarely requires medical intervention in immunocompetent individuals.

NTS infection of immunocompromised hosts can result in invasive nontyphoidal *Salmonella* infection (iNTS), which shares features of both enteric fever and typical NTS infection. Disease symptoms can include fever and a lack of diarrhea similar to enteric fever; however, most iNTS are not host-restricted and can still cause inflammatory disease in other hosts. iNTS infection is an important cause of bloodstream infections in children and HIV-infected adults in sub-Saharan Africa, with a case fatality rate of 20-25%[40]. Sequencing has revealed that a single *S.* Typhimurium sequence type, ST313, is responsible for most of the bacteremia seen in this region. This sequence type has undergone genomic decay in a manner similar to typhoidal serovars, leading to a loss of phenotypes required for survival outside of the human host, such as oxidative stress resistance and multicellular organization[41].

Typhoid fever is a protracted febrile illness accompanied by non-specific symptoms including fatigue, anorexia, and abdominal tenderness. It can be difficult to distinguish from other causes of fever, such as malaria. Mucosal inflammation and diarrhea, hallmarks of NTS enteritis,

are usually absent in typhoid fever. The incubation period for typhoid fever is one to two weeks, much longer than the incubation period of NTS enteritis[42]. In the absence of specific treatment with antibiotics, typhoid may persist for 3-4 weeks, and relapses are common. While the fatality rate is 1-4% with treatment, in the absence of treatment it can rise to 10-30%[4]. Lack of treatment can lead to complications including delirium, intestinal hemorrhage, and perforation[43]. Paratyphoid fever caused by *S.* Paratyphi A is often clinically indistinguishable from typhoid fever[44,45]. It is estimated that up to 5% of typhoid patients can become chronically infected[7]; chronic carriage can also occur with *S.* Paratyphi A infection, although not as frequently as with *S.* Typhi[46].

Chronic carriers of *S.* Typhi are usually asymptomatic and can shed *S.* Typhi in their feces for the rest of their lives[7]. Mary Mallon was the most infamous carrier of typhoid fever; known as "Typhoid Mary", she infected dozens of clients while working as a cook at the beginning of the 20th century, leading to her eventual forced quarantine[47]. It is thought that the gallbladder can serve as a reservoir for bacteria shed by chronic carriers, as asymptomatic carriage has been associated with gallstones[48]. Indeed, a gallstone-producing diet in *S.* Typhimurium-infected mice promoted a carrier state[49]. *Salmonella* has been shown to form biofilms on gallstones, where the bacteria are protected from bile and antibiotic treatment[50]. However, not all chronic typhoid carriers have gallstones[51]. Studying chronic carriage is challenging, as identifying a true carrier requires sampling over an entire year, and antibody detection is not a reliable method of identifying carriers[52,53]. Current treatments for chronic carriers include prolonged antibiotics and gallbladder removal, but these are not always effective[52].

1.3.2 Natural History of Salmonella Infection

Comparisons between typhoidal and non-typhoidal *Salmonella* infections are relevant because of the model systems used to study *Salmonella* infection. Because typhoidal serovars like *S.* Typhi and *S.* Paratyphi A are human-restricted, much of the information on systemic *Salmonella* pathogenesis has been gained from studies using *S.* Typhimurium in a mouse model, which is thought to approximate systemic infection. Despite the potential problems with translating these findings[18], the murine model has provided important insights into how *Salmonella* traffics through various body sites and causes disease.

After oral ingestion, both NTS and typhoidal *Salmonella* invade the intestinal mucosa in the distal ileum, particularly through Microfold (M) cells which overlay lymphoid structures called Peyer's Patches (PP)[54]. Invasion is mediated by the SPI1 Type-III Secretion System (T3SS), which facilitates secretion of effector proteins to promote internalization by host cells[55]. Tissues underlying the PP are rich in phagocytic cells, so that *Salmonella* is quickly internalized by macrophages and dendritic cells[56]. Lack of a mucosal inflammatory response is a key feature of typhoid, allowing persistence within phagocytes. In humans, NTS infection remains localized due to inflammatory responses such as IL-8 production and a massive neutrophil influx to the intestinal mucosa during the acute stage[57–59], a response that is largely absent during typhoid. From the PP, *Salmonella* can travel via the afferent lymphatics to the mesenteric lymph nodes (MLN), eventually gaining access to the blood and systemic tissues through the efferent lymphatics. Travel through the lymphatics is thought to primarily occur within dendritic cells and macrophages, although it is possible that extracellular bacteria also travel via these routes[60]. A SPI1-independent pathway of systemic invasion has also been demonstrated, mediated by intestinal dendritic cells which carry *Salmonella* to the mesenteric lymph nodes, spleen, and liver[61]. After arriving at

systemic tissues, *Salmonella* can replicate within phagocytes in the liver, spleen, bone marrow, and gallbladder[62]. Once inside phagocytes, *Salmonella* utilizes the SPI2 T3SS to disrupt vesicular trafficking and promote intracellular survival[63,64].

1.3.3 Protective Immunity to Salmonella Infection

As described above, innate immunity to *Salmonella* infection involves a number of cell types including macrophages, dendritic cells, and neutrophils present in gut lymphoid tissues. Differences in IL-8 secretion during NTS versus typhoidal *Salmonella* infection account for differences in the recruitment of neutrophils. RB6-8C5 antibody depletion of neutrophils during *Salmonella* infection in mice rendered them more susceptible and led to higher bacterial burdens in the PP and spleens[65], although these observations must be interpreted with caution, as this antibody targets the Gr-1 antigen that is also expressed on dendritic cells and subpopulations of lymphocytes and monocytes[66]. Lymphoid tissue-resident dendritic cells can be activated by *Salmonella* pathogen-associated molecular patterns (PAMPs) and inform naive T cells to initiate an adaptive immune response[67].

Murine infection models using *S.* Typhimurium indicate that adaptive immune responses are also important for controlling *Salmonella* infection, with cell-mediated immunity likely playing a dominant role. CD4+ T cells are activated early during infection in PP, and later in the MLNs, after which there is rapid and efficient expansion of *Salmonella*-specific T cells. Despite reports that *Salmonella*-specific CD4+ T cells can comprise up to 50% of all T cells several weeks after infection[68], there is evidence that these do little to clear early *Salmonella* infection, and in fact replicating bacteria have been shown to inhibit their effector function[69]. Few natural *Salmonella* MHC class II peptides have been characterized, although previously *Salmonella*-infected mice mount a robust CD4+ T cell response against purified flagellin[70]. *Salmonella*

infection also elicits humoral responses, but the role of these responses in clearance is not well understood. *Salmonella* are thought to spend a relatively brief time in the extracellular milieu where they would be exposed to antibody, but infection-induced cell death could contribute to the pool of extracellular bacteria[71]. Examining the antibody response to natural *Salmonella* infection in humans shows that antibodies directed against *Salmonella* outer membrane proteins are protective against NTS bacteremia in African children[72,73], but excess antibody directed against LPS can antagonize antibody-mediated killing[74]. Anti-*S.* Typhi specific antibodies from naturally-infected individuals target LPS, flagellin, and the Vi capsular polysaccharide. Indeed, a Vi parenteral vaccine is protective, and high titers of anti-Vi antibodies are recovered from patients in endemic areas[75]. During *Salmonella* infection, B cells may not only serve to produce these antibodies, but may have antigen-presenting functions[76]. There are also important roles suggested for Treg and Th17 cells during *Salmonella* infection based on murine studies[77].

Examination of the effect of various inherited and acquired immunodeficiencies in humans on susceptibility to *Salmonella* infection reveals that the host determinants of immunity to NTS and typhoidal *Salmonella* and fundamentally different, particularly in regard to T_H1 cellular responses. The T_H1 response is essential for clearance of many intracellular pathogens, including NTS[78]. Classic M1-polarized macrophages initiate T_H1 immunity in response to inflammatory signals by producing cell surface markers, transcription factors, cytokines, and chemokines[78–80]. T_H1 helper T cells in turn produce the cytokine IFNγ, which augments the antimicrobial actions of macrophages. Although humans with autosomal mutations in the IL-12/IFNγ signaling axis exhibit enhanced susceptibility to infections with mycobacteria and NTS, these individuals do not appear to be more susceptible to typhoid fever [81,82]. A lack of association between IFNγ/IL12B/IFNγR1 polymorphisms and typhoid or paratyphoid fever has been specifically confirmed[83]. Additionally,

acquired immunodeficiency of CD4+ T cells in patients with HIV infection is associated with higher susceptibility to NTS infection but does not correlate with increased incidence or severity of typhoid fever[72,84,85]. Together, these observations indicate that NTS and typhoidal *Salmonella* have significantly different interactions with both innate and adaptive immunity, the details of which are not fully recapitulated with current murine models.

1.3.4 Current Treatment and Prevention Strategies

Salmonella enteric fever often requires antibiotic treatment and can be susceptible to fluoroquinolones, third-generation cephalosporins or azithromycin. Antibiotic treatment reduces the case-fatality rate from 10-30% to about 1% [86]. Chloramphenicol was used from 1948 up until the 1970s, when widespread resistance emerged; ampicillin and trimethoprim-sulfamethoxazole (TMP-SMZ) were used until the 1980s. Although fluoroquinolones are still commonly used, multidrug-resistant (MDR) *S.* Typhi strains are now increasingly widespread, especially those carrying *gyrA* mutations that confer resistance to fluoroquinolone treatment[87]. Recently, third-generation cephalosporins have been used more frequently. The H58 *S.* Typhi lineage is associated with multiple MDR phenotypes and is widespread in countries with a high prevalence of typhoid[88]. More than 60% of H58 isolates are resistant to ampicillin, TMP-SMZ, chloramphenicol and streptomycin. Extensively drug resistant (XDR) *S.* Typhi was first reported in 2017 and harbors a plasmid containing multiple antibiotic resistance genes[88].

There are currently two widely available vaccines for typhoid fever: the Vi antigen parenteral vaccine containing purified Vi capsule and an oral live attenuated vaccine comprised of the Ty21a strain[89,90]. Ty21a contains multiple attenuating mutations, including the loss of Vi antigen and metabolic processes such as galactose breakdown by GalE, rendering it unable to survive in host cells[90]. Ty21a elicits both-cell mediated and humoral responses, and antibodies

generated against this vaccine exhibit some cross-reactivity with *S.* Paratyphi A and B [91]. However, the live attenuated vaccine requires cold-chain storage, making it less suited for distribution in endemic areas, and is not recommended for immunocompromised individuals[76]. The Vi parenteral vaccine elicits T-cell independent humoral responses, does not confer long-term protection, and does not provide protection against other typhoidal serovars. Both vaccines offer incomplete protection ranging from 50-80% efficacy, are relatively expensive, and require boosting. Recent development of conjugate subunit vaccines has been promising. The Vi capsule conjugated to tetanus toxin (Vi-TT or Typbar-TCV) has been used India and Nepal. This vaccine provides protection in children as young as 6 months-2 years old, unlike previous vaccines.

1.4 Models to Study *Salmonella* Infection

Because typhoidal serovars are human-restricted, and humans are the only known reservoir, most of the current understanding of *Salmonella* pathogenesis comes from studies using *S.* Typhimurium in mice. *S.* Typhimurium-murine infections are often stated to mimic *S.* Typhi-human interactions[92], however more recent studies are challenging some of the previous assumptions about these models.

1.4.1 Mouse Models of Systemic Infection

S. Typhimurium infection of mice can result in a systemic infection that resembles typhoid fever in some respects, including lesions in internal organs and bacterial distribution to tissues beyond the intestines[76,93]. Mice that are either intrinsically susceptible or resistant to *Salmonella* infection can be used to analyze mechanisms of host resistance to *Salmonella*. Mice that are deficient in the divalent metal transporter Nramp1 are *Salmonella*-susceptible and have been extensively used in systemic infection models; this includes BALB/c and C57BL/6 strains, which

are naturally deficient in Nramp1[94]. Nramp1-deficient mice can be infected orally or parenterally with *S.* Typhimurium at moderate doses to achieve lethal systemic infection. To achieve a similar degree of infection, resistant mice can be infected intrapertioneally or intravenously at moderate doses, orally at very high doses, or intraperitoneally with the additional of hog gastric mucin to impair host phagocytes[95]. Infection of Nramp1$^{+/+}$ mice has also been used as a model of persistent infection[96]. Many *Salmonella* vaccine candidates have been tested using systemic mouse models [97,98].

Although it has been reported that mice lacking toll-like receptor 11 (Tlr11) are susceptible to lethal infection with *S.* Typhi after oral or systemic inoculation[99], these results have not been confirmed. It was hypothesized that recognition of *Salmonella* flagellin by Tlr11, which is present in mice but not in humans, is responsible for the resistance of mice to *S.* Typhi. However, follow-up studies by five separate groups using identical murine and *Salmonella* strains found that Tlr11$^{-/-}$ mice are not susceptible to *S.* Typhi infection[100]. Even the original group subsequently reported that their original results were not always reproducible [101].

1.4.2 Gastroenteritis Models

Mice and other experimental animals can also be used to study human enteritis with NTS. Pre-treatment of mice with streptomycin depletes their normal gut microbiota and allows *Salmonella* to colonize the cecum and colon, causing a colitis that resembles NTS-induced inflammation in humans. Other models used for studying acute *Salmonella* infection include oral infection of calves, ileal loops in various animals, and non-human primates[102].

1.4.3 Humanized Mouse Models

"Humanized" mice, specifically those reconstituting functional human immune cells, have been a useful innovation for studying human pathogens such as *Mycobacterium tuberculosis,* HIV, hepatitis viruses, and *Plasmodium* spp.[103–106]. This technology is of particular interest for understanding host-pathogen interactions involving human-restricted pathogens such as *S.* Typhi, which has historically lacked a small animal model. There have been several humanized mouse models reported for the study of *S.* Typhi infection, with varying results in terms of bacterial persistence, induction of disease, and elicitation of protective immunity.

The engineering of immunodeficient mice allows both the removal of murine immune cells and their replacement with engrafted human cells. A mutation in *PRKCD* results in deficiencies in T and B cell development, also known as severe combined immunodeficiency syndrome (*scid*)[107]. The combination of the *scid* mutation with a non-obese diabetic (NOD) background results in a reduction in T, B and NK cells[108]. Both backgrounds support only poor engraftment, but knockout of the IL-2 receptor common γ-chain impairs production of IL-2, IL-4, IL-7, IL-9, and IL-15, leading to superior engraftment[109,110]. Mice carrying deletions of the recombination inactivating genes (*RAG1*^{null} and *RAG2*^{null}) cannot perform V(D)J recombination and are also deficient in T and B cell development, similarly to *scid*[111,112]. Engraftment of immunodeficient mouse strains can be performed with stem cells derived from fetal liver, umbilical cord blood, bone marrow, or stimulated peripheral blood, and can also include transplantation of fetal liver and thymus under the kidney capsule (BLT mice)[113].

Although the mouse backgrounds used for the construction of humanized mice are severely immunocompromised, NOD-s*cidIL2rγ*^{null} mice are completely resistant to infection with *S.* Typhi in the absence of engrafted cells[114]. The presence of human hematopoietic cells in engrafted mice

appears to be the key factor required to support progressive infection *in vivo*. *In vitro* studies comparing human and murine macrophages have suggested that *S.* Typhi is better able to replicate and survive in human macrophages[115–118], and human macrophages appear to be required for *S.* Typhi can cause productive infections in humanized mice.

In 2010, two different groups reported the use of $Rag2^{-/-}\gamma c^{-/-}$ models to study *S.* Typhi infection. Song et al. used $Rag2^{-/-}\gamma c^{-/-}$ mice engrafted with human fetal liver hematopoietic stem and progenitor cells. They observed dissemination of *S.* Typhi to the spleen and liver, with bacterial replication at those sites, but no signs of infection or mortality. Analysis of cell populations in organs showed a depletion of human cells following infection, but pro-inflammatory serum cytokine levels were elevated[119]. Firoz Mian et al. used $Rag2^{-/-}\gamma c^{-/-}$ mice engrafted with CD34+-enriched hematopoietic stem cells and observed evidence of meningitis and spread of *S.* Typhi to the liver, spleen, blood and bone marrow[120].

The only lethal small animal model of *S.* Typhi infection appears to be the hu-SRC-SCID model, which uses NOD-s*cidIL2rγ*^{null} mice engrafted with CD34+ hematopoietic stem cells derived from umbilical cord blood[114,121]. The pathology observed in *S.* Typhi-infected hu-SRC-SCID mice resembles that of human typhoid, including hepatic Kupffer cell swelling and splenic multinucleated giant cells[114,122,123]. Elevated serum human cytokines are detected in infected hu-SRC-SCID mice, including IL-6, TNFα, and IFNγ. Hu-SRC-SCID mice provide a unique model for studying various aspects of *S.* Typhi infection; advantages and limitations of this model are discussed in Chapter 2.

1.4.4 Human Challenge Model

Recently, a human challenge model of typhoid was re-established by the Oxford Vaccine Group after a lapse of nearly 40 years since earlier human infection studies. Typhoid human

challenge studies were first performed at the University of Maryland from 1952-1974, using male volunteers from the Maryland House of Corrections. Studies during this period yielded important insights into the pathogenesis of *S.* Typhi and with regard to methods for improving reproducible challenge results, paving the way for future vaccine research[124] . Most initial studies used the *S.* Typhi Quailes strain, which was isolated in 1958 from the gallbladder of a chronic carrier[125]; current studies also use this strain. The University of Maryland studies originally administered *S.* Typhi suspended in milk, but later discovered the importance of a stronger neutralizing buffer to allow the bacteria to withstand exposure to gastric acid. The recent human challenge studies suspend the bacterium in a sodium bicarbonate solution, which also allows a lower dose and improves reproducibility of clinical infection[126]. Carefully pre-screened volunteers are infected and then monitored for 14 days for signs of infection including temperature and blood culture. Antibiotics are administered at the first sign of clinical typhoid or after 14 days, whichever comes first[126].

The human challenge model is a uniquely useful tool for studying typhoid pathogenesis for several reasons. Samples can be collected longitudinally from volunteers, allowing "healthy" baseline samples to be used as controls for samples taken during disease progression. The model provides a platform for the study of novel vaccine candidates with the potential to accelerate licensure. Finally, it provides a unique opportunity for testing sensitivity and efficacy of new diagnostic tests[126]. Limitations include the need to ensure the safety of experimental subjects and the 14-day maximal duration of the studies, making it a poor model for severe or chronic typhoid infection. The stringent selection of healthy participants limits understanding of vaccine efficacy in a population of diverse health statuses.

Recent studies using the Oxford human challenge model included determination of the efficacy of vaccine candidate M01ZH09 and the virulence of a typhoid toxin mutant strain. M01ZH09 carries mutations in *aroC* (metabolism) and *ssaV* (SPI2 T3SS), rendering it safe yet immunogenic, inducing production of a high amount of anti-LPS antibodies[127,128]. However, a single dose failed to provide protection in the human challenge model[129]. The typhoid toxin was suggested to be a major *S.* Typhi virulence factor, but a typhoid toxin deletion mutant exhibited comparable human infectivity to a wild-type parent strain and a longer duration of bacteremia[130].

1.5 *Salmonella*-Macrophage Interactions

Both typhoidal and nontyphoidal *Salmonella* are facultative intracellular pathogens that invade host cells and survive and replicate within them. A hallmark of *Salmonella* pathogenesis is residence within the reticuloendothelial system, specifically, macrophages. *S.* Typhimurium mutants unable to survive within macrophages are avirulent in mice[131], highlighting the importance of survival within this niche.

1.5.1 Macrophage Intracellular Defenses

As part of the innate immune response, macrophages are considered the first line of defense against pathogens, and as such possess a wide array of effector functions to kill or eliminate pathogens. Paradoxically, a great number of intracellular pathogens preferentially reside within macrophages, including *Salmonella*[132]. As such, *Salmonella* is uniquely adapted to survive within macrophages. After entry into a macrophage, *Salmonella* resides within a membrane-bound vacuole, which is formed shortly after invasion and rapidly acidifies to approximately pH5[133]. Acidification serves as an environmental signal that triggers transcriptional regulators – like two component systems EnvZ/OmpR and PhoP/PhoQ, and the alternative sigma factor σ^E – to modofy

expression of factors involved in *Salmonella* intracellular survival [134]. Macrophages also generate microbicidal reactive oxygen species (ROS) and reactive nitrogen species (RNS) in response to infection. The NADPH phagocyte oxidase Nox2 produces superoxide ($O_2 \cdot -$), which can be converted to hydrogen peroxide, hydroxyl radical, or other ROS; inducible nitric oxide synthase (iNOS) produces nitric oxide ($NO\cdot$)[135–138]. Macrophages also withhold essential nutrients from the phagosomal compartment in what is termed nutritional immunity. The natural resistance-associated membrane protein 1 (Nramp1 or Slc11a1) was first discovered for its ability to confer resistance to *Mycobacteria* in mice; it was later identified as a divalent metal transporter that removes magnesium and iron from the *Salmonella*-containing phagosome[139,140]. Mice deficient in Nramp1 are severely susceptible to *Salmonella* infection[141]. Expression of the metal transporter Nramp1 (Slc11a1) is associated with inflammatory molecules such TNFα , $NO\cdot$, and IL-12[139], demonstrating the intimate ties between macrophage activation and iron sequestration. Finally, macrophage TLRs can recognize *Salmonella* PAMPs including LPS and flagellin, and can also sense cytosolic flagellin using NLRC4. Signaling cascades resulting from PAMP sensing determine cell fate, and control of infection may require an infected cell to undergo programmed cell death. However, *Salmonella* may interfere with this strategy, as described in further detail below.

1.5.2 Macrophage Cell Death

Salmonella can induce cell death in multiple host cell types, although only macrophage cell death will be discussed here. Cell death is a host strategy to limit infection of intracellular pathogens by exposing them to the extracellular space for clearance by other cells. *Salmonella* has adapted to subvert this response by interfering with cell death pathways through the secretion of effector proteins, which can interact with multiple types of cell death cascades.

1.5.2.1 Pyroptosis

Pyroptosis is the most well-characterized form of macrophage cell death triggered by *Salmonella* infection. It is highly inflammatory, releasing intracellular bacteria and cellular contents to the extracellular milieu, where bacteria can potentially be killed by other immune cells, notably neutrophils in the lymphoid tissues[142]. Stimulation of other cell types is also achieved through release of inflammatory cytokines such as IL-1β and IL-18 [143–146]. Growth conditions of *Salmonella* prior to infection, such as growth phase or opsonization with serum, have a profound effect on the type of cell death. The use of nonopsonized bacteria grown under conditions to stimulate SPI1 leads to the rapid onset of pyroptosis[145,147,148]. Secretion of SPI1 rod protein PrgJ or flagellin through the T3SS is recognized by host cytosolic pattern recognition receptors known as NAIPs (NLR family apoptosis inhibitory protein)[149,150]. NAIPs then trigger NOD-like receptor NLRC4, which assembles and activates the inflammasome complex[147,151]. Cleavage of pro-caspase-1 to its active form by this complex processes proinflammatory cytokines IL-1β and IL-18 and creates pores in the cell membrane that lead to cell lysis[143,146].

When bacteria are grown under conditions that do not induce SPI1 expression (e.g., stationary phase), and particularly when they are opsonized, cytotoxicity is delayed up to 12 hours after infection[152–154]. This delayed-onset pyroptosis is dependent on SPI2. The specific inflammasome components involved in this process are unknown[155], although the rod protein of SPI2, SsaI, is not involved[142]. *S.* Typhi has been shown to induce both rapid and delayed pyroptosis in human macrophages[152,156,157], although less delayed pyroptosis was seen in *S.* Typhi- than *S.* Typhimurium-infected macrophages[117].

1.5.2.2 Apoptosis

Apoptosis is a programmed form of cell death that is non-inflammatory and can be triggered by intrinsic or extrinsic pathways. The intrinsic pathway is triggered by DNA damage, ROS, or ER stress, leading to the activation of caspase-9. Caspase-9 in turn activates caspase-3 and caspase-7, executioner caspases that carry out the morphological changes seen during apoptosis. These include blebbing to form apoptotic bodies, DNA fragmentation, phosphatidylserine exposure, and cell shrinkage. The extrinsic pathway is triggered by ligand or cytokine binding to transmembrane receptors on the cell surface, such as the TNFR1 receptor. When bound to TNF, this receptor recruits adaptor proteins such as TRADD, TRAF2, and RIPK1. RIPK1 can be ubiquitinated and phosphorylated to direct the cell towards the pro-survival NF-κB pathway; without these modifications, RIPK1 associates with pro-caspase-8, TRADD, and FADD to form a signaling complex that activates caspase-8, which then activates caspases-3/7[158].

Pro-survival signaling through NF-κB is one of a myriad of functions regulated by this transcription factor. NF-κB-responsive genes include those that encode proinflammatory cytokines and defensins as well as anti-apoptotic factors like Bcl-2. Activation of NF-κB begins through binding of ligands to TLRs, NLRs, cytokine receptors, CD40, and others, which signal through adaptor proteins to activate the Iκκ complex. This complex phosphorylates the binding partner of NF-κB, IκB, causing its degradation and release of NF-κB, which is then translocated to the nucleus[159,160]. Numerous *Salmonella* effector proteins can interfere with this pathway, detailed in **Table 1-1.**

1.5.2.3 Necroptosis and Autophagy

Other forms of cell death that occur during *Salmonella* infection include necroptosis and autophagy. Necroptosis is another form of inflammatory programmed cell death that occurs when

TNFR1 is triggered in the absence of caspase-8, allowing RIPK1 and RIPK3 to form a necrosome, which triggers membrane permeabilization and lytic cell death. Manipulation of NF-κB signaling by *Salmonella* effectors can inhibit necroptosis[161]. Autophagy is a process by which the cell can recycle various components; *Salmonella* is also able to manipulate autophagy through effectors like SseF and SseG[162].

1.5.3 Macrophage Modulation by SPI2 Effectors

Salmonella uses T3SSs encoded on SPI1 and SPI2 to inject effector proteins directly into the host cell in order to modulate host cell processes and promote intracellular *Salmonella* survival. Effectors are moved across the needle-like machinery of the T3SS apparatus through both the inner and outer membrane into the host cell. Effectors are targeted to this machinery via an N-terminal signal of 20-30 amino acids; these sequences are not well conserved but may share some sequence patterns. Some effectors are also guided by a chaperone protein, which can bind the 50-100 amino acid region. Effectors may have redundant functions and do not necessarily share sequence similarity, and may be encoded both within and outside of pathogenicity islands, making their comprehensive identification challenging. Identification of secreted effectors has been accomplished by looking for: 1) co-regulation with SPI1 or SPI2; 2) sequence similarity (which is rare); 3) secretion via fusion systems, such as fusions with the catalytic domain of CyaA, a calmodulin-dependent adenylate cyclase that allows detection of an increase of cAMP in *Salmonella*-infected cells[163]; 4) contents of cell culture supernatants by proteomic analysis[164]. Functions of the effector repertoire include remodeling host cellular functions, immune subversion, establishment of the SCV, and promotion of replication[165,166] (**Table 1-1**).

Whereas SPI1 is utilized for invasion of host epithelial cells, once inside the macrophage *Salmonella* relies on the SPI2 T3SS. Infection of murine macrophages with *S.* Typhimurium has

shown that SPI2 mutants are defective for survival and proliferation within the macrophage and cannot cause systemic disease[63]. While *S.* Typhi also upregulates SPI2 during infection of human macrophages[167,168], SPI2 does not appear to be required for *S,* Typhi survival in either primary or immortalized macrophages[17] in contrast to *S.* Typhimurium. Conclusions regarding *Salmonella*-macrophage interactions made on the basis of the *S.* Typhimurium-murine model alone may miss important differences between typhoidal and non-typhoidal *Salmonella* serovars.

An additional observation suggesting that SPI2 may serve different roles in NTS and typhoidal *Salmonella* infections is the significant loss of the SPI2 effector repertoire in the typhoidal serovars *S.* Typhi and *S.* Paratyphi A[169] (**Table 1-1**). This loss is due to genomic decay in the form of both large deletions as well as premature stop codons. A large proportion of SPI2 effectors are absent in both *S.* Typhi and *S.* Paratyphi A, although not typically due to the same inactivating mutations, indicating that these serovars may have undergone convergent evolution towards a similar infection lifestyle. Effectors specifically implicated in inhibition of NF-κB signaling are noticeably absent. Previous studies looking at the effects of NF-κB manipulation by *S.* Typhimurium have primarily focused on the effects on induction of inflammatory gene expression. However, although regulation of inflammation is an important function of NF-κB, this pleotropic transcription factor also has an important role in determining cell survival.

1.6 Dissertation Summary

Enteric fever is a significant contributor to the global burden of disease, particularly in developing countries. Improved therapeutic approaches for enteric fever will require a better understanding of the pathogenesis of typhoidal *Salmonella*. Our current understanding of systemic *Salmonella* infection has primarily relied on studies of the non-typhoidal serovar *S.* Typhimurium in a murine model, which cannot fully recapitulate all aspects of human typhoid. This dissertation

focuses on the use of improved models for studying systemic *Salmonella* Typhi infection, including cultured human macrophages and a humanized mouse model, which allow has revealed important differences in the pathogenesis of *S.* Typhi in humans and *S.* Typhimurium in mice. Chapter 2 describes a genome-wide screen of virulence determinants of *S.* Typhi in the humanized mouse model. Chapter 3 explores the ability of *S.* Typhi to avoid macrophage cell death in order to cause persistent systemic infection. Chapter 4 details how bacterial iron acquisition differs in typhoidal and non-typhoidal *Salmonella* infections. Finally, a summary of the findings, conclusions, and future directions of this work is provided in Chapter 5.

1.7 FIGURES & TABLES

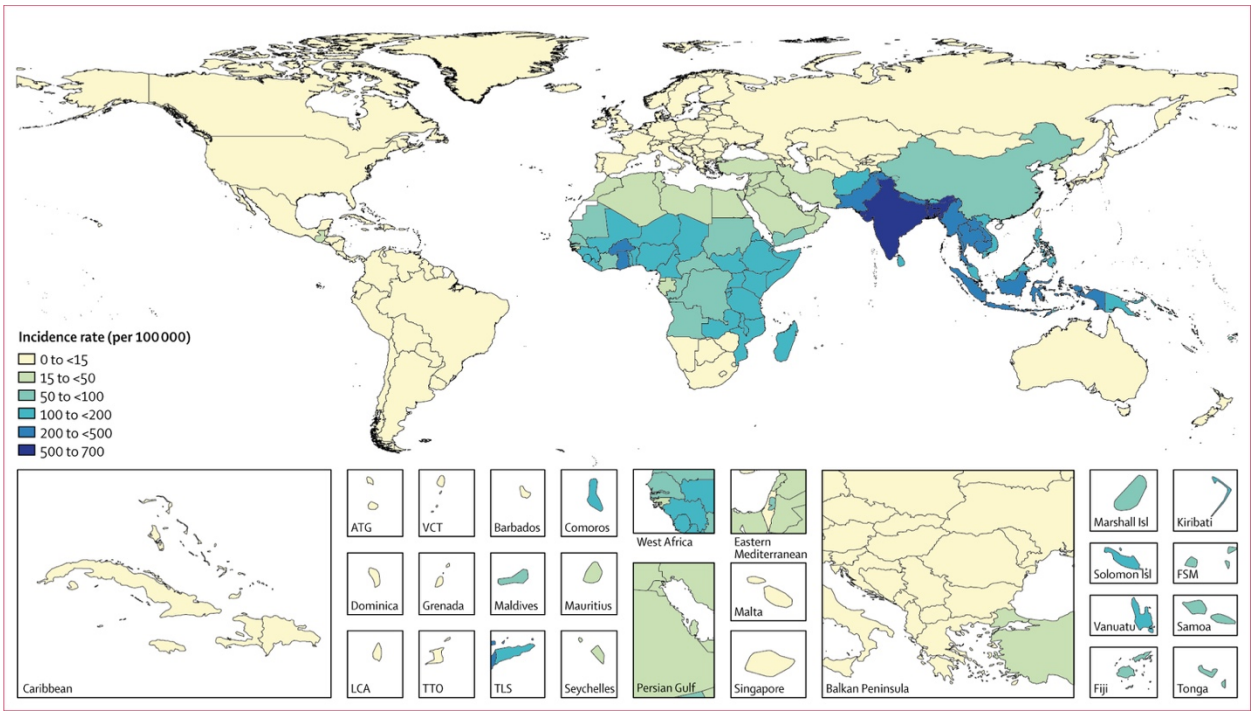

Figure 1-1. Global Burden of Typhoid Fever.

Shown are the incidence rates per 100,000 of typhoid and paratyphoid fevers by country in 2017.

Data are adapted from GBD 2017 Typhoid and Paratyphoid Collaborators[3].

Table 1-1. SPI2 T3SS Effectors in *Salmonella enterica* serovars Typhimurium, Typhi, and Paratyphi A.

Effectors in red are absent in *S.* Typhi.

Effector (*S.* Typhimurium)	T3SS	Genomic Location	*S.* Typhi	*S.* Paratyphi A	Function(s)
AvrA	SPI1/SPI2	SPI1	absent	absent	An acetyltransferase [170] that inhibits NF-κB, JNK, and mTOR pathways. Participates in early and late stages of infection [171]. Prevents macrophage cell death by dampening the pro-apoptotic response [172], although other studies suggest pro-apoptotic functions [173–175]. Stabilizes tight junctions [176,177]. Deubiquitinase activity against NF-κB inhibitors IκBα, β-catenin, and Wnt2 [178].
CigR	SPI2	SPI3	pseudogene	+	Secreted after 3h of infection [179]. Identified via CyaA screen [180]. Required for replication in BMDM [181].
GogA	SPI1/SPI2		absent	absent	Related to proteases PipA and GtgA; targets NF-κB by cleavage of RelA and RelB [182]. Unknown if secreted by SPI1 or SPI2.
GogB	SPI2	Gifsy-1 bacteriophage	absent	absent	Secreted mainly through SPI2 during infection but does not affect mouse colonization [183]. LRR domain targets host FBOX22 to the ubiquitin ligase complex to inhibit IκBα degradation and NF-κB activation [184].
GtgA	SPI2	Gifsy-2 bacteriophage	absent	absent	Protease closely related to PipA and GogA [182]. Inhibits NF-κB signaling through unknown function [180].
GtgE	SPI1/SPI2	Gifsy-2 bacteriophage	absent	absent	Discovered due to requirement for virulence in a mouse model [185]. Proteolytically targets GTPases Rab29, Rab32, and Rab38, promoting replication inside murine macrophages. Absence in typhoidal strains reported to mediate host restriction [35,186].
PipA	SPI1/SPI2	SPI5	+	+	Closely related to GtgA. Inhibits NF-κB signaling [182].
PipB	SPI2	SPI5	+	+	Important for a calf model of infection [187]. Localizes to SCV membranes and SIFs [188,189].
PipB2	SPI2		+	+	Similar to PipB; localizes to SCV and SIFs [179]. Interacts with kinesin light chain (antagonistic to SifA), affecting distribution of late endosomal compartments to the cell periphery [190,191]. May be important in later stages of infection for cell-to-cell spread [192].
SifA	SPI2		+	+	Required for the formation of *Salmonella*-induced filaments (glycoprotein-containing tubules) which maintains integrity of SCV [193–196]. SifA mutants have replication defect [194]. Directs recruitment of LAMP1 enriched membranes [197].
SifB	SPI2		+	pseudogene	30% identical to SifA; a member of the WxxxE family [198]. Targets SCV and SIFs in association with LAMP1 [199].

SlrP	SPI1/SPI2		pseudogene	pseudogene	First identified as a host-range factor [200]. Can be secreted through SPI1 or SPI2 [201]. E3 ubiquitin ligase [202] that mediates ubiquitination of mammalian thioredoxin and interacts with chaperone ERdj3, leading to cell death [203].
SopD2	SPI2		pseudogene	pseudogene	Similar in structure but not function to SopD. Binds membranes independent of ATP during late endosome formation (an antagonist of SifA) [204]. Interacts with Rab7 to regulate endosomal trafficking [205]. Expression in STy redcues invasion [206]. Involved in Sif formation, Required for virulence in mice [207]. Inhibits vesicle traffic to the SCV [208].
SpiC/SsaB	SPI2	SPI2	+	+	Targets TassC (localizes with lipid rafts) [209] and Hook3 (vesicle trafficking or fusion) [210]. Required for secretion of SseB, SseC, and SseD (parts of translocon) [211]. Mediates switch from translocon to effector secretion [212]. Inhibits endosomal trafficking [213].
SptP/StpA	SPI1/SPI2	SPI1	+	+	Tyrosine phosphatase that reverses activation of MAPK ERK [214]. Reverses the effects of SopE and SopE2 through GTPase-activating protein domain [215]. Role in early membrane ruffling but also later SCV maintenance. Promotes intracellular replication during late infection [216]. Mainly translocated through SPI1and requires chaperone SicP [217].
SpvB	SPI2	pSLT	absent	absent	An ADP ribosyltransferase [218] that prevents F-actin filament formation [219]. Required for delayed cell death [220].
SpvC	SPI2	pSLT	absent	absent	Has phosphothreoninelyase activity [221]. Removes phosphate from threonine of ERK to inactivate MAPK [219].
SpvD	SPI1/SPI2	pSLT	absent	absent	Cysteine protease that inhibits NF-κB signaling [180,222,223].
SrfJ	SPI2		absent	unknown	Identified via the SsrB regulon [224]. Similar to human lysosomal glucosylceramidase, which alters sphingolipid metabolism [225,226].
SseF	SPI2	SPI2	+	+	Together, associate with the SCV; required for SIF formation. Target SCV to Golgi network [227–229].
SseG	SPI2	SPI2	+	+	
SseI / SrfH	SPI2	Gifsy-2 bacteriophage	absent	absent	Interacts with IQGAP1 resulting in inhibition of macrophage and dendritic cell migration [230]. Mutant led to enhanced dissemination [231].
SseJ	SPI2		pseudogene	absent	Regulates SCV membrane dynamics along with SifA [197,232]. Expression in *S.* Typhi increases intracellular replication [233].
SseK1	SPI2		absent	absent	Initial studies showed they were not essential for infection [234]. All share homology to NleE from *E. coli* and inhibit TRADD and FADD [235]. SseK1 and SseK3 have been shown to inhibit TNF-mediated but not Tlr4- or interleukin-mediated NF-κB signaling [161].
SseK2	SPI2		absent	absent	

SseK3	SPI2	ST64B bacteriophage	absent	absent	
SseL	SPI2		+	+	Deubiquitinase that inhibits autophagy [236]. Interferes with lipid metabolism [237]. Required for delayed macrophage cytotoxicity but does not affect macrophage cytokine production. Mutants were attenuated for virulence in mice [238].
SspH1	SPI1/2	Gifsy-3 bacteriophage	absent	absent	E3 ubiquitin ligase that interacts with PKN1 and inhibits NF-κB signaling [239,240].
SspH2	SPI2	Bacteriophage remnant	+	absent	E3 ubiquitin ligase that interacts with SGT1 and ubiquitinates Nod1 to modulate immune response [241].
SteA	SPI2		+	+	Binds to (PI(4)P) on Sifs to localize to the SCV [163,242].
SteB	SPI2		absent	absent	Unknown function [163].
SteC	SPI2		+	pseudogene	Phosphorylates MAPK to induce actin formation around SCVs and regulate intracellular replication [163,243,244].
SteD	SPI2		+	+	Inhibits MHCII presentation and inhibits T cell activation [180,245].
SteE/SarA	SPI2	Gifsy-3 bacteriophage	absent	absent	Identified in CyaA screen (SteE) [180], via the PhoPQ regulon (PagJ) [246], and also through comparative genomics (SarA) [247]. Activates phosphorylation of STAT3 to promote IL-10 production [247,248]. Alters phosphorylation activity of host GSK3 to influence macrophage polarization [249]. Neutralizes TNF signaling to alter macrophage polarization [250].
SipA	SPI1	SPI1	+	+	Promotes actin polymerization near adherent bacteria [251]. Contributes to invasion [252]. Persists in infected cells to regulates SCV morphology with SifA [253].
SipB	SPI1	SPI1	+	+	A component of the SPI1 T3SS translocon [254]. Induces apoptosis in macrophages by binding caspase-1 [144].
SipC/SspC	SPI1	SPI1	+	+	A component of the SPI1 T3SS translocon [254]. Bundles and nucleates actin to promote invasion [255].
SipD	SPI1	SPI1	+	+	A component of the SPI1 T3SS translocon [256].
SopA	SPI1		?	+	E3 ubiquitin ligase that promotes leukocyte transmigration and stimulates immune signaling via TRIM E3 ligases [257–259].
SopB/SigD	SPI1	SPI5	+	+	Inositol phosphatase that activates the kinase Akt, inhibiting apoptosis of infected cells at early and late timepoints [260,261]. Contributes to invasion [252].

SopD	SPI1		+	+	Functions with SopB to manipulate membrane dynamics [262]. Contributes to invasion [252].
SopE	SPI1	SopEϕ bacteriophage / SPI7	+	+	Both are guanine exchange factors that activate Rac1 and Cdc42 to manipulate cytoskeleton and promote invasion [187,263–265]. SopE is located on a phage in *S.* Typhimurium but within SPI7 in *S.* Typhi.
SopE2	SPI1	Bacteriophage remnant	pseudogene	+	

Chapter 2. GENOME-WIDE ANALYSIS OF *SALMONELLA* TYPHI VIRULENCE LOCI IN HUMANIZED MICE

The figures and text in this chapter have been adapted from the following publication:

Joyce E. Karlinsey*, **Taylor A. Stepien***, Matthew Mayho, Larissa A. Singletary, Lacey K. Bingham-Ramos, Michael A. Brehm, Dale L. Greiner, Leonard D. Shultz, Larry A. Gallagher, Matthew Bawn, Robert A. Kingsley, Stephen J. Libby and Ferric C. Fang. (2019) Genome-wide Analysis of *Salmonella enterica* serovar Typhi in Humanized Mice Reveals Key Virulence Features. **Cell Host & Microbe**, vo. 26, no. 3, DOI: 10.1016/j.chom.2019.08.001.

**equal contribution*

2.1 ABSTRACT

Salmonella enterica serovar Typhi causes typhoid fever only in humans. Murine infection with *S.* Typhimurium is used as a typhoid model, but its relevance to human typhoid is limited. Non-obese diabetic-*scid IL2rγnull* mice engrafted with human hematopoietic stem cells (hu-SRC-SCID) are susceptible to lethal *S.* Typhi infection. In this study, we used a high-density *S.* Typhi transposon library in hu-SRC-SCID mice to identify virulence loci using transposon-directed insertion site sequencing (TraDIS). Vi capsule, lipopolysaccharide (LPS), and aromatic amino acid biosynthesis were essential for virulence, along with the siderophore salmochelin. However, in contrast to the murine *S.* Typhimurium model, neither the PhoPQ two-component system nor the SPI2 pathogenicity island was required for lethal *S.* Typhi infection, nor was the CdtB typhoid toxin. These observations highlight major differences in the pathogenesis of typhoid and non-typhoidal *Salmonella* infections and demonstrate the utility of humanized mice for understanding the pathogenesis of a human-specific pathogen. (**Figure 2-1**)

2.2 INTRODUCTION

Salmonella enterica serovars Typhi and Paratyphi cause enteric fever and infect only humans. *S*. Typhi infrequently causes diarrhea, instead producing a severe systemic illness with bloodstream invasion and fever, headache, and prostration[59]. A hallmark of typhoid is the development of a carrier state in which infected individuals exhibit prolonged fecal *S*. Typhi shedding[42]. The World Health Organization estimates that 11–20 million cases of typhoid fever result in 128,000–161,000 related deaths per year, mainly in Asia and Africa[86]. Recent emergence of drug-resistant *S*. Typhi strains poses a major public health challenge[266,267]. Understanding the molecular and immunological mechanisms of *S*. Typhi pathogenesis can lead to more effective typhoid vaccines and therapies.

Insight into how *S*. Typhi causes human disease has been hampered by the lack of a small animal model. Non-human primates are resistant to typhoid and exhibit only mild self-limited illness after *S*. Typhi challenge[268,269]. Non-typhoidal *S*. Typhimurium causes an acute systemic infection in most laboratory mice and is commonly described as a model for typhoid. This model has uncovered many important *Salmonella* virulence determinants. However, the relevance of these observations to human typhoid is uncertain, as *S*. Typhimurium causes enteritis rather than enteric fever in humans, and *S*. Typhi and *S*. Typhimurium have numerous genetic differences[18].

We previously reported that hu-SRC-SCID mice develop lethal *S*. Typhi infection, along with characteristic pathology and cytokine responses of typhoid fever[114]. A small number of candidate virulence loci were identified in a transposon site hybridization (TraSH) screen in this model[114]. However, each pool was limited to approximately 10^3 insertions and yielded a number of false-positive results due to genetic bottlenecks. We have subsequently employed transposon-directed insertion site sequencing (TraDIS)[270], a high-throughput method that allows the parallel

analysis of high-complexity transposon (Tn) libraries in individual mice. Here, we report a genome-wide analysis of loci required for *S.* Typhi infection following intraperitoneal (i.p.) inoculation of hu-SRC-SCID mice. This systematic analysis of *S.* Typhi virulence in an infection model demonstrates the unique ability of a humanized mouse model to allow the comprehensive identification of virulence determinants of a human-specific pathogen.

2.3 RESULTS

2.3.1 Identification of S. Typhi Genes Required for Virulence in hu-SRC-SCID Mice

A high-density Tn library of *S.* Typhi with 50× genome coverage by a Tn5-based Tn was used to infect hu-SRC-SCID mice. After i.p. inoculation of 4×10^5 colony-forming units (CFU), mice were monitored for signs of illness and euthanized when moribund. As seen previously[114], most animals rapidly developed illness and were euthanized 24 h post-infection (hpi), although some were less severely ill and were euthanized 64 to 79 hpi. Variation in severity is expected because of differences in donor genetic backgrounds and levels of engraftment in individual mice. Organism burdens in the liver and spleen of infected hu-SRC-SCID mice were higher than in infected non-engrafted NOD-*scidIL2rγnull* mice (**Figure 2-2**). Two "input" libraries, representing the inoculum (T2 and JZ01), and one "output" library per mouse, generated from spleen CFU outgrowth, were constructed and sequenced on an Illumina 2500 platform[270,271]. Sequences were analyzed with the Bio-TraDIS analysis pipeline[271]. The input *S.* Typhi library contained over 185,370 unique insertions, whereas the output libraries from spleens had 53,154 to 125,183 unique insertions. Underrepresentation of mutants within specific genes in the output pool ("counter-selection") identifies genes essential for virulence in the hu-SRC-SCID model.

Initial analysis of differences in reads between input and output libraries showed variable and indiscriminate counter-selection for mice euthanized 64 to 79 hpi. Therefore, only mice

euthanized 24 hpi were used for comparison of input and output pools (T3, T4, T5, T6, T13, T14, T15, T16, and T17). Analysis of the nine output pools and two input pools revealed 72 counter-selected genes that met pre-determined criteria of a false discovery rate of <0.05 and log fold change <−2; these genes are categorized into functional groups in **Table 2-1**. Counter-selected loci include genes for purine and amino acid biosynthesis (*pur* and *aro*), lipopolysaccharide (LPS) and O-antigen synthesis (*waa* and *rfb*), DNA repair (*rec*), protein folding (*dsb* and *fkp*), iron acquisition (*ent* and *iro*), and Vi capsular synthesis (*vex* and *tvi*) (**Table 2-1**).

2.3.2 Comparison of Sequence Reads in Input and Output Libraries for S. Typhi Virulence Genes

Regions of counter-selected Tn insertions were visualized with Artemis software[272]. **Figure 2-3** shows read maps from representative input and output samples; counter-selected loci include Vi capsule (**Figure 2-3a**), salmochelin (**Figure 2-3b),** and LPS biosynthetic operons (**Figure 2-3c**). Counter-selected genes had high read numbers of input but not output samples, whereas flanking genomic regions showed similar read numbers in both input and output samples, indicating that chromosomal location did not affect counter-selection. Unexpectedly, some genes important during murine *S*. Typhimurium infection were not significantly counter-selected in *S*. Typhi-infected hu-SRC-SCID mice. The importance of *Salmonella* Pathogenicity Island-1 (SPI1) and SPI2 genes for *S*. Typhimurium invasion, macrophage survival, and systemic infections in mice is well documented[273–275]. However, *S*. Typhi carrying Tn insertions in SPI1 or SPI2 genes were not counter-selected in hu-SRC-SCID mice (**Figure 2-3 d and e**). The PhoPQ two-component system is a regulator of SPI2[276] and other genes required for *S.* Typhimurium virulence[277,278] but was only weakly counter-selected in *S*. Typhi-infected humanized mice (logFC phoP = 2.1 phoQ = −0.27, Data Not Shown). In addition, the *cdtB* locus encoding the typhoid toxin was not counter-selected (**Figure 2-3f**).

2.3.3 Confirmation of Selected Mutants in hu-SRC-SCID Mice

Validation of the TraDIS analysis was performed by competitive infections of wild-type (WT) and selected mutant strains in hu-SRC-SCID mice. WT and isogenic mutant *S*. Typhi Ty2 strains in a 1:1 ratio (10^5 CFU of each strain) were administered by i.p. inoculation. Mice infected with WT and *iroCDEN*, *ssrB*, *phoP*, or *cdtB* mutants were euthanized 24 hpi; WT and *vexA*- or *entA*-infected mice were euthanized after 72 h. Competitive indexes were determined from liver and spleen CFUs. Mutants lacking the Vi antigen (*vexA*) or enterobactin synthesis (*entA*) were significantly outcompeted by WT *S.* Typhi in both liver and spleen (**Figure 2-4a**), confirming that Vi- or enterobactin-deficient mutant *S.* Typhi have reduced virulence. An *iroCDEN* mutant was outcompeted by WT in the three mice from which sufficient numbers of bacteria were recovered (**Figure 2-4a**). Therefore, the conversion of enterobactin to salmochelin appears to be essential for virulence after i.p. infection. A *phoP* mutant was outcompeted only in the spleen. Mutants lacking *ssrB* (SPI2) or *cdtB* (typhoid toxin) were recovered as well as WT (**Figure 2-4a**), confirming that these genes are not essential for virulence in hu-SRC-SCID mice. Hu-SRC-SCID mice challenged with up to 2.5×10^6 CFUs of an *aroA* mutant of S. Typhi did not succumb to infection, unlike mice infected with WT (**Figure 2-5**).

2.3.4 Effect of Virulence Genes on S. Typhi Persistence in Macrophages

Selected *S*. Typhi mutants were also assayed for survival in THP-1-derived human macrophages. Uptake was measured by comparing intracellular CFUs at t = 0 with the infective dose (**Figure 2-4b**), and survival was measured by comparing intracellular CFUs at t = 0 and t = 24 hpi. (**Figure 2-4c**). Only a *vexA* mutant showed a difference in uptake, an expected finding given the ability of Vi to interfere with phagocytosis[20]. Mutants lacking *aroA*, *entA*, *iroCDEN* or *phoP* demonstrated reduced survival in macrophages (**Figure 2-4c**). However, *invA* (SPI1) or *ssrB*

(SPI2) mutants were not impaired in macrophage survival (**Figure 2-4c**), corroborating the TraDIS results. Mutants lacking the PhoP-regulated typhoid toxin CdtB[279] were also able to survive in macrophages (**Figure 2-4c**). Expression of virulence-associated genes was measured in *S.* Typhi and *S.* Typhimurium during macrophage infection using regulated GFP reporter plasmids (**Figure 2-6**). Modest differences in expression fold change from 0 to 24 h were seen between *S.* Typhi and *S.* Typhimurium, including salmochelin (*iroB*), SPI2 (*ssaG*), and the PhoP regulon (*mig14*).

2.4 DISCUSSION

Human host specificity has posed a formidable challenge in identifying unique determinants of *S.* Typhi virulence. Murine infection with *S.* Typhimurium is used as a model of human typhoid, but major differences between typhoidal and non-typhoidal *Salmonella* serovars limit what can be inferred about typhoid pathogenesis from this model. The hu-SRC-SCID mouse model is a unique research tool to study the pathology and immunology of human typhoid[114]. *S.* Typhi virulence in mice engrafted with human hematopoietic cells suggests that human mononuclear cells are essential for typhoid pathogenesis. Here, we report the genome-wide analysis of *S.* Typhi virulence determinants in humanized mice, confirming some expectations but also revealing unexpected findings.

Biosynthesis of aromatic amino acids, Vi capsular polysaccharide, and the siderophore salmochelin appears to be particularly important for *S.* Typhi virulence in hu-SRC-SCID mice. Aromatic amino acid biosynthesis has long been known to be required for *Salmonella* virulence, as these amino acids are not freely available in the mammalian host[33]. *S.* Typhimurium and *S.* Typhi strains deficient in aromatic amino acid biosynthesis are attenuated for virulence in mice and humans, respectively, and have been used as live attenuated vaccines[280,281]. Our results confirm that *aroA* mutant *S.* Typhi is strongly counter-selected in hu-SRC-SCID mice.

The Vi (virulence) antigen was initially described in association with highly virulent strains of *S.* Typhi Ty2[282] and later shown to be a capsular polysaccharide[20]. Although Vi expression may be lost during lab passage, bloodstream isolates from patients with typhoid are nearly always Vi positive[283], suggesting that Vi is important for *S.* Typhi virulence. A variety of functions for Vi have been described from in vitro studies, including prevention of complement-mediated clearance[284], antibody binding[285] and Tlr4 signaling[286]. Here, we show that Vi is essential for systemic infection of humanized mice. Genes required for biosynthesis, transport, and assembly of the Vi capsular polysaccharide were highly counter-selected in hu-SRC-SCID mice.

In addition to protection conferred by Vi, *S.* Typhi requires specific LPS modifications for resistance to antibodies and complement[287]. LPS biosynthetic genes, especially those involved in O-antigen synthesis and modifications of the outer core, were highly counter-selected in hu-SRC-SCID mice. The O-antigen is important for *S.* Typhi serum resistance and macrophage survival[288,289], while the outer core is required for host cell invasion[288,290]. The outer core terminal glucose plays a critical role in *S.* Typhi internalization by host cells[288] and is added by the WaaB glucosyltransferase, which was identified by TraDIS. Interestingly, this terminal residue is not required for internalization of *S.* Typhimurium, highlighting a key difference between these serovars.

Mutants deficient in iron acquisition and utilization or iron-sulfur cluster repair were counter-selected in hu-SRC-SCID mice, including the siderophore salmochelin. The importance of salmochelin was confirmed by competitive infection and shown to be required for *S.* Typhi survival in macrophages. Iron acquisition is known to be required for *Salmonella* survival in macrophages[291]. Enterobactin is glucosylated by *iro* genes to produce salmochelin, which counteracts the neutralizing effects of host-derived lipocalin-2[292–294]. Reduced survival of an *S.*

Typhi *iroCDEN* mutant in macrophages demonstrates the importance of evading lipocalin-2 neutralization for *S.* Typhi survival. Although salmochelin loss attenuates *S.* Typhimurium virulence in mice[292,295,296], salmochelin is not required for *S.* Typhimurium growth in murine macrophages unless other iron uptake systems are also impaired[296], and salmochelin loss has a more profound impact on *S.* Typhi virulence, suggesting that non-glucosylated enterobactin may be less effective as a siderophore in *S.* Typhi than in *S.* Typhimurium.

Studies in murine *S.* Typhimurium infection have highlighted the importance of SPI2 for macrophage survival and systemic infection[274,275]. It was therefore surprising that our TraDIS analysis did not show significant counter-selection of SPI2. Dispensability of SPI2 was confirmed by competitive infection. Although previous studies have shown that *S.* Typhi SPI2 genes are upregulated in human THP-1 macrophages[168], SPI2 was not required for macrophage survival[17] (**Figure 2-4c**). Collectively, these observations suggest a marked difference in the dependence of *S.* Typhi and *S.* Typhimurium on SPI2.

An additional factor long recognized as essential for *S.* Typhimurium virulence is the transcriptional regulator PhoP, which was only weakly counter-selected in hu-SRC-SCID mice. PhoP is required for *S.* Typhimurium survival in murine macrophages[131,297], and we observed reduced survival of *phoP* mutant *S.* Typhi in THP-1 cells. However, PhoP-regulated genes were not highly counter-selected in our study, and a *phoP* mutant had only a modest competitive disadvantage in humanized mice. This suggests that PhoP may be less important during acute typhoid fever than in non-typhoidal *Salmonella* infections, at least during the early infection stages examined in this model. An analysis of PhoP-regulated proteins in *S.* Typhi and *S.* Typhimurium found some *S.* Typhi-specific proteins including the typhoid toxin (CdtB)[279]. We failed to observe counter-selection of mutants lacking *cdtB* or the associated genes *pltA* and *pltB*, and competitive

infection showed that a *cdtB* mutant has no defect in hu-SRC-SCID mice. A previous study similarly showed increased replication of *cdtB* mutant *S*. Typhi in humanized Rag2$^{-/-}\gamma c^{-/-}$ mice engrafted with human fetal liver and hematopoietic progenitor cells[119]. In an experimental challenge study, a *cdtB* mutant was not attenuated for virulence in human subjects[130]. Collectively, these observations indicate that the typhoid toxin is not required for *S*. Typhi virulence during early acute typhoid infection in hu-SRC-SCID mice and in humans.

A limitation of our study is the acute nature of *S*. Typhi infection in hu-SRC-SCID mice, which differs from the prolonged systemic infection that characterizes typhoid fever. While the presence of human mononuclear cells allows *S*. Typhi to proliferate, the residual presence of murine immune cells creates a chimeric immune environment in which artificial interactions may be detrimental to the host. In addition, the absence of non-hematopoietic human cells prevents *S*. Typhi interactions with other human cell types. For example, although human hematopoietic stem cells used to engraft hu-SRC-SCID mice express the typhoid toxin receptor CD45, toxin interactions with human epithelial cells cannot be studied using this model[298]. Oral inoculation of hu-SRC-SCID mice is infeasible due to the absence of the IL-2 receptor gamma chain molecule, which prevents the development of mucosal lymphoid tissue[121]. Finally, the labor-intensive generation of hu-SRC-SCID mice limits sample size in this and similar studies, and subject-to-subject variation is expected due to differences in engraftment levels and donor heterogeneity. Despite these constraints, we observed consistent counter-selection of many genes across all mice analyzed, validating the importance of these genetic loci for *S*. Typhi virulence. The hu-SRC-SCID model is unique in its ability to support lethal *S*. Typhi infection and recapitulates important aspects of typhoid pathogenesis such as systemic spread, histopathological findings, and cytokine profile[114], suggesting that our observations are relevant to human typhoid.

Live attenuated *S*. Typhi strains are presently under investigation, both as typhoid vaccines and as carriers to elicit immunity to heterologous antigens[299]. Our studies in hu-SRC-SCID mice confirm that mutations in pathways required for aromatic amino acid biosynthesis reduce the virulence of vaccine strains. However, mutations in SPI2 genes or *phoP* are also used in vaccine strains but may not have attenuating effects in *S*. Typhi. Hu-SRC-SCID mice provide an improved model to assess candidate virulence-attenuating mutations and a new starting point from which to investigate typhoid pathogenesis.

2.5 Materials and Methods

2.5.1 Bacterial Growth Conditions and Strain Constructions

Bacterial strains used in this study are listed in **Table 2-2**. *S. enterica* cultures were grown in Miller's Luria Broth (LB) medium at 37°C with shaking at 250 rpm. Medium was supplemented with "aromix" (40 μg ml^{-1} L-phenylalanine, 40 μg ml^{-1} L-tryptophan, 10 μg ml^{-1} 2,3-dihydroxybenzoic acid, 10 μg ml^{-1} p-amino benzoic acid), ampicillin (100 μg ml^{-1}), carbenicillin (100 μg ml^{-1}), kanamycin (50 μg ml^{-1}), X-gal (40 μg ml^{-1}) or 2,6-diaminopimelic acid (0.4 mM), as indicated. Plasmids and primers used in this study are listed in **Table 2-2** and **Table 2-3**. Primers were purchased from Integrated DNA Technologies (IDT, Skokie, IL). Mutant alleles of *S*. enterica serovars were constructed using λ-Red recombination as described[300,301] with primers sets listed in **Table 2-3**. All plasmids were constructed using NEBuilder HiFi Assembly Master mix (NEB, Ipswich, MA) with the following vectors and PCR products using primer sets listed in **Table 2-3** as follows: pJK741, pJK745, pJK747, pJK749 and pJK750 with pMPMA3Δnull-gfp digested with EcoRI and PCR products generated with gDNA from S. Typhi Ty2; pJK744, pJK746, pJK748 and pJK754 with pMPMA3Δnull-gfp and PCR products generated with gDNA from *S*. Typhimurium 14028s; pJK753 with pWSK130 digested with BamHI and PCR products generated with pDNA

from pFPVmCherry. All mutant strains and plasmid constructs were confirmed by DNA sequencing (Genewiz, South Plainfield, NJ).

2.5.2 S. Typhi Transposon Library Construction

Transposon mutagenesis in *S.* Typhi Ty2 was performed by conjugal mating of pLG100 containing transposable element T22 (ISlacZ-Tn2/FRT with a selectable kanamycin marker)[302] as follows: The donor strain FLS232 (Rho3/pLG100) was grown in LB broth with carbenicillin and 2,6-diaminopimelic acid to OD_{600}∼1.0. This was mixed with recipient strain *S.* Typhi Ty2 grown in LB broth with "aromix" to OD_{600}∼1.0 at a ratio of (0.1:1), then spotted onto a sterile 0.45μM nitrocellulose membrane filter seeded on a LB plate. Eleven independent matings were performed, and after 1 h incubation at 37°C, the filters were added to 1 ml LB broth with "aromix," vortexed, then pooled together. The pooled matings were subsequently plated onto ten QTrays (240x240x20mm) plates (Molecular Devices, San Jose, CA) containing LB agar with "aromix" and kanamycin (lacking DAP) and incubated at 37°C for ∼18 h. Each plate was harvested with 15 ml of LB broth, and all plate harvests were pooled together for a total of ∼300,000 kanamycin-resistant mutant colonies. DMSO was added to 10%, and 1 ml aliquots were frozen at -80°C. One aliquot was thawed, and the viable titer of the transposon library was found to be $8.7x10^9$ CFU ml^{-1}. The construction of an *S.* Typhi transposon library for Illumina-based sequencing was performed as described below, and the subsequent sequences were processed using the Bio-TraDIS analysis pipeline[271]. Eighty-one percent of the total mapped reads of 7,067,870 matched to the transposon tag, to which 64% of these sequences were mapped to *S.* Typhi genome sequence AE014613.1. A total of 253,439 unique insertion sites were found, with an average of one insertion site for every 19 bp of sequence.

2.5.3 Libraries for Illumina-based TraDIS

Construction of *S.* Typhi transposon libraries for Illumina-based TraDIS is based on the TdT method[303] modified for transposon T22[302], outlined in **Figure 2-7**. Genomic DNA (gDNA) from transposon library outgrowths were isolated from ~1x10^9 cells using a DNeasy Blood & Tissue Kit (Qiagen, Germantown, MD), per the manufacturer's protocol. The gDNA was additionally purified by ethanol precipitation and resuspended in 100 µl TE (10mM Tris-HCL,1 mM EDTA pH 8.0). The gDNA was quantified with the Invitrogen Qubit ds DNA BR assay kit on a Qubit fluorometer (Invitrogen, ThermoFisher Scientific, Waltham, MA).

One to 1.5 µg of gDNA in a final volume 130 µl TE was transferred to a Covaris microtube AFA Fiber Crimp-cap and sheared to fragment size ~300bp using an LE220 focused-ultrasonicator with Rack PN500282 and duty factor 30%, (W) 450 and cycles 200, for 60 s (Covaris, Woburn, MA). The sheared gDNA was end-repaired using NEBNext End Repair in a final volume of 155 µl per the manufacturer's protocol (New England Biolabs, Ipswich, MA). The end-repaired DNA was purified using a MinElute PCR Clean up kit (Qiagen, Germantown, MD), and the DNA was eluted twice with 10 µl EB. The purified end-repaired DNA was C-tailed with Terminal Transferase (TdT) in the following reaction: 18.6 µl end-repaired DNA, 2.8 µl freshly prepared solution of 9.5 mM dCTP (and 0.5 mM ddCTP (Millipore-Sigma, St. Louis, MO), 5.6 µl of 5X TdT reaction buffer, 1.0 µl Terminal Transferase 30U/µl (Promega, Madison, WI). The C-tailing reaction was incubated at 37°C for 60 m then 75°C for 20 m. C-tailed DNA was purified using a Performa DTR gel filtration column per the manufacturer's protocol (EdgeBio, SanJose, CA) and quantified by fluorometry.

The first PCR reaction (PCR1) was performed using a transposon-specific primer T22-87_Left and primer olj376 specific to the C-tailed end (**Figure 2-7**) in the following reaction: 7.4

µl of EDGE-purified C-tailed DNA (~150 ng), 25 µl of 2X KAPA HiFi Hot Start Ready Mix (Kapa Biosystems, Wilmington, MA), 3 µl of 10 µM primer olj376, 1 µl of 10 µM primer T22-87_Left, 0.25 µl of 100x SYBR Green 1 (Invitrogen, ThermoFisher Scientific, Waltham, MA), 13.35 of µl PCR-grade water. Thermocycling was performed in a BioRAD CFX96 with the following conditions: 95°C-2:00; 24X{98°C-0:30, 64°C-0:30, 72°C-1:30, read} 72°C-2:00; 10°C hold. Under these conditions using 150 ng of C-tailed DNA, the inflection point was observed at approximately 24 cycles. As a control, no amplification was seen in a PCR1 reaction where a C-tailed DNA sample was performed without TdT enzyme. Subsequent PCR purification was not required after the PCR1 reaction.

The second PCR reaction (PCR2) added the P5-Tn and P7-Index primers (**Figure 2-7**) in the following reaction: 1.2 µl of PCR1 product, 25 µl of 2X KAPA HiFi Hot Start Ready Mix, 3 µl of 10 µM primer T22_PAIR_AmpF_Left, 3 µl of 10µM primer TdT_Index_XX, 0.25 µl of 100x SYBR Green 1, 17.55 µl PCR grade water. Thermocycling was performed in a BioRAD CFX96 with the following conditions: 95°C-2:00; ~14X{98°C-0:30, 64°C-0:30, 72°C-1:30, read} 72°C-2:00; 10°C hold. To determine the number of cycles to run, a PCR2 reaction was piloted for 25-30 cycles to calculate the inflection point for each sample. Two reactions of PCR2 were performed per PCR1 sample with the number of cycles (inflection point) determined in the pilot PCR2 reaction. Twenty-four indexed TdT_Index_XX primers (**Table 2-2**) were used for multiplexing up to 24 libraries for subsequent Illumina sequencing.

The PCR2 reactions were purified by SPRI beads using a ratio left-right 0.8-0.61 size selection method for a range of 230-660 bps, per the manufacturer's protocol (Beckman Coulter Life Sciences, Indianapolis, IN). This method first selects the right side of the bp range, then the left. Size selection was performed in a 96-well round bottom microtiter plate (Costar 3795).

Ninety-five µl of PCR2∗(0.61X) SPRI beads = (58 µl) were mixed 10X, then incubated for 1 m at RT. The microtiter plate was placed on an Agencourt SPRIPlate 96R ring super magnet plate (Beckman Coulter) for 2 m. One-hundred forty-five µl of supernatant were removed into a new well. One hundred forty-five µl of (0.8X-0.61X)=0.19X SPRI beads = (27.6 µl) were added, mixed 10X, and incubated for 1 m at RT. The plate was placed on the magnet for 2 m, and supernatants were discarded. While the plate was on the magnet, 180 µl of freshly made 85% ethanol were added before incubation for 30 s at RT. Ethanol was discarded before air-drying for 2 m at RT. The plate was removed from the magnet and 35 µl EB (Qiagen) added before mixing and incubation for 5 m at RT. The plate was then placed on the magnet for 2 m and supernatant transferred to a new 0.65 ml Eppendorf tube for storage at -20°C.

Quantification of the purified libraries was performed by three different methods as follows: One µl of SPRI sized select library was quantified using a High Sensitivity DNA Kit on an Agilent Bioanalyzer 2100 (Agilent, Santa Clara, CA). Quantification of the purified libraries was also performed by qPCR with the KAPA Library Quantification kit Illumina platform (KAPA Biosystems, Wilmington, MA), per the manufacturer's protocol. Finally, libraries were quantified using an Invitrogen Qubit ds DNA HS assay kit on a Qubit fluorometer.

For multiplexing, the libraries were pooled to a final concentration of 2 nM of each library. The libraries were sequenced at the Fred Hutch Cancer Research Center Genomics Facility on platform HiSeq 2500 Rapid Run (65°C) (2-lanes if multiplexing), 50SR with a custom primer T22_custom_1stRead_SEQ_Left with a 15 pM final library concentration, and a 6% spike-in of 12.5 pM PhiX library.

2.5.4 Library Infection in Humanized Mice

Mouse experiments in this study were approved by the University of Washington Institutional Animal Care and Use Committee (IACUC) and performed as described in protocol 3373-01. NOD-*Prkdc*^{scid}*IL2r*γ^{tm1Wjl} (NSG) mice were purchased from The Jackson Laboratory (Bar Harbor, ME) and engrafted with human CD34+ hematopoietic stem cells derived from umbilical cord blood[121,304]. Umbilical cord blood was obtained from donors that were consented under an approved IRB protocol at the UMass Memorial Medical Center, Department of General Obstetrics and Gynecology (Worcester, MA), and all samples used for engraftment were de-identified. Non-engrafted NSG mice and human hematopoietic stem cell-engrafted hu-SRC-SCID mice[121,304] were infected with a total of ~4 x 10^5 CFU of an *S.* Typhi transposon library by i.p. injection with 0.5 ml of ~8 x 10^5 CFU ml^{-1} in PBS. In addition, 0.5 ml of the inoculum was added to a 125 ml Erlenmeyer flask containing 25 ml LB broth with "aromix" and kanamycin before incubation for ~18 h at 37°C with shaking at 200 rpm. DMSO was added to the outgrowth "input" sample to 10% and aliquots stored at -80°C for subsequent transposon-specific library construction and Illumina sequencing.

The infected mice were closely monitored for signs of illness, and moribund animals were euthanized. The majority of the animals were euthanized at approximately 24 hpi; however, a small number of animals showed less severe signs of illness and were euthanized at 64 to 79 hpi. Livers and spleens were harvested and homogenized in PBS. A portion of each organ was plated for CFU counts and the remainder of the homogenates were transferred to a 125 ml Erlenmeyer flask containing 25 ml LB broth with "aromix" and kanamycin before incubation for ~18 h at 37°C with shaking at 200 rpm. The outgrowth "output" samples were passed through a 70 μM cell strainer, DMSO was added to 10%, and aliquots stored at -80°C for subsequent transposon-specific

library construction for Illumina sequencing. Sequence reads with a transposon tag were identified, mapped to *S.* Typhi strain Ty2 whole genome sequence (Accession number AE014613.1) with SMALT (smalt-0.7.6) and quantified using the Bio-TraDIS analysis pipeline[271].

2.5.5 Competitive Infections in Humanized Mice

Human HSC-engrafted NSG (hu-SRC-SCID)[121,304] mice were infected with an equal ratio of wild-type and mutant strains of *S.* Typhi Ty2. For each competitive infection, six hu-SRC-SCID mice were inoculated i.p. with a total of 2 x 10^5 CFU in PBS each. Mice were closely monitored for illness and euthanized when moribund (e.g., exhibiting reduced spontaneous movement or oral intake, hypothermia). Livers and spleens were harvested and homogenized in PBS. Dilutions of the homogenates were plated for CFU on LB plates with "aromix" and incubated overnight at 37°C. Colonies were enumerated and 100 colonies patched onto LB plates with "aromix" and the appropriate antibiotic to determine the ratio of wild-type to mutant bacteria. The competitive index (CI) was calculated as a ratio of $(\text{mutant/wild-type})_{\text{output}}$ / $(\text{mutant/wild-type})_{\text{input}}$. Statistical significance was determined using a Wilcoxson signed rank test using Prism v. 8.1.2 (GraphPad).

2.5.6 Macrophage Infections

Human THP-1 monocytes were obtained from ATCC and cultured in RPMI 1640 medium (Corning) supplemented with 10% heat-inactivated fetal bovine serum (Millipore-Sigma), sodium pyruvate (Corning), non-essential amino acids (Gibco), 50 U ml^{-1} penicillin and 50 µg ml^{-1} streptomycin (Corning) at 37°C in 5% CO2. Monocytes were differentiated with 100 nM phorbol 12-myristate 13-acetate (PMA) for 48 h; the medium was changed to PMA- and antibiotic-free RPMI 24 h prior to infection. *Salmonella* strains were grown in LB broth with "aromix," amplicillin and kanamycin for 18 h with shaking at 37°C, then adjusted to OD_{600}=1.0 and washed

twice with sterile PBS. *Salmonella* were mixed with equal parts human pooled serum (MP Biomedicals LLC) and incubated at 37°C for 20 m to opsonize the bacteria. Opsonized bacteria were used to infect THP-1 human macrophage-like cells at an MOI of 10:1. Infected monolayers were centrifuged for 5 m at 1000 rpm to synchronize infection, then incubated at 37°C for 1 h to promote internalization. Following internalization, monolayers were washed with RPMI supplemented with 20 μg ml^{-1} gentamicin to kill extracellular bacteria. All macrophage infections were performed in biological triplicate. For survival studies, infected macrophages were lysed in 1% Triton X-100 at 0 h and 24 h post-infection. Lysates were serially diluted and plated on LB plates with "aromix" to determine the number of intracellular CFU. For gene expression analysis, infected macrophages were lysed after 24 h with 1% Triton X-100. Lysates were gently centrifuged at 2500 rcf for 5 m, supernatants were removed, and bacteria pelleted by centrifugation at 15000 rpm for 5 m. Bacterial pellets were resuspended in 2.5% paraformaldehyde and fixed for 15 m at 37°C. Fixed bacteria were washed once in PBS then analyzed for GFP expression using a BD LSRII flow cytometer (Becton, Dickinson) at the Pathology Flow Cytometry Core Facility (Department of Pathology, University of Washington, Seattle, WA) with the following gating scheme: All *Salmonella* strains assayed by flow cytometry had a constitutive expressing mCherry plasmid (pJK743) as well as various promoter fusions to GFP to assay for expression. Bacteria were first gated on forward and side scatter to logarithmic amplification, then mCherry fluorescence was detected after 561nM excitation and emission collected through a 595LP, 610/20 nm filter. A total of 10,000 mCherry counts were collected and GFP fluorescence was detected after 488 nM excitation and emission collected through a 505LP, 530/30 nm filter. Data were processed using FlowJo v. 10.3 software (Treestar). Total GFP fluorescence was calculated from

the GFP-positive cells and statistical significance calculated using a Student's unpaired two-tailed t-test with software Excel v. 16.19 (Microsoft) or Prism v. 8.1.2 (GraphPad).

2.5.7 Statistical Analysis

Statistical method and sample size for experiments are indicated in the corresponding figure legends. The TraDIS input and output libraries were analyzed using the tradis_comparison.R script in the BioTraDIS pipeline, which applies an edgeR package[305] to quantitatively analyze significant differences of read counts in genes between two conditions. Genes that were counter-selected in hu-SRC-SCID mice with a false discovery rate (Q value) of <0.05 and log fold change (logFC) of <-2 were deemed significant. Statistical analysis of the competitive infections in mice and macrophage infections was performed using Prism v. 8.1.2 software (GraphPad). An unpaired two-tailed Student's t-test was performed on the means of parametric data, and a Wilcoxson signed rank test was performed on the means of non-parametric data. Statistical significance was defined as $p<0.05$. Error bars on figures show standard deviation.

2.5.8 Data and Code Availability

Datasets generated during this study are available at the NCBI Sequence Read Archive (SRA: PRJNA546274).

2.6 Acknowledgments, Author Contributions, and Conflicts of Interest

2.6.1 Acknowledgments

We thank Dr. Gemma Langridge of Quadram Institute Bioscience for advice on TraDIS methodology; Davin Hoover and James Januik for dedicated laboratory assistance; Dr. Thea Brabb of UW Comparative Medicine for assistance with animal care; Dr. Jeffery Delrow, Andy Marty,

and Qing Zhang at the Fred Hutchinson Cancer Research Center Genomics Facility for help with Illumina sequencing and analysis; Chris Frazer and Dr. Debra Nickerson of UW Genome Sciences for use of the Covaris LE220; Dr. Hillary Hayden and Dr. Samuel Miller of UW Microbiology for use of the Qubit; Dr. Rafael Hernandez and Dr. Lakshmi Rajagopal at Seattle Children's Research Institute for use of the Agilent 2100 bioanalyzer; and Dr. Olivia Steele-Mortimer at NIAID for the pMPMA3 ΔPlac P*ssaG* GFP and pMPMA3 ΔPlac null GFP expression plasmids. This work was supported by NIH grants AI112640 (F.C.F.), AI132963 (M.A.B. and L.D.S.), OD018259 (L.D.S.), and CA034196 (L.D.S.).

2.6.2 Author Contributions

J.E.K., T.A.S., S.J.L., and F.C.F. designed the study; J.E.K., T.A.S., L.A.S., L.K.B.-R., and S.J.L. performed the experiments; L.A.G., M.A.B., D.L.G., and L.D.S. contributed reagents; J.E.K., T.A.S., M.M., L.A.S., L.K.B.-R., M.A.B., D.L.G., L.D.S., L.A.G., M.B., R.A.K., S.J.L., and F.C.F. analyzed the data; J.E.K., T.A.S., and F.C.F. wrote the paper with input from all authors.

2.6.3 Conflicts of Interest

The authors declare no competing interests.

2.7 FIGURES

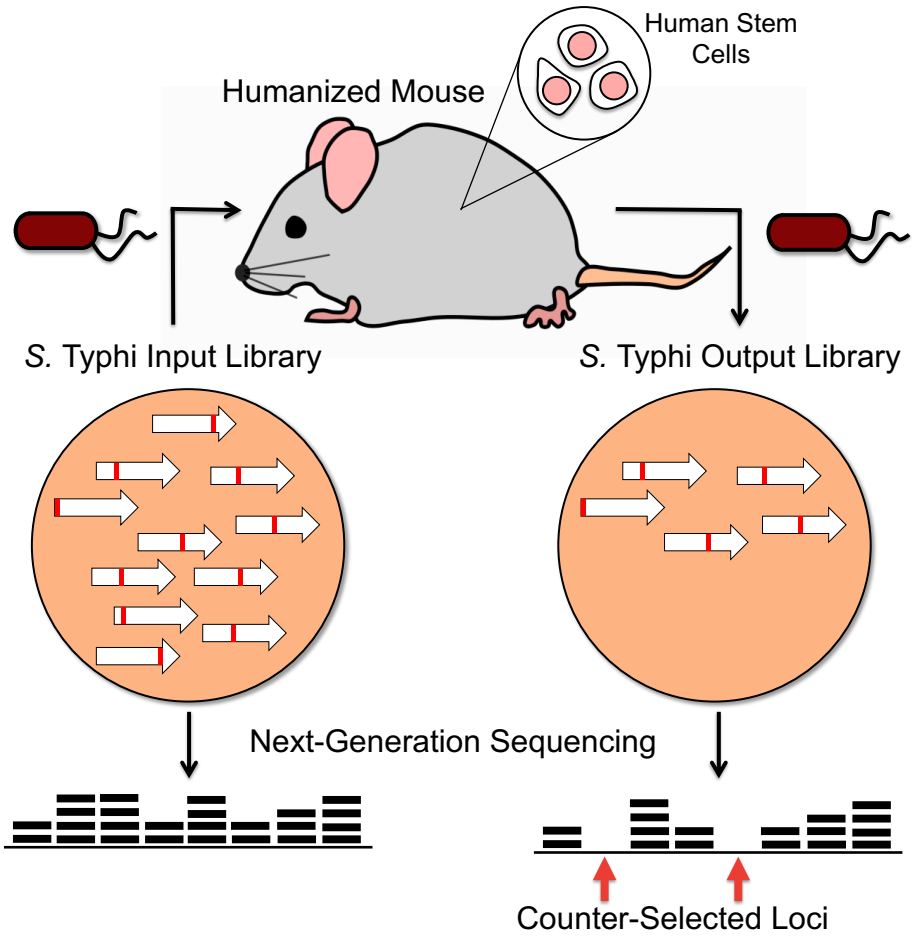

Figure 2-1. Graphical Representation of TraDIS Screen in Humanized Mice.

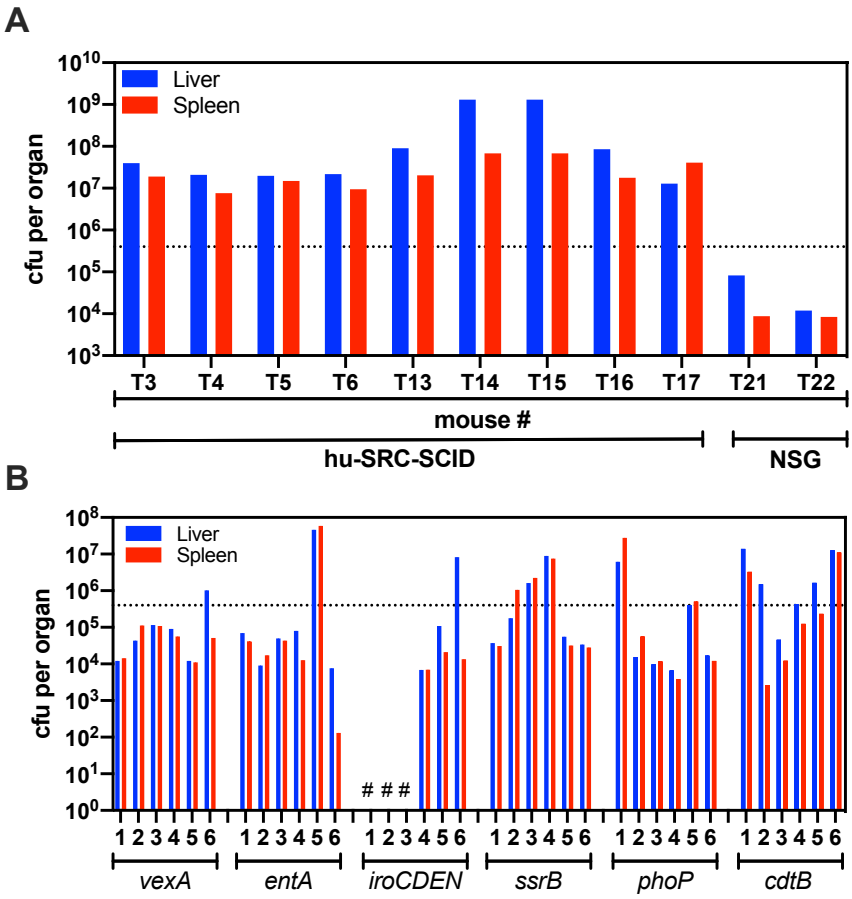

Figure 2-2. Bacterial Burdens in Liver and Spleen of hu-SRC-SCID and Non-engrafted NSG Mice Infected with *S.* Typhi.

(**A**) Hu-SRC-SCID mice (T2, T3, T5, T6, T13, T14, T15, T16 and T17) and non-engrafted NSG mice (T21 and T22) were infected i.p. with ~4 x 10^5 cfu *S.* Typhi transposon library (y-axis dotted line). Twenty-four hours p.i., the organs were harvested, homogenized and a sample plated for CFU determination in livers (blue bars) and spleens (red bars). The remaining homogenates were processed for Illumina-based TraDIS. (**B**) The competitive indexes (CI) of *S.* Typhi mutants *vexA, entA, iroCDEN, ssrB, phoP* and *cdtB* compared to wild-type were determined by mixed infections in hu-SRC-SCID mice (see Figure 2-3a). The organism burdens in livers (blue bars) and spleens (red bars) from hu-SRC-SCID mice infected i.p. with 2x10^5 cfu (y-axis dotted line) with

an equal mixture of wild-type and mutant strain. The animals were monitored daily and sacrificed before moribund. Mixed infections of wild-type and *iroCDEN*, *ssrB*, *phoP* or *cdtB* mutants were sacrificed at 24 h p.i. and *vexA*, *entA* at 72 hpi. Six mice were infected in each group; the # indicates samples where no colonies were isolated in the organs for subsequent CI determination.

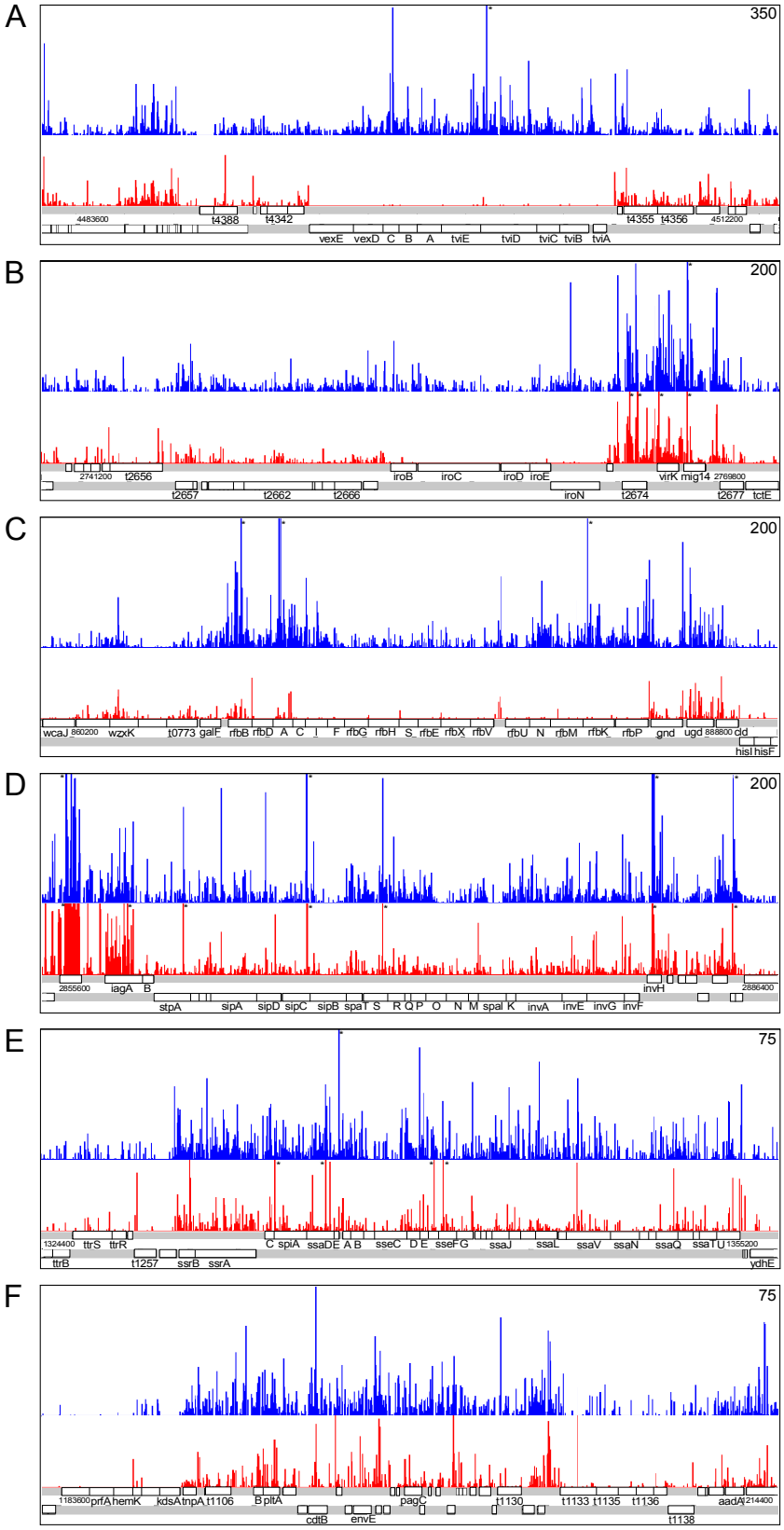

Figure 2-3. Selection of *S.* Typhi Loci Identified by TraDIS in hu-SRC-SCID Mice.

The frequency and distribution of mapped sequence reads were generated using Artemis. Counter-selected loci: (**A**) Vi antigen, (**B**) salmochelin biosynthesis and utilization, and (**C**) LPS biosynthesis. Non-counter-selected loci: (**D**) SPI1 region, (**E**) SPI2 region, and (**F**) typhoid toxin. The y axis shows the frequency of mapped reads. Maximum read maps are shown in the upper right except where * indicates map reads greater than shown. Input S. Typhi transposon library (blue) and a representative output S. Typhi transposon library from hu-SRC-SCID mouse 24 hpi (red) are shown.

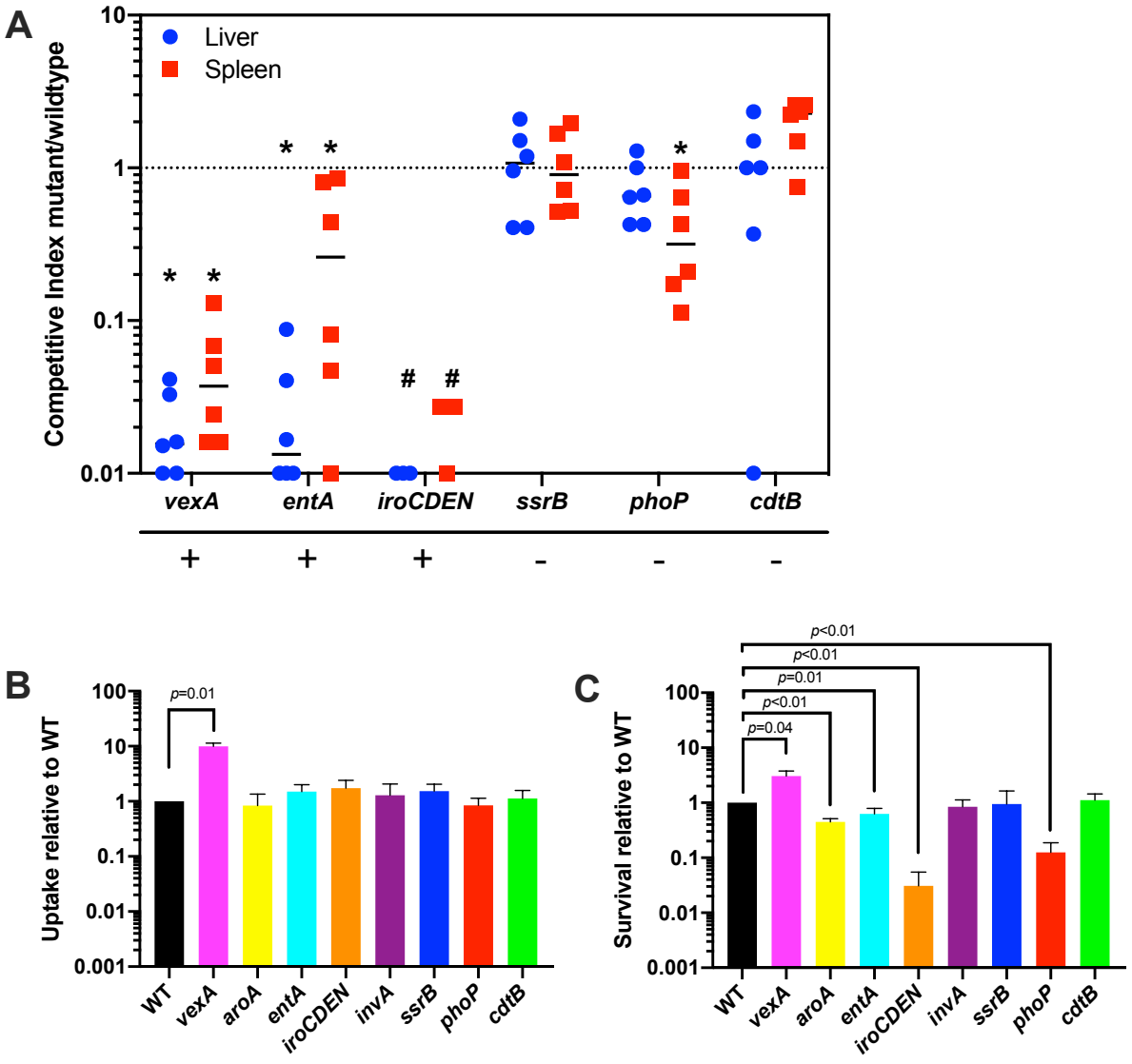

Figure 2-4. Confirmation of *S.* Typhi Mutants in hu-SRC-SCID Mouse and Human Macrophage Infections.

(**A**) Competitive indices (CIs) of *S.* Typhi *vexA*, *entA*, *iroCDEN*, *ssrB*, *phoP*, or *cdtB* mutants compared to wild-type were measured in hu-SRC-SCID mice. *S.* Typhi mutants counter-selected or not counter-selected in the TraDIS analysis are indicated with a (+) or (−), respectively. Six hu-SRC-SCID mice for each group were infected with an equal mixture of wild-type and mutant strains. Solid lines represent median CI in the livers (blue circles) and spleens (red squares). Dotted

line represents the expected CI if neither strain has a competitive disadvantage. Significance of the CI was determined by Wilcoxon signed-rank test to a hypothetical median of 1; ⋆p = 0.03; # indicates animals with too few colonies isolated for CI determination. Uptake (B) and survival (C) of WT (black bars), *vexA* (magenta bars), *aroA* (yellow bars), *entA* (cyan bars), *iroCDEN* (orange bars), *invA* (purple bars), *ssrB* (blue bars), *phoP* (red bars) and *cdtB* (green bars) *S.* Typhi strains in THP-1 macrophages. Bar graphs show mean values of mutant strains relative to wild-type (WT), and error bars show standard deviations from at least 3 biological replicates. Statistical significance p was determined by paired two-tailed Student's t test.

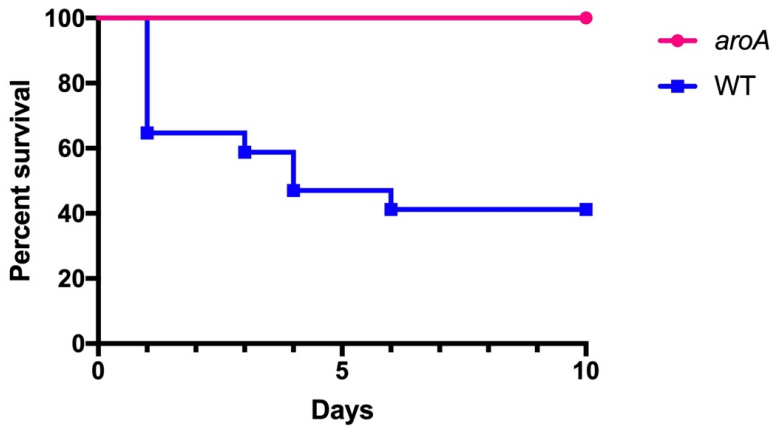

Figure 2-5. *S.* Typhi Carrying an *aroA* Mutation is Attenuated for Virulence in Humanized Mice.

Humanized hu-SRC-SCID mice were challenged with i.p. inoculation of wild-type *S.* Typhi Ty2 (1-3.5x10^5 cfu) or an isogenic *aroA* mutant strain (3x10^5 to 2.5x10^6 cfu) (n=17 per group). Differences in survival were highly significant (p = 0.0002 by Mantel-Cox test).

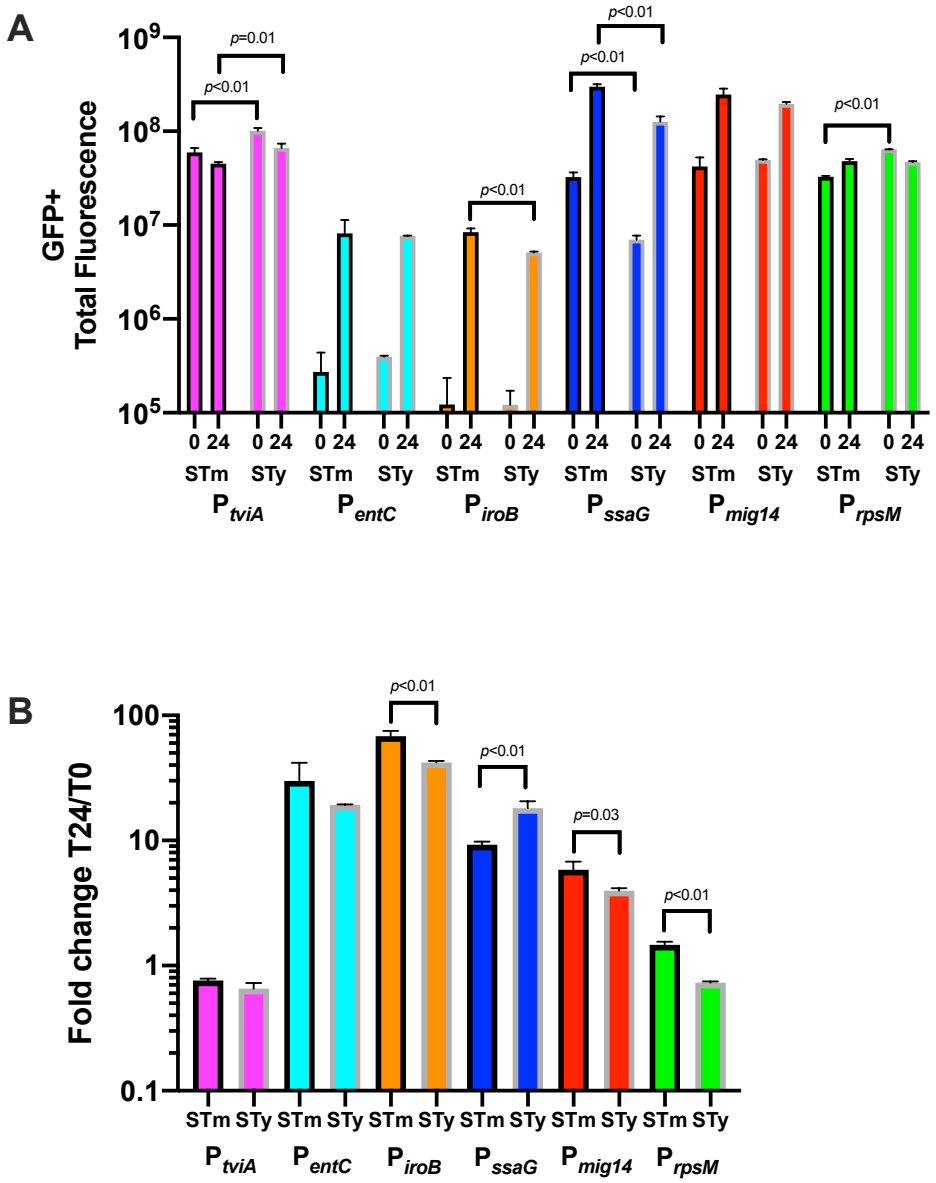

Figure 2-6. Infection with *Salmonella* Strains in Human THP-1 Macrophages.

(**A**) Comparison of gene expression between *S.* Typhi (STy) and *S.* Typhimurium (STm) of representative promoters involved in *Salmonella* pathogenesis. *Salmonella* strains with GFP fusions to representative promoters for Vi antigen (*tviA*), Iron acquisition (*entC* and *iroB*), SPI2 (*ssaG*), PhoP regulon (*mig14*) and a constitutive promoter (*rpsM*) were assayed for GFP expression by FACS analysis. All reporter-carrying *Salmonella* strains also carried a plasmid constitutively expressing mCherry to identify viable intracellular bacteria. THP-1 macrophages

infected with S*almonella* strains (STm black bordered bars, STy grey bordered bars) with GFP promoter fusions to *tviA* (magenta bars), *entC* (cyan bars), *iroB* (orange bars), *ssaG* (blue bars), *mig14* (red bars) or *rpsM* (green bars) at a MOI of ~15:1 for 24 h. The bar graph shows total fluorescence intensity of GFP+ cells at pre-infection (0) and 24 h p.i. (24) where the error bars are the means from 3 biological replicates. Statistical significance *p* between STm and STy reporter plasmids was determined by unpaired two-tailed Student t test. (**B**) Fold change T24/T0 of total fluorescence intensity of GFP+ cells.

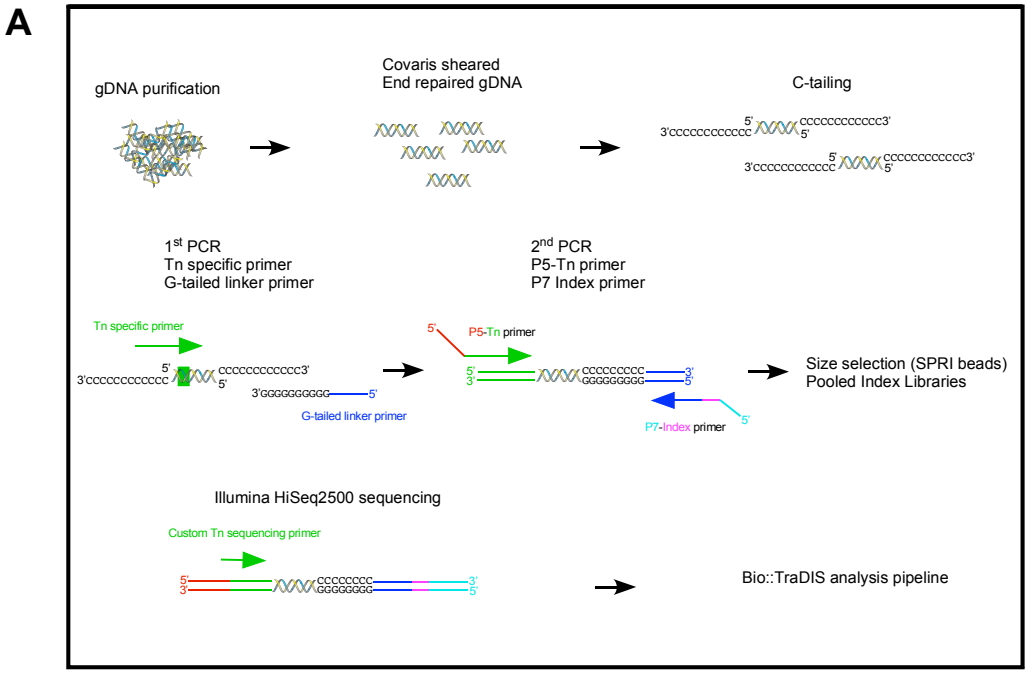

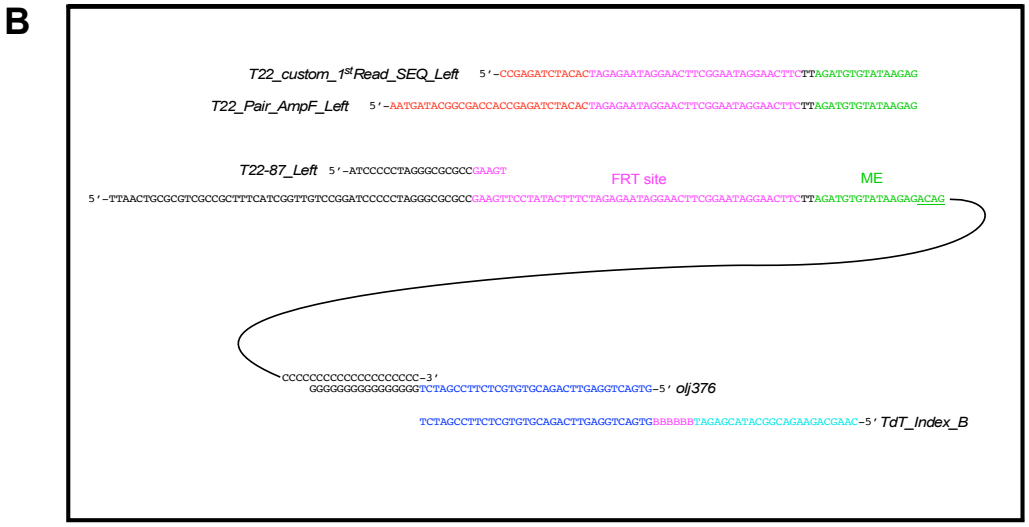

Figure 2-7. Overview of Illumina-based Transposon-Directed Insertion Site Sequencing (TraDIS).

(**A**) Construction of transposon specific libraries using the TdT method for Illumina sequencing. Genomic DNA was isolated from the "input" and "output" cultures and Covaris-sheared to ~300bp. The sheared DNA ends were end-repaired, and the 3'-ends were C-tailed using

terminal deoxynucleotidyl transferase (TdT). The transposon specific fragments were PCR-amplified using a transposon-specific primer and a G-tailed linker primer. A second PCR reaction was performed to add the P5 and P7-indexed sequences. The libraries were size-selected using SPRI beads, and the indexed transposon specific libraries were pooled and sequenced using a custom transposon specific sequencing primer on an Illumina HiSeq2500 platform. The sequences were processed using Bio::TraDIS analysis pipeline[271]. (**B**) Primer design for Illumina-based transposon-directed insertion site sequencing for the left end of transposable element T22.

2.8 TABLES

Table 2-1. *S.* Typhi Ty2 Genes Counter-Selected in hu-SRC-SCID Mice 24 hpi.

Gene name	Locus tag	Function	logFC
LPS biosynthesis; O-antigen			
rfbD/rmlD	t0776	dTDP-4-dehydrorhamnose reductase	-5.03
rfbC/rmlC	t0778	dTDP-4-dehydrorhamnose 3,5-epimerase	-4.9
rfbI/ddhD	t0779	putative reductase RfbI	-3.52
rfbG/ddhB	t0781	CDP-glucose 4,6-dehydratase	-3.5
rfbH/ddhC	t0782	putative dehydratase RfbH	-3.12
rfbE/tyv	t0784	CDP-tyvelose-2-epimerase	-2.89
rfbX/wzx	t0785	putative O-antigen transporter	-2.9
rfbV/wbaV	t0786	putative glycosyl transferase	-2.79
rfbN/wbaN	t0788	putative rhamnosyltransferase	-4.55
rfbM/manC	t0789	mannose-1-phosphate guanylyltransferase	-3.27
rfbK/manK	t0790	phosphomannomutase	-3.82
rfbP/wbaP	t0791	undecaprenyl-phosphate galactosephosphotransferase	-3.77
wzxE	t3371	putative lipopolysaccharide biosynthesis protein	-4.47
waaL	t3806	O-antigen ligase	-4.67
LPS biosynthesis; Outer core			
waaB	t3800	lipopolysaccharide 1,6-galactosyltransferase	-4.51
waaI	t3801	lipopolysaccharide 1,3-galactosyltransferase	-3.92
waaJ	t3802	lipopolysaccharide 1,2-glucosyltransferase	-4.11
waaK	t3805	lipopolysaccharide 1,2-N-acetylglucosaminetransferase	-4.61
Metabolism and enzymes			
purL	t0291	phosphoribosylformylglycineamide synthetase	-5.38
purN	t0357	phosphoribosylglycinamidine myltransferase	-5.53
purM	t0358	phosphoribosylformylglycinamidine cyclo-ligase	-5.57
cvpA	t0501	colicin V production protein	-6.39
purF	t0502	amidophosphoribosyltransferase	-5.54
pabB	t1053	para-aminobenzoate synthase component I	-3.47
gpmA	t2115	phosphoglycerate mutase 1	-3.78
purE	t2327	phosphoribosylaminoimidazole carboxylase catalytic subunit	-5.45
purH	t3455	phosphoribosylaminoimidazolecarboxamide formyltransferase	-3.45
purD	t3456	phosphoribosylglycineamide synthetase	-4.47
gntK	t3980	putative gluconokinase	-4.24
purA	t4417	adenylosuccinate synthetase	-3.93
Vi antigen biosynthesis			
vexE	t4344	Vi polysaccharide export protein	-4.61
vexD	t4345	Vi polysaccharide export inner-membrane protein	-5.5
vexC	t4346	Vi polysaccharide export ATP-binding protein	-4.99
vexB	t4347	Vi polysaccharide export inner-membrane protein	-5.16
vexA	t4348	Vi polysaccharide export protein	-5.69
tviE	t4349	Vi polysaccharide biosynthesis protein TviE	-5.39
tviD	t4350	Vi polysaccharide biosynthesis protein	-5.21

tviC	t4351	Vi polysaccharide biosynthesis protein, epimerase	-5.77
tviB	t4352	Vi polysaccharide biosynthesis protein, UDP-glucose/GDP-mannose dehydrogenase	-4.83
tviA	t4353	Vi polysaccharide biosynthesis protein	-4.75
Iron acquisition/utilization/cluster repair			
entA	t2270	2,3-dihydro-2,3-dihydroxybenzoate dehydrogenase	-4.55
ybdZ	t2281	conserved hypothetical protein	-5.52
iroC	t2669	putative ABC transporter protein	-5.14
iroD	t2670	putative ferric enterochelin esterase	-5.66
iroE	t2671	putative exported protein	-2.32
iroN	t2672	TonB-dependent outer membrane siderophore receptor protein	-4.9
exbD	t3078	biopolymer transport ExbD protein	-4.58
exbB	t3079	biopolymer transport ExbB protein	-4.4
yggX	t3024	conserved hypothetical protein probable Fe(2+)-trafficking protein	-3.74
Unclassified			
t1103	t1103	putative regulator sirB1	-4.15
t2640	t2640	conserved hypothetical protein	-4.05
t3486	t3486	hypothetical protein	-5.02
yhgE	t4007	putative membrane protein DUF4153 domain-containing protein	-5.33
t4182	t4182	entericidin B precursor	-6.21
Cell membrane			
yfgC/bepA	t0363	putative Zn-dependent protease, contains TPR repeats	-4.14
yejM/pbgA	t0626	putative sulphatase cardiolipin transport	-3.74
ybiS	t2050	putative exported protein L,D-transpeptidase	-5.87
yrfF/igaA	t4011	negative regulator Rcs regulatory system	-5.09
Amino acid synthesis			
aroC	t0480	chorismate synthase	-6.96
aroA	t1956	3-phosphoshikimate 1-carboxyvinyltransferase	-5.02
serC	t1957	phosphoserine aminotransferase	-3.65
Transcription			
nagC	t2193	N-acetylglucosamine repressor	-2.61
greA	t3216	transcription elongation factor	-5.26
fabR	t3498	HTH-type transcriptional repressor FabR	-4.68
Chaperone			
fkpA	t4052	FKBP-type peptidyl-prolyl isomerase	-3.51
ytfN/tamB	t4464	autotransporter assembly complex protein TamB	-5.1
Respiration and ATP synthesis			
ndh	t1709	NADH dehydrogenase	-5.04
corE/ypjD	t2633	putative membrane protein	-3.23
Transport			
tolB	t2128	tolB protein precursor	-4.68
tolQ	t2131	tolQ protein	-4.51
Cell redox homeostasis			
dsbA	t3623	thiol:disulfide interchange protein	-4.17
DNA replication, modification			
recA	t2730	recA protein	-5.95

Table 2-2. Strains, Plasmids, and Resources.

Bacterial Strains		
Salmonella enterica serovar Typhi Ty2 wild-type JSG624	J. Gunn	TY01
S. Typhi Ty2 Δ*phoP::FRTaphFRT*	[306]	TY53
S. Typhi Ty2 Δ*aroA::FRTaphFRT*	[306]	TY57
S. Typhi Ty2 Δ*vexA::FRTaphFRT*	[306]	TY76
S. Typhi Ty2 Δ*invA::FRTaphFRT*	[306]	TY88
S. Typhi Ty2 Δ*ssrB::FRTaphFRT*	[306]	TY144
S. Typhi Ty2 Δ*cdtB::FRTaphFRT*	[306]	TY198
S. Typhi Ty2 Δ*entA::FRTaphFRT*	[306]	TY262
S. Typhi Ty2 Δ*iroCDEN::FRTaphFRT*	[306]	TY300
S. Typhi Ty2 / P_{null}-GFP pJK753	[306]	TY346
S. Typhi Ty2 / pJK754 pJK753	[306]	TY356
S. Typhi Ty2 / pJK741 pJK753	[306]	TY348
S. Typhi Ty2 / pJK745 pJK753	[306]	TY350
S. Typhi Ty2 / pJK747 pJK753	[306]	TY351
S. Typhi Ty2 / pJK749 pJK753	[306]	TY352
S. Typhi Ty2 / pJK750 pJK753	[306]	TY353
Salmonella enterica serovar Typhimurium 14028s wild-type	S. Miller	JK1324
S. Typhimurium 14028s / P_{null}-GFP pJK753	[306]	JK1532
S. Typhimurium 14028s / pJK754 pJK753	[306]	JK1541
S. Typhimurium 14028s / pJK744 pJK753	[306]	JK1534
S. Typhimurium 14028s / pJK746 pJK753	[306]	JK1535
S. Typhimurium 14028s / pJK748 pJK753	[306]	JK1536
S. Typhimurium 14028s / pJK750 pJK753	[306]	JK1537
E. coli SM10λpirλpir Δ*asd::FRT* Δ*aphA::FRT*	[307]	Rho3
Rho3 / pLG100	[306]	FLS232
Chemicals, Peptides, and Recombinant Proteins		
RPMI 1640, 1x with L-glutamine and 25mM HEPES	Corning	Cat#10-041-CV
Sodium Pyruvate 100mM solution	Corning	Cat#25-000-CI
MEM Non-Essential Amino Acids 100X	Gibco	Cat#11140-050
Penicillin Streptomycin	Corning	Cat#30-001-CI
Fetal Bovine Serum, heat-inactivated (USA sourced)	Millipore-Sigma	F4135
Phorbal 12-myristate 13-acetate	Millipore-Sigma	P1585
Human pooled serum	MP Biomedicals LLC	Cat#2930149
Phosphate-Buffered Saline	Corning	Cat#21-040-CV
Triton X-100	Fisher BioReagents	BP151-100
2,2-Dipyridyl	Millipore-Sigma	D216305
Paraformaldehyde, 16% solution	Electron Microscopy Sciences	Cat#15710
Ferric Chloride	Millipore-Sigma	Cat#F-7134
LB Broth, Miller	Fisher BioReagents	Cat#BP1426
LB Agar, Miller	Fisher BioReagents	Cat#BP1425
L-Phenylalanine	Millipore-Sigma	Cat#P2126
L-Tryptophan	Millipore-Sigma	Cat#T0254
2,3-Dihydroxybenzoic acid	Millipore-Sigma	Cat#126209
4-Aminobenzoic acid	Millipore-Sigma	Cat#A9878
2,6-Diaminopimelic acid	Millipore-Sigma	Cat#33240

Ampicillin, sodium salt	Research Products International	Cat#A40040
Carbenicillin disodium salt	Research Products International	Cat#C46000
Kanamycin sulfate	VWR	Cat#0408
X-GAL	Research Products International	Cat#B71800
RNaseA	Qiagen	Cat#19101
Terminal Deoxynucleotidyl Transferase, Recombinant	Promega	Cat#M1871
2'-Deoxycytidine 5'-triphosphate disodium salt	Millipore-Sigma	Cat#D4913
2',3'-Dideoxycytidine 5'Triphosphate	GE Healthcare	Cat#27-2061-01
SYBR Green 1		
SPRIselect Reagent	Beckman Coulter Life Sciences	Cat#B23318
Critical Commercial Assays		
Qubit dsDNA BR Assay Kit	Invitrogen	Cat#Q32850
Qubit dsDNA HS Assay Kit	Invitrogen	Cat#Q32851
DNeasy Blood & Tissue Kit	Qiagen	Cat#69504
MinElute PCR Purification Kit	Qiagen	Cat#28004
NEBuilder HiFi DNA Assembly Master Mix	New England BioLabs	Cat#E2621
NEBNext End Repair Module	New England BioLabs	Cat#E6050L
Agilent High Sensitivity DNA Kit	Agilent	Cat#5067-4626
KAPA HiFi HotStart Library Amplification Kit	KAPABiosystems	Cat#KK2612
Library Quantification Kit-Illumina/Universal	KAPABiosystems	Cat#KK4824
Deposited Data		
SRA accession		https://www.ncbi.nlm.gov/sra/PRJNA546274
Experimental Models: Cell Lines		
THP-1 monocyte	ATCC	ATCC TIB-202
Experimental Models: Organisms/Strains		
NOD-*scid IL2rγ^{null}γ^{null}* mice	Dale Greiner University of Massachusetts Medical School	NSG
Humanized-NOD-*scid IL2rγ^{null}γ^{null}* mice	Dale Greiner University of Massachusetts Medical School	hu-SRC-SCID
Recombinant DNA		
T22 ISlacZ-Fn2/FRT (kan^{Fn}) oriRK6 *bla tnpA mob*	[302]	pLG100
araC-P$_{araB}$-γβ*exo* oriR101 repA101ts *bla*	[300]	pKD46
Low copy cloning vector ori pSC101 *aph*	[308]	pWSK130
P$_{STM\text{-}rpsM}$-mCherry ori pBR322 *bla*	[309]	pFPV-mCherry
pMPMA3ΔP$_{lac}$ null-*gfp* oriP15A *bla*	Olivia Steele-Mortimer NIAID	P$_{null}$-GFP
pMPMA3ΔP$_{lac}$ P$_{STM\text{-}ssaG}$-*gfp* oriP15A *bla*	Olivia Steele-Mortimer NIAID	P$_{ssaG}$-GFP
P$_{STY\text{-}ssaG}$-*gfp* oriP15A *bla*	[306]	pJK741
P$_{STM\text{-}mig14}$-*gfp* oriP15A *bla*	[306]	pJK744
P$_{STY\text{-}mig14}$-*gfp* oriP15A *bla*	[306]	pJK745
P$_{STM\text{-}entC}$-*gfp* oriP15A *bla*	[306]	pJK746

$P_{STY\text{-}entC}$-*gfp* oriP15A *bla*	[306]	pJK747
$P_{STM\text{-}iroB}$-*gfp* oriP15A *bla*	[306]	pJK748
$P_{STY\text{-}iroB}$-*gfp* oriP15A *bla*	[306]	pJK749
$P_{STY\text{-}tviA}$-*gfp* oriP15A *bla*	[306]	pJK750
$P_{STM\text{-}rpsM}$-mCherry ori pSC101 *aph*	[306]	pJK753
$P_{STM\text{-}rpsM}$-*gfp* oriP15A *bla*	[306]	pJK754
Software and Algorithms		
Artemis	[272]	https://www.sanger.ac.uk/science/tools/artemis
Bio-TraDIS analysis pipeline	[271]	https://sanger-pathogens.github.io/Bio-Tradis/
Canvas Draw 4 Version 4.0.2	Canvas	https://www.canvasgfx.com/
FlowJo Version 10.3	Treestar, Inc.	https://www.flowjo.com/solutions/flowjo
MacVector Version 17.0.4	MacVector	https://www.macvector.com/
Microsoft Excel Version 16.24	Office 365	https://www.office.com/
Prism Version 8.1.1	GraphPad	https://www.graphpad.com/
MacVector Version 17.05.5	MacVector, Inc.	https://macvector.com/

Table 2-3. Primers.

Primer	Sequence 5'-3'	Purpose
TYP5	GTACTGGTTGTAGAGGATAATGCATTATTACGCCACCACCGTGTAGGCTGGAGCTGCTTC	Deletion of *phoP* in STy and STm
TYP6	TCAAAAAGATATCCTTGTCCGCGTACGGTGGTAATGACATCATATGAATATCCTCCTTAG	Deletion of *phoP* in STy and STm
TYP9	CTGACGTTACAACCCATCGCGCGGGTCGATGGCGCCATTAGTGTAGGCTGGAGCTGCTTC	Deletion of *aroA* in STy
TYP10	CGTACTCATCCGCGCCAGTTGTTCGAAATAATCAGGGAACCATATGAATATCCTCCTTAG	Deletion of *aroA* in STy
TYP45	ATCATCATATTACTAACGACATTTTTCCTGCTTTCGGGATGTGTAGGCTGGAGCTGCTTC	Deletion of *vexA* in STy
TYP46	TTAGTGCCGCGGGTCAAAAAGCTATCGAATGCGGCTTTCACATATGAATATCCTCCTTAG	Deletion of *vexA* in STy
TYP13	TATAAGATCTTATTAGTAGACGATCATGAAATCATCATTAGTGTAGGCTGGAGCTGCTTC	Deletion of *ssrB* in STy
TYP14	ATTAACCTCATTCTTCGGGCGCAGTTAAGTAACTCTGTCACATATGAATATCCTCCTTAG	Deletion of *ssrB* in STy
TYP17	TCTCTACTTAACAGTGCTCGTTTACGACCTGAATTACTGAGTGTAGGCTGGAGCTGCTTC	Deletion of *invA* in STy

TYP18	TTTATAACATTCACTGACTTGCTATCTGCTATCTCACCGACATATGAATATCCTCCTTAG	Deletion of *invA* in STy
JKP696	CGCGAGGGCAGCAAAATGAAAGAATATAAGATCTTATTAGGTGTAGGCTGGAGCTGCTTC	Deletion of *ssrB* in STm
JKP697	AGTTAAGTAACTCTGTCACTTTATGAACCTGTAGCTTTCTC	Deletion of *ssrB* in STm
TSP303	GCTTTGATTTTTCAGACAAAACGGTATGGGTGACCGGGGCGTGTAGGCTGGAGCTGCTTC	Deletion of *entA* in STy and STm
TSP304	TCAGGCTCCCAATGTTGAACCGCCGTCCACCACGATATCCCATATGAATATCCTCCTTAG	Deletion of *entA* in STy and STm
JKP899	ATGCCCGCGACTCATTCCCCCATGCCCGCTCGTGCCTGGAGTGTAGGCTGGAGCTGCTTC	Deletion of *iroCDEN* in STy and STm
JKP912	ATGAGAGTTAAGAAGTTCATCTGGTTAATAACCGTGGTTTCATATGATTATCCTCCTTAG	Deletion of *iroCDEN* in STy and STm
JKP684	TGTTTTTTTCCTTCTGACCATGATCATCTGCAGCTATATGTGTAGGCTGGAGCTGCTTC	Deletion of *cdtB* in STy
JKP685	TAATGCTTCAACCCTTTGTGAATAAGGTGCTCGATCGACACATATGAATATCCTCCTTAG	Deletion of *cdtB* in STy
JKP965	TGGATCCCCCGGGCTGCAGGTGGGAGTTTGGGACTACAG	Construction of pJK741
JKP966	GGCATGCAAGCTTGATATCGATAACCGTTAGCGCTGGTAAC	Construction of pJK741
JKP969	TGGATCCCCCGGGCTGCAGGAACTATTTCATACGCGGATGTG	Construction of pJK744 and pJK745
JKP970	GGCATGCAAGCTTGATATCGTATTGATACTACCGCCGTATTGC	Construction of pJK744 and pJK745
JKP971	TGGATCCCCCGGGCTGCAGGAGTCTCACAATAGCGTCCTG	Construction of pJK746 and pJK747
JKP972	GGCATGCAAGCTTGATATCGAAGCGATCGGGAGCAAGC	Construction of pJK746 and pJK747
JKP973	TGGATCCCCCGGGCTGCAGGTCCACGGGCGTCTGGTATG	Construction of pJK748 and pJK749
JKP974	GGCATGCAAGCTTGATATCGGACAGCACAGGGTATAGCAGTC	Construction of pJK748 and pJK749
JKP975	TGGATCCCCCGGGCTGCAGGCCAGTATGACGTTCTGACG	Construction of pJK750
JKP976	GGCATGCAAGCTTGATATCGTAATGCCAGCAGCTCCAAC	Construction of pJK750
JKP979	GGCCGCTCTAGAACTAGTGTTCGAGCTCGGTACCCGG	Construction of pJK753
JKP980	GAATTCCTGCAGCCCGGGGTTACTTGTACAGCTCGTCCATGC	Construction of pJK753
JKP981	TGGATCCCCCGGGCTGCAGGTTCGAGCTCGGTACCCGG	Construction of pJK754
JKP982	GGCATGCAAGCTTGATATCGGATCTTAACATTTTCAGCGATACCCG	Construction of pJK754
T22—87_Left	ATCCCCCTAGGGCGCGCCGAAGT	TraDIS
olj376	GTGACTGGAGTTCAGACGTGTGCTCTTCCGATCTGGGGGGGGGGGGGGGG	TraDIS
T22_PAIR_AmpF_LEFT	AATGATACGGCGACCACCGAGATCTACACTAGAGAATAGGAACTTCGGAATAGGAACTTCTTAGATGTGTATAAGAG	TraDIS
TdT_Index_01_ATCACG	CAAGCAGAAGACGGCATACGAGATCGTGATGTGACTGGAGTTCAGACGTGTGCTCTTCCGATCT	TraDIS
TdT_Index_02_CGATGT	CAAGCAGAAGACGGCATACGAGATACATCGGTGACTGGAGTTCAGACGTGTGCTCTTCCGATCT	TraDIS
TdT_Index_03_TTAGGC	CAAGCAGAAGACGGCATACGAGATGCCTAAGTGACTGGAGTTCAGACGTGTGCTCTTCCGATCT	TraDIS
TdT_Index_04_TGACCA	CAAGCAGAAGACGGCATACGAGATTGGTCAGTGACTGGAGTTCAGACGTGTGCTCTTCCGATCT	TraDIS

TdT_Index_05_ACAGTG	CAAGCAGAAGACGGCATACGAGATCACTGTGTGACTGGAGTTCAGACGTGTGCTCTTCCGATCT	TraDIS
TdT_Index_06_GCCAAT	CAAGCAGAAGACGGCATACGAGATCACTGTGTGACTGGAGTTCAGACGTGTGCTCTTCCGATCT	TraDIS
TdT_Index_07_CAGATC	CAAGCAGAAGACGGCATACGAGATGATCTGGTGACTGGAGTTCAGACGTGTGCTCTTCCGATCT	TraDIS
TdT_Index_08_ACTTGA	CAAGCAGAAGACGGCATACGAGATTCAAGTGTGACTGGAGTTCAGACGTGTGCTCTTCCGATCT	TraDIS
TdT_Index_09_GATCAG	CAAGCAGAAGACGGCATACGAGATCTGATCGTGACTGGAGTTCAGACGTGTGCTCTTCCGATCT	TraDIS
TdT_Index_10_TAGCTT	CAAGCAGAAGACGGCATACGAGATAAGCTAGTGACTGGAGTTCAGACGTGTGCTCTTCCGATCT	TraDIS
TdT_Index_11_GGCTAC	CAAGCAGAAGACGGCATACGAGATGTAGCCGTGACTGGAGTTCAGACGTGTGCTCTTCCGATCT	TraDIS
TdT_Index_12_CTTGTA	CAAGCAGAAGACGGCATACGAGATTACAAGGTGACTGGAGTTCAGACGTGTGCTCTTCCGATCT	TraDIS
TdT_Index_13_AGTCAA	CAAGCAGAAGACGGCATACGAGATTTGACTGTGACTGGAGTTCAGACGTGTGCTCTTCCGATCT	TraDIS
TdT_Index_14_AGTTCC	CAAGCAGAAGACGGCATACGAGATGGAACTGTGACTGGAGTTCAGACGTGTGCTCTTCCGATCT	TraDIS
TdT_Index_15_ATGTCA	CAAGCAGAAGACGGCATACGAGATTGACATGTGACTGGAGTTCAGACGTGTGCTCTTCCGATCT	TraDIS
TdT_Index_16_CCGTCC	CAAGCAGAAGACGGCATACGAGATGGACGGGTGACTGGAGTTCAGACGTGTGCTCTTCCGATCT	TraDIS
TdT_Index_18_GTCCGC	CAAGCAGAAGACGGCATACGAGATGCGGACGTGACTGGAGTTCAGACGTGTGCTCTTCCGATCT	TraDIS
TdT_Index_19_GTGAAA	CAAGCAGAAGACGGCATACGAGATTTTCACGTGACTGGAGTTCAGACGTGTGCTCTTCCGATCT	TraDIS
TdT_Index_20_GTGGCC	CAAGCAGAAGACGGCATACGAGATGGCCACGTGACTGGAGTTCAGACGTGTGCTCTTCCGATCT	TraDIS
TdT_Index_21_GTTTCG	CAAGCAGAAGACGGCATACGAGATCGAAACGTGACTGGAGTTCAGACGTGTGCTCTTCCGATCT	TraDIS
TdT_Index_22_CGTACG	CAAGCAGAAGACGGCATACGAGATCGTACGGTGACTGGAGTTCAGACGTGTGCTCTTCCGATCT	TraDIS
TdT_Index_23_GAGTGG	CAAGCAGAAGACGGCATACGAGATCCACTCGTGACTGGAGTTCAGACGTGTGCTCTTCCGATCT	TraDIS
TdT_Index_25_ACTGAT	CAAGCAGAAGACGGCATACGAGATATCAGTGTGACTGGAGTTCAGACGTGTGCTCTTCCGATCT	TraDIS
TdT_Index_27_ATTCCT	CAAGCAGAAGACGGCATACGAGATAGGAATGTGACTGGAGTTCAGACGTGTGCTCTTCCGATCT	TraDIS
T22_custom_1stRead_SEQ_Left	CCGAGATCTACACTAGAGAATAGGAACTTCGGAATAGGAACTTCTTAGATGTGTATAAGAG	TraDIS

Chapter 3. *SALMONELLA* TYPHI AVOIDS CELL DEATH AND PRO-INFLAMMATORY POLARIZATION IN HUMAN MACROPHAGES AND HUMANIZED MICE

3.1 ABSTRACT

Salmonella enterica serovar Typhi causes typhoid fever, a prolonged febrile illness that is distinct from the acute enteritis caused by nontyphoidal *Salmonella*. Human host-restriction of *S.* Typhi has limited our understanding of typhoid to murine models using nontyphoidal *S.* Typhimurium. However, these serovars differ in important respects, and the murine model fails to recapitulate important aspects of human typhoid. A key feature of *Salmonella* pathogenesis is survival within phagocytes, and here we show that *S.* Typhimurium and *S.* Typhi have markedly different interactions with human macrophages. In contrast to *S.* Typhi, which persists in human macrophages and induces minimal cytotoxicity, *S.* Typhimurium induces cell death. Macrophage cell death induced by *S.* Typhimurium is dependent on effector proteins secreted by *Salmonella* Pathogenicity Island-2 (SPI2). *S.* Typhi lacks SPI2 effector proteins with pro-apoptotic functions, including those that inhibit the NF-κB pathway. Chemical inhibition of NF-κB is sufficient to cause apoptosis in *Salmonella*-infected but not uninfected macrophages. *S.* Typhi infection also fails to activate STAT1 signaling due to the absence of the effector SarA, leading to a decrease in inflammatory IL-12 production. Finally, humanized mice infected with *S.* Typhi exhibit an impaired T_H1 response in contrast to mice infected with *S.* Typhimurium as measured by human cytokines in the serum. Collectively, these observations suggest that *S.* Typhi avoids causing cell death and inflammatory activation in order to persist within human macrophages, leading to chronic infection.

3.2 INTRODUCTION

Enteric fever caused by *Salmonella enterica* serovars Typhi and Paratyphi A is a life-threatening febrile illness affecting 11-20 million persons each year[2]. Global incidence is difficult to estimate, because the gold standard for diagnosis rquires a positive culture of a clinical sample[6]. Transmission occurs via contaminated food or water, primarily in developing nations with limited access to proper sanitation systems, with the greatest impact on children living in poverty in South Asia[310]. Treatment is complicated by the emergence of multidrug-resistant strains[88]. Current vaccines for typhoid fever offer incomplete protection (50-80% efficacy), are relatively expensive, require boosting, and are not ideal for distribution in endemic areas[90]; moreover, there are no vaccines for paratyphoid fever. The development of improved preventative and therapeutic measures will require a better understanding of typhoid pathogenesis.

Because *S.* Typhi and *S.* Paratyphi A are human host-restricted, much of what is known about *Salmonella* infection comes from studies in mice using the non-typhoidal *Salmonella* (NTS) serovar Typhimurium. Although *S.* Typhimurium infection in immunocompetent individuals causes acute gastroenteritis, infection of susceptible mouse strains can recapitulate some aspects of typhoid fever, such as bacterial dissemination [311]. Murine *Salmonella* models have demonstrated the importance of two pathogenicity island-encoded type-three secretion systems (T3SS) for *Salmonella* infection, known as *Salmonella* Pathogenicity Islands 1 and 2 (SPI1 and SPI2). SPI1 mediates invasion of the intestinal epithelium[312], whereas SPI2 is important for survival within macrophages[64,275]. Both systems secrete effector proteins into the host cell that can interfere with numerous host cell processes including ubiquitination, cytoskeletal function, signal transduction, and cell survival[164,166].

Although a wealth of knowledge has been gleaned from studies with *S.* Typhimurium, the clinical syndromes caused by different *Salmonella* serovars in humans are distinct, and the genetic basis for this distinction is presently unknown. *S.* Typhi differs from *S.* Typhimurium with regard to both gene loss and acquisition. Genomic decay has led to the loss of ~5% of the *S.* Typhi genome, including a substantial number of T3SS-secreted effectors[12,169]. *S.* Typhi also possesses virulence factors not shared with *S.* Typhimurium, such as the Vi capsular polysaccharide and the CdtB cytolethal distending toxin. *S.* Typhimurium has its own unique virulence factors, such as the pSLT virulence plasmid[18]. Therefore, studies using *S.* Typhimurium cannot provide a comprehensive understanding of typhoid pathogenesis.

Both NTS and typhoidal *Salmonella* are internalized by phagocytes, but a hallmark of typhoid infection is prolonged bacterial replication and persistence within host macrophages, allowing systemic dissemination within these cells to multiple sites[313,314]. This is in contrast to the acute and self-limiting infection caused by NTS, which tends to remain within the intestinal tract. Epidemiological evidence suggests that T_H1 cellular immune responses and IFNγ signaling do not play a significant role in susceptibility to or clinical outcomes of enteric fever[81,84], despite their importance for the clearance of NTS infections[78,315]. In this study, we sought to understand the mechanisms underlying the ability of *S.* Typhi to persist and disseminate in contrast to *S.* Typhimurium, focusing on the interactions between *Salmonella* and macrophages, with the hope of understanding how similar pathogens can cause dramatically different infections in human hosts.

3.3 RESULTS

3.3.1 S. *Typhi Persists in Human Macrophages by Promoting Cell Survival*

S. Typhi disseminates from the intestinal tract to systemic sites within host phagocytic cells, mainly macrophages and dendritic cells[131,316,317]. While the murine typhoid model has shown that *S.* Typhimurium is able to persist within murine macrophages, *S.* Typhi is unable to survive within murine cells; the reverse is true in human macrophages – *S.* Typhimurium is unable to survive while *S.* Typhi survives and replicates[117]. We hypothesized that the ability of *S.* Typhi to cause persistent infection in humans is linked to its ability to survive within human macrophages. THP-1-derived macrophages were differentiated with phorbol 12-myristate 13-acetate (PMA) and infected with human serum-opsonized, stationary phase *Salmonella* to limit SPI1 induction[318]. Macrophages were lysed and intracellular *Salmonella* enumerated. After 3 days of infection, intracellular colony-forming units (CFU) of *S.* Typhimurium had decreased significantly, while *S.* Typhi continued to survive and replicate within THP-1 macrophages (**Figure A-1a**); *S.* Typhi survived in THP-1 macrophages up to two weeks (data not shown). Macrophages infected with *S.* Typhi showed significantly less cell death than those infected with *S.* Typhimurium 24 hours post-infection (hpi), as measured by the release of lactate dehydrogenase (LDH). (**Figure A-1b**) *Salmonella* is known to manipulate host cells through the secretion of effector proteins via SPI1 and SPI2 T3SS. Mutants of these two T3SS were generated in *S.* Typhimurium by deleting part of the SPI1 secretion apparatus (*invA*) or the response regulator of a two-component regulatory system that controls expression of SPI2 genes (*ssrB*). Infection of macrophages with mutant *S.* Typhimurium strains showed that macrophage LDH release under these experimental conditions was dependent on SPI2 (Δ*ssrB*) but not on SPI1 (Δ*invA*) (**Figure A-1b**). The lack of cell death caused by the *ssrB* mutant of *S.* Typhimurium correlated with its

ability to replicate in human macrophages (**Figure A-1a**). Taken together, *S.* Typhimurium appears to cause human macrophage cell death via SPI2, whereas *S.* Typhi avoids cell death in human macrophages despite the presence of SPI2.

3.3.2 S. *Typhi Avoids Induction of Apoptosis in Human Macrophages*

As the experimental conditions were selected to minimize SPI1-dependent pyroptosis, we hypothesized that macrophage cell death is due to apoptosis. Using TUNEL staining as a measurement of apoptosis, THP-1 cells infected for 24 h with *S.* Typhimurium revealed ~ 97% TUNEL-positivity. This process was dependent on SPI2, as infection with an isogenic *ssrB* mutant strain exhibited a 60% reduction in TUNEL positivity (**Figure 3-1a**). Macrophages infected with either wild-type or *ssrB* mutant *S.* Typhi also exhibited significantly lower levels of TUNEL positivity (**Figure 3-1a**). To determine whether the TUNEL-positive cells contained bacteria, *Salmonella* expressing the fluorochrome Ypet were used to infect THP-1 macrophages. Although *S.* Typhimurium infected a higher percentage of macrophages than *S.* Typhi, the percent of *S.* Typhimurium-containing cells that were TUNEL positive was also significantly higher compared to *S*. Typhi-containing cells (**Figure 3-1b**). Nearly all of the wild-type *S.* Typhimurium-infected macrophages were TUNEL-positive by 24 hpi, while only 46% and 44% of *ssrB* mutant *S.* Typhimurium- or wild-type *S.* Typhi-infected cells, respectively, were TUNEL-positive (**Figure 3-1b**). Macrophage infection with *S.* Typhimurium rapidly induces DNA fragmentation indicative of apoptosis, dependent on SPI2, whereas *S.* Typhi fails to induce this response in human macrophages.

3.3.3 SPI2-Secreted Effectors Are Absent in S. *Typhi*

The contribution of SPI2 to *Salmonella* pathogenesis has been studied for decades using the nontyphoidal serovar *S.* Typhimurium in the murine model and has been shown to be important for survival within macrophages[64,275]. However, recent studies indicate a different role for SPI2 in *S.* Typhi. Although SPI2 is expressed by *S.* Typhi following macrophage internalization, levels of gene expression are lower than observed in *S.* Typhimurium[17,306]. Interestingly, a large proportion of the SPI2 effector repertoire is absent in *S.* Typhi due to genomic decay, with either inactivating mutations or complete deletions in 20 out of 34 SPI2-secreted effectors that are present in *S.* Typhimurium[169] (**Table 3-1**). To test the effects of individual SPI2-secreted effectors on cell fate, each SPI2 effector absent in *S.* Typhi was individually deleted in *S.* Typhimurium. Individual effector mutants of *S.* Typhimurium were used to infect THP-1 macrophages, and LDH release was assayed 24 hpi. However, no single effector mutant showed a decrease in macrophage LDH release similar to the *ssrB* mutant of *S.* Typhimurium (**Figure 3-2a**).

However, SPI2 effectors have redundant functions, as multiple effectors may interfere with the same host pathway. Examination of the SPI2 effectors that are absent in *S.* Typhi revealed several host pathways that could be redundantly targeted by effectors in *S.* Typhimurium, including caspase activation, the transcription factor NF-κB, and the JAK/STAT signaling pathway. To examine the effect of *Salmonella* infection on these pathways in infected human macrophages, markers were assayed by Western Blot 24 hpi. *S.* Typhimurium infection was found to induce activation of caspase-3, the executioner caspase of apoptosis, and phosphorylation of the signaling molecule STAT1, an important regulator of macrophage activation and cell death[319,320] (**Figure 3-2b**). In contrast, *S.* Typhi infection failed to activate these pathways. The transcription factor NF-κB is involved in numerous host cell processes including promotion of cell survival[321]. *S.*

Typhimurium infection did not induce activation of NF-κB, as measured by phosphorylation of the p65 subunit, whereas *S.* Typhi infection resulted in activation of NF-κB (**Figure 3-2b**). Macrophages infected with an *ssrB* (SPI2) mutant strain of *S.* Typhimurium showed that modulation of these three pathways, all of which are involved in the regulation of apoptotic cell death, is dependent on SPI2 (**Figure 3-2b**). Therefore, while the inability of *S.* Typhimurium to persist in human macrophages is due to SPI2-induced cell death, it is likely that the absence of specific SPI2 effectors in *S.* Typhi allows it to avoid cell death in order to persist within human macrophages.

3.3.4 S. *Paratyphi A Persists in Human Macrophages*

Salmonella enterica Paratyphi A is also human-restricted and causes paratyphoid fever, which can be clinically indistinguishable from typhoid fever. Like *S.* Typhi, *S.* Paratyphi has undergone genomic decay resulting in loss of the same pro-apoptotic SPI2 effectors that are absent from *S.* Typhi (**Table 3-1**). In view of the similar clinical presentations of these two enteric fever serovars, we hypothesized that they might exhibit similar interactions with human macrophages. This was confirmed, as both *S.* Typhi and *S.* Paratyphi A are able to persist within THP-1-derived macrophages for 48 hpi (**Figure 3-3a**). LDH release was reduced in *S.* Paratyphi-infected macrophages at 24 h (**Figure 3-3b**), as was apoptosis, in comparison to *S.* Typhimurium infection (**Figure 3-3c**). We conclude that *S.* Typhi and *S.* Paratyphi A have convergently evolved the ability to persistently infect human macrophages as a result of the loss of pro-apoptotic SPI2 effectors.

3.3.5 The SPI2 Effector SpvB Prevents S. *Typhimurium Persistence in Human Macrophages*

In order to determine specific SPI2 effectors that contribute to macrophage apoptosis during *S.* Typhimurium infection, isogenic *S.* Typhimurium mutant strains lacking individual SPI2 effectors were screened for their ability to activate caspase-3 in infected THP-1 macrophages by Western Blot 24 hpi (selected data shown). The absence of a single *S.* Typhimurium SPI2 effector, SpvB, was sufficient to abrogate caspase-3 cleavage in infected macrophages, similar to an *ssrB* mutant (**Figure A-2a**). The *spv* genes are encoded on the pSLT virulence plasmid in *S.* Typhimurium (and absent in *S.* Typhi), and have been previously been implicated in apoptosis of *S.* Typhimurium-infected macrophages[220,322,323]. The *S.* Typhimurium *spvB* mutant also exhibited greater persistence within THP-1 macrophages as measured by intracellular CFU after 1, 2, or 3 days of infection (**Figure A-2b**). Surprisingly, neither the *spvB* mutant nor an *spvR* mutant lacking the plasmid virulence regulator demonstrated reduced levels of macrophage LDH release at 24 hpi (**Figure A-2c**). This suggests that *S.* Typhimurium promotes macrophage cytotoxicity by both caspase-3-dependent and -independent mechanisms.

3.3.6 The SPI2 Effector SarA is Responsible for Differential Activation of STAT1 in S. *Typhimurium- and* S. *Typhi-infected Macrophages*

The eukaryotic transcription factor STAT1 promotes macrophage polarization, activation of inflammatory responses, and the expression of pro-apoptotic genes encoding TNFα and caspases[320]. Isogenic *S.* Typhimurium mutant strains lacking single SPI2 effectors were screened for their ability to activate STAT1 in infected macrophages, as measured by Wester Blot of phosphorylated STAT1 at 24 hpi. The absence of a single *S.* Typhimurium SPI2 effector, SarA, was sufficient to abrogate STAT1 phosphorylation in infected macrophages, similar to an *ssrB* mutant (**Figure 3-4a**). SarA, also known as SteE, has been shown to interact with STAT proteins,

specifically STAT3[247,248]. Phosphorylation of STAT1 could be restored during infection with a *sarA* mutant *S.* Typhimurium complemented with a *sarA*-expressing plasmid, and the expression of SarA was able to increase levels of phosphorylated STAT1 during *S.* Typhi macrophage infection as well (**Figure 3-4b**). To distinguish whether *S.* Typhi infection prevents phosphorylation of STAT1 or promotes dephosphorylation of activated STAT1, levels of phospho-STAT1 were measured in *S.* Typhi- and *S.* Typhimurium-infected THP1-derived macrophages over time. Early after infection (1 and 6 hpi), phospho-STAT1 levels were similarly increased in both *S.* Typhi- and *S.* Typhimurium-infected cells, while at later timepoints *S.* Typhi-infected cells contained reduced levels of phospho-STAT1 (**Figure A-3a**), suggesting that *S.* Typhi may promote STAT1 dephosphorylation. Furthermore, treatment of uninfected or *Salmonella*-infected cells with exogenous IFNβ induced STAT1 phosphorylation, but *S.* Typhi-infected cells exhibited lower levels of STAT1 phosphorylation in comparison to *S.* Typhimurium-infected cells (**Figure A-3b**). Although the absence of SarA in *S.* Typhi is responsible, at least in part, for lower levels of STAT1 phosphorylation, additional factors may be involved.

3.3.7 S. *Typhi Avoids T_H1 Polarization of Human Macrophages and Humanized Mice*

STAT1 signaling promotes a T_H1 inflammatory immune response, which is required for the clearance of non-typhoidal *Salmonella* infection but does not appear to be important in typhoid fever. To determine whether the ability of *S.* Typhi to avoid activation of STAT1 dampens the inflammatory macrophage phenotype that leads to a T_H1 response, production of IL-12 by infected macrophages was measured. THP-1 macrophages were infected with *S.* Typhi or *S.* Typhimurium as prevously, and supernatants were assayed by ELISA for IL-12 concentrations at 24 hpi . *S.* Typhimurium-infected macrophages produced significantly higher levels of IL-12 than *S.* Typhi-infected macrophages (**Figure A-4a**). However, THP-1-derived macrophages produced only the

p40 subunit of IL-12, whereas physiological activity requires the full p70 heterodimer[78]. Therefore, IL-12p70 was measured in infected PBMC-derived macrophages; similar to THP-1 infection, *S.* Typhimurium induced high levels of IL-12p70 production, while *S.* Typhi-infected cells produced lower levels (**Figure A-4b**).

As *S.* Typhi and *S.* Typhimurium cause different amounts of macrophage cell death (**Figures A-1a, 3-1**), measurement of cytokines in the supernatant might not account for differences in surviving macrophage numbers. Therefore, intracellular cytokine staining was performed to normalize the concentration of IL-12 to viable cell numbers. Infected PBMC-derived macrophages were treated with Brefeldin A 2 h prior to harvest to prevent cytokine release, then macrophages were lifted from the wells and stained for IL-12 with fluorescently-conjugated antibody. *S.* Typhi-infected macrophages produced significantly lower levels of IL-12p70 than *S.* Typhimurium even when equal numbers of macrophages were compared (**Figure 3-4c**). An *S.* Typhimurium *ssrB* mutant induced less IL-12 production, as did a *sarA* mutant strain, implicating STAT1 activation in the elicitation of inflammatory cytokines by *S.* Typhimurium (**Figure 3-4c**).

A humanized mouse model was used to determine whether *S.* Typhimurium and *S.* Typhi infections differ in the induction of inflammatory cytokine production *in vivo*. Hu-SRC-SCID mice are susceptible to *S.* Typhi infection due to the presence of functional human hematopoietic cells[114]. Hu-SRC-SCID mice were infected with wild-type *S.* Typhi, wild-type *S.* Typhimurium, or *ssrB* mutant *S.* Typhimurium by intraperitoneal inoculation and monitored for morbidity, at which point serum was collected for cytokine analysis. *S.* Typhimurium infection of humanized mice resulted in high levels of the inflammatory human cytokines IL-12 and IFNγ, whereas infection with *ssrB* mutant *S.* Typhimurium or *S.* Typhi elicited significantly lower serum levels of these cytokines (**Figure A-4c**). As a T_H1 response is required for the clearance of NTS

infections[82,324], the ability of *S.* Typhi to avoid such a response may help to explain its ability to cause chronic infections.

3.3.8 Chemical Inhibition of NF-κB Causes Apoptosis in Salmonella*-Infected Macrophages*

Nine of the SPI2 effectors that are present in *S.* Typhimurium but absent in *S.* Typhi and *S.* Paratyphi A have been implicated in the inhibition of the NF-κB regulatory complex. NF-κB has myriad effects on gene expression and plays a central role in cell survival through the inhibition of apoptotic factors such as Bcl-2[160]. We screened individual effector mutants of *S.* Typhimurium for their ability to activate NF-κB by p65 Western Blot (**Figure 3-5a**) and a THP-1 Blue reporter cell line (**Figure 3-5b**). THP-1 Blue cells express the SEAP (secreted alkaline phosphatase) enzyme under the control of a promoter activated by NF-κB (Invivogen). None of the mutant *S.* Typhimurium strains lacking single SPI2 effectors phenocopied the lack of NF-κB activation observed in *ssrB* mutant *S.* Typhimurium, suggesting that these effectors have redundant effects on the NF-κB pathway.

To determine the importance of NF-κB activation in determining macrophage cell fate during *Salmonella* infection, *Salmonella*-infected cells were treated with the chemical NF-κB inhibitor BMS345541 (BMS, Cayman Chemical). BMS345541 treatment resulted in dose-dependent inhibition of NF-κB activation in macrophages infected with either wild-type or *ssrB* mutant derivatives of *S.* Typhimurium and *S.* Typhi, as measured in the THP-1 Blue reporter cell line (**Figure 3-6a**). Inhibition of NF-κB correlated with an increase in macrophage cell death measured by LDH release (**Figure 3-6b**). NF-κB p65 phosphorylation was observed in untreated macrophages and in macrophages infected with *ssrB* mutant *S.* Typhimurium, *S.* Typhi or *S.* Paratyphi A, but not in macrophages infected with *S.* Typhimurium (**Figure 3-6c,** top panel).

Treatment with BMS345541 inhibited p65 phosphorylation in all infected macrophages, even at low doses (**Figure 3-6c**). To measure the effect of NF-κB inhibition on apoptosis, infected macrophages were treated with BMS345541 and stained with the TUNEL (terminal deoxynucleotidyl transferase dUTP nick end labeling) assay for the detection of apoptotic cells. Low doses of BMS were sufficient to induce apoptosis of all *Salmonella*-infected cells (**Figure 3-6d**), whereas high doses were required to induce apoptosis of uninfected cells (**Figure 3-6d**). The ability of a chemical NF-κB inhibitor to induce apoptosis of *S.* Typhi-infected macrophages might be exploited for the treatment of chronic infections with intracellular bacteria that rely on NF-κB signaling to persist in macrophages.

3.4 DISCUSSION

Nontyphoidal *Salmonella* serovars such as *S.* Typhimurium and the enteric fever serovars *S.* Typhi and *S.* Paratyphi A exhibit fundamentally different interactions with the human immune system. *Salmonella* disseminates from the intestine within host mononuclear cells, and survival within this niche is central for understanding *Salmonella* pathogenesis. Here we show that *S.* Typhi survives within human macrophages through the sustained expression of cell survival pathways regulated by NF-κB, while in contrast *S.* Typhimurium rapidly induces the apoptosis of host macrophages and promotes the initiation of T_H1 T cell immune response. This fundamental difference underlies the striking clinical differences between enteric fever and *Salmonella* enteritis and accounts for the differences in their epidemiology.

Macrophage cytotoxicity during *S.* Typhimurium infection is dependent on as many as twelve effector proteins secreted by the SPI2 type 3 secretion system, which stimulate apoptosis and inhibit NF-κB-dependent cell survival pathways. The enteric fever serovars *S.* Typhi and *S.*

Paratyphi A lack these effectors, allowing them to persist within macrophages and avoid induction of an inflammatory response, leading to chronic infection. Chemical or genetic inhibition of NF-κB is sufficient to induce apoptosis of *S.* Typhi-infected macrophages and may provide a novel approach to eliminate a key reservoir for intracellular pathogens including not only *Salmonella,* but *Mycobacterium tuberculosis* and *Legionella pneumophila* as well[325–327].

Until recently, understanding the pathogenesis of typhoid fever has relied on models that compare the interactions of nontyphoidal *S.* Typhimurium with murine immune cells. Although important aspects of *Salmonella* infection have been gleaned from these models, typhoidal serovars differ from NTS in important ways. The contrasting interactions of *S.* Typhimurium and *S.* Typhi with human macrophages are likely to underlie the differences in the clinical features of *Salmonella* enteritis and typhoid fever. Systemic dissemination, a prolonged incubation period, sustained and relapsing infections, and chronic carriage depend on the ability of *S.* Typhi to survive within macrophages while avoiding an inflammatory immune response that could lead to clearance[7,52]. Studies of *S.* Typhimurium in conventional laboratory mice are unable to recapitulate the crucial features of persistence and the absence of protective T_H1 immune responses that are hallmarks of typhoid pathogenesis. However, recent evidence suggests that there are important differences in the contribution of SPI2 and its effectors to the virulence of NTS and enteric fever *Salmonella* serovars.

Early studies determined that the SPI2 virulence genes play an important role in *Salmonella*-macrophage interactions and systemic infection in mice[63,274,275,328]. However, recent evidence suggests that there are important differences in the contribution of SPI2 and its effectors to the virulence of NTS and enteric fever *Salmonella* serovars. In contrast to *S.* Typhimurium[274], SPI2 was not counter-selected in a transposon-mutant screen of *S.* Typhi genetic loci required for

virulence in humanized mice, and was found to be expressed at much lower levels than in *S.* Typhimurium following macrophage internalization[306]. SPI2 is not required for persistent infection of human macrophages with *S.* Typhi[17] (**Figure A-1a**).

Although some secreted SPI2 effectors are conserved in NTS and enteric fever serovars, *S.* Typhi has evolved a distinctive strategy of intracellular persistence that is linked to the loss of effectors associated with macrophage cytotoxicity. The SPI2 effectors implicated in macrophage cytotoxicity include both factors that elicit apoptosis, such as SpvB[329], and those that inhibit the NF-κB pathway, which plays a critical role in the regulation of cell survival[330]. Nine different SPI2 effectors of *S.* Typhimurium have been implicated in the inhibition of NF-κB, which attests to its central importance but also makes the assignment of specific roles to individual effects challenging.

The involvement of NF-κB in both cell survival and host defense creates an additional challenge. Engagement of TLRs by microbial ligands leads to activation of the NF-κB signaling cascade, generating a pro-inflammatory response that can promote pathogen clearance. However, some pathogens can exploit NF-κB-dependent pathways to promote their replication in the host[331]. Here we show that *S.* Typhi requires NF-κB activation in order to avoid the apoptosis of *S.* Typhi-infected cells. This may prove to be a useful therapeutic target, as chemical inhibition of NF-κB results in the selective killing of *S.* Typhi-infected macrophages and the elimination of persistent intracellular bacteria. Other intracellular pathogens, such as *Mycobacterium tuberculosis* and *Legionella pneumophila*, have also been shown to promote NF-κB activation during infection infection[326,332]. The minimal effect of NF-κB inhibition in uninfected cells suggests that NF-κB inhibitors might be useful for the eradication of bacterial reservoirs during persistent infections. Future studies can utilize models of chronic *Salmonella* infection such as 129svJ Nramp$^{+/+}$ mice[96]

to determine whether treatment with chemical NF-κB inhibitors can promote the clearance of persistent *Salmonella* infections.

The ability of *S.* Typhi to persist in the host is also facilitated by a deficient pro-inflammatory immune response, in contrast to NTS infection. Host determinants of immunity to *S.* Typhi and *S.* Typhimurium are fundamentally different, particularly with regard to T_H1 cellular responses. Individuals with inherited or acquired defects in T_H1 immunity, such as those with IFNγ/IL12B/IFNγR1 polymorphisms or HIV/AIDS, are more susceptible to nontyphoidal *Salmonella* infections, but not to typhoid fever[81–83]. The transcription factor STAT1 regulates inflammatory gene activation in response to IFNγ secreted by differentiated T or NK cells, or IFNβ secreted by macrophages following TLR4 stimulation[333]. Here we show that STAT1 is differentially activated in macrophages infected with *S.* Typhimurium or *S.* Typhi. IL-12 production by macrophages and humanized mice, which is regulated by STAT1[334], is also specifically impaired by *S.* Typhi infection. The differences in SPI2-dependent macrophage polarization induced by *S.* Typhimurium and *S.* Typhi can now be understood to be a consequence of differences in their complements of SPI2 effectors, in particular SarA (SteE)[247], which explains why acquired or inherited deficiencies in the IFNγ signaling axis result in opportunistic NTS infections, but not enteric fever[84,335].

Although the murine typhoid model has been an invaluable resource for understanding *Salmonella* infections, the observations presented here demonstrate the importance of studying pathogens in their native hosts . Genetic differences between *S.* Typhi and *S.* Typhimurium account for important differences in their pathogenesis, but even factors that are present in both *S.* Typhimurium and *S.* Typhi may play different roles in these two serovars, as shown by their different reliance on SPI2. Our observations reveal a fundamental divergence between

nontyphoidal *Salmonella*, which induce macrophage apoptosis and exploit the host intestinal inflammatory response, and enteric fever *Salmonella* serovars, which avoid the induction of T_H1 immunity and persist in the intracellular compartment. This represents an important insight into the pathogenesis of human typhoid and identifies a new avenue for therapeutic approaches to treat chronic bacterial infections.

3.5 MATERIALS AND METHODS

3.5.1 Bacterial Growth Conditions and Strain Constructions

Bacterial strains and plasmids used in this study are listed in **Table 3-2**. *S. enterica* cultures were grown in Miller's Luria Broth (LB) medium at 37°C with shaking at 250 rpm. Medium was supplemented with "aromix" (40 μg ml^{-1} L-phenylalanine, 40 μg ml^{-1} L-tryptophan, 10 μg ml^{-1} 2,3-dihydroxybenzoic acid, 10 μg ml^{-1} p-amino benzoic acid), ampicillin (100 μg ml^{-1}), or kanamycin (50 μg ml^{-1}), as indicated.

Primers were purchased from Integrated DNA Technologies (IDT, Skokie, IL) and are listed in **Table 3-3**. Mutant alleles of *S. enterica* serovars were constructed using λ-Red recombination as described[300,301]. To construct the SarA complementation plasmid, the *sarA* gene and promoter region were amplified using primers listed in **Table 3-3** and ligated into pJK392 digested with KpnI and HindIII. pJK392 contains a pBR322 origin of replication and a β-lactamase gene for antibiotic selection. All PCR products were generated with gDNA from *S.* Typhimurium 14028s or *S.* Typhi Ty2. All mutant strains and plasmid constructs were confirmed by DNA sequencing (Genewiz, South Plainfield, NJ).

Transduction was performed with transducing phage P22. One-hundred μl of stationary phase culture of the recipient strain were mixed with 100 μl of P22 lysate. After 1 h of incubation

at 37°C, transductants were selected on LB agar plates with antibiotic selection for the appropriate selectable marker. Colonies were streaked on indicator Green Plates, and P22-free colonies were selected for further experiments.

3.5.2 THP-1 Macrophage Cell Culture and Infection

Human THP-1 monocytes were obtained from ATCC and cultured in RPMI 1640 medium (Corning Inc.) supplemented with 10% heat-inactivated fetal bovine serum (Millipore-Sigma), sodium pyruvate (Corning Inc.), non-essential amino acids (Gibco), 50 U ml^{-1} penicillin and 50 μg ml^{-1} streptomycin (Corning Inc.) at 37°C in 5% CO_2.

Human THP-1-derived macrophages were infected as described previously[306]. Briefly, THP-1 monocytes were seeded at 10^5 per well in 96-well plates or $5x10^6$ in 24-well plates and differentiated with 100 nM phorbol 12-myristate 13-acetate (PMA, Millipore-Sigma) for 48 h; the medium was changed to PMA-minus and antibiotic-free RPMI 24 h prior to infection. *Salmonella* strains were grown in LB broth for 18 h with shaking at 37°C, then adjusted to OD_{600}=1.0 and washed twice with sterile PBS. *Salmonella* were mixed with equal parts human pooled serum (MP Biomedicals LLC) and incubated at 37°C for 20 min to opsonize the bacteria. Opsonized bacteria were used to infect THP-1 human macrophage-like cells at a MOI of 10:1. Infected monolayers were centrifuged for 5 min at 1000 rpm to synchronize infection, then incubated at 37°C for 1 h to promote internalization. Following internalization, monolayers were washed with RPMI supplemented with 20 μg ml^{-1} gentamicin to kill extracellular bacteria.

For infections treated with the NF-κB inhibitor BMS345541 (Cayman Chemical), culture medium was changed to medium containing the desired concentration of the inhibitor 1 h prior to the application of *Salmonella* and maintained throughout the remainder of the infection.

3.5.3 Salmonella *Intramacrophage Quantification*

For *Salmonella* intramacrophage survival studies, infected macrophages were lysed in 1% Triton X-100 at the designated time point post-infection. Lysates were serially diluted and plated on LB plates to determine the number of intracellular CFU. Percent intramacrophage *Salmonella* survival was determined as the number of CFU at the given timepoint divided by the number of CFU at 1 hpi.

3.5.4 Macrophage Cytotoxicity Assay

For quantification of macrophage cell death, the concentration of lactate dehydrogenase (LDH) in the supernatants was measured using the CytoTox96 Cytotoxicity Kit (Promega) per the manufacturer's instructions. Percent cytotoxicity was calculated as ((experimental release - spontaneous release) / (maximum release - spontaneous release))*100.

3.5.5 Western Blots

Infected macrophages were lysed in 1X RIPA buffer (Cell Signaling Technology) with added 1X protease and phosphatase inhibitors (Cell Signaling Technology) at the designated time point. Total protein was quantified using the BCA Protein assay kit (Pierce). Fifty µg total protein were combined with SDS loading dye and heated at 95C for 5 min before proteins were separated on a 4-15% SDS polyacrylamide gel (Bio-Rad). Proteins were wet-transferred to an Immobilon-P Polyvinylidene fluoride (PVDF) membrane (Millipore-Sigma), then blocked for 1 h with 5% bovine serum albumin (BSA, Research Products International). Primary antibody incubations were done at 1:1000 in BSA overnight at 4°C. Membranes were washed three times in 1X Tris-buffered saline with 0.05% Tween (TBST), then incubated with secondary HRP-conjugated antibody for 1 h at room temperature in 5% milk. After three more washes, chemiluminescent substrate was

applied (ECL western blotting substrate, Thermo Scientific) and the membranes were exposed to CL-X Posure film (Thermo Scientific). Film was developed using an AFP Imageworks MM90.

3.5.6 TUNEL Staining

Adherent infected macrophages were removed from infection wells by adding ice-cold PBS with 0.5 M EDTA for 5 min, then pipetting to loosen macrophages. Cells were fixed using IC Fixation buffer (Invitrogen) for 20 min at room temperature. After washing, macrophages were permeabilized in 70% ethanol and kept at 20°C until TUNEL staining. TUNEL staining was performed per the manufacturer's protocol (Phoenix Biosystems). Stained cells were analyzed on an LSRII cytometer (Becton Dickinson). Data were acquired with DIVA software (BD Biosciences) and analyzed using FlowJo software (TreeStar).

3.5.7 Measurement of NF-κB Activity

THP-1 cells transfected with an NF-κB reporter system (THP-1 Blue) were obtained from Invivogen (San Diego, CA) and were cultured as above in RPMI 1640 with 10% heat-inactivated FBS, sodium pyruvate (Corning Inc.), non-essential amino acids (Gibco), 50 U ml^{-1} penicillin, 50 μg ml^{-1} streptomycin, and 100 μg ml^{-1} normocin at 37°C in 5% CO_2; cells were cultured with added 10 μg ml^{-1} blasticidin every other passage. THP-1 Blue cells were infected as above. Upon NF-κB activation, secreted embryonic alkaline phosphatase (SEAP) is expressed and measured in cell supernatants by the addition of Quanti-Blue (Invivogen) per the manufacturer's instructions. The assay is read spectrophotometrically on an OptiMax Tunable Microplate reader (Molecular Devices, Sunnyvale, CA) at OD_{622}.

3.5.8 PBMC-Derived Macrophage Cell Harvest

Leukocyte reduction filters (Bloodworks NW, Seattle, WA) were backflushed with 100 mL sterile PBS with 5 mM EDTA. Eluate was overlaid on Ficoll-Paque PLUS (GE Healthcare) and centrifuged at 25°C for 35 m at 2000 rpm (brake off). Following gradient separation, the monocyte-containing layer was removed and washed twice in sterile PBS. Cells were filtered using a sterile 70 μM nylon mesh cell strainer (Fisherbrand) and suspended in RPMI 1640 with 10% human AB serum (Corning Inc.), sodium pyruvate (Corning Inc.), non-essential amino acids (Gibco), 50 U mL^{-1} penicillin, 50 μg mL^{-1} streptomycin, and 10 ng mL^{-1} GM-CSF (PeproTech). Cells were incubated in untreated tissue culture flasks for 48 h; adherent cells were then scraped and seeded into tissue culture wells and allowed to adhere for 5 d. Medium was exchanged for GM-CSF-free, antibiotic-free medium 24 h prior to infection; PBMC-derived macrophages were infected as with THP-1-macrophages above.

3.5.9 Intracellular Cytokine Staining

Infected PBMC-derived macrophages were treated with Brefeldin A (Thermo Scientific) to a final concentration of 3.0 μg mL^{-1} in infection wells for 2 h prior to fixation and staining. Cells were washed once with PBS and scraped into ice-cold PBS with 0.5M EDTA in round-bottom polypropylene tubes. Cells were washed once by centrifugation at 600 x g for 5 min at 25°C and resuspended at approximately $1x10^6$ cells mL^{-1} in PBS. Cells were stained with fixable viability dye (Thermo Scientific) at 1:1000 for 30 min on ice, then washed with Flow Cytometry Staining Buffer (Thermo Scientific). Fc receptor binding inhibitor was added for 20 min on ice, then surface antigens were stained for 30 min on ice in the dark (see **Table 3-2** for list of antibodies). Cells were washed with Flow Cytometry Staining Buffer followed by fixation with IC Fixation Buffer

(Thermo Scientific) for 20 min at room temperature. Cells were washed twice with Permeabilization Buffer (Thermo Scientific) and stained for intracellular hIL-12p70 for 30 min at room temperature in the dark. After washing, cells were resuspended in Flow Cytometry Staining Buffer and analyzed on a LSRII cytometer (Becton Dickinson). Data were acquired with DIVA software (BD Biosciences) and analyzed using FlowJo software (TreeStar).

3.5.10 Humanized Mouse Infections

Mouse experiments in this study were approved by the University of Washington Institutional Animal Care and Use Committee (IACUC) and performed as described in protocol 3373-01. NOD-*Prkdc*^{scid}*IL2rg*^{tm1Wjl} (NSG) mice were purchased from The Jackson Laboratory (Bar Harbor, ME) and engrafted with human CD34+ hematopoietic stem cells derived from umbilical cord blood[121,304]. Umbilical cord blood was obtained from donors that were consented under an approved IRB protocol at the UMass Memorial Medical Center, Department of General Obstetrics and Gynecology (Worcester, MA), and all samples used for engraftment were de-identified. Mice were maintained under ABSL-2 containment at the University of Washington Animal Care and Research Facility on a 14-h light cycle and housed up to 5 animals per cage in Allentown cages with micro-isolator tops. Mice were checked daily during infection studies, and veterinary care was provided 7 days a week.

Hu-SRC-SCID mice were infected with a total of ~6 x 10^4 CFU of wild-type *S.* Typhi, ~1 x 10^3 CFU of wild-type *S.* Typhimurium, or ~1 x 10^3 CFU of *S.* Typhimurium Δ*ssrB*. Infection inocula were chosen to obtain similar infection lengths between strains. The infected mice were closely monitored for signs of illness and sacrificed when moribund or 7 d post-infection, whichever came first. Intracardiac blood was harvested and centrifuged in serum separator tubes (BD Biosciences) for 5 min at 15000 rpm before storage at -80°C. Serum cytokines were measured

using a multiplex bead array assayed by Luminex 200. Livers and spleens were aseptically harvested and homogenized in PBS using a Power Gen 125 tissue homogenizer (Fisher Scientific), then serially diluted and plated on LB agar + "aromix" for CFU counts.

3.5.11 Statistical Analysis

Statistical method and sample size for experiments are indicated in the corresponding figure legends. Statistical analysis of macrophage and mouse infections was performed using Prism v. 8.1.2 software (GraphPad). A paired two-tailed Student's t-test was performed on the means of parametric data, and a Kruskal-Wallis test was performed on the means of non-parametric data. Statistical significance was defined as $p < 0.05$. Error bars on figures show standard deviation.

3.6 ACKNOWLEDGMENTS, AUTHOR CONTRIBUTIONS, AND CONFLICTS OF INTEREST

3.6.1 Acknowledgments

Thank you to Dan Vyshnevskyi, Davin Hoover, James Januik, Tessa Warheit-Niemi, Helen Warheit-Niemi and Alexandria McCarthy for their dedicated laboratory assistance; Dr. Thea Brabb of UW Comparative Medicine for help with animal work; Donna Prunkard and Xiaoping Wu of the UW Pathology Flow Core for assistance running flow cytometry; Nutthakarn Suwankitwat, Dr. Kevin Labadie, Alyse Douglas, and Dr. Nichole Lieberman for their advice on cell staining and flow cytometry; and Dr. Dirk Bumann of Biozentrum at the University of Basel for providing the Ypet fluorescent constructs. This work was supported by NIH grants AI112640 (F.C.F.), AI132963 (M.A.B. and L.D.S.), OD018259 (L.D.S.), and CA034196 (L.D.S.).

2.6.2 Author Contributions

T.A.S., Larissa A. Singletary, and Ferric C. Fang designed the study (for L.A.S. contribution, see Appendix); T.A.S., L.A.S., Stephen J. Libby and Joyce E. Karlinsey performed the experiments; Michael A. Brehm, Dale L. Greiner, Leonard D. Shultz, Sarah L. Jaslow, and Dennis C. Ko contributed reagents; T.A.S., L.A.S., S.J.L., J.E.K., Fermin E. Guerra, and F.C.F. analyzed the data; T.A.S. and F.C.F. wrote the manuscript.

2.6.3 Conflicts of Interest

The authors declare no competing interests.

3.7 FIGURES

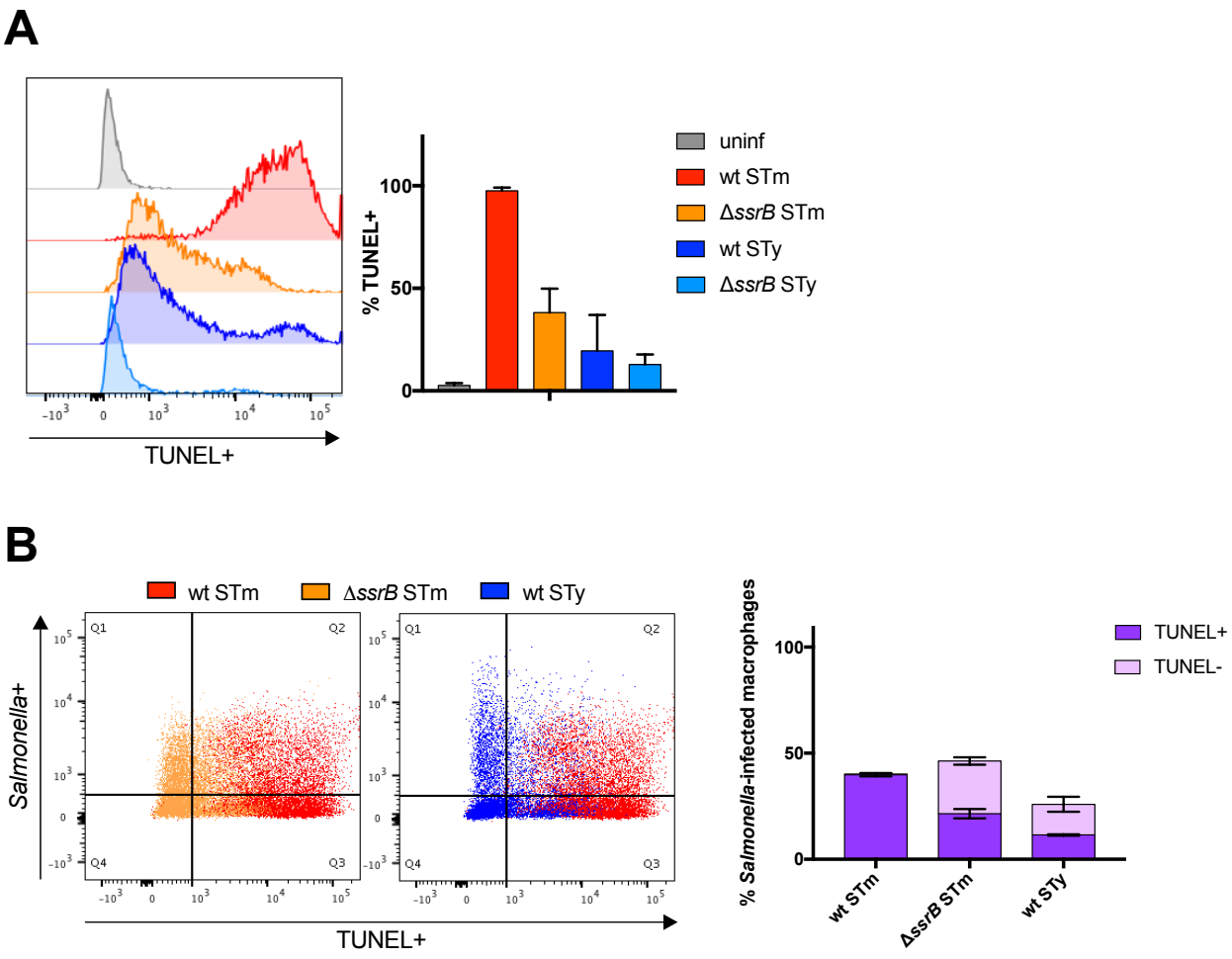

Figure 3-1. SPI2-dependent Apoptosis in *Salmonella*-infected Human Macrophages.

THP-1 cells were differentiated with PMA and infected with opsonized stationary-phase *Salmonella* at an MOI of 10:1. *S.* Typhimurium 14028s = STm, *S.* Typhi Ty2 = STy. (**A**) Infected macrophages were harvested 24 hpi and stained for TUNEL as a measure of apoptosis. The left panel shows representative histograms with TUNEL positivity on the x-axis; the right panel summarizes the means of three biological replicates. (**B**) *Salmonella* expressing the fluorochrome Ypet were used to infect macrophages and determine the population of infected cells during TUNEL analysis. Left panels show representative scatter plots with TUNEL positivity on the x-

axis and *Salmonella* positivity on the y-axis; the right panel summarizes the means of three biological replicates. Error bars represent standard deviation.

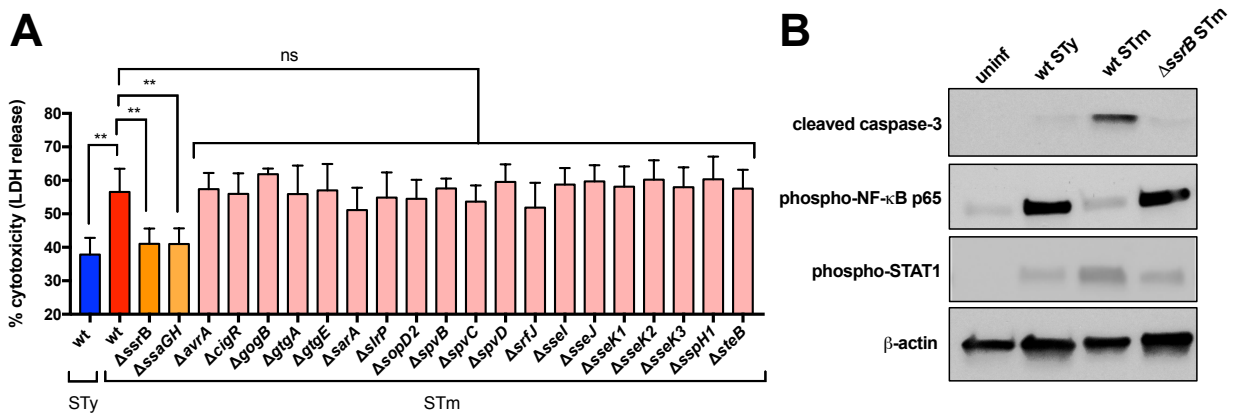

Figure 3-2. SPI2-dependent Cytotoxicity in *Salmonella*-infected Human Macrophages.

THP-1 cells were differentiated with PMA and infected with opsonized stationary-phase *Salmonella* at an MOI of 10:1. *S.* Typhimurium 14028s = STm, *S.* Typhi Ty2 = STy. (**A**) Macrophage cytotoxicity was measured as the amount of LDH released in supernatants 24 hpi with indicated strains. Shown are the means of two biological replicates, with error bars representing the standard deviation. Statistical significance (p) was determined by paired two-tailed Student's t test, ** $P < 0.01$. (**B**) Fifty µg of total protein from THP-1 cells infected with *Salmonella* for 24 h were subjected to Western blot analysis for cleaved caspase-3, phosphorylated STAT1, and activated NF-κB p65. Measurement of β-actin was included as a loading control.

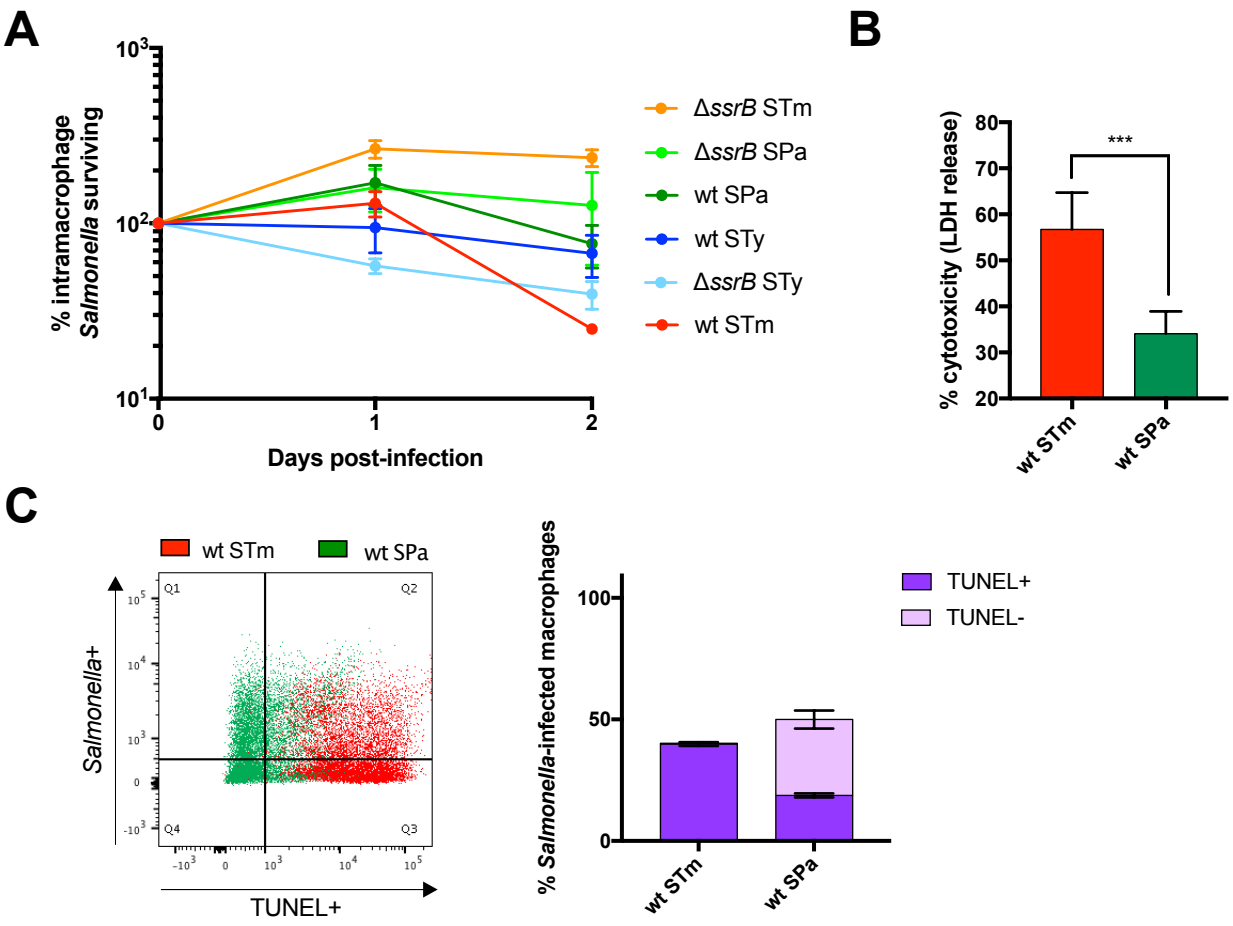

Figure 3-3. SPI2-dependent Apoptosis of *S.* Paratyphi A-infected Human Macrophages.

THP-1 cells were differentiated with PMA and infected with opsonized stationary-phase *Salmonella* at an MOI of 10:1. *S.* Typhimurium 14028s = STm, *S.* Typhi Ty2 = STy, *S.* Paratyphi A ATCC9150 = SPa. (**A**) Macrophages were lysed at indicated time post-infection and intracellular CFU enumerated. Survival is expressed as the proportion of intracellular *Salmonella* remaining compared to internalized bacteria 1 hpi. The means of three biological replicates are shown. (**B**) Macrophage cytotoxicity was measured as the amount of LDH released in supernatants 24 hpi with indicated strains. Shown are the means of two biological replicates, with error bars representing the standard deviation. Statistical significance (p) was determined by paired two-tailed Student's t test, *** $P < 0.001$. (**C**) *Salmonella* expressing the fluorochrome Ypet were used

to infect macrophages and determine the population of cells that were infected during TUNEL analysis. TUNEL positivity is shown on the x-axis and *Salmonella* positivity on the y-axis; the right panel summarizes the means of three biological replicates. Error bars represent standard deviation.

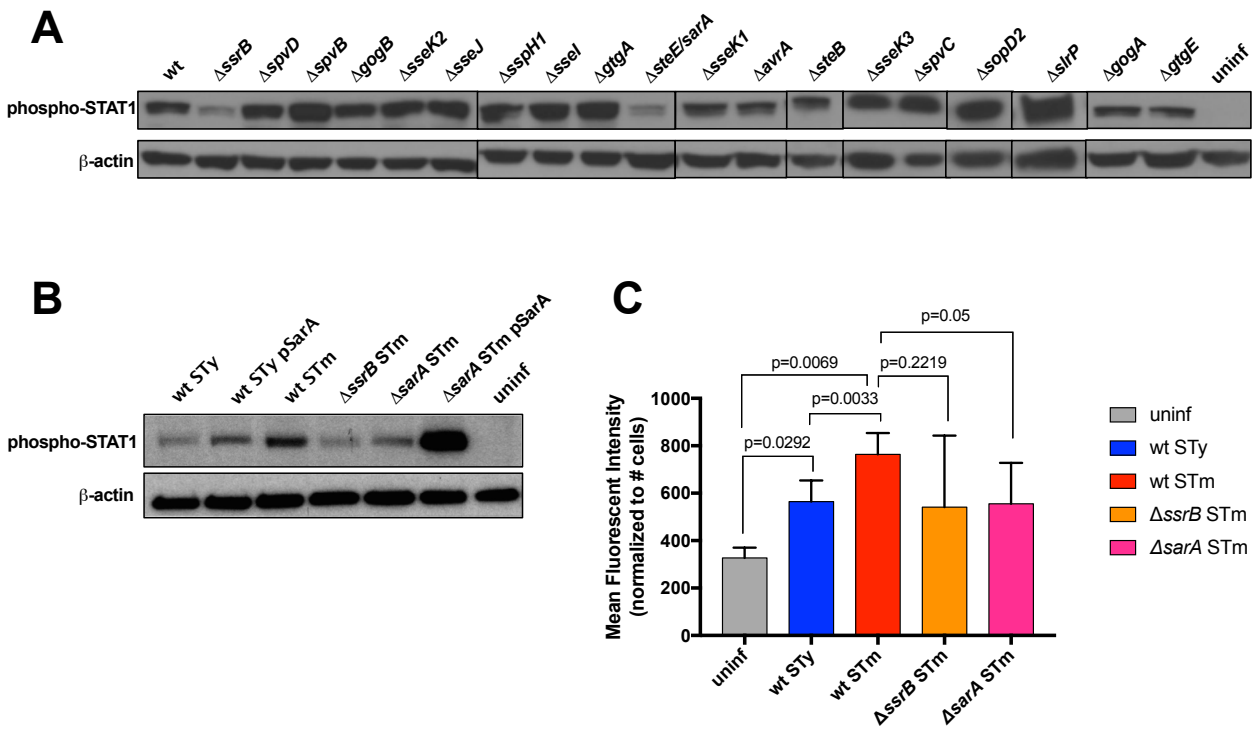

Figure 3-4. SPI2-dependent STAT1 Activation in *Salmonella*-infected Human Macrophages.

THP-1- or PBMC-derived macrophages were infected with opsonized stationary-phase *Salmonella* at an MOI of 10:1. *S.* Typhimurium 14028s = STm, *S.* Typhi Ty2 = STy. (**A** and **B**) Fifty µg of total protein from THP-1 cells infected with *Salmonella* for 24 h were subjected to Western blot analysis for phosphorylated STAT1. Measurement of β-actin was included as a loading control. (**C**) Infected PBMC-derived macrophages were treated with Brefeldin A and stained for intracellular retention of IL-12p70 after 24 h of infection. The means of three biological replicates are shown, with error bars representing standard deviation. Statistical significance (p) was determined by paired two-tailed Student's t test.

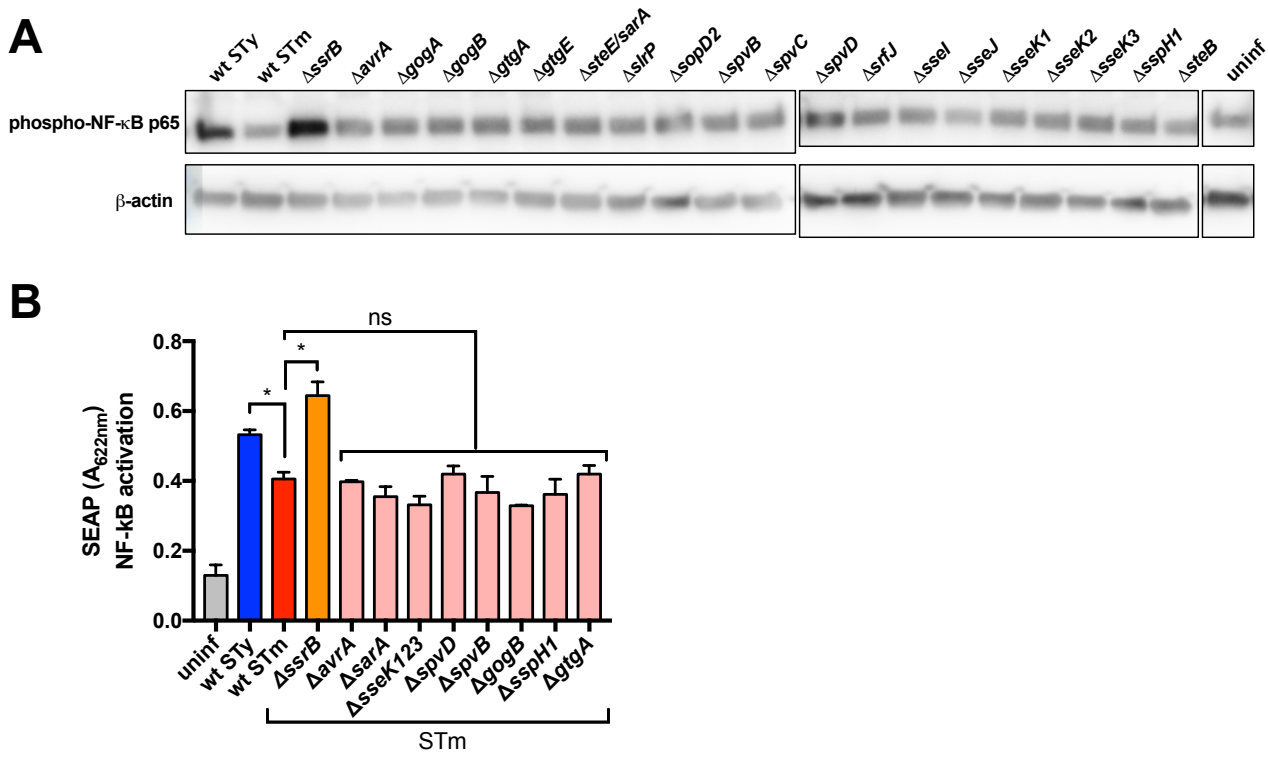

Figure 3-5. SPI2-dependent NF-κB Inhibition in Human Macrophages.

THP-1 cells were differentiated with PMA and infected with opsonized stationary-phase *Salmonella* at an MOI of 10:1. *S.* Typhimurium 14028s = STm, *S.* Typhi Ty2 = STy. (**A**) Fifty µg of total protein from THP-1 cells infected with *Salmonella* for 24 h were subjected to Western blot analysis for activated NF-κB p65. Measurement of β-actin was included as a loading control. (**B**) THP-1 NF-κB Blue reporter cells were infected with *Salmonella* and NF-κB activation was measured 24 hpi using the colorimetric Quanti-Blue assay. Shown are the means of three biological replicates, with error bars representing standard deviation, and statistical significance (p) was determined by paired two-tailed Student's t test, * $P < 0.05$.

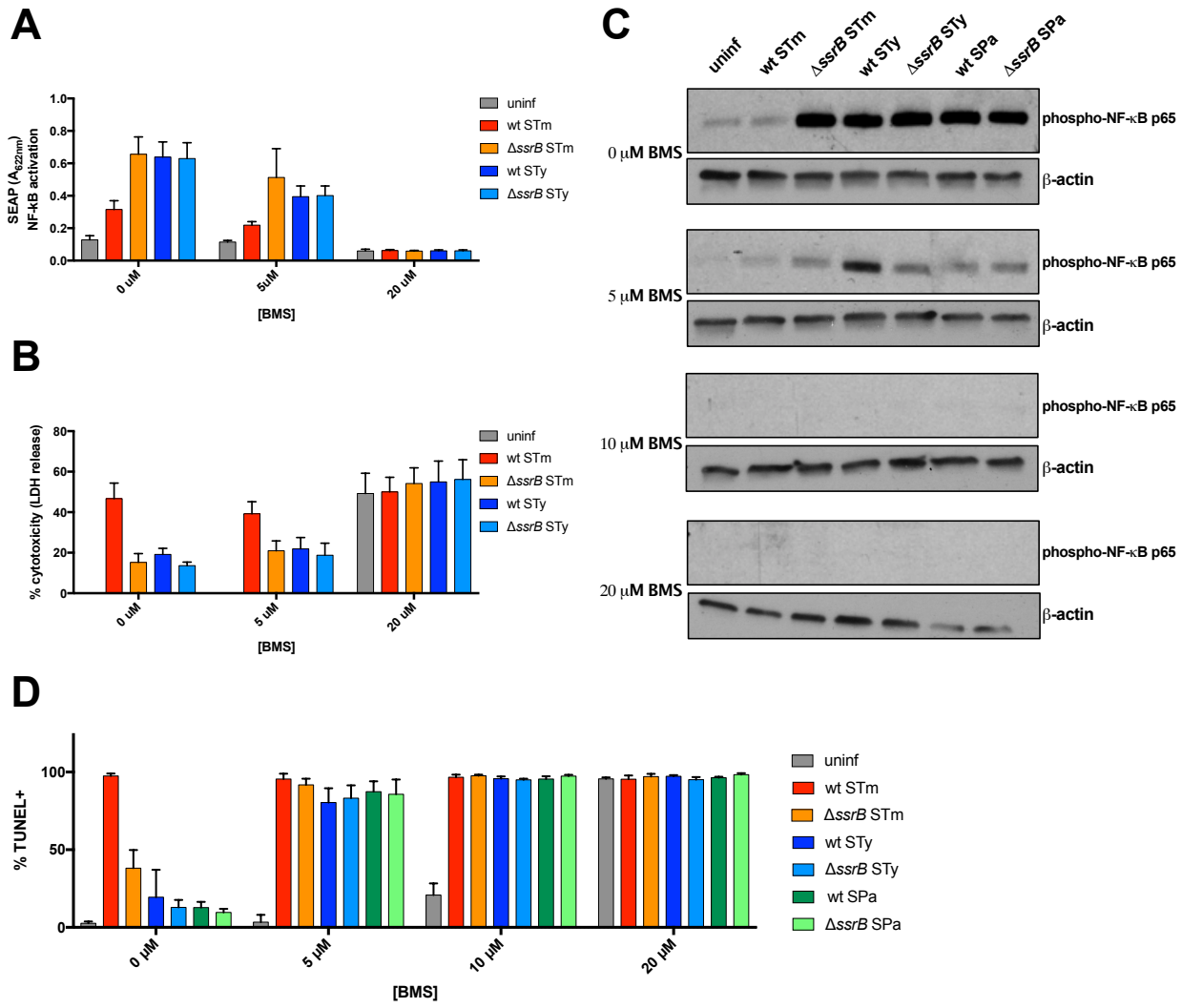

Figure 3-6. NF-κB Inhibition During *Salmonella* Infection Results in Human Macrophage Apoptosis.

Macrophages were treated with the indicated concentration of the NF-κB inhibitor BMS345541 1 h prior to infection and treatment was maintained throughout the infection. *S.* Typhimurium 14028s = STm, *S.* Typhi Ty2 = STy, *S.* Paratyphi A ATCC9150 = SPa. (**A**) THP-1 NF-κB Blue reporter cells were infected with *Salmonella* and NF-κB activation was measured 24 hpi using the colorimetric Quanti-Blue assay. (**B**) Macrophage cytotoxicity was measured as the amount of LDH released in supernatants 24 hpi with the indicated strains. (**C**) Fifty μg of total protein from THP-

1 cells infected with *Salmonella* for 24 h were subjected to Western blot analysis for activated NF-κB p65. (**D**) Macrophages were stained for TUNEL 24 h after *Salmonella* infection. All bar graphs represent the means of three biological replicates, with error bars representing standard deviation.

3.8 TABLES

Table 3-1. SPI2 Effector Repertoire of *S.* Typhimurium, *S.* Typhi, and *S.* Paratyphi A.

Absent in *S.* Typhi and *S.* Paratyphi A	Absent in *S.* Typhi	Absent in *S.* Paratyphi A

S. Typhimurium SPI2-Secreted Effector	*S.* Typhi	*S.* Paratyphi A
AvrA	absent	absent
CigR	pseudogene	+
GogA	absent	absent
GogB	absent	absent
GtgA	absent	absent
GtgE	absent	absent
PipA	+	+
PipB	+	+
PipB2	+	+
SifA	+	+
SifB	+	pseudogene
SlrP	pseudogene	pseudogene
SopD2	pseudogene	pseudogene
SpiC / SsaB	+	+
SptP / StpA	+	+
SpvB	absent	absent
SpvC	absent	absent
SpvD	absent	absent
SrfJ	absent	unknown
SseF	+	+
SseG	+	+
SseI / SrfH	absent	absent
SseJ	pseudogene	absent
SseK1	absent	absent
SseK2	absent	absent
SseK3	absent	absent
SseL	+	+
SspH1	absent	absent
SspH2	+	absent
SteA	+	+
SteB	absent	absent
SteC	+	pseudogene
SteD	+	+
SteE / SarA	absent	absent

Table 3-2. Strains, Plasmids, and Resources.

Bacterial Strains		
Salmonella enterica serovar Typhimurium 14028s wild-type	S. Miller	JK1324, LAS5, TAS8
S. Typhimurium 14028S Δ*invA::FRTaphFRT*	[41]	JK1217
S. Typhimurium 14028S Δ*ssrB::FRTaphFRT*	This study	LAS18, TAS9
S. Typhimurium 14028S Δ*ssaGH::FRTaphFRT*	This study	TAS210
S. Typhimurium 14028S Δ*avrA::FRTaphFRT*	This study	TAS12
S. Typhimurium 14028S Δ*cigR::FRTaphFRT*	This study	TAS20
S. Typhimurium 14028S Δ*gogB::FRTaphFRT*	This study	LAS86
S. Typhimurium 14028S Δ*gtgA::FRTaphFRT*	This study	LAS91
S. Typhimurium 14028S Δ*gtgE::FRTaphFRT*	This study	TAS22
S. Typhimurium 14028S Δ*sarA::FRTaphFRT*	This study	TAS199
S. Typhimurium 14028S Δ*slrP::FRTaphFRT*	This study	LAS82
S. Typhimurium 14028S Δ*sopD2::FRTaphFRT*	This study	LAS83
S. Typhimurium 14028S Δ*spvB::FRTaphFRT*	This study	LAS85
S. Typhimurium 14028S Δ*spvC::FRTaphFRT*	This study	LAS81
S. Typhimurium 14028S Δ*spvD::FRTaphFRT*	This study	LAS84
S. Typhimurium 14028S Δ*spvR::FRTaphFRT*	This study	LAS16
S. Typhimurium 14028S Δ*srfJ::FRTaphFRT*	This study	LAS211
S. Typhimurium 14028S Δ*sseI::FRTaphFRT*	This study	LAS90
S. Typhimurium 14028S Δ*sseJ::FRTaphFRT*	This study	LAS88
S. Typhimurium 14028S Δ*sseK1::FRTaphFRT*	This study	TAS10
S. Typhimurium 14028S Δ*sseK2::FRTaphFRT*	This study	LAS87
S. Typhimurium 14028S Δ*sseK3::FRTaphFRT*	This study	LAS80
S. Typhimurium 14028S Δ*sspH1::FRTaphFRT*	This study	LAS89
S. Typhimurium 14028S Δ*steB::FRTaphFRT*	This study	TAS18
S. Typhimurium 14028S Δ*sseK1::FRT* Δ*sseK2::FRTaphFRT* Δ*sseK1::FRTcatFRT*	This study	TAS255
S. Typhimurium 14028S Δ*sarA::FRTaphFRT* / pTS11	This study	TAS214
S. Typhimurium 14028S wild-type / pYpet	This study	JK1606
S. Typhimurium 14028S Δ*ssrB::FRTaphFRT* / pBC19-Ypet	This study	JK1619
Salmonella enterica serovar Typhi Ty2 wild-type JSG624	J. Gunn	TY01
S. Typhi Ty2 Nal^R (mouse infections)	This study	TY196
S. Typhi Ty2 Δ*vexA::FRTaphFRT*	[306]	TY76
S. Typhi Ty2 Δ*ssrB::FRTaphFRT*	[306]	TY144
S. Typhi Ty2 wild-type / pBC20-Ypet	This study	TY399
Salmonella enterica serovar Paratyphi A ATCC9150 wild-type	ATCC	TY363
S. Paratyphi A ATCC9150 Δ*ssrB::FRTaphFRT*	This study	TY377
S. Paratyphi A ATCC9150 wild-type / pBC20-Ypet	This study	TY407
Chemicals, Peptides, and Recombinant Proteins		
RPMI 1640, 1x with L-glutamine and 25mM HEPES	Corning	Cat#10-041-CV
Sodium Pyruvate 100mM solution	Corning	Cat#25-000-CI
MEM Non-Essential Amino Acids 100X	Gibco	Cat#11140-050
Penicillin Streptomycin	Corning	Cat#30-001-CI
Fetal Bovine Serum, heat-inactivated (USA sourced)	Millipore-Sigma	F4135
Phorbal 12-myristate 13-acetate	Millipore-Sigma	P1585

Human pooled serum	MP Biomedicals LLC	Cat#2930149
Phosphate-Buffered Saline	Corning	Cat#21-040-CV
Triton X-100	Fisher BioReagents	BP151-100
LB Broth, Miller	Fisher BioReagents	Cat#BP1426
LB Agar, Miller	Fisher BioReagents	Cat#BP1425
L-Phenylalanine	Millipore-Sigma	Cat#P2126
L-Tryptophan	Millipore-Sigma	Cat#T0254
2,3-Dihydroxybenzoic acid	Millipore-Sigma	Cat#126209
4-Aminobenzoic acid	Millipore-Sigma	Cat#A9878
2,6-Diaminopimelic acid	Millipore-Sigma	Cat#33240
Ampicillin, sodium salt	Research Products International	Cat#A40040
Carbenicillin disodium salt	Research Products International	Cat#C46000
Kanamycin sulfate	VWR	Cat#0408
Gentamicin sulfate	Research Products International	Cat#G3800
Normocin	Invivogen	Cat#ant-nr-1
Blasticidin	Invivogen	Cat#ant-bl-05
Ficoll-Paque PLUS	GE Healthcare	Cat#17-1440-02
hGM-CSF	PeproTech	
Human AB Serum	Corning	Cat#35-060-CI
Lowfat powdered milk	Saco Foods Inc.	
Bovine Serum Albumin	MP Biomedicals LLC	Cat#30075
Brefeldin A	Invitrogen	Cat#00-4506-51
Fixable Viability Dye eFluor450	Invitrogen	Cat#65-0863-14
Recombinant human IFNβ	PeproTech	Cat#300-02BC
BMS345541	Cayman Chemical	
IC Fixation Buffer	Invitrogen	Cat#00-8222-49
Permeabilization Buffer 10X	Invitrogen	Cat#00-8333-56
EDTA 0.5M	Corning	Cat#14-034-CI
Quanti-Blue Solution	Invivogen	Cat: rep-qbs
Pierce ECL Western Blotting Substrate	ThermoFisher Scientific	Cat#32209
RIPA Buffer		
Phosphatase Inhibitor Cocktail	Cell Signaling Technologies	Cat#5870
Protease Inhibitor Cocktail	Cell Signaling Technologies	Cat#5871
Critical Commercial Assays		
DNeasy Blood & Tissue Kit	Qiagen	Cat#69504
MinElute PCR Purification Kit	Qiagen	Cat#28004
NEBuilder HiFi DNA Assembly Master Mix	New England BioLabs	Cat#E2621
Cytotox96 Non-Radioactive Cytotoxicity Assay	Promega	Cat#G1780
Apo-BrdU TUNEL Kit	Phoenix Flow Systems	Cat#AU1001
Experimental Models: Cell Lines		

THP-1 monocyte	ATCC	ATCC TIB-202
THP-1 Blue NF-κB Reporter	Invivogen	Cat: thp-nfkb
Experimental Models: Organisms/Strains		
NOD-*scid IL2rγ*^{null} mice	Dale Greiner University of Massachusetts Medical School	NSG
Humanized-NOD-*scid IL2rγ*^{null} mice	Dale Greiner University of Massachusetts Medical School	hu-SRC-SCID
Recombinant DNA		
araC-P$_{araB}$-γβ*exo* oriR101 repA101ts *bla*	[300]	pKD46
FRTaphFRT PS1 PS2 oriR *bla*	[300]	pKD4
FRTaphFRT PS1 PS4 oriR *bla*	[300]	pKD13
Medium copy cloning vector ori pBR322 *bla*	This study	pJK392
pJK392::*sarA*	This study	pTS11
P*ybaJ*-Ypet 10% ori pSC101 *aph*	D. Bumann	pBC19
P*ybaJ*-Ypet 3% ori pSC101 *aph*	D. Bumann	pBC20
Antibodies		
Rabbit monoclonal anti-phosphoSTAT1 (Y701,clone D47A)	Cell Signaling Technologies	Cat#7649
Rabbit monoclonal anti-cleaved Caspase-3 (Asp175, clone 5A1E)	Cell Signaling Technologies	Cat#9664
Rabbit monoclonal anti-phospho- NF-κB p65 (Ser536, clone 93H1)	Cell Signaling Technologies	Cat#3033
Rabbit monoclonal anti-beta-Actin	Cell Signaling Technologies	Cat#4967
Goat anti-Rabbit IgG, HRP-linked	Cell Signaling Technologies	Cat#7074
Mouse monoclonal anti-BrdU Alexa Fluor647-conjugated (clone 3D4)	BioLegend	Cat#364108
Mouse monoclonal anti-CD11b PECy7-conjugated (clone ICRF44)	Invitrogen	Cat#25-0118-42
Mouse monoclonal anti-IL-12p35 PE-conjugated (clone 27537)	Invitrogen	Cat#MA5-23559
Mouse IgG1 kappa isotype control PE-conjugated	Invitrogen	Cat#12-4714-41
Biological Samples		
Leukocyte Reduction Filters	Bloodworks NW, Seattle, WA	
Software and Algorithms		
FlowJo Version 10.3	Treestar, Inc.	https://www.flowjo.com/solutions/flowjo
Microsoft Excel Version 16.24	Office 365	https://www.office.com/
Prism Version 8.1.1	GraphPad	https://www.graphpad.com/
MacVector Version 17.05.5	MacVector, Inc.	https://macvector.com/

Table 3-3. Primers.

Primer	Sequence 5'-3'	Purpose
TYP45	ATCATCATATTACTAACGACATTTTTCCTGCTTTCGGGATGTGTAGGC TGGAGCTGCTTC	Deletion of *vexA* in STY
TYP46	TTAGTGCCGCGGGTCAAAAAGCTATCGAATGCGGCTTTCACATATGA ATATCCTCCTTAG	Deletion of *vexA* in STY
TYP13	TATAAGATCTTATTAGTAGACGATCATGAAATCATCATTAGTGTAGG CTGGAGCTGCTTC	Deletion of *ssrB* in STY
TYP14	ATTAACCTCATTCTTCGGGCGCAGTTAAGTAACTCTGTCACATATGAA TATCCTCCTTAG	Deletion of *ssrB* in STY
JKP696	CGCGAGGGCAGCAAAATGAAAGAATATAAGATCTTATTAGGTGTAG GCTGGAGCTGCTTC	Deletion of *ssrB* in STM
JKP697	AGTTAAGTAACTCTGTCACTTTATGAACCTGTAGCTTTCTC	Deletion of *ssrB* in STM
TSP481	GTCAAAGTAATACTCAAACCATCGCACCTACGCTCAGTCCGTGTAGG CTGGCGCTGCTTC	Deletion of *sseK2* in STm
TSP482	TTACCTCCAAGAACTGGCAGTTAAACTGCTTGTGTTCATACATATGA ATATCCTCCTTAG	Deletion of *sseK2* in STm
TSP485	ATGTTTTCTCGAGTCAGAGGTTTTCTTTCATGCCAGAACTGTGTAGGC TGGAGCTGCTTC	Deletion of *sseK3* in STm
TSP486	TTATCTCCAGGAGCTGATAGTCAAACTGCTGGTATCCATACATATGA ATATCCTCCTTAG	Deletion of *sseK3* in STm
TSP1	ATGATCCCACCATTAAATAGATATGTTCCCGCGCTTTCAATGTGTAGG CTGGAGCTGCT	Deletion of *sseK1* in STm
TSP2	CTACTGCACATGCCTCGCCCATGAACTTTGCGTAAACTGACATATGA ATATCCTCCTTAG	Deletion of *sseK1* in STm
TSP4	TTAGCATAACGGCATTGTTATCGAATCGCTCATAAAGCGTTGTGTAG GCTGGAGCTGCT	Deletion of *avrA* in STm
TSP5	ATGATATTTTCGGTGCAGGAGCTATCATGTGGAGGGAAAACATATGA ATATCCTCCTTA	Deletion of *avrA* in STm
TSP13	ATGCCTATTTCGATTTGTAAACATGGTGCTCCTTTTGTTGTGTGTAGG CTGGAGCTGCT	Deletion of *steB* in STm
TSP14	TTATCTGACATTACCATTTGAGTGACAGGTTAGCAGATGTCATATGA ATATCCTCCTTA	Deletion of *steB* in STm
TSP16	TTAATCAAATACGCCATTAATAATCGCCGTGACCACCGCGTGTGTAG GCTGGAGCTGCT	Deletion of *cigR* in STm
TSP17	ATGAATAATCGTCGTGGTTTAACCGCCGTCCTGGCGACGTCATATGA ATATCCTCCTTA	Deletion of *cigR* in STm
TSP19	TCATAAAATGGTACACCAGTCTTTCCAGGCGGCGGCGTGTTGTGTAG GCTGGAGCTGCT	Deletion of *gtgE* in STm

TSP20	ATGTTAAGACACATTCAAAATAGTTTAGGCAGCGTTTACACATATGAATATCCTCCTTA	Deletion of *gtgE* in STm
slrPkop1	ATGTTTAATATTACTAATATACAATCTACGGCAAGGCATCTGTGTAGGCTGGACCTGCTT	Deletion of *slrP* in STm
slrPkop2	CTATCGCCAGTAGGCGCTCATGAGCGAGCTCACCTCTTTTCATATGAATATCCTCCTTAG	Deletion of *slrP* in STm
sopD2kop1	ATGCCAGTTACGTTAAGTTTTGGTAATCGTCATAACTATGTGTGTAGGCTGGAGCTGCTT	Deletion of *sopD2* in STm
sopD2kop2	TTATATAAGCATATTGCGACAACTCGACTTTTCACTTATACATATGAATATCCTCCTTAG	Deletion of *sopD2* in STm
sseJkop1	ATGCCATTGAGTGTTGGACAGGGTTATTTCACATCATCTATGTGTAGGCTGGAGCTGCTT	Deletion of *sseJ* in STm
sseJkop2	TTATTCAGTGGAATAATGATGAGCTATAAAACTTTCTAACCATATGAATATCCTCCTTAG	Deletion of *sseJ* in STm
sseIkop1	ATGCCCTTTCATATTGGAAGCGGATGTCTTCCCGCCATCATGTGTAGGCTGGAGCTGCTT	Deletion of *sseI* in STm
sseIkop2	TTACATTTTACCTATTAAGGAATATTTTTGCTTTTTAAAGCATATGAATATCCTCCTTAG	Deletion of *sseI* in STm
sspH1kop1	ATGTTTAATATCCGCAATACACAACCTTCTGTAAGTATGCTGTGTAGGCTGGAGCTGCTT	Deletion of *sspH1* in STm
sspH1kop2	TCAGTTAAGACGCCACCGGGCTGTCAGATAGCTACCCAGCCATATGAATATCCTCCTTAG	Deletion of *sspH1* in STm
gogBkop1	TTGACATATAGATTGAAAAAGCGCATGAAAATAGGATTCCTGTGTAGGCTGGAGCTGCTT	Deletion of *gogB* in STm
gogBkop2	TCAACGATTTCTATTTTTAGGCTTATATTTATCCCAACCACATATGAATATCCTCCTTAG	Deletion of *gogB* in STm
gtgAKop1	TCAATTACTAAATTCGTAGGCGATTCTTGGTGGTGATGTGTGTGTAGGCTGGAGCTGCTT	Deletion of *gtgA* in STm
gtgAkop2	ATGCCAACGGGAATTAAACCAATATTTATCAATAATATGACATATGAATATCCTCCTTAG	Deletion of *gtgA* in STm
sseK2kop1	ATGGCACGTTTTAATGCCGCTTTTACAAGGATTAAAATAATGTGTAGGCTGGAGCTGCTT	Deletion of *sseK2* in STm
sseK2kop2	TTACCTCCAAGAACTGGCAGTTAAACTGCTTGTGTTCATACATATGAATATCCTCCTTAG	Deletion of *sseK2* in STm
spvBkop1	CTATGAGTTGAGTACCCTCATGTTTATTATTCTTTTTATCTGTGTAGGCTGGAGCTGCTT	Deletion of *spvB* in STm
spvBkop2	ATGTTGATACTAAATGGTTTTTCATCTGCCACTTTAGCGCCATATGAATATCCTCCTTAG	Deletion of *spvB* in STm
spvCkop1	TTACTCTGTCATCAAACGATAAAACGGTTCCTCACGTAAATGTGTAGGCTGGAGCTGCTT	Deletion of *spvC* in STm
spvCkop2	ATGCCCATAAATAGGCCTAATCTAAATCTAAACATCCCTCCATATGAATATCCTCCTTAG	Deletion of *spvC* in STm
spvDkop1	TCAATCGTGTTTTTCATCATAAGCCCTGACATAAAATTCCTGTGTAGGCTGGAGCTGCTT	Deletion of *spvD* in STm
spvDkop2	ATGAGAGTTTCTGGTAGTGCGTCATCCCAAGATATAATATCATATGAATATCCTCCTTAG	Deletion of *spvD* in STm

steAkop1	TTAATAATTGTCCAAATAGTTATGGTAGCGAGCTTTTATGTGTGTAGGCTGGAGCTGCTT	Deletion of *steA* in STm
steAkop2	ATGCCATATACATCAGTTTCTACCTATGCCAGAGCTTTATCATATGAATATCCTCCTTAG	Deletion of *steA* in STm
sseK3kop1	ATGTTTTCTCGAGTCAGAGGTTTTCTTTCATGCCAGAACTTGTGTAGGCTGGAGCTGCTT	Deletion of *sseK3* in STm
sseK3kop2	TTATCTCCAGGAGCTGATAGTCAAACTGCTGGTATCCATACATATGAATATCCTCCTTAG	Deletion of *sseK3* in STm
steEkop1	GTGATGAGATTCGTATATATTTATATCTTAGTGATTTATGTGTGTAGGCTGGAGCTGCTT	Deletion of *steE* in STm
steEkop2	TTATTCATCCGGGAAAACCTCTGCAGAATGCCTGTATTGACATATGAATATCCTCCTTAG	Deletion of *steE* in STm
TSP369	GTGATGAGATTCGTATATATTTATATCTTAGTGATTTATGGTGTAGGCTGGAGCTGCTTC	Deletion of *sarA* in STm
TSP370	ATCCGGGAAAACCTCTGCAGAATGCCTGTATTGAGCGATACATATGAATATCCTCCTTAG	Deletion of *sarA* in STm
TSP390	GGAAGGAACCAAGCTTTCGGCGCAGCTATTTATAACG	Construction of pTS11
TSP418	GGAAGGAACCGGTACCTGGTGAGGCTATTTCACACGAA	Construction of pTS11
srfJkop1	ATGAAAGGCAGACTCATCTCTTCCGATCCGTATCGTCAGGTGTAGGCTGGAGCTGCTTC	Deletion of *srfJ* in STm
srfJkop4	CTGGACATCGCGGTTATACACCACCAGCACACGCTCGCCTTCTTCCGGGGATCCGTCGA	Deletion of *srfJ* in STm

Chapter 4. *SALMONELLA* TYPHI EXHIBITS INCREASED SENSITIVITY TO IRON RESTRICTION

Figure 4-2a and related text in this chapter have been adapted from the following publication:

Joyce E. Karlinsey*, **Taylor A. Stepien***, Matthew Mayho, Larissa A. Singletary, Lacey K. Bingham-Ramos, Michael A. Brehm, Dale L. Greiner, Leonard D. Shultz, Larry A. Gallagher, Matthew Bawn, Robert A. Kingsley, Stephen J. Libby and Ferric C. Fang. (2019) Genome-wide Analysis of *Salmonella enterica* serovar Typhi in Humanized Mice Reveals Key Virulence Features. **Cell Host & Microbe**, vo. 26, no. 3, DOI: 10.1016/j.chom.2019.08.001.

**equal contribution*

4.1 ABSTRACT

Iron is an essential nutrient for nearly all living organisms, and pathogenic bacteria are no exception. However, iron is sequestered within the mammalian host environment to limit its availability during infection. Although the importance of iron acquisition by bacterial pathogens such as non-typhoidal *Salmonella* (NTS) has been extensively studied, less is known about the mechanisms of host iron withholding during enteric fever and how *S.* Typhi overcomes nutritional immunity. Here we report the increased sensitivity of *S.* Typhi to iron restriction as compared to the NTS serovar *S.* Typhimurium. Attempts to ascertain a genetic mechanism for this sensitivity are presented. Previous studies demonstrating differential macrophage activation in response to infection with NTS versus typhoidal *Salmonella* indicate that iron availability in the macrophage may be different during infection with these serovars. A preliminary investigation of macrophage iron sequestration during NTS versus typhoidal *Salmonella* infection is provided. The importance of iron acquisition for *S.* Typhi virulence and the unique immune environment induced by enteric fever suggest that there are important differences in pathogen-host iron dynamics between NTS and typhoidal *Salmonella* serovars.

4.2 INTRODUCTION

Iron is an essential nutrient for both pathogen and host. It is the most common redox-active metal found in proteins that are involved in fundamental biochemical processes such as respiration, metabolism, and DNA repair. However, excess iron is toxic because it can participate in Fenton chemistry, generating oxygen-radical species that can damage DNA, lipids and proteins while mobilizing additional free iron[336,337]. Therefore, bacteria must tightly regulate iron concentrations through a variety of iron uptake and efflux systems (**Figure 4-1**). To acquire necessary iron, *Salmonella* employs cation uptake systems and iron-chelating siderophores. FeoAB is a ferrous iron uptake system consisting of the inner membrane ATP/GTP-driven transporter FeoB and the cytosolic protein FeoA, which aids FeoB activity[338]. SitABCD is an ABC-family transporter that transports divalent cations including Mn(II) and ferrous iron. It consists of the periplasmic binding protein SitA, the ATP-binding protein SitB, and two permeases, SitC and SitD[339,340]. The catecholate siderophores enterobactin (or enterochelin) and salmochelin are synthesized and secreted to chelate extracellular ferric iron. Secretion occurs by an active efflux mechanism involving the inner membrane transporters EntS or IroC and the outer membrane protein TolC[292,341]. Uptake of iron-bound siderophores also requires specialized proteins such as IroN and the Fep system[292,342]. FepA is the outer membrane receptor for ferric enterobactin and provides a gated pore that is activated by the transference of proton motive force from the cytoplasmic membrane to the pore by TonB[339,342].

Macrophages are the first line of defense against invading pathogens, and an important antimicrobial mechanism is their ability to prevent pathogen acquisition of important nutrients, termed nutritional immunity. Numerous studies have focused on the mechanisms by which host cells like macrophages subvert bacterial iron acquisition through iron compartmentalization and

sequestration. Of note is that much of the iron handling response by macrophages is controlled by the inflammatory response and macrophage immune activation[294,343–346]. Our lab has found that *S.* Typhi persists in human macrophages and fails to stimulate STAT1 phosphorylation and IL-12 production, key mediators of the T_H1 immune response, which is critical for resistance to *S.* Typhimurium (**Chapter 3**). The contrasting immune activation of macrophages infected with *S.* Typhi versus *S.* Typhimurium suggested that macrophage iron handling and sequestration might be altered during typhoidal *Salmonella* infection. This could explain why human disorders causing secondary iron overload increase susceptibility to NTS infection but are not associated with a greater predisposition to typhoid fever[347].

Previous studies have demonstrated the importance of iron uptake for *S.* Typhimurium virulence[292,348–350]. However, human restriction of *S.* Typhi and the lack of a small animal model have impeded the direct study of typhoid pathogenesis in the past. In Chapter 2, we used a humanized mouse model coupled with a high-complexity transposon mutant screen (TraDIS) to identify genetic loci required for *S.* Typhi virulence. TraDIS revealed high counter-selection of loci involved in iron acquisition, including the catecholate siderophores enterobactin and salmochelin, indicating that iron acquisition is essential for *S.* Typhi infection (**Figure 2-3, Table 2-1**). The importance of salmochelin was confirmed by competitive infection and shown to be required for *S.* Typhi survival in macrophages (**Figure 2-4**).

Due to the different immune environments described during *S.* Typhimurium and *S.* Typhi infection, we hypothesized that iron acquisition strategies may be different during NTS and typhoidal *Salmonella* infection. In this study, we characterize the differential ability of these two serovars to grow under iron-restricted conditions *in vitro* and seek to understand the mechanism for their contrasting sensitivity to iron restriction. We also attempted to distinguish iron handling

dynamics by the macrophage during infection with *S* Typhi versus *S.* Typhimurium. Clear differences emerged between *S.* Typhimurium and *S.* Typhi iron acquisition, but many questions remain.

4.3 RESULTS

4.3.1 S. Typhi is more sensitive to iron limitation than S. Typhimurium

Mutants deficient in the synthesis or transport of the siderophores enterobactin and salmochelin (*ent* and *iro*) were counter-selected in hu-SRC-SCID mice (**Figure 2-3, Table 2-1**), consistent with host iron restriction during S. Typhi infection. To test the ability of *S.* Typhi and *S.* Typhimurium to grow under iron restriction, *in vitro* growth was measured in LB medium with or without the divalent metal chelator 2,2-dipyridyl (DP). Although both serovars exhibited reduced growth rates with DP, *S.* Typhi growth was more severely restricted, indicating greater sensitivity to iron limitation (**Figure 4-2a**). Although DP can chelate other metals besides iron, growth of both S. Typhi and S. Typhimurium in DP-chelated medium was rescued by addition of $FeCl_3$, confirming that iron limitation was responsible for impaired growth in DP-chelated medium (**Figure 4-2a**).

Previous studies have demonstrated the requirement of various iron uptake systems for the ability of *S.* Typhimurium to persist in murine macrophages and for virulence in mice[292,349]. Isogenic mutants lacking known iron uptake systems were constructed in *S.* Typhimurium and *S.* Typhi using λ–red recombination[300]. These included the FeoAB ferrous iron transporter, the SitABCD divalent cation transporter, the siderophore enterobactin, whose biosynthetic pathway is encoded by the *entABCDEF* locus, and the glucosylated form of enterobactin called salmochelin, which is modified by the *iroBCDEN* locus. Strains were tested for their ability to grow under iron-limiting conditions using 200 μM DP in LB. All *S.* Typhi strains were more severely attenuated

for growth in DP-chelated media than *S.* Typhimurium; both *S.* Typhimurium and *S.* Typhi *entC* mutants were unable to grow in the presence of DP (**Figure 4-2b**).

To confirm that the inability of the *entC* mutants to grow is due to low iron, and to compare the low-iron sensitivity of *entC* mutant *S.* Typhi and *S.* Typhimurium, iron addback experiments were performed with both ferrous and ferric iron in DP-chelated media. As increasing concentrations of $FeCl_3$ or $FeSO_4$ were added to DP-chelated media, the *S.* Typhi *entC* mutant required higher amounts of exogenous iron to restore growth in comparison to the *S.* Typhimurium *entC* mutant (**Figure 4-3**). In the absence of ferric iron-transporting siderophores, addition of ferrous iron restored growth more quickly than ferric iron, likely due to the presence of ferrous iron transporters FeoAB and SitABCD.

4.3.2 S. Typhi Does Not Have a Higher Iron Content Than S. Typhimurium

One possibility for the increased sensitivity of *S.* Typhi to iron restriction as compared to *S.* Typhimurium is that *S.* Typhi requires more iron for normal cellular functions than *S.* Typhimurium. To test this, *S.* Typhi and *S.* Typhimurium were grown in iron-replete conditions in normal LB medium, and the iron content of the cell pellets was analyzed using inductively coupled plasma mass spectrometry (ICP-MS). No differences in the amount of iron per cell were observed between *S.* Typhi and *S.* Typhimurium during iron-replete growth (**Figure 4-4**).

4.3.3 Pseudogenes in Iron Uptake Systems of S. Typhi Do Not Explain Sensitivity to Low Iron

The genomic decay of human-restricted *S.* Typhi has led to the loss of 5% of its gene complement and only 89% sequence similarity to *S.* Typhimurium[169]. Notably, all of the host-restricted *Salmonella* serovars (Typhi, Paratyphi A, Gallinarum and Typhisuis) share gene loss due to pseudogenes in iron uptake systems (**Table 4-1**). Some of these genomic differences are

compatible with a limited lifestyle outside the host, for example the decreased likelihood of encountering fungal siderophores to be taken up by *fhu* systems[10]. The potential contribution of pseudogenes to *S.* Typhi low-iron sensitivity was examined further.

The *fepBDGC* operon for uptake of ferric enterobactin is essential in *S.* Typhi but not *S.* Typhimurium, indicating a requirement for ferric iron. Ferric iron is the primary form of iron in the bloodstream, a niche in which *S.* Typhi may be found[10]. In contrast, the intestinal lifestyle of *S.* Typhimurium allows utilization of the ferrous form of iron that is found in anaerobic environments, which can be taken up by the cationic transporters FeoAB and SitABCD[351]. FepE, part of the Fep ferric enterobactin transport system, is a pseudogene in *S.* Typhi. Although this does not prevent the Fep complex from transporting ferric enterobactin, we explored whether this affects the efficiency of the Fe-enterobactin system in *S.* Typhi. A *fepE* mutant of *S.* Typhimurium grown in the presence of DP did not have a defect as compared to wild-type *S.* Typhimurium (**Figure 4-5a**). Additionally, complementation plasmids containing either *S.* Typhimruium- or *S.* Typhi-derived *fepE* did not affect the growth of either *S.* Typhi or the *fepE* mutant of *S.* Typhimurium, further confirming that *fepE* does not contribute to *S.* Typhi sensitivity to iron restriction (**Figure 4-5a**). Despite the location of *fepE* within the enterobactin biosynthetic operon, it appears that *fepE* functions more in regulation of O-antigen chain length in *Salmonella,* despite being involved in iron uptake in *E. coli*[352].

Other pseudogenes in iron uptake systems in *S.* Typhi include *fhuA* and *fhuE* for uptake of fungal-derived siderophores. Mutants in *fhuA* and *fhuE* were generated in *S.* Typhimurium and tested for their ability to grow in the presence of DP; neither mutation affected growth of *S.* Typhimurium in DP as compared to wild-type (**Figure 4-5b**). *fhuA* or *fhuE* mutations in an *entA* mutant background of *S.* Typhi also did not affect growth compared to an *entA* mutation alone

(**Figure 4-5b**). Therefore, individual pseudogenes in *S.* Typhi iron uptake systems do not appear to explain its sensitivity to iron restriction.

Apart from pseuodgenes, *S.* Typhi iron uptake systems differ from those of *S.* Typhimurium by a number of polymorphisms, many leading to non-synonymous mutations that may affect the efficiency of these systems (**Table 4-2**). Paratyphoid fever caused by *S.* Paratyphi A is similar to typhoid, and in Chapter 2 we demonstrated the similarities in macrophage activation and cell death during infection with *S.* Typhi and *S.* Paratyphi A. A comparison of the polymorphisms in *S.* Paratyphi A showed that it shares many of these in common with *S.* Typhi (**Table 4-2**). *In vitro* growth in LB medium with or without DP revealed that *S.* Paratyphi A is also more sensitive to iron restriction than *S.* Typhimurium (**Figure 4-6**). Future work will analyze how shared polymorphisms between *S.* Typhi and *S.* Paratyphi A might affect their iron uptake efficiency.

4.3.5 No Unknown Factors were Identified in Screen for S. Typhimurium Genes that Improve S. Typhi Growth in Low Iron

To test whether an unknown *S.* Typhimurium gene that is absent or detective in *S.* Typhi might explain their differential growth in low iron, a cosmid library of *S.* Typhimurium 14028s[353] was screened in *S.* Typhi grown under iron limitation. pLAFR2::14028s is an RK2-derived, tetracycline-resistant cosmid cloning vector containing fragments of the *S.* Typhimurium 14028s genome averaging 25kbp in length. This library was moved into kanamycin-resistant *S.* Typhi Ty2 by triparental mating. The library was then screened on LB agar containing DP at a concentration that would allow growth of *S.* Typhimurium but inhibit growth of *S.* Typhi (**Figure 4-7a**). Clones were picked after overnight growth on LB + DP agar and further analyzed for the ability to grow under iron restriction by growing in LB + DP broth cultures for 18 h. Out of eight clones screened,

four grew better than wild-type *S.* Typhi in DP-chelated media (**Figure 4-7b**). These four clones were sub-cloned and sequenced to characterize their cosmid inserts. Sequencing revealed that all fragments contained some portion of the enterobactin biosynthesis and utilization loci of *S.* Typhimurium. Despite the inability to identify unknown factors involved in iron acquisition, the identification of *ent* and *fep* genes prompted investigation into whether these loci might be more efficient in *S.* Typhimurium. To test whether complementation of *S.* Typhi with enterobactin synthesis and utilization from *S.* Typhimurium could improve the growth of *S.* Typhi under iron restriction, portions of the operon (**Figure 4-7c**) were expressed in *trans* in *S.* Typhi and tested for growth in DP-chelated medium (**Figure 4-7d**). However, none of the complemented strains exhibited improved growth during iron limitation.

4.3.6 Iron Acquisition Genes are Upregulated in S. Typhi Compared to S. Typhimurium

To analyze the expression of genes involved in iron acquisition and storage, *S.* Typhimurium and *S.* Typhi gene expression was analyzed by qRT-PCR after growth under iron limitation. Cultures were grown to mid-log phase (OD_{600}~1.0) and treated with 200 μM DP for 2 h before RNA extraction. All of the iron-regulated genes analyzed were expressed to a higher level in *S.* Typhi than *S.* Typhimurium (**Figure 4-8a**).

To investigate expression of the siderophore enterobactin during infection, a reporter construct was added to wild-type *S.* Typhi and *S.* Typhimurium in which GFP is under control of the *S.* Typhimurium *entC* promoter. Macrophages were differentiated from THP-1 cells using phorbal myristate acetate (PMA) and infected with *Salmonella* at an MOI of 15:1. After 24 h of infection, macrophages were lysed with 1% Triton-X100, and intracellular bacteria were analyzed by flow cytometry for GFP expression. The reporter constitutively expresses mCherry under the control of the *rpsM* promoter to allow initial gating of viable cells that have retained the plasmid.

Expression of *entC* was significantly greater in intracellular *S.* Typhi in comparison to *S.* Typhimurium (**Figure 4-8b**). I conclude that iron restriction both *in vitro* and during macrophage infection induces higher levels of iron acquisition genes in *S.* Typhi compared to *S.* Typhimurium. This is consistent with reports that siderophore production is elevated in *S.* Typhi compared to *S.* Typhimurium[292,354]. However, it is uncertain whether *S.* Typhi is more iron-starved, or rather that iron acquisition is dysregulated in *S.* Typhi.

4.3.7 Both S. *Typhi and* S. *Typhimurium Infection Induce Macrophage Lipocalin-2 Production*

Iron acquisition is known to be required for *Salmonella* survival in macrophages[291]. Enterobactin is glucosylated by *iro* genes to produce salmochelin, which counteracts the neutralizing effects of host-derived Lipocalin-2 (Lcn2)[292–294]. Reduced survival of an *S.* Typhi *iroCDEN* mutant in macrophages and humanized mice demonstrates the importance of evading Lcn2 neutralization for *S.* Typhi survival (**Figure 2-4**). To better understand the dynamics between salmochelin and Lcn2 during *S.* Typhi-macrophage interactions, human macrophages were either treated with LPS, known to stimulate Tlr4 and induce Lcn2 production, or infected with *S.* Typhi or *S.* Typhimurium for 24 h, and Lcn2 in supernatants measured by ELISA (R&D Systems). THP-1-derived macrophages did not produce detectable Lcn2 under any conditions tested (**Figure 4-9**). PBMC-derived macrophages produced Lcn2, but production was not dependent on Tlr4 stimulation, as Lcn2 was detectable in supernatants even from untreated cells (**Figure 4-9**). Future studies should aim to optimize a system in which to study the dynamics of Lcn2 production during *Salmonella* infection of macrophages.

4.3.8 Examining the Role of Salmonella Infection on Hepcidin-Dependent Degradation of Fpn1

The hormone hepcidin is produced by the liver during infection in response to the inflammatory cytokine IL-6. Hepcidin restricts dietary absorption of iron, and also binds the sole cellular iron exporter, Ferroportin-1 (Fpn1), causing its internalization and degradation, and blocking the release of iron from macrophages[355–357]. A study using a human challenge model found that during the acute phase of typhoid infection, patients had elevated levels of serum hepcidin compared to baseline and a resultant hypoferremia as measured by serum iron levels[358]. During bacterial infection, flagellin is the major stimulus for the production of IL-6 through Tlr5 stimulation[359]; previous studies indicate that S. Typhi and S. Typhimurium differ in their regulation of flagellin during infection[168,360,361]. We measured the expression of flagellin during THP-1 macrophage infection using a reporter construct expressing GFP under the control of the *fliC* promoter. Macrophages infected with S. Typhi or S. Typhimurium carrying the construct were lysed after 24 h of infection, and intracellular bacteria were analyzed for GFP expression by flow cytometry. S. Typhi expresses significantly more flagellin during macrophage infection (**Figure 4-10a**). However, quantification of IL-6 production during macrophage infection by ELISA (R&D Systems) showed that IL-6 produced by S. Typhi-infected macrophages was not higher than S. Typhimurium-infected cells, despite higher flagellin expression (**Figure 4-10b**). To determine if elevated hepcidin levels in typhoid patients could reduce macrophage Fpn1 expression during Salmonella infection, exogenous human hepcidin (Peptides International, Inc.) was administered to THP-1 macrophages and Fpn1 levels measured by Western Blot (**Figure 4-10c**). The peptide does not appear to be biologically active, as no difference in Fpn1 levels was observed. It appears that studying the dynamics of hepcidin regulation of Fpn1 in infected macrophages will be

challenging. Future studies might employ Fpn1 knockout cell lines to investigate the role of iron efflux on Salmonella intramacrophage survival.

4.4 DISCUSSION

Iron acquisition plays a pivotal role in host-pathogen interactions, including both typhoidal and non-typhoidal *Salmonella enterica* serovars. Improved models to study human-restricted *S.* Typhi provide new opportunities to understand the importance of iron acquisition for the pathogenesis of typhoid fever. A genome-wide screen of *S.* Typhi virulence factors identified iron uptake via siderophores as essential for virulence in humanized mice. The requirement for salmochelin was more pronounced then in *S.* Typhimurium infection models[292,295,296], suggesting that non-glucosylated enterobactin may be less effective in typhoid than in non-typhoidal *Salmonella* infections. Further studies demonstrated that *S.* Typhi is more sensitive to iron restriction than the NTS serovar *S.* Typhimurium. Attempts to explain this difference genetically were unsuccessful thus far, although it may be possible to exploit this sensitivity in the development of novel typhoid therapies.

Pseudogenes in iron uptake genes in *S.* Typhi did not confer sensitivity to low iron when those loci were deleted from *S.* Typhimurium. Although gene loss cannot account for serovar differences in iron metabolism, a significant number of nucleotide polymorphisms exist in iron acquisition-related genes between *S.* Typhimurium and *S.* Typhi, including many non-synonymous mutations (**Table 4-2**). Additionally, the enteric fever serovar *S.* Paratyphi A shares a large number of these polymorphisms and is also sensitive to iron limitation (**Figure 4-6**). The possibility that these polymorphisms might render these systems less efficient in typhoidal *Salmonella* serovars should be further examined. As one example, FepB, part of the ferric enterobactin transport system, has five amino acids changes (P4S, I16L, T178A, R231Q, K270N) that could affect its

function. Additionally, in the absence of enterobactin synthesis and import, *Salmonella* must rely on its ferrous iron transport systems to obtain iron, including FeoAB and SitABCD. As seen in **Table 4-2**, *S.* Typhi has a number of polymorphisms in several genes of the *sit* operon and in *feoB*. Attempts to exchange the *S.* Typhi and *S.* Typhimurium-derived Feo and Sit systems in *ent*-deficient backgrounds to see how they affect the ability of these serovars to grow in low iron conditions are ongoing.

Another possible contributing factor MenF, a homolog of the isochorismate synthase EntC. MenF is specific to the menaquinone synthesis pathway and is regulated separately from EntC; MenF is expressed under anaerobic conditions, whereas EntC responds to iron deficiency, and each enzyme seems to feed isochorismate primarily into its respective pathway. However, one study found that chromosomal position could affect the ability of these enzymes to channel isochorismate to the mismatched pathway[362]. If MenF function is reduced or abrogated, *S.* Typhi may rely on EntC activity for menaquinone synthesis, which could burden the enterobactin synthesis system under iron limitation.

Higher expression of all iron acquisition genes in *S.* Typhi as compared to *S.* Typhimurium during iron restriction implies the possible global dysregulation of iron acquisition in *S.* Typhi. Fur is the master iron regulator and represses expression of iron acquisition genes when intracellular concentrations of iron are high; under low iron conditions, derepression of these genes allows iron uptake[363,364]. However, the Fur proteins of *S.* Typhi and *S.* Typhimurium are identical (**Table 4-2**), as are the Fur-binding boxes of *entC*. It remains conceivable that there are other Fur-binding boxes with different affinities for Fur between *S.* Typhi and *S.* Typhimurium. Additionally, Fur-regulated genes are subject to regulation by the small RNAs RhyA and RhyB[365]; their contribution to regulatory differences between *S.* Typhi and *S.* Typhimurium has yet to be explored.

The role of catecholate siderophores in iron uptake within the host has been extensively studied, but another possible role for these molecules is protection from oxidative stress[366] (Adler et al., 2014). Many iron uptake systems are regulated not only by the presence of iron but also of oxygen, and may protect bacteria from reactive species generated from the Fenton reaction[367,368]. One study showed that the ability to produce catecholate siderophores enhanced the ability of *Salmonella* to survive within macrophages and resist reactive oxygen species such as hydrogen peroxide and paraquat *in vitro*[369]. The sensitivity of *S.* Typhi to oxidative stress could be compared to that of *S.* Typhimrium. Another alternative function of siderophores their binding of other metals, either for acquisition or to prevent toxic intracellular accumulation[370,371].

Attempts in this chapter to understand iron acquisition in the context of *Salmonella*-macrophage interactions highlight the challenges of this endeavor. Nevertheless, the difference in macrophage immune modulation in response to infection with *S.* Typhi versus *S.* Typhimurium, as highlighted in Chapter 3, suggests that iron handling by macrophages may differ during infection with these *Salmonella* serovars. Clinical observations of the susceptibility of patients with iron overload to *Salmonella* infections support this hypothesis. Hemolytic disorders such as hemoglobinopathies and malaria promote secondary iron overload in macrophages, allowing NTS to proliferate[347,372,373]. However, these conditions are not associated with a greater predisposition to typhoid fever. Although salmochelin loss attenuates *S.* Typhimurium virulence in mice[292,295,296], salmochelin is not required for *S.* Typhimurium growth in murine macrophages unless other iron uptake systems are also impaired[296]. However, salmochelin loss has a profound impact on *S.* Typhi virulence, suggesting that Lcn2 may play a more prominent role in host resistance to typhoidal infection. We were not able to modulate Lcn2 or Fpn1 levels in macrophages in our studies, but the use of knockout cell lines might be informative for understanding how *S.* Typhi subverts iron

withholding. Finally, siderophores have been shown to modulate the host response, and this possibility might be explored in the context of macrophage infection[374–376].

The essentiality of iron for *S.* Typhi and other pathogenic bacteria makes iron acquisition an attractive target for the development of novel antimicrobial agents. The reliance of *Salmonella* and other bacteria on siderophores has led to attempts to exploit this process through toxic siderophore analogs, siderophore/antibiotic conjugates, inhibition of siderophore synthesis, or intoxication by alternative transition metals[377–379]. A hybrid siderophore-antibiotic was recently approved by the FDA for the treatment of resistant Gram-negative bacterial infections[380]. The revelation that *S.* Typhi is particularly sensitive to iron restriction suggests the potential for these strategies as novel treatments for typhoid fever.

4.5 Materials and Methods

4.5.1 Bacterial Growth Conditions and Strain Constructions

Bacterial strains and plasmids used in this study are listed in **Table 4-3**. *Salmonella enterica* serovar Typhimurium strain ATCC 14028s and serovar Typhi Ty2 were used as the wild-type strain for all experiments. *S. enterica* cultures were grown aerobically in Miller's Luria Broth (LB, Difco) medium at 37°C with shaking at 250 rpm. Medium was supplemented with antibiotics at the following concentrations: 100 μg ml^{-1} ampicillin (Amp), 50 μg ml^{-1} kanamycin (Kan), 20 μg ml^{-1} and 20 μg ml^{-1} tetracycline (Tet).

Primers were purchased from Integrated DNA Technologies (IDT, Skokie, IL) and are listed in **Table 4-4**. Mutant alleles of *S. enterica* serovars were constructed using λ-Red recombination as described[300,301]. To construct the pRU001 promoterless-GFP plasmid with constitutive mCherry expression, the PrspM-mCherry cassette was excised from pFPV-mCherry with HindIII and BamHI and ligated into pJK682 (unpublished) digested with BamHI and AvaI.

Plasmid pJK682 contains a pBR322 origin of replication, a β-lactamase gene for antibiotic selection, and a promoterless gfp3. Primer pair RU032 and RU034 was used for PCR-amplification of *entC* from *S.* Typhimurium 14028s gDNA. To construct the FepE complementation plasmids, the *fepE* gene was amplified from gDNA from either *S.* Typhimurium 14028S or *S.* Typhi Ty2 using primers TSP512 and TSP513. Plasmid pWSK29 and inserts were cut with EcoRV before ligation.

Transduction was performed with transducing phage P22. 100 µl of stationary phase culture of the recipient strain was mixed with 100 µl of P22 lysate. After 1 h of incubation at 37°C, transductants were selected on LB agar plates with antibiotics for the appropriate selectable marker. Colonies were streaked on indicator Green Plates, and P22-free colonies were selected for further experiments.

4.5.2 Bacterial Growth Curves

All strains were grown overnight in 5 mL Luria broth (LB), diluted 1:10 in fresh LB, then diluted 1:10 into 300 µL volume of LB or LB + DP in a microtiter plate. Cells were grown in a Labsystems Bioscreen C machine (Growth Curves USA) that measured OD_{600} every 15 min.

4.5.3 ICP-MS

Overnight *Salmonella* cultures were sub-cultured 1:100 into 10 ml fresh LB and grown to OD_{600} = 1.0. Four and one-half ml of culture were pelleted by centrifugation, washed once with 3 ml ultrapure water, and then resuspended in 250 µl analytical-grade nitric acid and incubated in an 85°C water bath for 30 min. The nitric acid solution was diluted 1:10 into MilliQ ultra-purified water before inductively coupled plasma-mass spectrometry (ICP-MS) analysis was performed by

the Environmental Health Laboratory and Trace Organics Analysis Center at the University of Washington using an Agilent 7500 CE instrument.

4.5.4 Cosmid Library Mating

Conjugal mating of the *S.* Typhimurium 14028s pLAFR2 cosmid library into *S.* Typhi Ty2 was performed by triparental mating as follows: the donor strain *E. coli* DH5a with cosmid pLAFR2 containing *S.* Typhimurium 14028s genomic fragments was grown in LB broth with Tet to OD_{600}~1.0. The recipient strain *S.* Typhi Ty2 *phoN*::Kan was grown in LB broth with "aromix" and Kan to OD_{600}~1.0. The helper strain *E. coli* MU12 containing the helper plasmid pRK2073 was grown in LB broth to OD_{600}~1.0. The three strains were mixed 1:1:1, then spotted onto a sterile 0.45 μm nitrocellulose membrane filter seeded on an LB plate. Five independent matings were performed, and after 4 h incubation at 37°C, the filters were added to 1 ml LB broth, vortexed, then plated in ten-fold dilutions on LB agar with Kan and Tet and incubated at 37°C for ~18 h. Plates were harvested by flooding with 2 mL LB broth and scraping, and all plates were pooled together for a total of ~$8.5*10^4$ Kan-and-Tet-resistant colonies representing ~472X genome coverage. One mL aliquots were frozen at -80°C, and one aliquot was thawed to determine the viable titer, which was found to be 2.2 x 10^9 CFU mL^{-1}.

4.5.5 Cosmid Library Screening

One vial of *S.* Typhi containing the 14028S cosmid library was thawed and added to 2 mL fresh LB broth with Tet, then placed at 37°C shaking at 250rpm for 30 min to warm. Culture was then plated in ten-fold dilutions on LB agar + DP in 100, 150, 200, 250, and 300 μM concentrations, and grown overnight at 37°C. Colonies were picked the following day and frozen at -80°C until further analysis.

4.5.6 Quantitative PCR

Wild-type *S.* Typhimurium and *S.* Typhi were grown overnight in LB at 37°C, then diluted 1:100 and grown to OD_{600}~1.0 Cultures were treated with DP to a final concentration of 200 μM for 2 h while shaking at 37°C, at which point cells were harvested for RNA extraction. Cells were pelleted and resuspended in TRIzol reagent (Life Technologies, Grand Island, NY) and incubated for a minimum of 30 min. RNA was then purified per the manufacturer's instructions. Residual DNA was removed by digestion with 5 U DNase I (Thermo Fisher Scientific, Pittsburgh, PA), followed by extraction with acid-phenol:chloroform (1:1). RNA was precipitated in 95% ethanol, and the resulting pellet was dissolved in RNase-free water. RNA was converted to cDNA using RevertAid reverse transcriptase (Thermo Fisher Scientific). qPCR was performed using SYBR green master mix on a Bio-Rad CFX96 real-time system. Data were analyzed using the comparative CT method $(2^{-\Delta\Delta CT})$[381] with the housekeeping gene *rpoD* amplified as an internal control, and normalization to untreated samples. Primers for quantitative PCR (qPCR) analysis are found in **Table 4-4**.

4.5.7 Macrophage Infections

THP-1- or PBMC-derived macrophages were harvested, cultured, treated, and infected as described in Chapter 3 (**3.5.2, 3.5.8**).

4.5.7 Fluorescent Reporter Assays

For bacterial intramacrophage gene expression analysis, infected macrophages were lysed after 24 h with 1% Triton X-100. Lysates were gently centrifuged at 2500 rcf for 5 min, supernatants were removed, and bacteria pelleted by centrifugation at 15000 rpm for 5 min. Bacterial pellets were resuspended in 2.5% paraformaldehyde and fixed for 15 min at 37°C. Fixed

bacteria were washed once in PBS, then analyzed using a BD LSRII flow cytometer (Becton, Dickinson) at the Pathology Flow Cytometry Core Facility (Department of Pathology, University of Washington, Seattle, WA) All bacteria were first gated on forward and side scatter to logarithmic amplification; if constitutive mCherry reporter was present, mCherry fluorescence was detected after 561 nM excitation and emission collected through a 595LP, 610/20 nm filter. For GFP, fluorescence was detected after 488 nM excitation and emission collected through a 505LP, 530/30 nm filter. Data were processed using FlowJo v. 10.3 software (Treestar). Total GFP fluorescence was calculated from the GFP-positive cells and statistical significance calculated using a Student's unpaired two-tailed t-test with software Excel v. 16.19 (Microsoft) or Prism v. 8.1.2 (GraphPad).

4.5.8 Western Blots

Infected macrophages were lysed in 1X RIPA buffer (Cell Signaling Technology) with added 1X protease and phosphatase inhibitors (Cell Signaling Technology) at the designated timepoint. Total protein was quantified using the BCA Protein assay kit (Pierce). Fifty µg total protein was combined with SDS loading dye and heated at 95C for 5 min before proteins were separated on a 4-15% SDS polyacrylamide gel (Bio-Rad). Proteins were wet-transferred to a Immobilon-P Polyvinylidene fluoride (PVDF) membrane (Millipore-Sigma), then blocked for 1 h in 5% bovine serum albumin (BSA, Research Products International). Primary antibody incubations were done at 1:1000 in BSA overnight at 4°C. Membranes were washed three times in 1X Tris-buffered saline with 0.05% Tween (TBST), then incubated with secondary HRP-conjugated antibody for 1 h at room temperature in 5% milk. After three more washes, chemiluminescent substrate was applied (ECL western blotting substrate, Thermo Scientific), and

the membranes were exposed to CL-X Posure film (Thermo Scientific). Film was developed using an AFP Imageworks MM90.

4.5.9 ELISA

Supernatants from infection macrophages were collected and stored at -20°C until assay by ELISA per the manufacturer's protocol.

4.5.10 Statistical Analysis

Statistical method and sample size for experiments are indicated in the corresponding figure legends. Statistical analysis of macrophage and mouse infections was performed using Prism v. 8.1.2 software (GraphPad). An unpaired two-tailed Student's t-test was performed on the means of parametric data. Statistical significance was defined as $p<0.05$. Error bars on figures show standard deviation.

4.6 Acknowledgments, Author Contributions, and Conflicts of Interest

4.6.1 Acknowledgments

We thank Joyce Karlinsey for her continued dedicated work on this project, as well as her guidance on experimental design; Dr. Elaine Frawley of Rhodes College for her advice on all things related to *Salmonella* and iron; Dr. Stephen Libby for providing the *S.* Typhimurium cosmid library; Dr. Rodolfo Urbano for construction of the enterobactin reporter plasmids; Dr. Brad Cookson of UW Department of Laboratory Medicine for providing the flagellin reporter plasmids; and Dr. Manfred Nairz and Dr. Gunter Weiss of the Medical University of Innsbruck for their advice on macrophage iron handling.

4.6.2 Author Contributions

T.A.S. and Ferric C. Fang designed the study; T.A.S. and Joyce E. Karlinsey performed the experiments; T.A.S., J.E.K., Stephen J. Libby, and F.C.F. analyzed the data; T.A.S. and F.C.F. wrote the manuscript.

4.6.3 Declaration of Interests

The authors declare no competing interests.

4.7 FIGURES

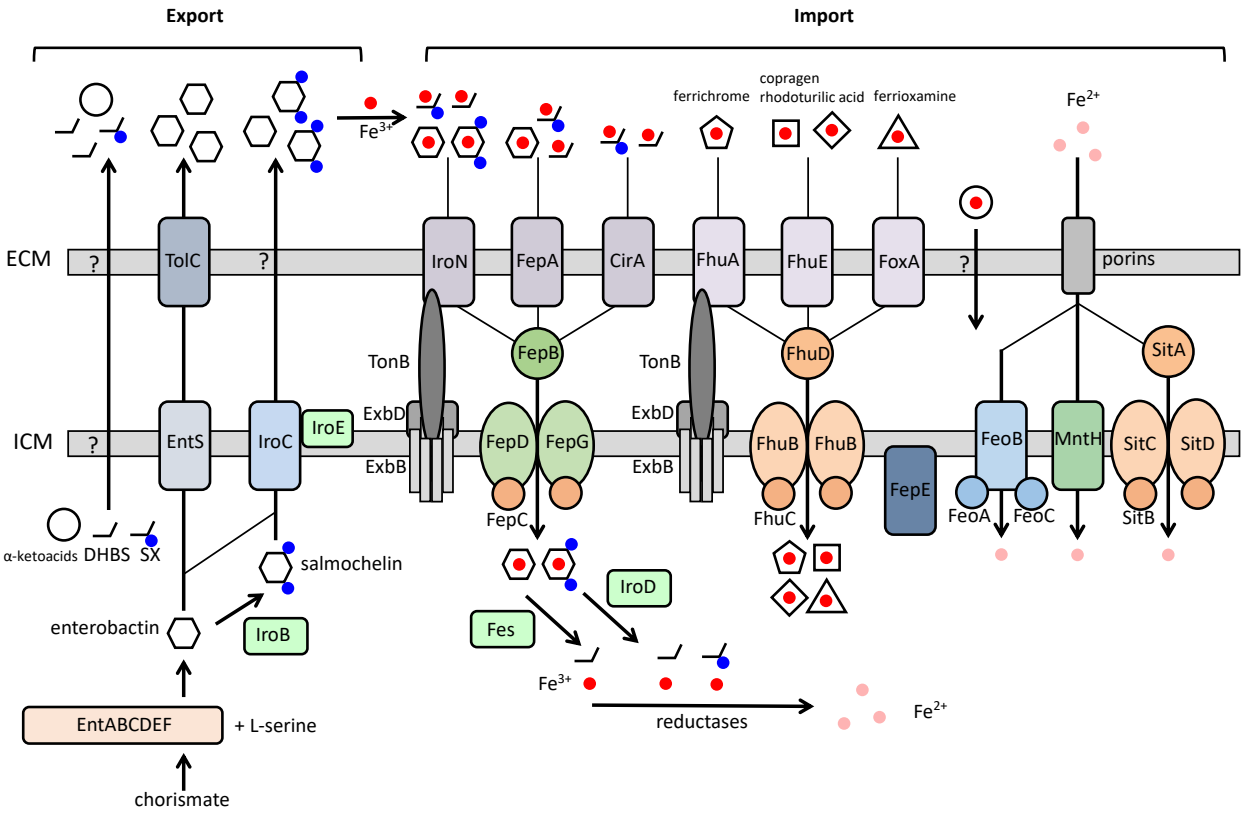

Figure 4-1. Iron Acquisition Systems of *Salmonella enterica.*

Salmonella synthesizes the catecholate siderophore enterobactin (*ent*), which can be glucosylated (*iro*) to form salmochelin. Ferric iron-bound siderophores is imported (*fep*) and converted to ferrous iron by reductases. Other iron-binding molecules can be taken up by other systems (*fhu*); both the Fep and Fhu systems are dependent on proton motive force transferred by TonB/ExbBD. Ferrous iron can also be taken up by divalent cation transporters including FeoAB and the ABC-family transporter SitABCD. A possible role of partial enterobactin products and alpha-ketoacids in iron uptake has been reported but less well studied.

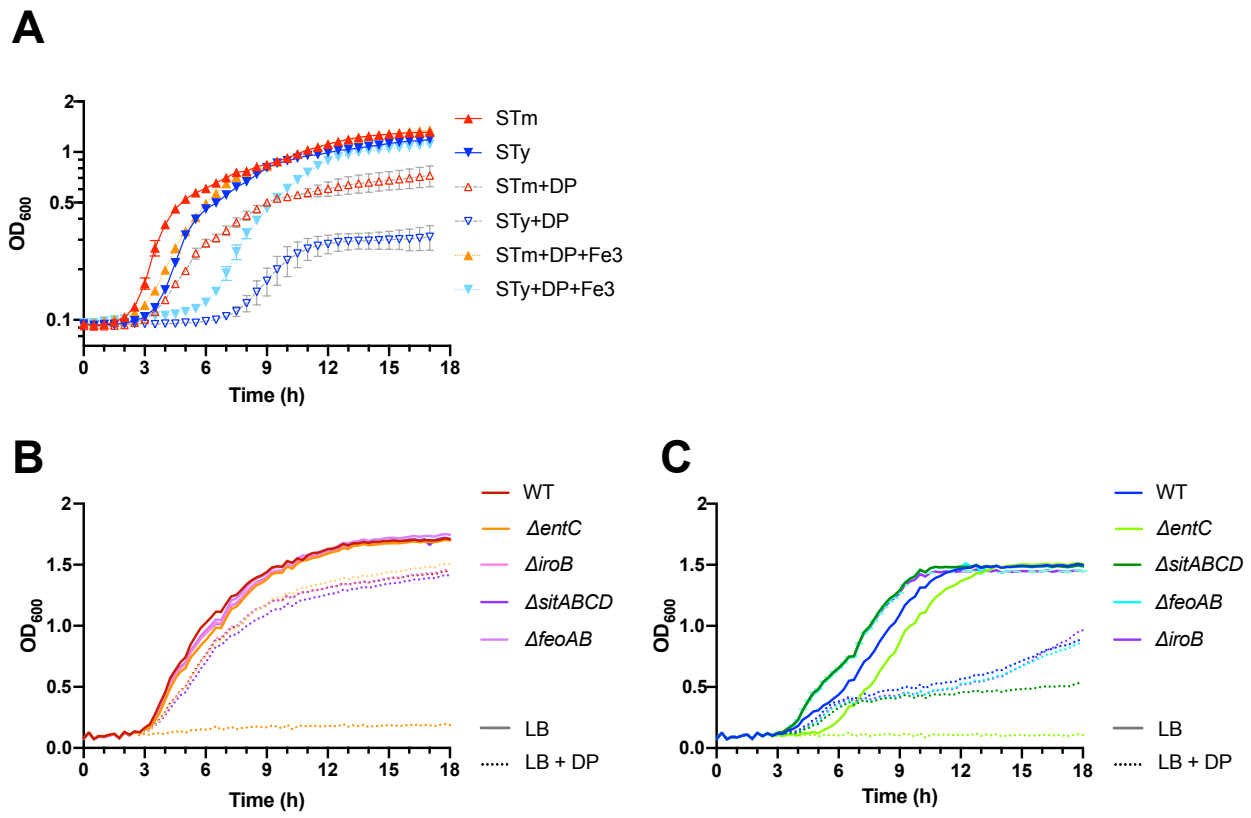

Figure 4-2. Growth of *Salmonella enterica* Under Iron Limitation.

(**A**) Wild-type *S.* Typhimurium (STm, red) and *S.* Typhi (STy, blue) were grown in LB or with 300 µM 2,2-dipyridyl (DP) (open triangles) or with 300 µM DP and 800 µM $FeCl_3$ (STm, orange triangles and STy, light blue triangles). OD_{600} was measured for 18 h; means and error bars representing standard deviation of three biological samples of OD_{600} are shown for each sample. Wild-type or isogenic mutants of *S.* Typhimurium (**B**) or *S.* Typhi (**C**) were grown in LB (solid lines) or with 300 µM DP (dotted lines) and OD_{600} measured for 18 h; daa shown are the means of three biological replicates. *S.* Typhi wild-type and mutant strains are more attenuated for growth in DP-chelated media than *S.* Typhimurium strains.

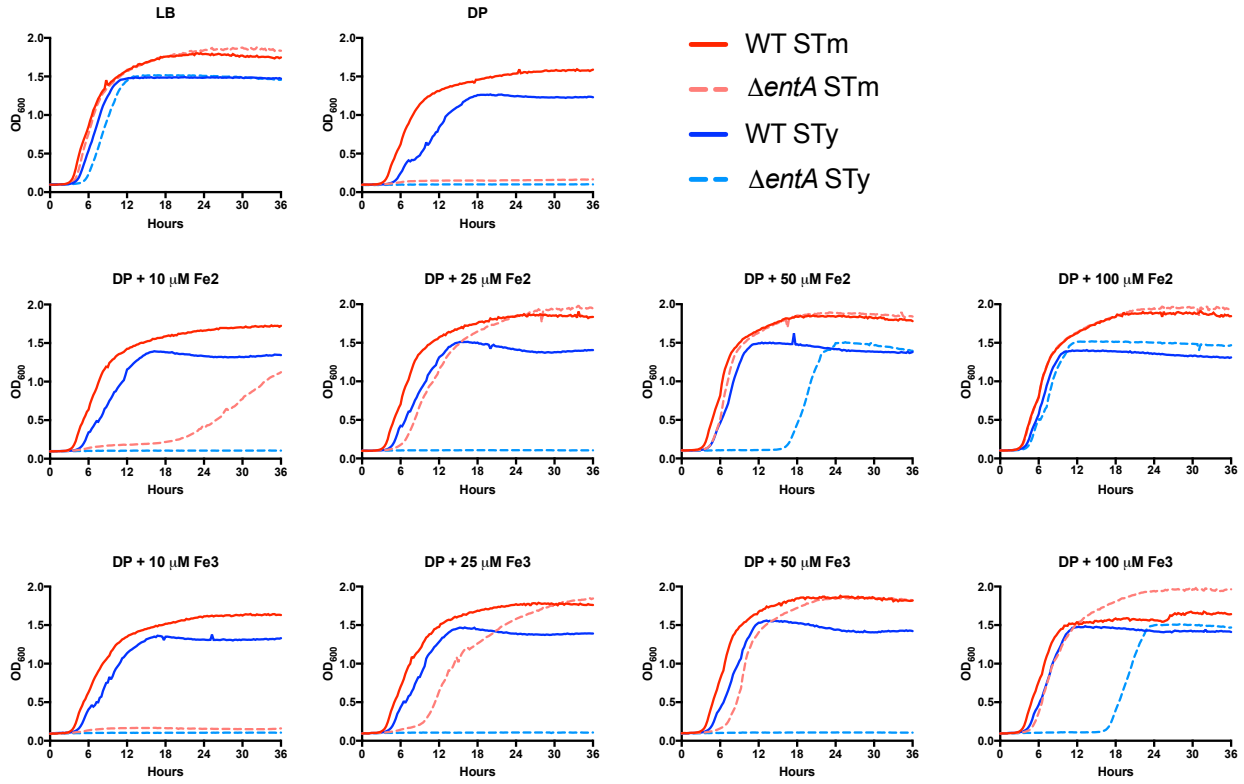

Figure 4-3. Growth of *Salmonella enterica* Under Iron Limitation With Iron Addback.

Wild-type (solid lines) or isogenic *entC* mutants (dashed lines) of *S.* Typhimurium (red hues) and *S.* Typi (blue hues) were grown in LB alone (top left panel) or with 200 μM DP (top right panel). LB + 200 μM DP was supplemented with either $FeSO_4$ to provide Fe(II) (middle row) or $FeCl_3$ to provide Fe(III) (bottom row) at the indicated concentration. OD_{600} was measured for 36 h; data shown are the means of three biological replicates. *entC* mutant *S.* Typhi requires more exogenous iron for growth than *entC* mutant *S.* Typhimurium.

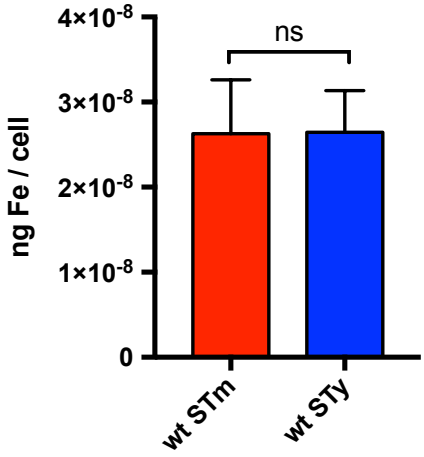

Figure 4-4. *S.* Typhi Does Not Have Higher Iron Content than *S.* Typhimurium.

Cultures of wild-type *S.* Typhimurium or *S.* Typhi were grown to early log phase in LB and analyzed for iron content by ICP-MS. Bars represent the mean of five biological replicates with error bars representing the standard deviation; no statistical significance was determined by paired two-tailed Student's t test.

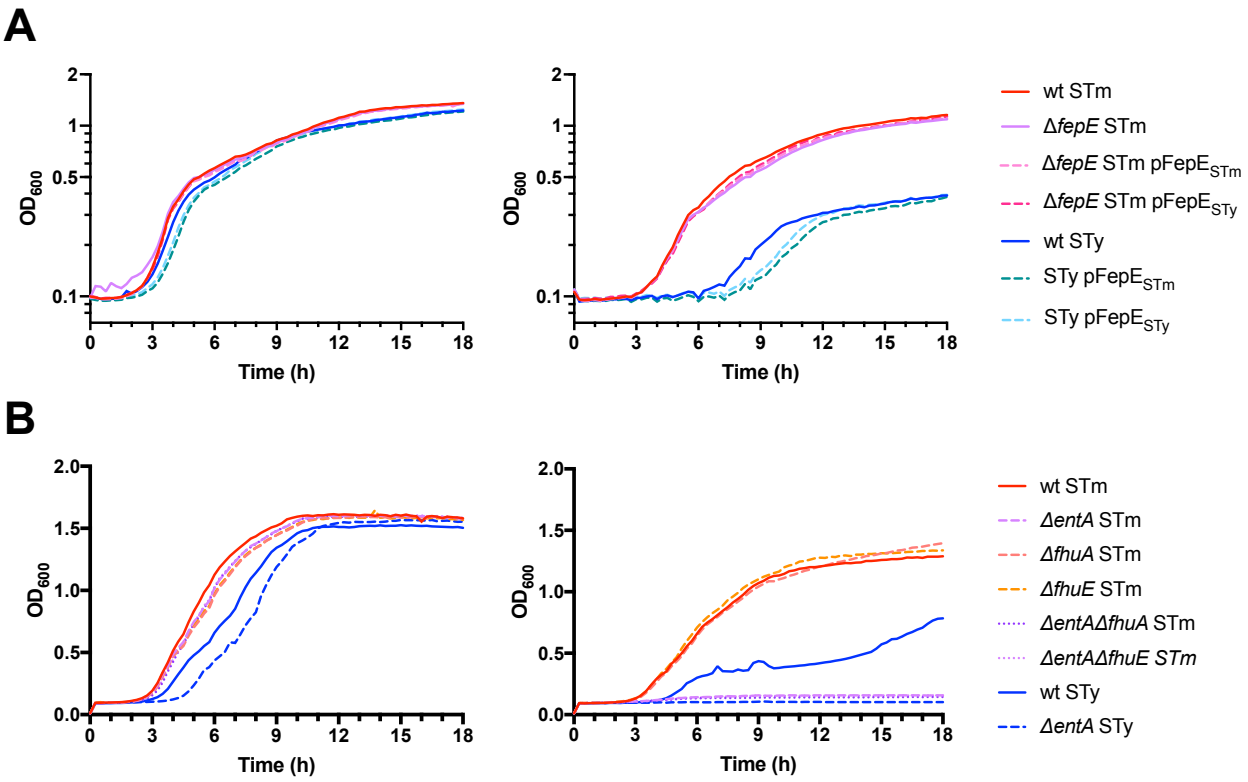

Figure 4-5. Pseudogenes in Iron Uptake Systems Do Not Make *S.* Typhi More Sensitive to Iron Limitation.

(**A**) Wild-type, isogenic mutants, or complementation plasmid-containing strains of *S.* Typhimurium and *S.* Typhi were grown in LB (left panel) or with 200 μM DP (right panel) with OD_{600} measured for 18 h. $pFepE_{STm}$ strains contain plasmid expressing *S.* Typhimurium-derived FepE; $pFepE_{STy}$ plasmids express FepE derived from *S.* Typhi. (**B**) Wild-type or isogenic mutant strains of *S.* Typhimurium and *S.* Typhi were grown in LB (left panel) or with 200 μM DP (right panel) with OD_{600} measured for 18 h. Data shown are the means of three biological replicates.

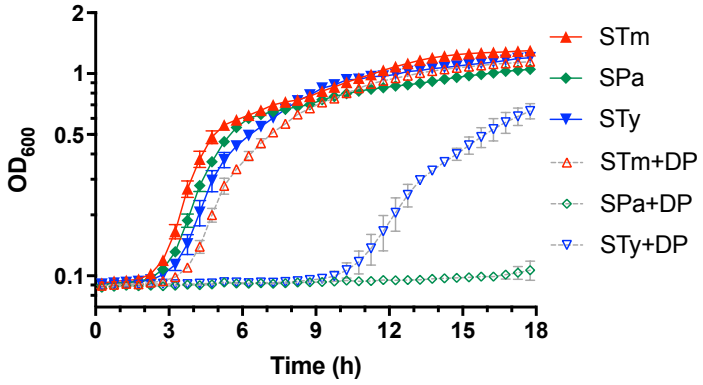

Figure 4-6. *S.* Paratyphi A Is Also Sensitive to Iron Restriction.

Wild-type *S.* Typhimurium (red), *S.* Typhi (blue), or *S.* Paratyphi A (green) were grown in LB with or without 300 μM DP. OD_{600} was measured for 18 h; means and error bars representing standard deviation of three biological samples of OD_{600} are shown for each sample.

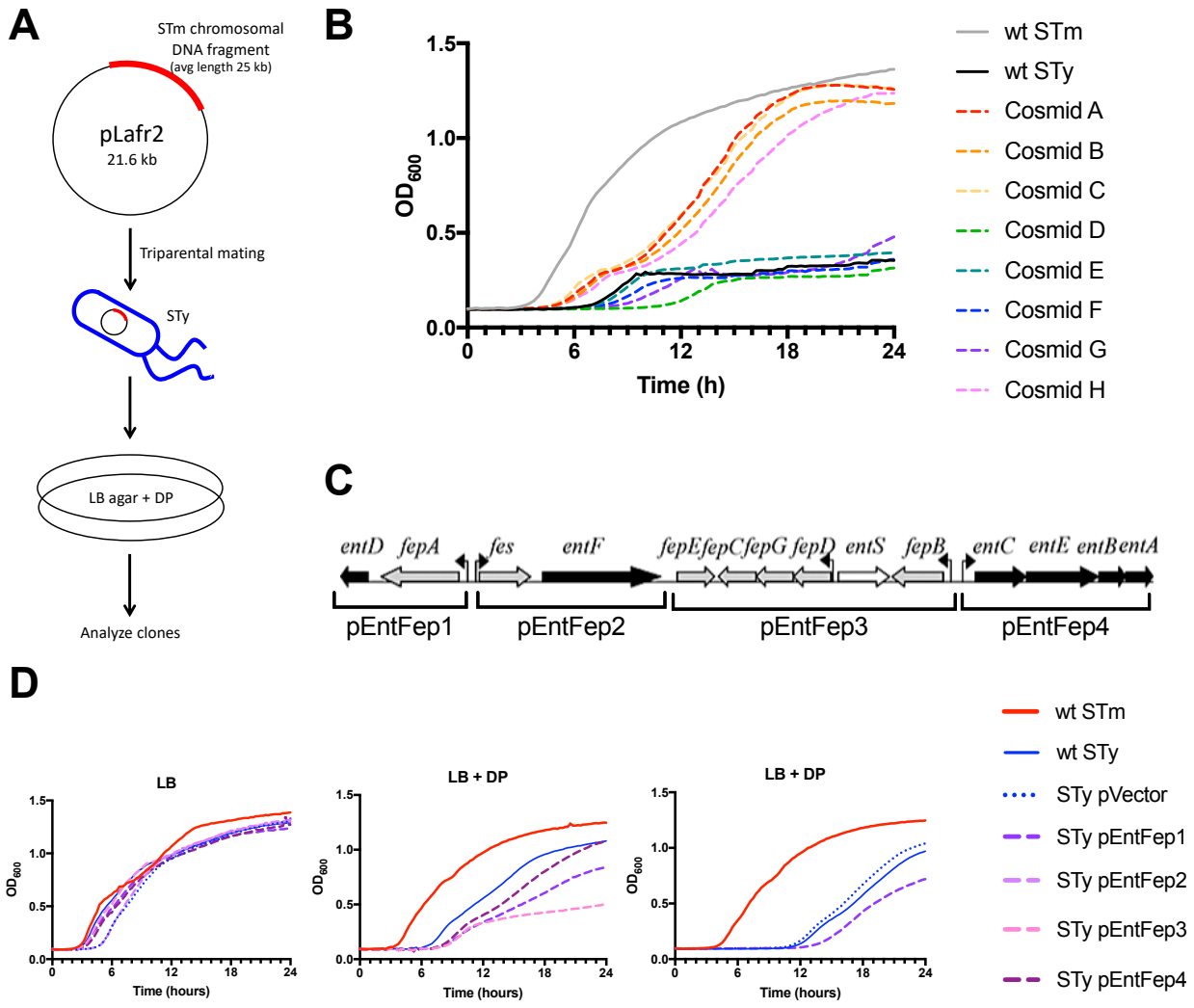

Figure 4-7. A Cosmid Library Screen for S. Typhimurium Loci that Enhance Growth of S. Typhi Under Iron Restriction.

(**A**) Schematic of the cosmid library screen. The pLAFR2 cosmid containing fragments of the *S.* Typhimurium 14028S genome was conjugated into *S.* Typhi by triparental mating. The library was screened by plating on LB agar with DP and growing overnight at 37°C. (**B**) Clones identified in the screen were tested for their ability to grow in LB media chelated with 200 μM DP. OD_{600} was measured for 24 h; the means of three biological replicates are shown. (**C**) Portions of the enterobactin synthesis and utilization operon were expressed *in trans* in *S.* Typhi. The top panel

shows the cloned fragments. OD_{600} was measured for 24 h; the means of three biological replicates are shown.

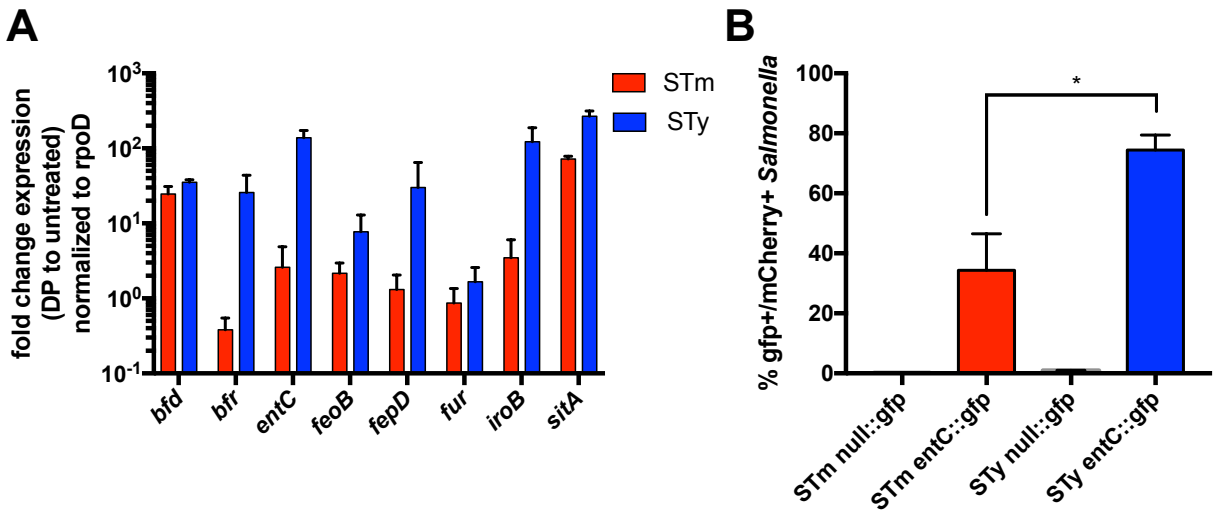

Figure 4-8. *S.* Typhi Upregulates Iron Acquisition Genes During Iron Limitation in vitro and During Macrophage Infection.

(**A**) Cultures of *S.* Typhimurium and *S.* Typhi were grown to mid-log and treated with 200 μM DP for 2 h. Expression of iron acquisition and storage genes were analyzed by qRT-PCR and normalized to expression of the housekeeping gene *rpoD*. Means and error bars representing standard deviations are shown for three biological replicates. (**B**) THP-1 macrophages were infected with *S.* Typhimurium or *S.* Typhi containing a reporter construct in which GFP expression is controlled by the *entC* promoter. Analysis of GFP expression from intracellular bacteria shows higher *entC* expression in *S.* Typhi than *S.* Typhimurium during macrophage infection. Medians and error bars representing standard deviation are shown from three biological replicates. Statistical significance (p) was determined by paired two-tailed Student's t test; * $p < 0.05$.

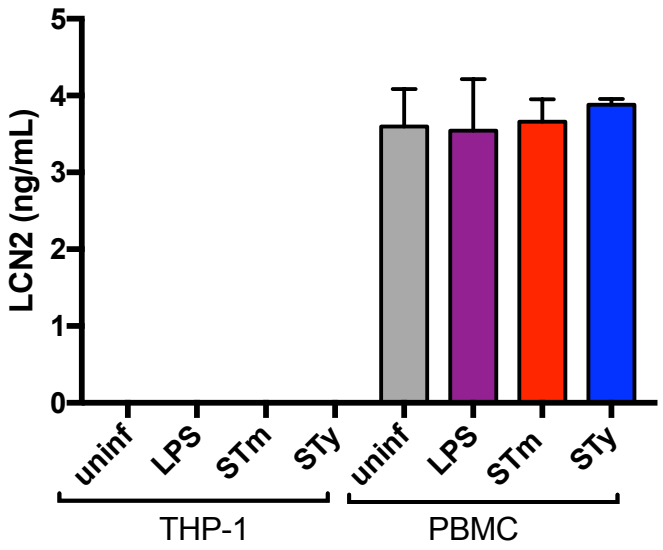

Figure 4-9. Effect of *Salmonella* Infection on Macrophage Lipocalin-2 Production.

THP-1- or PBMC-derived macrophages were treated with 100ng/mL LPS or infected with wild-type *S.* Typhimurium or *S.* Typhi for 24 h. Supernatants were analyzed for Lcn2 by ELISA. Only PBMC-derived macrophages produced Lcn2, and production was independent of stimulation. Shown are the means of two biological replicates with error bars representing the standard deviation.

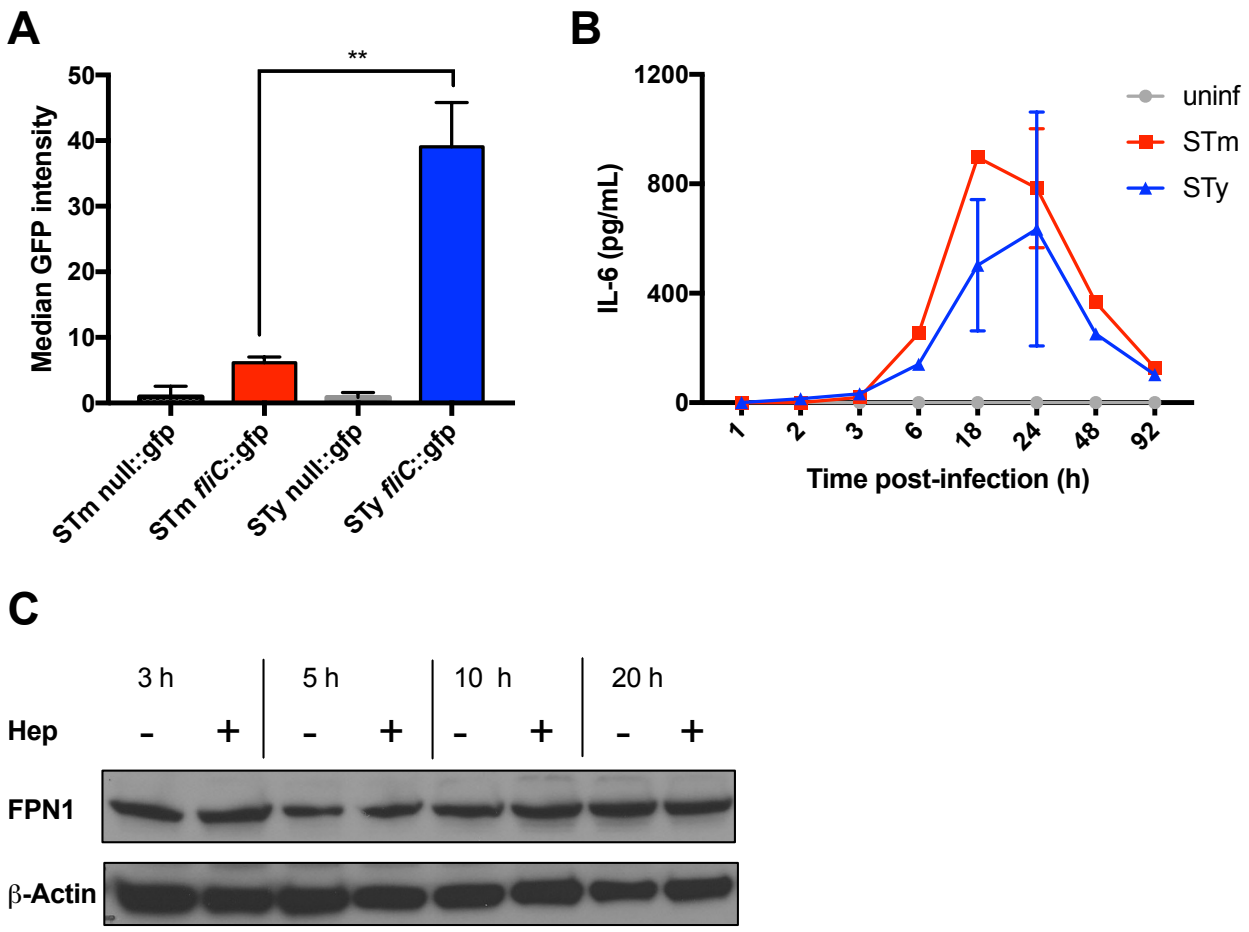

Figure 4-10. The Role of *Salmonella* Infection on Hepcidin-Dependent Degradation of Ferroportin-1.

(**A**) THP-1 macrophages were infected with *S.* Typhimurium or *S.* Typhi containing a reporter construct in which GFP expression is controlled by the *fliC* promoter of flagellin. Analysis of GFP expression from intracellular bacteria shows higher *fliC* expression in *S.* Typhi than *S.* Typhimurium during macrophage infection. Medians and error bars representing standard deviation are shown from three biological replicates. Statistical significance (p) was determined by paired two-tailed Student's t test; ** $p < 0.01$. (**B**) Supernatants from THP-1 macrophages infected with *S.* Typhi or *S.* Typhimurium were assayed for hIL-6 by ELISA. Means and error bars from two biological replicates are shown. (**C**) THP-1 macrophages were treated with 0.7 μM

human hepcidin for the indicated amount of time, and whole cell lysates were analyzed by Western Blot for Fpn1, with β-actin measured as a loading control.

4.8 TABLES

Table 4-1. Pseudogenes in *Salmonella enterica* Iron Uptake Systems.

Serovar	Iron uptake system pseudogene(s)
Typhi	*fepE, fhuA, fhuE*
Paratyphi A	*fhuA, fhuE*
Gallinarum	*iroD*
Typhisuis	*iroD, fhuE*

Table 4-2. Polymorphisms in Iron Uptake Systems: *S.* Typhimurium, *S.* Typhi, and *S.* Paratyphi A.

Polymorphisms presented as substitutions from *S.* Typhimurium genome.

Gene	Both STy and SPa	STy only	SPa only
EntD	R26H, T68A, M72I, T93S, L137S, N168D, T191M, D205G/S, V218F (9)	I104V, I106V, V172I, T176N (4)	L2R, R14W, G65D, R101Q (4)
FepA	D27E, N324D (2)	L452I (1)	0
Fes	V47A, L156R, P166S, P196T, S282N (5)	0	P34S (1)
YbdZ	D38G (1)	0	0
EntF	A42P, A443T, R590G (3)	H95L, A175V, L360F, A849V, E924D, A1104V, T1109I, E1177G, V1231A, G1249D (10)	M209I, D223G, R427C, A943T, R1102C, H1130N, R1155H (7)
FepE	0	Pseudogene – premature STOP at codon 79	0
FepC	0	0	R73H (1)
FepG	0	0	E34D, G36V, M200I (3)
FepD	0		S331N (1)
EntS	0	V310I (1)	I211L, S223C, P408S (3)
FepB	I16L, T178A, R231Q, K270N (4)	P4S (1)	A214T L222V (2)
EntC	0	S114P	V311A (1)
EntE	D223E, L398Q, V456A (3)	T141R, V149A, D173G, A401V, S260G	T40M (1)
EntB	0	V211I	0
EntA	T2A/P, G3S/C (2)	T74P, S95N, S145G (3)	F4I, A60G (2)
YbdB	I93V (1)	0	R30H (1)

IroB	0	G234S, V269I, A343T (3)	0
IroC	A404T, A476T, M803I, Q848K, S896T, G900E, _965G, L974R, I989T, P1065S, S1075I, R1079Q, D1188E, N1203A/D, I1205V, I1216V/M (16)	H63R, P613T, R639S, H1118Q, M1143I, R1148G (6)	T62P, N358T, P572S, N986K, A1005T, A1193T, G1213E (7)
IroD	G122D, A145T, R283Q, N334P, Y389C, S390C/N (6)	E119K, V204E, I245V (3)	T120A, R191C (2)
IroE	S177P (1)	R10C, M13V, I39M, V182I, V218A, T225A, L230P, D298G, Q306_, K307_, P308_, R309_, C310_, H311_ (14 – truncated)	T97A, P132S, A133V, D139E, D140S, N144S, V260I (7)
IroN	V19I, A606T (2)	M36I, G83S, V148M, Q187Y, T285N, D317G, Y469F, S634N (8)	G51S, I263L (2)
SitA	0	0	0
SitB	0	Q60R, K72Q, Q235L (3)	G31S (1)
SitC	0	A125T (1)	V104I, M222I (2)
SitD	A263V (1)	T4A (1)	I149V, A236T, G282V (3)
FeoA	0	0	0
FeoB	D186G, G694S, N759S, S761T (4)	0	0
TonB	E74_, P75_, _99K, _100P, K105E, V135M (6)	P12S, S140G, S187A, T238A (4)	0
ExbB	0	0	R200C (1)
ExbD	0	0	0
Fur	0	0	0

Table 4-3. Strains, Plasmids, and Resources.

Bacterial Strains		
Salmonella enterica serovar Typhimurium 14028s wild-type	S. Miller	TAS8
S. Typhimurium 14028s Δ*entC::FRTaphFRT*	This study	TAS58
S. Typhimurium 14028s Δ*entA::FRTaphFRT*	This study	TAS128
S. Typhimurium 14028s Δ*sitABCD::FRTaphFRT*	This study	TAS66
S. Typhimurium 14028s Δ*feoAB::FRTaphFRT*	This study	TAS68
S. Typhimurium 14028s Δ*iroB::FRTaphFRT*	This study	TAS62
S. Typhimurium 14028s Δ*fepE::FRTaphFRT*	This study	TAS242
S. Typhimurium 14028s Δ*fepE::FRTaphFRT* pFepE$_{STm}$	This study	TAS243
S. Typhimurium 14028s Δ*fepE::FRTaphFRT* pFepE$_{STy}$	This study	TAS244
S. Typhimurium 14028s Δ*fhuA::FRTaphFRT*	This study	TAS220
S. Typhimurium 14028s Δ*fhuE::FRTaphFRT*	This study	TAS221
S. Typhimurium 14028s Δ*entC::FRT*Δ*fhuA::FRTaphFRT*	This study	TAS258
S. Typhimurium 14028s Δ*entC::FRT*Δ*fhuE::FRTaphFRT*	This study	TAS259
S. Typhimurium 14028s pRU001::null	This study	TAS91
S. Typhimurium 14028s pRU001::*entC*	This study	TAS93
S. Typhimurium 14028s pSRB1	This study	TAS170
S. Typhimurium 14028s pDW6	This study	TAS172
Salmonella enterica serovar Typhi Ty2 wild-type JSG624	J. Gunn	TY01

S. Typhi Ty2 Nal^R	This study	TY196
S. Typhi Ty2 Δ*entC::FRTaphFRT*	This study	TY244
S. Typhi Ty2 Δ*entA::FRTaphFRT*	This study	TY262
S. Typhi Ty2 Δ*sitABCD::FRTaphFRT*	This study	TY221
S. Typhi Ty2 Δ*feoAB::FRTaphFRT*	This study	TY223
S. Typhi Ty2 Δ*iroB::FRTaphFRT*	This study	TY226
S. Typhi Ty2 $pFepE_{STm}$	This study	TY357
S. Typhi Ty2 $pFepE_{STy}$	This study	TY358
S. Typhi Ty2 pWSK219::empty	This study	TAS266
S. Typhi Ty2 pWSK129::EntFep1	This study	TAS267
S. Typhi Ty2 pWSK129::EntFep2	This study	TY384
S. Typhi Ty2 pWSK129::EntFep3	This study	TAS268
S. Typhi Ty2 pWSK129::EntFep4	This study	TAS269
S. Typhi Ty2 pRU001::null	This study	TY236
S. Typhi Ty2 pRU001::*entC*	This study	TY238
S. Typhi Ty2 pSRB1	This study	TY275
S. Typhi Ty2 pDW6	This study	TY274
Salmonella enterica serovar Paratyphi A ATCC9150 wild-type	ATCC	TY363
E. coli DH5α pLAFR2::14028S	[353]	14082S cosmid library
E. coli MU12 pRK2073		SL2115
Chemicals, Peptides, and Recombinant Proteins		
RPMI 1640, 1x with L-glutamine and 25mM HEPES	Corning	Cat#10-041-CV
Sodium Pyruvate 100mM solution	Corning	Cat#25-000-CI
MEM Non-Essential Amino Acids 100X	Gibco	Cat#11140-050
Penicillin Streptomycin	Corning	Cat#30-001-CI
Fetal Bovine Serum, heat-inactivated (USA sourced)	Millipore-Sigma	F4135
Phorbal 12-myristate 13-acetate	Millipore-Sigma	P1585
Human pooled serum	MP Biomedicals LLC	Cat#2930149
Phosphate-Buffered Saline	Corning	Cat#21-040-CV
Triton X-100	Fisher BioReagents	BP151-100
2,2-Dipyridyl	Millipore-Sigma	D216305
Paraformaldehyde, 16% solution	Electron Microscopy Sciences	Cat#15710
Ferric Chloride	Millipore-Sigma	Cat#F-7134
LB Broth, Miller	Fisher BioReagents	Cat#BP1426
LB Agar, Miller	Fisher BioReagents	Cat#BP1425
Ampicillin, sodium salt	Research Products International	Cat#A40040
Kanamycin sulfate	VWR	Cat#0408
SYBR Green 1		
Human Hepcidin	Peptides International Inc.	Cat#PLP-4392-s
Nitric Acid (Trace Metal Grade)	Fisher Chemical	Cat#A509-P500
Critical Commercial Assays		
DNeasy Blood & Tissue Kit	Qiagen	Cat#69504
MinElute PCR Purification Kit	Qiagen	Cat#28004
hIL-6 Quantikine ELISA Kit	R&D Systems	D6050

hLcn2 Quantikine ELISA Kit	R&D Systems	DLCN20
Antibodies		
Rabbit polyclonal anti-human Fpn1 (RRID: AB_11154326)	Invitrogen	Cat#PA5-22993
Experimental Models: Cell Lines		
THP-1 monocyte	ATCC	ATCC TIB-202
Recombinant DNA		
araC-P_{araB}-γβ*exo* oriR101 repA101ts *bla*	[300]	pKD46
FRTaphFRT PS1 PS2 oriR*bla*	[300]	pKD4
FRTaphFRT PS1 PS4 oriR*bla*	[300]	pKD13
Medium copy cloning vector ori pBR322 *bla*	[382]	pRB3-273C
Low copy cloning vector ori pSC101 *bla*	[308]	pWSK29
pWSK29::$FepE_{STm}$	This study	
pWSK29::$FepE_{STy}$	This study	
PrspM-mCherry Pgfp3 ori pBR322 *bla*	[383]	pRU001::null
PrspM-mCherry Pgfp3 ori pBR322 *bla*	[383]	pRU001::*entC*
p*fliC*::gfp (*gfp* mut3 downstream of *fliC* promoter in pRP3)	[384]	pSRB1
Promoterless *gfp* (pDW1 without pBR322 *tetA* promoter)	[384]	pDW6
Software and Algorithms		
FlowJo Version 10.3	Treestar, Inc.	https://www.flowjo.com/solutions/flowjo
Microsoft Excel Version 16.24	Office 365	https://www.office.com/
Prism Version 8.1.1	GraphPad	https://www.graphpad.com/
MacVector Version 17.05.5	MacVector, Inc.	https://macvector.com/

Table 4-4. Primers.

Primer	Sequence 5'-3'	Purpose
TSP162	GCCACTGGCGGATGGCGGCGTTCTGCTGGGCGCCAGCCCCGTGTAG GCTGGAGCTGCTTC	Deletion of *entC* from STm and STy
TSP177	GCGAAGAGGCAGGAACAATCCCGGCGCCGGCGAACAGGCGCATAT GAATATCCTCCTTAG	Deletion of *entC* from STm and STy
TSP303	GCTTTGATTTTTCAGACAAAACGGTATGGGTGACCGGGGCGTGTAG GCTGGAGCTGCTTC	Deletion of *entA* from STm and STy
TSP304	TCAGGCTCCCAATGTTGAACCGCCGTCCACCACGATATCCCATATG AATATCCTCCTTAG	Deletion of *entA* from STm and STy
TSP153	GATACTCGCGCTATCGCCAGCCTATGCAAAAGAGAAATTTGTGTAG GCTGGAGCTGCTTC	Deletion of *sitABCD* from STm and STy
TSP154	CCATGTTGCGTAAATAAATGCCGCAATAAACACGATGGCACATATG AATATCCTCCTTAG	Deletion of *sitABCD* from STm and STy
TSP180	ATGCAATTCACTCCTGACACTGCGTGGAAAATCACCGGCTGTGTAG GCTGGAGCTGCTTC	Deletion of *feoAB* from STm and STy
TSP183	TACGCCGCGCCCGCAGCCGTGTAGACATTGAACTGCTGGCCATATG AATATCCTCCTTAG	Deletion of *feoAB* from STm and STy

TSP170	GTCGGTCCACCACTGTATGGACTGCTATACCCTGTGCTGTGTGTAGG CTGGAGCTGCTTC	Deletion of *iroB* from STm and STy
TSP176	GACGCTTGCGATCAGGTGTACGTTCCCACCATTCTTCCCACATATGA ATATCCTCCTTAG	Deletion of *iroB* from STm and STy
TSP459	ATGCCATCTCTTAATGTAAAACAAGAAAAAAATCAGTCATGTGTGG CTGGAGCTGCTTC	Deletion of *fepE* from STm
TSP460	TCAGACTAACCGTTCATCTATCGCCAGCGCGTTTTCCATTCATATGA ATATCCTCCTTAG	Deletion of *fepE* from STm
TSP451	CTATCTGGATGGCCTGAAATTGCAGGGGAACTTCTACAACGTGTAG GCTGGAGCTGCTTC	Deletion of *fhuA* from STm
TSP452	TTAGAAACGGAAGGTTGCCGTTGCAACGACCTGACGTTCTCATATG AATATCCTCCTTAG	Deletion of *fhuA* from STm
TSP455	ATTCGACAGTAAAATGATGTATATCGATACGTTAGTCGATGTGTAG GCTGGAGCTGCTTC	Deletion of *fhuE* from STm
TSP456	TCAGAACTGATAATTGGCGGTGAGGCTGACGTTACGCGGTCATATG AATATCCTCCTTAG	Deletion of *fhuE* from STm
TSP230	GTG AAA TGG GCA CTG TTC AAC	Amplication of *rpoD* for qPCR
TSP231	TTC CAG CAG ATA GGT AAT GGC	Amplification of *rpoD* for qPCR
TSP238	TCA TCC ACA GTC ATT TCA ACA G	Amplification of *bfd* for qPCR
TSP239	GCG TTA ACT CAT CCT GCA TC	Amplification of *bfd* for qPCR
TSP240	TCG GTG AAG ATG TCG AAG AG	Amplification of *bfr* for qPCR
TSP241	CCT TCC TCG TCG GCA AG	Amplification of *bfr* for qPCR
TSP234	GTT GCG CAG AAT CCA GTT AG	Amplification of *entC* for qPCR
TSP235	TAA CGG CAG CGA ACT AAA CC	Amplification of *entC* for qPCR
TSP242	GGC AAG ACC ACC TTA TTT AAC C	Amplification of *feoB* for qPCR
TSP243	GAG ATG GTC GTC AGA GAA TAG G	Amplification of *feoB* for qPCR
TSP244	CCT GCA AAC GTT GAA AGT CG	Amplification of *fepD* for qPCR
TSP245	ACG GTA ATC GCC AGT AAA CC	Amplification of *fepD* for qPCR
TSP236	CAG GAA CCA GAT AAC CAT CAC G	Amplification of *fur* for qPCR
TSP237	AAA GTT ATG GCG GGT CAC G	Amplification of *fur* for qPCR
TSP228	GTG ACG AAA TCA CTT TCT AAC G	Amplification of *iroB* for qPCR
TSP229	ACG TAT TGC ATG GAG ATA ACC	Amplification of *iroB* for qPCR
TSP232	TCC ATG AGT ATC AGC CAA CG	Amplification of *sitA* for qPCR
TSP233	AGA CCA TTC GCG AGG ATA AG	Amplification of *sitA* for qPCR
RU032	AACCGAATTCAGTCTCACAATAGCGTCCTG	Cloning pRU001::*entC*
RU034	AACCGAATTCAAGCGATCGGGAGCAAGCGT	Cloning pRU001::*entC*
TSP512	CGA TAG TCG CCC ACA CAG ATG ACA AAG	Cloning *fepE* from STm and STy onto pWSK29
TSP 513	GAA ACT ATC GGG CCC ATC ATC AGC GAA C	Cloning *fepE* from STm and STy onto pWSK29

TSP471	TTATCGGGGTATTGCGCTAAGTATAGAAGCGG	Cloning “EntFep1” onto pWSK29
TSP472	CCCTGTGTTTATTATGAATTTTGTATATAAAAGGTG	Cloning “EntFep1” onto pWSK29
TSP473	CGTCAAAGGCATTGGCCGGGTGGTGAAATTGTG	Cloning “EntFep2” onto pWSK29
TSP474	ACTGATGACAAAGCCGGATATCGCTATCCGGCTTTTCGG	Cloning “EntFep2” onto pWSK29
TSP475	TGTGGGCGACTATCGCCGCCCCAGCGGTACCACC	Cloning “EntFep3” onto pWSK29
TSP476	TATCATCCTCCAATGATAAAGGCTTATATACAC	Cloning “EntFep3” onto pWSK29
TSP477	CTTCTCATTTTCATGTCAGCGGCAGCGAGATGC	Cloning “EntFep4” onto pWSK29
TSP478	CTATGGGATTACCGCCGTTCCCAGGCGACAGG	Cloning “EntFep4” onto pWSK29

Chapter 5. CONCLUSIONS AND FUTURE DIRECTIONS

5.1 SUMMARY OF FINDINGS

The work presented in this dissertation aims to understand the underlying mechanisms that lead to the distinct clinical syndromes caused by NTS and typhoidal *Salmonella* infection. Decades of research using the NTS serovar *S.* Typhimurium has provided a large body of *Salmonella* literature covering diverse topics. Yet research that focuses on *Salmonella* serovars that cause enteric fever has been significantly more limited. The work in this dissertation highlights some of the unique features of *S.* Typhi infection and aspects that distinguish it from assumptions made using the *S.* Typhimurium-murine model. Specifically, we show that the unique ability of *S.* Typhi to persist in human macrophages likely underlies its ability to cause persistent infection in the human host.

The development of a small animal model of *S.* Typhi infection had been a long-term goal in the *Salmonella* field, and the emergence of humanized mice has provided a unique opportunity for studies using typhoidal serovars. Engrafted mice adopt the human hematopoietic compartment, providing a replicative niche for typhoidal *Salmonella,* which has evolved to interact with human cells. In Chapter 2, we utilized hu-SRC-SCID humanized mice to perform the first genome-wide screen to identify *S.* Typhi virulence loci. While the TraDIS screen identified known virulence factors such as Vi, most importantly it demonstrated a reduced role for SPI2 in typhoid pathogenesis that differs significantly from findings using the *S.* Typhimurium-murine model.

Because of the requirement of human immune cells for *S.* Typhi infection, we further explored the interactions of both *S.* Typhi and *S.* Typhimurium with human macrophages in Chapter 3. *S.* Typhi is able to persist within human macrophages and avoid cell death, while *S.* Typhimurium-induced macrophage cell death is dependent on SPI2. The lack of full dependence

of *S.* Typhi on SPI2 demonstrated in Chapter 2 coincides with a substantial loss of SPI2-secreted effector proteins due to genomic decay. It is likely that the absence of pro-apoptotic effectors in *S.* Typhi and *S.* Paratyphi A, especially those that interfere with the NF-κB signaling pathway, allows these human-adapted serovars to persist in the host. Inhibition of NF-κB to induce apoptosis presents a potentially new strategy for targeting intracellular pathogens that persist by avoiding cell death.

Finally, the requirement for iron acquisition during *S.* Typhi infection demonstrated by the TraDIS screen in Chapter 2 led us to explore differences in iron acquisition by *S.* Typhi and *S.* Typhimurium in Chapter 4. We showed that *S.* Typhi is more sensitive to iron restriction, and explored the genetic basis for this distinction. Although we were unable to identify the genetic basis for sensitivity of *S.* Typhi to iron restriction, we present an extensive analysis of polymorphisms in iron-related genes among *S.* Typhi, *S.* Typhimurium, and *S.* Paratyphi A that could be analyzed for their contribution to iron acquisition. Polymorphisms that are shared between *S.* Typhi and *S.* Paratyphi A, both sensitive to low iron, should be the focus of studies that investigate iron uptake efficiency. We also present the intriguing concept of the effect of differential immune regulation by typhoidal *Salmonella* on iron availability in macrophages, which deserves further exploration.

Taken as a whole, these chapters represent valuable insights into the mechanisms governing acute versus persistent *Salmonella* infections. They also highlight the importance of using the appropriate model systems for understanding typhoid pathogenesis. A discussion of the potential future directions of this work is presented below.

5.2 Animal Models of Enteric Fever

5.2.1 Humanized Mouse Model

The hu-SRC-SCID humanized mouse model remains the only lethal model of *S.* Typhi infection and provides a unique tool to study typhoid pathogenesis, with many possible applications. We used this model to screen a mutant library of *S.* Typhi in Chapter 2 and to demonstrate skewing of the T_H1 immune response in Chapter 3. Given that not only hu-SRC-SCID but other humanized mouse models are permissive to *S.* Typhi infection, it appears that the presence of human immune cells is required for infection, most likely the macrophage niche. We are currently collaborating with Prof. Dirk Bumann (Universität Basel, Switzerland) to visualize the location of *S.* Typhi within infected hu-SRC-SCID organs, and determine whether *S.* Typhi preferentially infects human macrophages within these mice. Mice infected with fluorochrome-expressing *Salmonella* will be stained with fluorescently-conjugated anti-human antibodies and thick-section tomography will be used to identify the cell types in which *Salmonella* reside.

In Chapter 3, we described important differences in *S.* Typhi and *S.* Typhimurium interactions with human macrophages, including the ability of *S.* Typhi to persist in these cells due to the loss of pro-apoptotic SPI2 effectors. It will be of considerable interest to determine whether these phenomena occur in an *in vivo* model of infection. Our collaboration with Dr. Bumann presents the opportunity to identify not only the cells in which *Salmonella* reside within hu-SRC-SCID mice, but also whether these cells are undergoing apoptosis and immune activation. We will compare human macrophages from hu-SRC-SCID mice infected with wild-type and *ssrB* mutant *S.* Typhi and *S.* Typhimurium for levels of TUNEL, NF-κB, iNOS, IL-12 and pSTAT1. We predict that *S.* Typhi avoids apoptosis of human macrophages *in vivo* and that inflammatory activation markers would be lower in *S.* Typhi-infected cells compared to *S.* Typhimurium.

Preliminary studies in the lab have also explored the adaptive immune responses generated by hu-SRC-SCID mice against *S.* Typhi. Hu-SRC-SCID mice immunized with live attenuated *aroA* mutant *S.* Typhi were resistant to subsequent challenge with isogenic wild-type *S.* Typhi (unpublished, data not shown). Although hu-SRC-SCID mice possess human T and B cells, they lack full adaptive immunity, as the absence of the IL-2 receptor gamma chain molecule prevents development of gut-associated lymphoid tissue and limits antibody class type to IgM[121]. Still, the hu-SRC-SCID model holds promise for initial testing of novel vaccine candidates and for understanding adaptive immune responses to typhoid fever.

Despite the enormous potential of the hu-SRC-SCID model to advance our understanding of enteric fever, an awareness of the challenges and pitfalls of this model is critical. Production of these mice is laborious and costly, and the ever-changing source of donor stem cells results in variable susceptibility to *Salmonella* infection. Significant improvements in the levels of engraftment continue to be made, which can minimize the variability between individual mice, but also make it difficult to compare experiments over time. We have observed increased susceptibility of hu-SRC-SCID to *S.* Typhi as engraftment procedures have improved, making it difficult to estimate appropriate inocula prior to infection. Other limitations of the model are the requirement for i.p. inoculation due to the lack of gut-associated lymphoid tissue and the acute nature of the infection. Continued typhoid research will require careful selection of the appropriate model system for the question at hand.

5.2.2 Murine Persistence Models

To address questions involving oral infection with *S.* Typhi, our lab has recently developed an oral model of infection which supports bacterial persistence in the gut. We have shown that suppression of the normal gut microbiota by sustained aminoglycoside administration in C57BL/6

mice allows *S.* Typhi to persist indefinitely in the intestinal tract, while recovery of the gut flora corresponds to *S.* Typhi clearance (data not shown). This model provides an opportunity to study *S.* Typhi interactions with the gut and the gut microbiota. Infection of this model with the *S.* Typhi TraDIS library could be used to uncover loci required for gut persistence and for counteracting the antimicrobial activities of the normal flora.

There are no murine models to study long-term *Salmonella* persistence outside of the gut using *S.* Typhi at this time. The 129x1SvJ strain has a functional Nramp1 allele and supports sublethal systemic infection with *S.* Typhimurium, including bacterial persistence in macrophages in the spleen, liver, gallbladder, and MLNs, and sporadic shedding in the stool. *S.* Typhimurium was isolated from macrophages in the MLNs up to a year after infection[96], indicating *S.* Typhimurium persistence in murine macrophages similar to *S.* Typhi persistence in human macrophages as we describe. Understanding how SPI2 effectors affect bacterial persistence and macrophage cell death *in vivo* could be explored using this model.

5.2.3 Human Challenge Model

As the studies described here and elsewhere gravitate towards an ever better understanding of typhoid pathogenesis, there is hope of uncovering novel and improved vaccine candidates. The human challenge model will likely play a key role in preliminary testing of such candidates. Even so, like humanized mouse models, the human challenge model cannot serve as a model of chronic infection or of more severe disease sequelae, as volunteers are treated with antibiotics no later than 14 days after infection. Untreated prolonged fever can lead to severe neurological symptoms, intestinal hyperplasia and even perforation and peritonitis. Although studies presented here and elsewhere indicate typhoid toxin is not important for acute *S.* Typhi infection, it is possible the toxin plays a role in more severe forms of infection. One study found more CdtB-specific T cells

in human subjects who were bacteremic following typhoid challenge[385]. Given that hyperplasia is likely driven by the immune response to *S.* Typhi, the toxin could be one immune target driving this response. Use of the appropriate model to study particular questions about enteric fever will have to suffice until new models are proposed.

5.3 *SALMONELLA*-MACROPHAGE INTERACTIONS

5.3.1 SPI2 Effector Functions

The loss of a significant portion of the SPI2 effector compliment by typhoidal *Salmonella* appears to contribute to the ability of *S.* Typhi and *S.* Paratyphi A to persist within human macrophages and cause persistent infection. As highlighted in Chapter 3, a significant portion of the effectors still present in *S.* Typhimurium but absent in *S.* Typhi and *S.* Paratyphi A participate in inhibition of the NF-κB pathway. While many SPI2 effector functions have been described in the past several decades (**Table 1-1**), the functions of some effectors remain controversial or elusive. Out of the effectors absent in *S.* Typhi, very little is known about SrfJ and SteB, and SarA/SteE has only recently been studied more intensely[248–250]. It can be difficult to trust effector binding partners identified using techniques like yeast two-hybrid and overexpression in mammalian cells, which may not represent the true interactions and activities of effectors during an infection. The use of more sophisticated techniques such as click chemistry could help to identify primary effector functions[166].

More difficult than understanding the specific functions of individual effectors is understanding how their activities work in concert to contribute to the overall fate of the host cell. It is unknown whether all SPI2-active *Salmonella* secrete all effector proteins during host cell infection, or if distinct cells deliver different effector subsets. Bistable growth of *Salmonella* during

infection has been described for some time[386–389] and appears to represent bacteria which are slow-growing while expressing virulence genes and those that grow more rapidly while forgoing expression. This suggests differential regulation of effector expression even under the same environmental conditions. Additionally, the temporal nature of effector expression is complicated, with the precise timing of secretion and dependence on the prior secretion of other effectors unknown. Therefore, a more unified understanding of effector dynamics could help pinpoint the mechanistic consequences of a particular effector repertoire during macrophage infection.

Studies in Chapter 3 focused on removing effectors from *S.* Typhimurium that are absent in *S.* Typhi, but future studies should also aim to add these effectors to *S.* Typhi. We would hypothesize that complementation of *S.* Typhi with SPI2 effectors that are normally absent may reduce its ability to persist in the macrophage.

5.3.2 Functional Studies of Infected Human Macrophages

Besides approaching a better understanding of *Salmonella*-macrophage interactions from the perspective of effector function and kinetics, it will also be useful to approach studies from the host side as well. Our lab has only begun to fully utilize tools such as FACS analysis of *Salmonella*-infected cells to understand their polarization and functional capacity. Left open is the opportunity to measure more complex panels of macrophage markers coupled with infections using different *Salmonella* mutants to further understand how *Salmonella* factors affect macrophage activation. Future studies can also measure markers in macrophages isolated from infected hu-SRC-SCID mice, whether by FACS from digested organs or using immunohistochemistry on organ sections. Finally, the ability to sort out infected cells from hu-SRC-SCID mice opens up opportunities for whole-transcriptome analysis by RNAseq or proteomic analysis.

5.4 *SALMONELLA* PARATYPHI A

S. Paratyphi A infection poses a growing global health challenge as reports of drug-resistant isolates are on the rise[8]. Despite the ability to cause severe enteric fever, similar to typhoid[44], *S.* Paratyphi A is only distantly related to *S.* Typhi, and appears to have undergone convergent evolution resulting in similar loss of gene function[31]. Comparisons of the shared genetic strategies employed by *S.* Paratyphi A and *S.* Typhi to cause enteric fever have the potential to teach us a great deal about mechanisms of persistent infection in the host. Here we show that *S.* Paratyphi A infection relies on the presence of human immune cells and survival in human macrophages is enhanced compared to *S.* Typhimurium, similar to *S.* Typhi. Studies using *S.* Paratyphi A at this time are extremely limited, thus there is a great potential to apply strategies used in this dissertation to the study of *S.* Paratyphi A.

Having constructed a TraDIS library of both *S.* Typhi and *S.* Typhimurium, our lab is interested in similarly constructing a library of *S.* Paratyhi A for use in virulence screening. Infection of hu-SRC-SCID mice with the library would present the first such genome-wide screen of *S.* Paratyphi A virulence determinants. The previous TraDIS screen of *S.* Typhi mutants demonstrated strong counter-selection of numerous genes involved in serum resistance, including Vi, LPS and O-antigen synthesis (**Table 2-1**). Vi is not present in *S.* Paratyphi A, but the production of very long O-antigen mediated by genes *fepE* and *wzzB* is thought to serve a similar role[390]. In *S.* Typhi, *fepE* is a pseudogene, likely due to interference of very long O-antigen with Vi. Current work in the lab is focusing on the differences in mechanisms of serum resistance between *S.* Paratyphi A, *S.* Typhi, and *S.* Typhimurium.

Preliminary studies of *S.* Paratyphi A interactions with human macrophages are presented in Chapter 3, and there remains much to explore in this area. Functional studies of *S.* Paratyphi A-

infected human macrophages from both culture and hu-SRC-SCID mice are needed and could be carried out as described above.

5.5 *Salmonella* Iron Acquisition

The difference in sensitivity to iron restriction between *S.* Typhi and *S.* Typhimurium is striking, and is likely related to their adaptation to the host niche. Iron availability in the host is modulated by immune factors such as IFNγ, therefore, differences in iron availability during NTS versus typhoidal *Salmonella* infection could be a result of their differential modulation of the immune response. Many questions remain for this project, and potential future directions are discussed in detail in Chapter 4.

5.6 Final Thoughts

The rationale for making comparisons between NTS and typhoidal *Salmonella* pathogenesis is multifold. One, given the history of *Salmonella* studies using almost exclusively *S.* Typhimurium, it is valuable to make comparisons with typhoidal *Salmonella* serovars in order to advance our knowledge of typhoid pathogenesis. Two, it highlights the particular benefits and challenges of using different model systems to understand host-pathogen interactions. And three, an improved understanding of the mechanisms underlying chronic infection can potentially be applied to a wide array of intracellular pathogens. The studies presented in this dissertation are some of the first to challenge long-held assumptions about typhoid pathogenesis based on the *S.* Typhimurium model. We also present a unifying hypothesis that the absence of SPI2 effectors in typhoidal *Salmonella* serovars allows these serovars to persist within human macrophages to cause severe disease. Improvements to our understanding of typhoid pathogenesis will not only inform

therapeutic research for enteric fevers but potentially other persistent infections of global health importance.

APPENDIX

The following unpublished figures were conceived and generated by Larissa A. Singletary.

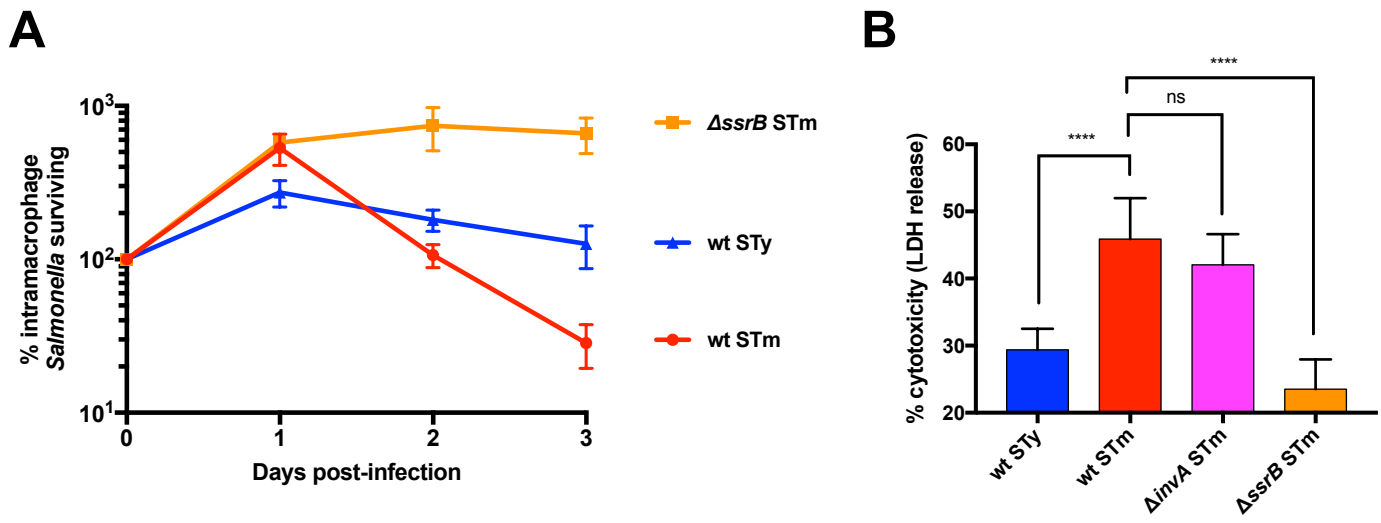

Figure A-1. *S.* Typhi Persists in Human Macrophages, *S.* Typhimurium Causes Macrophage Cell Death Dependent on SPI2. THP-1 cells were differentiated with PMA and infected with opsonized stationary-phase *Salmonella* at an MOI of 15:1. *S.* Typhi Ty2 = STy, *S.* Typhimurium 14028s = STm. (**A**) Macrophages were lysed at the indicated time post-infection and intracellular CFU enumerated. Survival is expressed as the proportion of intracellular *Salmonella* remaining compared to internalized bacteria 1 hpi. Shown are the means of three biological replicates, with error bars representing the standard deviation. (**B**) Macrophage cytotoxicity was measured as the amount of LDH released in supernatants 24 hpi with indicated strains. Shown are the means of three biological replicates, with error bars representing standard deviation; statistical significance (p) was determined by paired two-tailed Student's t test, **** $P < 0.0001$.

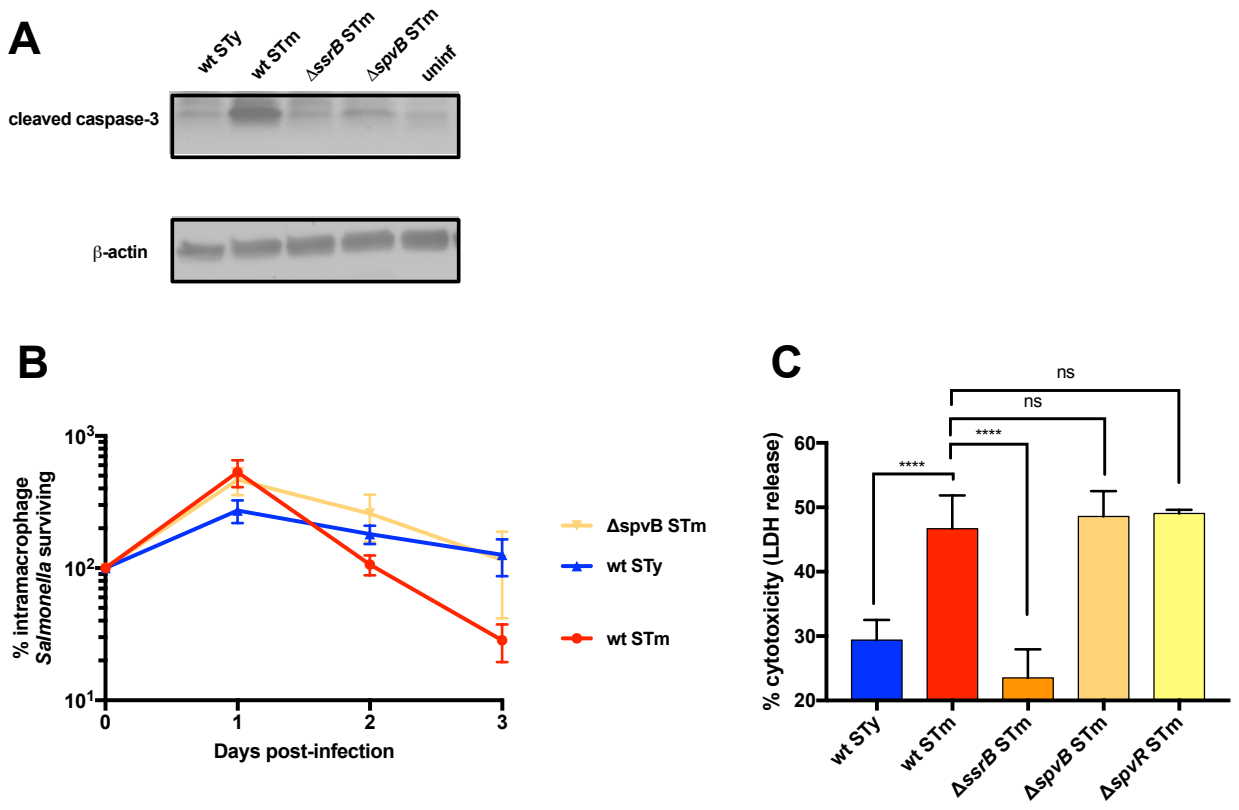

Figure A-2. The SPI2 Effector SpvB Induces Apoptosis and Prevents *S.* Typhimurium Persistence in Human Macrophages. THP-1 cells were differentiated with PMA and infected with opsonized stationary-phase *Salmonella* at an MOI of 15:1. *S.* Typhi Ty2 = STy, *S.* Typhimurium 14028s = STm. (**A**) Fifty µg of total protein from THP-1 cells infected with *Salmonella* for 24 h were subjected to Western blot analysis for cleaved caspase-3. Activation of caspase-3 is dependent on the effector SpvB, which is absent in S. Typhi. Measurement of β-actin was included as a loading control. (**B**) Macrophages were lysed at indicated time post-infection and intracellular CFU enumerated. Survival is expressed as the proportion of intracellular *Salmonella* remaining compared to internalized bacteria 1 hpi. (**C**) Macrophage cytotoxicity was measured as the amount of LDH released in supernatants 24 hpi with indicated strains. Shown are the means of three biological replicates, with error bars representing standard deviation; statistical significance (p) was determined by paired two-tailed Student's t test, **** $P < 0.0001$.

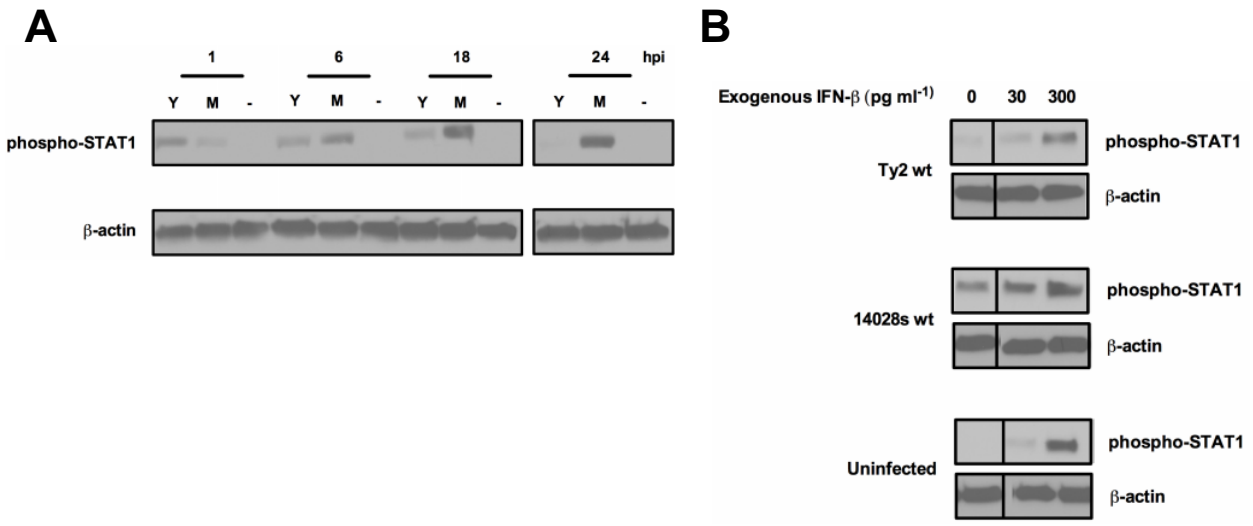

Figure A-3. *S.* Typhi Actively Inhibits STAT1 Phosphorylation. THP-1 cells were differentiated with PMA and infected with opsonized stationary-phase *Salmonella* at an MOI of 15:1. **(A)** Fifty µg of total protein from THP-1 cells infected with *Salmonella* for the indicated amount of time were subjected to Western Blot analysis for phosphorylated STAT1. Wild-type *S.* Typhi Ty2 = Y, wild-type *S.* Typhimurium 14028s = M, uninfected = –. (**B**) Thirty or 300 pg mL^{-1} were administered to THP-1 macrophages 18 hpi to stimulate STAT1 phosphorylation. Fifty µg of total protein from THP-1 cells 48 hpi were subjected to Western Blot analysis for phosphorylated STAT1. Measurement of β-actin was included as a loading control.

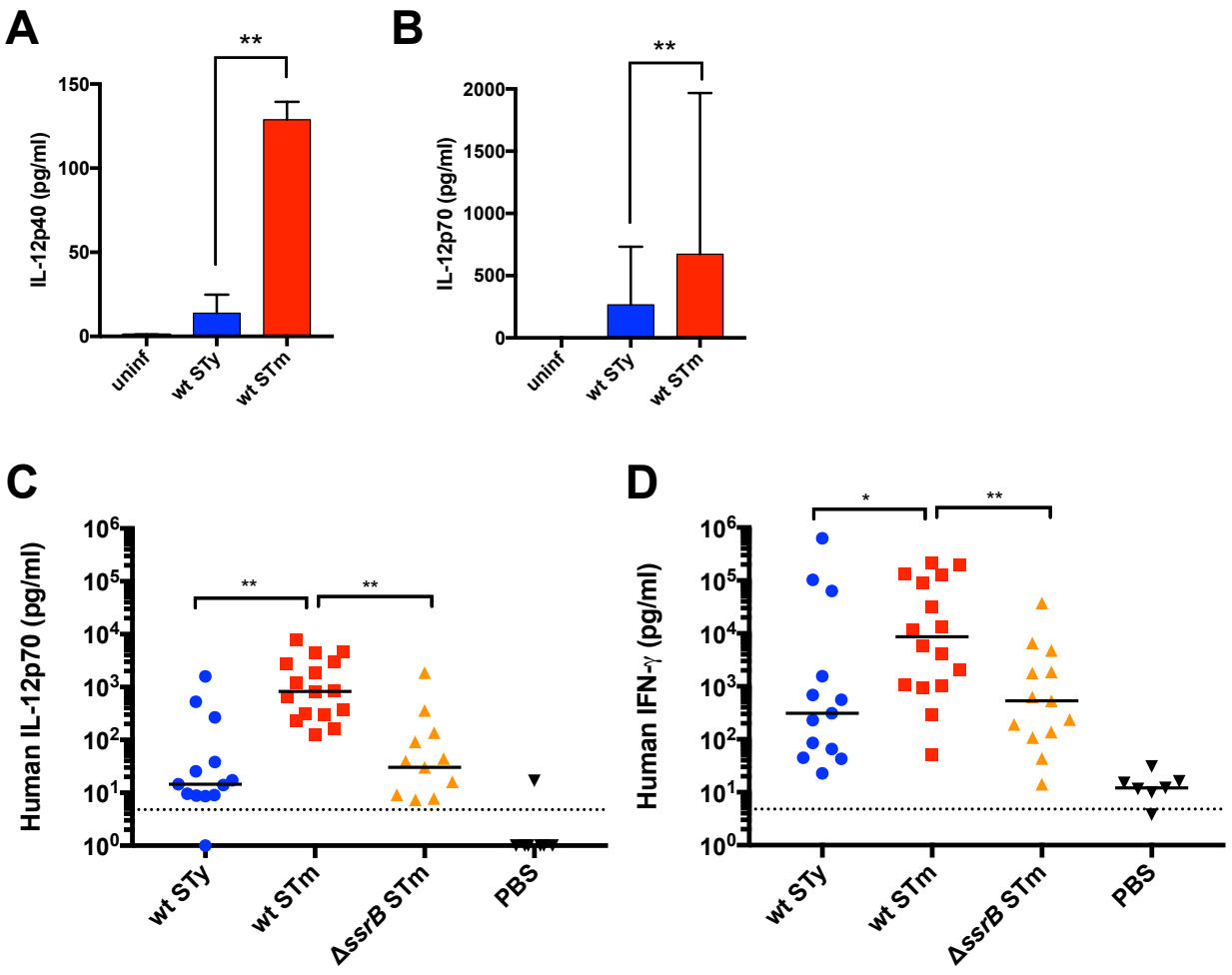

Figure A-4. *S.* Typhi Avoids an Inflammatory Response in Human Macrophages and Humanized Mice. *S.* Typhi Ty2 = STy, *S.* Typhimurium 14028s = STm, uninfected = uninf or PBS (mock-infected control). THP-1- (**A**) or PBMC- (**B**) derived macrophages were infected opsonized stationary-phase *Salmonella* at an MOI of 15:1. 24 hpi, culture supernatants were assayed for the presence of human IL-12 by ELISA. Shown are the means of three biological replicates, with error bars representing standard deviation; statistical significance (p) was determined by paired two-tailed Student's t test, ** $P < 0.01$. (**C** and **D**) Humanized hu-SRC-SCID mice were infected ip with wild-type *S.* Typhimurium, *ssrB* mutant *S.* Typhimurium, or wild-type

S. Typhi and sacrificed when moribund. Serum was analyzed for human cytokines IL-12p70 (**C**) or IFNγ (**D**) by multiplex microbead cytokine array (Luminex). Dotted line indicates assay limit of detection. Statistical significance (p) was determined suing a Kruskal-Wallis test, * $P < 0.05$, ** $P < 0.01$.

REFERENCES

1. Harris, J. B. & Brooks, W. A. Typhoid and Paratyphoid (Enteric) Fever. *Hunter's Tropical Medicine and Emerging Infectious Disease: Ninth Edition* 568–576 (2012) doi:10.1016/B978-1-4160-4390-4.00069-2.

2. Crump, J. A. Updating and refining estimates of typhoid fever burden for public health action. *Lancet Glob Health* **2**, e551–e553 (2014).

3. Stanaway, J. D. *et al.* The global burden of typhoid and paratyphoid fevers: a systematic analysis for the Global Burden of Disease Study 2017. *The Lancet Infectious Diseases* **19**, 369–381 (2019).

4. Crump, J. A., Luby, S. P. & Mintz, E. D. The global burden of typhoid fever. *Bull. World Health Organ.* **82**, 346–353 (2004).

5. Buckle, G. C., Walker, C. L. F. & Black, R. E. Typhoid fever and paratyphoid fever: Systematic review to estimate global morbidity and mortality for 2010. *J Glob Health* **2**, (2012).

6. Dougan, G. & Baker, S. *Salmonella enterica* serovar Typhi and the pathogenesis of typhoid fever. *Annu. Rev. Microbiol.* **68**, 317–336 (2014).

7. Parry, C. M., Hien, T. T., Dougan, G., White, N. J. & Farrar, J. J. Typhoid Fever. *New England Journal of Medicine* **347**, 1770–1782 (2002).

8. Fangtham, M. & Wilde, H. Emergence of *Salmonella paratyphi* A as a major cause of enteric fever: need for early detection, preventive measures, and effective vaccines. *J Travel Med* **15**, 344–350 (2008).

9. Wain, J., Hendriksen, R. S., Mikoleit, M. L., Keddy, K. H. & Ochiai, R. L. Typhoid fever. *The Lancet* **385**, 1136–1145 (2015).

10. Langridge, G.C. Metabolic capability in host-restricted serovars of *Salmonella enterica.* (Darwin College, Univerisity of Cambridge, 2010).

11. Bäumler, A. J., Tsolis, R. M., Ficht, T. A. & Adams, L. G. Evolution of host adaptation in *Salmonella enterica*. *Infect. Immun.* **66**, 4579–4587 (1998).

12. Bäumler, A. & Fang, F. C. Host Specificity of Bacterial Pathogens. *Cold Spring Harb Perspect Med* **3**, (2013).

13. Grimont, P. & Weill, F. Antigenic Formulae of the *Salmonella* Serovars. in *WHO Collaborating Centre for Reference and Research on Salmonella* (2007).

14. Zhang, S. *et al.* Molecular pathogenesis of *Salmonella enterica* serotype typhimurium-induced diarrhea. *Infect. Immun.* **71**, 1–12 (2003).

15. Roumagnac, P. *et al.* Evolutionary history of *Salmonella typhi*. *Science* **314**, 1301–1304 (2006).

16. Ochman, H. & Groisman, E. A. Distribution of pathogenicity islands in *Salmonella* spp. *Infect Immun* **64**, 5410–5412 (1996).

17. Forest, C. G., Ferraro, E., Sabbagh, S. C. & Daigle, F. Intracellular survival of *Salmonella enterica* serovar Typhi in human macrophages is independent of *Salmonella* pathogenicity island (SPI)-2. *Microbiology (Reading, Engl.)* **156**, 3689–3698 (2010).

18. Sabbagh, S. C., Forest, C. G., Lepage, C., Leclerc, J.-M. & Daigle, F. So similar, yet so different: uncovering distinctive features in the genomes of *Salmonella enterica* serovars Typhimurium and Typhi. *FEMS Microbiol. Lett.* **305**, 1–13 (2010).

19. Tanner, J. R. & Kingsley, R. A. Evolution of *Salmonella* within Hosts. *Trends Microbiol.* **26**, 986–998 (2018).

20. Robbins, J. D. & Robbins, J. B. Reexamination of the protective role of the capsular polysaccharide (Vi antigen) of *Salmonella typhi*. *J. Infect. Dis.* **150**, 436–449 (1984).

21. Looney, R. J. & Steigbigel, R. T. Role of the Vi antigen of *Salmonella typhi* in resistance to host defense in vitro. *J. Lab. Clin. Med.* **108**, 506–516 (1986).

22. Sharma, A. & Qadri, A. Vi polysaccharide of *Salmonella typhi* targets the prohibitin family of molecules in intestinal epithelial cells and suppresses early inflammatory responses. *Proc. Natl. Acad. Sci. U.S.A.* **101**, 17492–17497 (2004).

23. Raffatellu, M. *et al.* The Vi capsular antigen of *Salmonella enterica* serotype Typhi reduces Toll-like receptor-dependent interleukin-8 expression in the intestinal mucosa. *Infect. Immun.* **73**, 3367–3374 (2005).

24. Wangdi, T. *et al.* The Vi Capsular Polysaccharide Enables *Salmonella enterica* Serovar Typhi to Evade Microbe-Guided Neutrophil Chemotaxis. *PLOS Pathogens* **10**, e1004306 (2014).

25. Haghjoo, E. & Galán, J. E. *Salmonella typhi* encodes a functional cytolethal distending toxin that is delivered into host cells by a bacterial-internalization pathway. *Proc. Natl. Acad. Sci. U.S.A.* **101**, 4614–4619 (2004).

26. Song, J., Gao, X. & Galán, J. E. Structure and function of the *Salmonella* Typhi chimaeric A(2)B(5) typhoid toxin. *Nature* **499**, 350–354 (2013).

27. Deng, L. *et al.* Host adaptation of a bacterial toxin from the human pathogen *Salmonella* Typhi. *Cell* **159**, 1290–1299 (2014).

28. Galán, J. E. Typhoid toxin provides a window into typhoid fever and the biology of *Salmonella* Typhi. *PNAS* **113**, 6338–6344 (2016).

29. Parkhill, J. *et al.* Genome sequence of *Yersinia pestis*, the causative agent of plague. *Nature* **413**, 523–527 (2001).

30. McClelland, M. *et al.* Complete genome sequence of *Salmonella enterica* serovar Typhimurium LT2. *Nature* **413**, 852–856 (2001).

31. Holt, K. E. *et al.* Pseudogene accumulation in the evolutionary histories of *Salmonella enterica* serovars Paratyphi A and Typhi. *BMC Genomics* **10**, 36 (2009).

32. Spanò, S. Host restriction in *Salmonella*: insights from Rab GTPases. *Cellular Microbiology* **16**, 1321–1328 (2014).

33. Hoiseth, S. K. & Stocker, B. a. D. Aromatic-dependent *Salmonella typhimurium* are non-virulent and effective as live vaccines. *Nature* **291**, 238–239 (1981).

34. Fowler, C. C. & Galán, J. E. Decoding a *Salmonella* Typhi Regulatory Network that Controls Typhoid Toxin Expression within Human Cells. *Cell Host Microbe* **23**, 65-76.e6 (2018).

35. Spanò, S. & Galán, J. E. A Rab32-dependent pathway contributes to *Salmonella typhi* host restriction. *Science* **338**, 960–963 (2012).

36. Ramachandran, G., Aheto, K., Shirtliff, M. E. & Tennant, S. M. Poor biofilm-forming ability and long-term survival of invasive *Salmonella* Typhimurium ST313. *Pathog Dis* **74**, (2016).

37. Tükel, C. *et al.* Neutrophil influx during non-typhoidal salmonellosis: who is in the driver's seat? *FEMS Immunol. Med. Microbiol.* **46**, 320–329 (2006).

38. Chanput, W., Mes, J. J. & Wichers, H. J. THP-1 cell line: an in vitro cell model for immune modulation approach. *Int. Immunopharmacol.* **23**, 37–45 (2014).

39. Lee, S. D. & Surawicz, C. M. Infectious causes of chronic diarrhea. *Gastroenterology Clinics of North America* **30**, 679–692 (2001).

40. Feasey, N. A., Dougan, G., Kingsley, R. A., Heyderman, R. S. & Gordon, M. A. Invasive non-typhoidal *Salmonella* disease: an emerging and neglected tropical disease in Africa. *Lancet* **379**, 2489–2499 (2012).

41. Singletary, L. A. *et al.* Loss of Multicellular Behavior in Epidemic African Nontyphoidal *Salmonella enterica* Serovar Typhimurium ST313 Strain D23580. *mBio* **7**, (2016).

42. Gunn, J. S. *et al. Salmonella* chronic carriage: epidemiology, diagnosis, and gallbladder persistence. *Trends Microbiol.* **22**, 648–655 (2014).

43. Chanh, N. Q. *et al.* A Clinical, Microbiological, and Pathological Study of Intestinal Perforation Associated with Typhoid Fever. *Clin Infect Dis* **39**, 61–67 (2004).

44. Maskey, A. P. *et al. Salmonella enterica* serovar Paratyphi A and *S. enterica* serovar Typhi cause indistinguishable clinical syndromes in Kathmandu, Nepal. *Clin. Infect. Dis.* **42**, 1247–1253 (2006).

45. Woods, C. W. *et al.* Emergence of *Salmonella enterica* serotype Paratyphi A as a major cause of enteric fever in Kathmandu, Nepal. *Trans. R. Soc. Trop. Med. Hyg.* **100**, 1063–1067 (2006).

46. Khatri, N. S. *et al.* Gallbladder carriage of *Salmonella paratyphi* A may be an important factor in the increasing incidence of this infection in South Asia. *Annals of Internal Medicine* **150**, 567–568 (2009).

47. Marineli, F., Tsoucalas, G., Karamanou, M. & Androutsos, G. Mary Mallon (1869-1938) and the history of typhoid fever. *Ann Gastroenterol* **26**, 132–134 (2013).

48. Lai, C. W., Chan, R. C., Cheng, A. F., Sung, J. Y. & Leung, J. W. Common bile duct stones: a cause of chronic salmonellosis. *Am. J. Gastroenterol.* **87**, 1198–1199 (1992).

49. Crawford, R. W. *et al.* Gallstones play a significant role in *Salmonella* spp. gallbladder colonization and carriage. *PNAS* **107**, 4353–4358 (2010).

50. Prouty, A. M., Schwesinger, W. H. & Gunn, J. S. Biofilm formation and interaction with the surfaces of gallstones by *Salmonella* spp. *Infect. Immun.* **70**, 2640–2649 (2002).

51. Tynes, B. S. & Utz, J. P. Factors influencing the cure of *Salmonella* carriers. *Ann. Intern. Med.* **57**, 871–882 (1962).

52. Gopinath, S., Carden, S. & Monack, D. Shedding light on *Salmonella* carriers. *Trends Microbiol.* **20**, 320–327 (2012).

53. Levine, M. M., Black, R. E. & Lanata, C. Precise estimation of the numbers of chronic carriers of *Salmonella typhi* in Santiago, Chile, an endemic area. *J. Infect. Dis.* **146**, 724–726 (1982).

54. Jones, B. D., Ghori, N. & Falkow, S. *Salmonella typhimurium* initiates murine infection by penetrating and destroying the specialized epithelial M cells of the Peyer's patches. *J Exp Med* **180**, 15–23 (1994).

55. Que, F., Wu, S. & Huang, R. *Salmonella* pathogenicity island 1(SPI-1) at work. *Curr. Microbiol.* **66**, 582–587 (2013).

56. Haraga, A., Ohlson, M. B. & Miller, S. I. Salmonellae interplay with host cells. *Nat. Rev. Microbiol.* **6**, 53–66 (2008).

57. House, D., Bishop, A., Parry, C., Dougan, G. & Wain, J. Typhoid fever: pathogenesis and disease. *Current Opinion in Infectious Diseases* **14**, 573 (2001).

58. Wangdi, T., Winter, S. E. & Bäumler, A. J. Typhoid fever: 'you can't hit what you can't see'. *Gut Microbes* **3**, 88–92 (2012).

59. Raffatellu, M., Wilson, R. P., Winter, S. E. & Bäumler, A. J. Clinical pathogenesis of typhoid fever. *J Infect Dev Ctries* **2**, 260–266 (2008).

60. Tam, M. A., Rydström, A., Sundquist, M. & Wick, M. J. Early cellular responses to *Salmonella* infection: dendritic cells, monocytes, and more. *Immunol. Rev.* **225**, 140–162 (2008).

61. Vazquez-Torres, A. *et al.* Extraintestinal dissemination of *Salmonella* by CD18-expressing phagocytes. *Nature* **401**, 804–808 (1999).

62. Watson, K. G. & Holden, D. W. Dynamics of growth and dissemination of *Salmonella* in vivo. *Cell. Microbiol.* **12**, 1389–1397 (2010).

63. Cirillo, D. M., Valdivia, R. H., Monack, D. M. & Falkow, S. Macrophage-dependent induction of the *Salmonella* pathogenicity island 2 type III secretion system and its role in intracellular survival. *Mol. Microbiol.* **30**, 175–188 (1998).

64. Vazquez-Torres, A. *et al. Salmonella* pathogenicity island 2-dependent evasion of the phagocyte NADPH oxidase. *Science* **287**, 1655–1658 (2000).

65. Cheminay, C., Chakravortty, D. & Hensel, M. Role of neutrophils in murine salmonellosis. *Infect. Immun.* **72**, 468–477 (2004).

66. Daley, J. M., Thomay, A. A., Connolly, M. D., Reichner, J. S. & Albina, J. E. Use of Ly6G-specific monoclonal antibody to deplete neutrophils in mice. *J. Leukoc. Biol.* **83**, 64–70 (2008).

67. Sierro, F. *et al.* Flagellin stimulation of intestinal epithelial cells triggers CCL20-mediated migration of dendritic cells. *PNAS* **98**, 13722–13727 (2001).

68. Srinivasan, A., Foley, J. & McSorley, S. J. Massive number of antigen-specific CD4 T cells during vaccination with live attenuated *Salmonella* causes interclonal competition. *J. Immunol.* **172**, 6884–6893 (2004).

69. Srinivasan, A., Nanton, M., Griffin, A. & McSorley, S. J. Culling of Activated CD4 T Cells during Typhoid Is Driven by *Salmonella* Virulence Genes. *The Journal of Immunology* **182**, 7838–7845 (2009).

70. McSorley, S. J., Cookson, B. T. & Jenkins, M. K. Characterization of CD4+ T cell responses during natural infection with *Salmonella typhimurium*. *J. Immunol.* **164**, 986–993 (2000).

71. Ravindran, R. & McSorley, S. J. Tracking the dynamics of T-cell activation in response to *Salmonella* infection. *Immunology* **114**, 450–458 (2005).

72. MacLennan, C. A. *et al.* The neglected role of antibody in protection against bacteremia caused by nontyphoidal strains of *Salmonella* in African children. *J Clin Invest* **118**, 1553–1562 (2008).

73. Gondwe, E. N. *et al.* Importance of antibody and complement for oxidative burst and killing of invasive nontyphoidal *Salmonella* by blood cells in Africans. *Proc. Natl. Acad. Sci. U.S.A.* **107**, 3070–3075 (2010).

74. MacLennan, C. A. *et al.* Dysregulated Humoral Immunity to Nontyphoidal *Salmonella* in HIV-Infected African Adults. *Science* **328**, 508–512 (2010).

75. Pulickal, A. S. *et al.* Kinetics of the natural, humoral immune response to *Salmonella enterica* serovar Typhi in Kathmandu, Nepal. *Clin. Vaccine Immunol.* **16**, 1413–1419 (2009).

76. Pham, O. H. & McSorley, S. J. Protective host immune responses to *Salmonella* infection. *Future Microbiol* **10**, 101–110 (2015).

77. Johanns, T. M., Ertelt, J. M., Rowe, J. H. & Way, S. S. Regulatory T Cell Suppressive Potency Dictates the Balance between Bacterial Proliferation and Clearance during Persistent *Salmonella* Infection. *PLoS Pathog* **6**, (2010).

78. Mastroeni, P., Harrison, J. A., Chabalgoity, J. A. & Hormaeche, C. E. Effect of interleukin 12 neutralization on host resistance and gamma interferon production in mouse typhoid. *Infect Immun* **64**, 189–196 (1996).

79. Benoit, M., Desnues, B. & Mege, J.-L. Macrophage Polarization in Bacterial Infections. *The Journal of Immunology* **181**, 3733–3739 (2008).

80. Martinez, F. O. Regulators of macrophage activation. *Eur. J. Immunol.* **41**, 1531–1534 (2011).

81. Dougan, G., John, V., Palmer, S. & Mastroeni, P. Immunity to salmonellosis. *Immunol. Rev.* **240**, 196–210 (2011).

82. MacLennan, C. *et al.* Interleukin (IL)-12 and IL-23 are key cytokines for immunity against *Salmonella* in humans. *J. Infect. Dis.* **190**, 1755–1757 (2004).

83. Ali, S. *et al.* Polymorphisms in proinflammatory genes and susceptibility to typhoid fever and paratyphoid fever. *J. Interferon Cytokine Res.* **27**, 271–279 (2007).

84. Gordon, M. A. *Salmonella* infections in immunocompromised adults. *Journal of Infection* **56**, 413–422 (2008).

85. Reddy, E. A., Shaw, A. V. & Crump, J. A. Community-acquired bloodstream infections in Africa: a systematic review and meta-analysis. *Lancet Infect Dis* **10**, 417–432 (2010).

86. WHO | Typhoid. *WHO* http://www.who.int/mediacentre/factsheets/typhoid/en/.

87. Mirza, S. H., Beeching, N. J. & Hart, C. A. Multi-drug resistant typhoid: a global problem. *J. Med. Microbiol.* **44**, 317–319 (1996).

88. Dyson, Z. A., Klemm, E. J., Palmer, S. & Dougan, G. Antibiotic Resistance and Typhoid. *Clin Infect Dis* **68**, S165–S170 (2019).

89. Guzman, C. A. *et al.* Vaccines against typhoid fever. *Vaccine* **24**, 3804–3811 (2006).

90. Yang, Y.-A., Chong, A. & Song, J. Why Is Eradicating Typhoid Fever So Challenging: Implications for Vaccine and Therapeutic Design. *Vaccines (Basel)* **6**, (2018).

91. Pakkanen, S. H., Kantele, J. M. & Kantele, A. Cross-reactive gut-directed immune response against *Salmonella enterica* serovar Paratyphi A and B in typhoid fever and after oral Ty21a typhoid vaccination. *Vaccine* **30**, 6047–6053 (2012).

92. Mittrücker, H. W. & Kaufmann, S. H. Immune response to infection with *Salmonella typhimurium* in mice. *J. Leukoc. Biol.* **67**, 457–463 (2000).

93. Santos, R. L. *et al.* Animal models of *Salmonella* infections: enteritis versus typhoid fever. *Microbes Infect.* **3**, 1335–1344 (2001).

94. O'Brien, A. D., Rosenstreich, D. L. & Taylor, B. A. Control of natural resistance to *Salmonella typhimurium* and *Leishmania donovani* in mice by closely linked but distinct genetic loci. *Nature* **287**, 440–442 (1980).

95. Hone, D. M., Harris, A. M., Chatfield, S., Dougan, G. & Levine, M. M. Construction of genetically defined double aro mutants of *Salmonella typhi*. *Vaccine* **9**, 810–816 (1991).

96. Monack, D. M., Bouley, D. M. & Falkow, S. *Salmonella typhimurium* persists within macrophages in the mesenteric lymph nodes of chronically infected Nramp1+/+ mice and can be reactivated by IFNγ neutralization. *J. Exp. Med.* **199**, 231–241 (2004).

97. Simon, R., Tennant, S. M., Galen, J. E. & Levine, M. M. Mouse models to assess the efficacy of non-typhoidal *Salmonella* vaccines: revisiting the role of host innate susceptibility and routes of challenge. *Vaccine* **29**, 5094–5106 (2011).

98. Tennant, S. M. & Levine, M. M. Live attenuated vaccines for invasive *Salmonella* infections. *Vaccine* **33 Suppl 3**, C36-41 (2015).

99. Mathur, R. *et al.* A mouse model of *Salmonella typhi* infection. *Cell* **151**, 590–602 (2012).

100. Song, J. *et al.* Absence of TLR11 in mice does not confer susceptibility to *Salmonella* Typhi. *Cell* **164**, 827–828 (2016).

101. Mathur, R., Zeng, W., Hayden, M. S. & Ghosh, S. Mice Lacking TLR11 Exhibit Variable *Salmonella typhi* Susceptibility. *Cell* **164**, 829–830 (2016).

102. Higginson, E. E., Simon, R. & Tennant, S. M. Animal Models for Salmonellosis: Applications in Vaccine Research. *Clin. Vaccine Immunol.* **23**, 746–756 (2016).

103. Grover, A. *et al.* Humanized NOG mice as a model for tuberculosis vaccine-induced immunity: a comparative analysis with the mouse and guinea pig models of tuberculosis. *Immunology* **152**, 150–162 (2017).

104. Berges, B. K. & Rowan, M. R. The utility of the new generation of humanized mice to study HIV-1 infection: transmission, prevention, pathogenesis, and treatment. *Retrovirology* **8**, 65 (2011).

105. Zeisel, M. B., Da Costa, D. & Baumert, T. F. Opening the door for hepatitis C virus infection in genetically humanized mice. *Hepatology* **54**, 1873–1875 (2011).

106. Jiménez-Díaz, M. B. *et al.* Improved Murine Model of Malaria Using *Plasmodium falciparum* Competent Strains and Non-Myelodepleted NOD-scid IL2Rγnull Mice Engrafted with Human Erythrocytes. *Antimicrob Agents Chemother* **53**, 4533–4536 (2009).

107. Bosma, M. J. & Carroll, A. M. The SCID mouse mutant: definition, characterization, and potential uses. *Annu. Rev. Immunol.* **9**, 323–350 (1991).

108. van der Loo, J. C. *et al.* Nonobese diabetic/severe combined immunodeficiency (NOD/SCID) mouse as a model system to study the engraftment and mobilization of human peripheral blood stem cells. *Blood* **92**, 2556–2570 (1998).

109. Ito, M. *et al.* NOD/SCID/γ_c^{null} mouse: an excellent recipient mouse model for engraftment of human cells. *Blood* **100**, 3175–3182 (2002).

110. Brehm, M. A. *et al.* Parameters for establishing humanized mouse models to study human immunity: analysis of human hematopoietic stem cell engraftment in three immunodeficient strains of mice bearing the IL2rγ^{null} mutation. *Clin. Immunol.* **135**, 84–98 (2010).

111. P, M. *et al.* RAG-1-deficient Mice Have No Mature B and T Lymphocytes. *Cell* vol. 68 https://pubmed.ncbi.nlm.nih.gov/1547488/ (1992).

112. Y, S. *et al.* RAG-2-deficient Mice Lack Mature Lymphocytes Owing to Inability to Initiate V(D)J Rearrangement. *Cell* vol. 68 https://pubmed.ncbi.nlm.nih.gov/1547487/ (1992).

113. Yong, K. S. M., Her, Z. & Chen, Q. Humanized Mice as Unique Tools for Human-Specific Studies. *Arch Immunol Ther Exp (Warsz)* **66**, 245–266 (2018).

114. Libby, S. J. *et al.* Humanized nonobese diabetic-scid IL2rγ^{null} mice are susceptible to lethal *Salmonella* Typhi infection. *PNAS* **107**, 15589–15594 (2010).

115. Vladoianu, I. R., Chang, H. R. & Pechère, J. C. Expression of host resistance to *Salmonella typhi* and *Salmonella typhimurium*: bacterial survival within macrophages of murine and human origin. *Microb. Pathog.* **8**, 83–90 (1990).

116. Ishibashi, Y. & Arai, T. *Salmonella typhi* does not inhibit phagosome-lysosome fusion in human monocyte-derived macrophages. *FEMS Immunol Med Microbiol* **12**, 55–61 (1995).

117. Schwan, W. R., Huang, X. Z., Hu, L. & Kopecko, D. J. Differential bacterial survival, replication, and apoptosis-inducing ability of *Salmonella* serovars within human and murine macrophages. *Infect. Immun.* **68**, 1005–1013 (2000).

118. Pascopella, L. *et al.* Host restriction phenotypes of *Salmonella typhi* and *Salmonella gallinarum*. *Infect. Immun.* **63**, 4329–4335 (1995).

119. Song, J. *et al.* A Mouse Model for the Human Pathogen *Salmonella* Typhi. *Cell Host & Microbe* **8**, 369–376 (2010).

120. Firoz Mian, M., Pek, E. A., Chenoweth, M. J. & Ashkar, A. A. Humanized mice are susceptible to *Salmonella typhi* infection. *Cell Mol Immunol* **8**, 83–87 (2011).

121. Pearson, T., Greiner, D. L. & Shultz, L. D. Creation of 'humanized' mice to study human immunity. *Curr Protoc Immunol* **Chapter 15**, Unit 15.21 (2008).

122. Mallory, F. A. histological study of typhoid fever. *J Exp Med* **3**, 611–638 (1898).

123. Bharadwaj, S., Anim, J. T., Ebrahim, F. & Aldahham, A. Granulomatous Inflammatory Response in a Case of Typhoid Fever. *Med Princ Pract* **18**, 239–241 (2009).

124. Waddington, C. S. *et al.* Advancing the management and control of typhoid fever: a review of the historical role of human challenge studies. *J. Infect.* **68**, 405–418 (2014).

125. Hornick, R. B. *et al.* Typhoid fever: pathogenesis and immunologic control. *N. Engl. J. Med.* **283**, 686–691 (1970).

126. Darton, T., Blohmke, C. & Pollard, A. Typhoid epidemiology, diagnostics and the human challenge model. *Current Opinion in Gastroenterology* **30**, 7–17 (2014).

127. Hindle, Z. *et al.* Characterization of *Salmonella enterica* Derivatives Harboring Defined aroC and *Salmonella* Pathogenicity Island 2 Type III Secretion System (*ssaV*) Mutations by Immunization of Healthy Volunteers. *Infect Immun* **70**, 3457–3467 (2002).

128. Kirkpatrick, B. D. *et al.* Evaluation of *Salmonella enterica* serovar Typhi (Ty2 *aroC-ssaV-*) M01ZH09, with a defined mutation in the *Salmonella* pathogenicity island 2, as a live, oral typhoid vaccine in human volunteers. *Vaccine* **24**, 116–123 (2006).

129. Darton, T. C. *et al.* Using a Human Challenge Model of Infection to Measure Vaccine Efficacy: A Randomised, Controlled Trial Comparing the Typhoid Vaccines M01ZH09 with Placebo and Ty21a. *PLOS Neglected Tropical Diseases* **10**, e0004926 (2016).

130. Gibani, M. M. *et al.* Investigation of the role of typhoid toxin in acute typhoid fever in a human challenge model. *Nature Medicine* **25**, 1082–1088 (2019).

131. Fields, P. I., Swanson, R. V., Haidaris, C. G. & Heffron, F. Mutants of *Salmonella typhimurium* that cannot survive within the macrophage are avirulent. *PNAS* **83**, 5189–5193 (1986).

132. Price, J. V. & Vance, R. E. The macrophage paradox. *Immunity* **41**, 685–693 (2014).

133. Rathman, M., Sjaastad, M. D. & Falkow, S. Acidification of phagosomes containing *Salmonella typhimurium* in murine macrophages. *Infect. Immun.* **64**, 2765–2773 (1996).

134. Muller, C. *et al.* Acid stress activation of the σ^E stress response in *Salmonella enterica* serovar Typhimurium. *Mol Microbiol* **71**, 1228–1238 (2009).

135. Fang, F. C. Antimicrobial reactive oxygen and nitrogen species: concepts and controversies. *Nat. Rev. Microbiol.* **2**, 820–832 (2004).

136. Quinn, M. T. & Gauss, K. A. Structure and regulation of the neutrophil respiratory burst oxidase: comparison with nonphagocyte oxidases. *J. Leukoc. Biol.* **76**, 760–781 (2004).

137. Nathan, C. & Xie, Q. W. Nitric oxide synthases: roles, tolls, and controls. *Cell* **78**, 915–918 (1994).

138. Kamijo, R. *et al.* Requirement for transcription factor IRF-1 in NO synthase induction in macrophages. *Science* **263**, 1612–1615 (1994).

139. Nairz, M. *et al.* Slc11a1 limits intracellular growth of *Salmonella enterica* sv. Typhimurium by promoting macrophage immune effector functions and impairing bacterial iron acquisition. *Cell. Microbiol.* **11**, 1365–1381 (2009).

140. Cunrath, O. & Bumann, D. Host resistance factor SLC11A1 restricts *Salmonella* growth through magnesium deprivation. *Science* **366**, 995–999 (2019).

141. Vidal, S. *et al.* The *Ity/Lsh/Bcg* locus: natural resistance to infection with intracellular parasites is abrogated by disruption of the Nramp1 gene. *J. Exp. Med.* **182**, 655–666 (1995).

142. Miao, E. A. *et al.* Caspase-1-induced pyroptosis is an innate immune effector mechanism against intracellular bacteria. *Nat. Immunol.* **11**, 1136–1142 (2010).

143. Fantuzzi, G. & Dinarello, C. A. Interleukin-18 and interleukin-1 beta: two cytokine substrates for ICE (caspase-1). *J. Clin. Immunol.* **19**, 1–11 (1999).

144. Hersh, D. *et al.* The *Salmonella* invasin SipB induces macrophage apoptosis by binding to caspase-1. *PNAS* **96**, 2396–2401 (1999).

145. Brennan, M. A. & Cookson, B. T. *Salmonella* induces macrophage death by caspase-1-dependent necrosis. *Mol. Microbiol.* **38**, 31–40 (2000).

146. Fink, S. L. & Cookson, B. T. Caspase-1-dependent pore formation during pyroptosis leads to osmotic lysis of infected host macrophages. *Cell. Microbiol.* **8**, 1812–1825 (2006).

147. Mariathasan, S. *et al.* Differential activation of the inflammasome by caspase-1 adaptors ASC and Ipaf. *Nature* **430**, 213–218 (2004).

148. Lundberg, U., Vinatzer, U., Berdnik, D., von Gabain, A. & Baccarini, M. Growth Phase-Regulated Induction of *Salmonella*-Induced Macrophage Apoptosis Correlates with Transient Expression of SPI-1 Genes. *J Bacteriol* **181**, 3433–3437 (1999).

149. Kofoed, E. M. & Vance, R. E. Innate immune recognition of bacterial ligands by NAIPs determines inflammasome specificity. *Nature* **477**, 592–595 (2011).

150. Zhao, Y. *et al.* The NLRC4 inflammasome receptors for bacterial flagellin and type III secretion apparatus. *Nature* **477**, 596–600 (2011).

151. Zhao, Y. *et al.* Genetic functions of the NAIP family of inflammasome receptors for bacterial ligands in mice. *J. Exp. Med.* **213**, 647–656 (2016).

152. van der Velden, A. W., Lindgren, S. W., Worley, M. J. & Heffron, F. *Salmonella* pathogenicity island 1-independent induction of apoptosis in infected macrophages by *Salmonella enterica* serotype typhimurium. *Infect. Immun.* **68**, 5702–5709 (2000).

153. Monack, D. M., Detweiler, C. S. & Falkow, S. *Salmonella* pathogenicity island 2-dependent macrophage death is mediated in part by the host cysteine protease caspase-1. *Cell. Microbiol.* **3**, 825–837 (2001).

154. Monack, D. M., Navarre, W. W. & Falkow, S. *Salmonella*-induced macrophage death: the role of caspase-1 in death and inflammation. *Microbes Infect.* **3**, 1201–1212 (2001).

155. Fink, S. L. & Cookson, B. T. Pyroptosis and host cell death responses during *Salmonella* infection. *Cell. Microbiol.* **9**, 2562–2570 (2007).

156. Chen, L. M., Kaniga, K. & Galán, J. E. *Salmonella* spp. are cytotoxic for cultured macrophages. *Mol. Microbiol.* **21**, 1101–1115 (1996).

157. Monack, D. M., Raupach, B., Hromockyj, A. E. & Falkow, S. *Salmonella typhimurium* invasion induces apoptosis in infected macrophages. *Proc. Natl. Acad. Sci. U.S.A.* **93**, 9833–9838 (1996).

158. Wemyss, M. A. & Pearson, J. S. Host Cell Death Responses to Non-typhoidal *Salmonella* Infection. *Front. Immunol.* **10**, (2019).

159. Hayden, M. S. & Ghosh, S. Shared principles in NF-κB signaling. *Cell* **132**, 344–362 (2008).

160. Hayden, M. S. & Ghosh, S. NF-κB, the first quarter-century: remarkable progress and outstanding questions. *Genes Dev.* **26**, 203–234 (2012).

161. Günster, R. A., Matthews, S. A., Holden, D. W. & Thurston, T. L. M. SseK1 and SseK3 Type III Secretion System Effectors Inhibit NF-κB Signaling and Necroptotic Cell Death in *Salmonella*-Infected Macrophages. *Infect. Immun.* **85**, (2017).

162. Feng, Z.-Z. *et al.* The *Salmonella* effectors SseF and SseG inhibit Rab1A-mediated autophagy to facilitate intracellular bacterial survival and replication. *J. Biol. Chem.* **293**, 9662–9673 (2018).

163. Geddes, K., Worley, M., Niemann, G. & Heffron, F. Identification of new secreted effectors in *Salmonella enterica* serovar Typhimurium. *Infect. Immun.* **73**, 6260–6271 (2005).

164. Ramos-Morales, F. Impact of *Salmonella enterica* Type III Secretion System Effectors on the Eukaryotic Host Cell. *ISRN Cell Biology* (2012) doi:10.5402/2012/787934.

165. Figueira, R. & Holden, D. W. Functions of the *Salmonella* pathogenicity island 2 (SPI-2) type III secretion system effectors. *Microbiology (Reading, Engl.)* **158**, 1147–1161 (2012).

166. Jennings, E., Thurston, T. L. M. & Holden, D. W. *Salmonella* SPI-2 Type III Secretion System Effectors: Molecular Mechanisms And Physiological Consequences. *Cell Host Microbe* **22**, 217–231 (2017).

167. Daigle, F., Graham, J. E. & Curtiss, R. Identification of *Salmonella typhi* genes expressed within macrophages by selective capture of transcribed sequences (SCOTS). *Mol. Microbiol.* **41**, 1211–1222 (2001).

168. Faucher, S. P., Porwollik, S., Dozois, C. M., McClelland, M. & Daigle, F. Transcriptome of *Salmonella enterica* serovar Typhi within macrophages revealed through the selective capture of transcribed sequences. *Proc. Natl. Acad. Sci. U.S.A.* **103**, 1906–1911 (2006).

169. Langridge, G. C. *et al.* Patterns of genome evolution that have accompanied host adaptation in *Salmonella*. *PNAS* **112**, 863–868 (2015).

170. Hardt, W.-D. & Galán, J. E. A secreted *Salmonella* protein with homology to an avirulence determinant of plant pathogenic bacteria. *PNAS* **94**, 9887–9892 (1997).

171. Giacomodonato, M. N. *et al.* AvrA effector protein of *Salmonella enterica* serovar Enteritidis is expressed and translocated in mesenteric lymph nodes at late stages of infection in mice. *Microbiology* **160**, 1191–1199 (2014).

172. Jones, R. M. *et al. Salmonella* AvrA Coordinates Suppression of Host Immune and Apoptotic Defenses via JNK Pathway Blockade. *Cell Host Microbe* **3**, 233–244 (2008).

173. Collier-Hyams, L. S. *et al.* Cutting edge: *Salmonella* AvrA effector inhibits the key proinflammatory, anti-apoptotic NF-kappa B pathway. *J. Immunol.* **169**, 2846–2850 (2002).

174. Wu, H., Jones, R. M. & Neish, A. S. The *Salmonella* effector AvrA mediates bacterial intracellular survival during infection in vivo. *Cell. Microbiol.* **14**, 28–39 (2012).

175. Liu, X., Lu, R., Wu, S. & Sun, J. *Salmonella* regulation of intestinal stem cells through the Wnt/beta-catenin pathway. *FEBS Lett.* **584**, 911–916 (2010).

176. Lin, Z. *et al. Salmonella* Enteritidis effector AvrA stabilizes intestinal tight junctions via the JNK pathway. *J. Biol. Chem.* jbc.M116.757393 (2016) doi:10.1074/jbc.M116.757393.

177. Liao, A. P. *et al. Salmonella* type III effector AvrA stabilizes cell tight junctions to inhibit inflammation in intestinal epithelial cells. *PLoS ONE* **3**, e2369 (2008).

178. Ye, Z., Petrof, E. O., Boone, D., Claud, E. C. & Sun, J. *Salmonella* effector AvrA regulation of colonic epithelial cell inflammation by deubiquitination. *Am. J. Pathol.* **171**, 882–892 (2007).

179. Eriksson, S., Lucchini, S., Thompson, A., Rhen, M. & Hinton, J. C. D. Unravelling the biology of macrophage infection by gene expression profiling of intracellular *Salmonella enterica*. *Molecular Microbiology* **47**, 103–118 (2003).

180. Niemann, G. S. *et al.* Discovery of Novel Secreted Virulence Factors from *Salmonella enterica* Serovar Typhimurium by Proteomic Analysis of Culture Supernatants. *Infect Immun* **79**, 33–43 (2011).

181. Figueira, R., Watson, K. G., Holden, D. W. & Helaine, S. Identification of *Salmonella* Pathogenicity Island-2 Type III Secretion System Effectors Involved in Intramacrophage Replication of *S. enterica* Serovar Typhimurium: Implications for Rational Vaccine Design. *mBio* **4**, (2013).

182. Sun, H., Kamanova, J., Lara-Tejero, M. & Galán, J. E. A Family of *Salmonella* Type III Secretion Effector Proteins Selectively Targets the NF-κB Signaling Pathway to Preserve Host Homeostasis. *PLOS Pathogens* **12**, e1005484 (2016).

183. Coombes, B. K. *et al.* Genetic and molecular analysis of GogB, a phage-encoded type III-secreted substrate in *Salmonella enterica* serovar Typhimurium with autonomous expression from its associated phage. *J. Mol. Biol.* **348**, 817–830 (2005).

184. Pilar, A. V. C., Reid-Yu, S. A., Cooper, C. A., Mulder, D. T. & Coombes, B. K. GogB Is an Anti-Inflammatory Effector that Limits Tissue Damage during *Salmonella* Infection through Interaction with Human FBXO22 and Skp1. *PLOS Pathogens* **8**, e1002773 (2012).

185. Ho, T. D. *et al.* Identification of GtgE, a novel virulence factor encoded on the Gifsy-2 bacteriophage of *Salmonella enterica* serovar Typhimurium. *J. Bacteriol.* **184**, 5234–5239 (2002).

186. Spanò, S., Liu, X. & Galán, J. E. Proteolytic targeting of Rab29 by an effector protein distinguishes the intracellular compartments of human-adapted and broad-host *Salmonella*. *Proc. Natl. Acad. Sci. U.S.A.* **108**, 18418–18423 (2011).

187. Wood, M. W. *et al.* Identification of a pathogenicity island required for *Salmonella* enteropathogenicity. *Molecular Microbiology* **29**, 883–891 (1998).

188. Knodler, L. A. *et al. Salmonella* effectors within a single pathogenicity island are differentially expressed and translocated by separate type III secretion systems. *Mol. Microbiol.* **43**, 1089–1103 (2002).

189. Knodler, L. A. *et al. Salmonella* type III effectors PipB and PipB2 are targeted to detergent-resistant microdomains on internal host cell membranes. *Molecular Microbiology* **49**, 685–704 (2003).

190. Knodler, L. A. & Steele-Mortimer, O. The *Salmonella* Effector PipB2 Affects Late Endosome/Lysosome Distribution to Mediate Sif Extension. *MBoC* **16**, 4108–4123 (2005).

191. Henry, T. *et al.* The *Salmonella* effector protein PipB2 is a linker for kinesin-1. *PNAS* **103**, 13497–13502 (2006).

192. Szeto, J., Namolovan, A., Osborne, S. E., Coombes, B. K. & Brumell, J. H. *Salmonella*-Containing Vacuoles Display Centrifugal Movement Associated with Cell-to-Cell Transfer in Epithelial Cells. *Infection and Immunity* **77**, 996–1007 (2009).

193. Stein, M. A., Leung, K. Y., Zwick, M., Portillo, F. G. & Finlay, B. B. Identification of a *Salmonella* virulence gene required for formation of filamentous structures containing lysosomal membrane glycoproteins within epithelial cells. *Molecular Microbiology* **20**, 151–164 (1996).

194. Beuzón, C. R. *et al. Salmonella* maintains the integrity of its intracellular vacuole through the action of SifA. *The EMBO Journal* **19**, 3235–3249 (2000).

195. Jackson, L. K., Nawabi, P., Hentea, C., Roark, E. A. & Haldar, K. The *Salmonella* virulence protein SifA is a G protein antagonist. *Proc. Natl. Acad. Sci. U.S.A.* **105**, 14141–14146 (2008).

196. Eswarappa, S.M. *et al.* Differentially evolved genes of *Salmonella* pathogenicity islands: insights into the mechanism of host specificity in *Salmonella*. *PLoS ONE* **3,** e3829 (2008).

197. Ruiz-Albert, J. *et al.* Complementary activities of SseJ and SifA regulate dynamics of the *Salmonella typhimurium* vacuolar membrane. *Molecular Microbiology* **44**, 645–661 (2002).

198. Alto, N. M. *et al.* Identification of a Bacterial Type III Effector Family with G Protein Mimicry Functions. *Cell* **124**, 133–145 (2006).

199. Freeman, J. A., Ohl, M. E. & Miller, S. I. The *Salmonella enterica* Serovar Typhimurium Translocated Effectors SseJ and SifB Are Targeted to the *Salmonella*-Containing Vacuole. *Infection and Immunity* **71**, 418–427 (2003).

200. Tsolis, R. M., Adams, L. G., Ficht, T. A. & Bäumler, A. J. Contribution of *Salmonella typhimurium*Virulence Factors to Diarrheal Disease in Calves. *Infection and Immunity* **67**, 4879–4885 (1999).

201. Miao, E. A. & Miller, S. I. A conserved amino acid sequence directing intracellular type III secretion by *Salmonella typhimurium*. *PNAS* **97**, 7539–7544 (2000).

202. Quezada, C. M., Hicks, S. W., Galán, J. E. & Stebbins, C. E. A family of *Salmonella* virulence factors functions as a distinct class of autoregulated E3 ubiquitin ligases. *PNAS* **106**, 4864–4869 (2009).

203. Bernal-Bayard, J., Cardenal-Muñoz, E. & Ramos-Morales, F. The *Salmonella* Type III Secretion Effector, *Salmonella* Leucine-rich Repeat Protein (SlrP), Targets the Human Chaperone ERdj3. *J. Biol. Chem.* **285**, 16360–16368 (2010).

204. Brumell, J. H. *et al.* SopD2 is a Novel Type III Secreted Effector of *Salmonella typhimurium* That Targets Late Endocytic Compartments Upon Delivery Into Host Cells. *Traffic* **4**, 36–48 (2003).

205. D'Costa, V. M. *et al. Salmonella* Disrupts Host Endocytic Trafficking by SopD2-Mediated Inhibition of Rab7. *Cell Rep* **12**, 1508–1518 (2015).

206. Trombert, A. N., Rodas, P. I. & Mora, G. C. Reduced invasion to human epithelial cell lines of *Salmonella enterica* serovar Typhi carrying *S.* Typhimurium sopD2. *FEMS Microbiology Letters* **322**, 150–156 (2011).

207. Jiang, X. *et al.* The related effector proteins SopD and SopD2 from *Salmonella enterica* serovar Typhimurium contribute to virulence during systemic infection of mice. *Molecular Microbiology* **54**, 1186–1198 (2004).

208. Schroeder, N. *et al.* The virulence protein SopD2 regulates membrane dynamics of *Salmonella*-containing vacuoles. *PLoS Pathog.* **6**, e1001002 (2010).

209. Lee, A. H., Zareei, M. P. & Daefler, S. Identification of a NIPSNAP homologue as host cell target for *Salmonella* virulence protein SpiC. *Cellular Microbiology* **4**, 739–750 (2002).

210. Shotland, Y., Krämer, H. & Groisman, E. A. The *Salmonella* SpiC protein targets the mammalian Hook3 protein function to alter cellular trafficking. *Molecular Microbiology* **49**, 1565–1576 (2003).

211. Freeman, J. A., Rappl, C., Kuhle, V., Hensel, M. & Miller, S. I. SpiC Is Required for Translocation of *Salmonella* Pathogenicity Island 2 Effectors and Secretion of Translocon Proteins SseB and SseC. *Journal of Bacteriology* **184**, 4971–4980 (2002).

212. Yu, X.-J., McGourty, K., Liu, M., Unsworth, K. E. & Holden, D. W. pH sensing by intracellular *Salmonella* induces effector translocation. *Science* **328**, 1040–1043 (2010).

213. Uchiya, K. *et al.* A *Salmonella* virulence protein that inhibits cellular trafficking. *EMBO J.* **18**, 3924–3933 (1999).

214. Lin, S. L., Le, T. X. & Cowen, D. S. SptP, a *Salmonella typhimurium* type III-secreted protein, inhibits the mitogen-activated protein kinase pathway by inhibiting Raf activation. *Cellular Microbiology* **5**, 267–275 (2003).

215. Fu, Y. & Galán, J. E. A *salmonella* protein antagonizes Rac-1 and Cdc42 to mediate host-cell recovery after bacterial invasion. *Nature* **401**, 293–297 (1999).

216. Humphreys, D., Hume, P. J. & Koronakis, V. The *Salmonella* effector SptP dephosphorylates host AAA+ ATPase VCP to promote development of its intracellular replicative niche. *Cell Host Microbe* **5**, 225–233 (2009).

217. Johnson, R. *et al.* The Type III Secretion System Effector SptP of *Salmonella enterica* Serovar Typhi. *Journal of Bacteriology* **199**, (2017).

218. Lesnick, M. L., Reiner, N. E., Fierer, J. & Guiney, D. G. The *Salmonella spvB* virulence gene encodes an enzyme that ADP-ribosylates actin and destabilizes the cytoskeleton of eukaryotic cells. *Molecular Microbiology* **39**, 1464–1470 (2001).

219. Matsui, H. *et al.* Virulence plasmid-borne spvB and spvC genes can replace the 90-kilobase plasmid in conferring virulence to *Salmonella enterica* serovar Typhimurium in subcutaneously inoculated mice. *J. Bacteriol.* **183**, 4652–4658 (2001).

220. Libby, S. J., Lesnick, M., Hasegawa, P., Weidenhammer, E. & Guiney, D. G. The *Salmonella* virulence plasmid *spv* genes are required for cytopathology in human monocyte-derived macrophages. *Cellular Microbiology* **2**, 49–58 (2000).

221. Mazurkiewicz, P. *et al.* SpvC is a *Salmonella* effector with phosphothreonine lyase activity on host mitogen-activated protein kinases. *Molecular Microbiology* **67**, 1371–1383 (2008).

222. Grabe, G. J. *et al.* The *Salmonella* Effector SpvD is a Cysteine Hydrolase with a Serovar-Specific Polymorphism Influencing Catalytic Activity, Suppression of Immune Responses and Bacterial Virulence. *J. Biol. Chem.* **291,** 25853-25863 (2016).

223. Rolhion, N. *et al.* Inhibition of Nuclear Transport of NF-κB p65 by the *Salmonella* Type III Secretion System Effector SpvD. *PLOS Pathogens* **12**, e1005653 (2016).

224. Worley, M. J., Ching, K. H. L. & Heffron, F. *Salmonella* SsrB activates a global regulon of horizontally acquired genes. *Molecular Microbiology* **36**, 749–761 (2000).

225. Canals, D., Perry, D. M., Jenkins, R. W. & Hannun, Y. A. Drug targeting of sphingolipid metabolism: sphingomyelinases and ceramidases. *Br J Pharmacol* **163**, 694–712 (2011).

226. Cordero-Alba, M., Bernal-Bayard, J. & Ramos-Morales, F. SrfJ, a *Salmonella* Type III Secretion System Effector Regulated by PhoP, RcsB, and IolR. *J Bacteriol* **194**, 4226–4236 (2012).

227. Deiwick, J. *et al.* The Translocated *Salmonella* Effector Proteins SseF and SseG Interact and Are Required To Establish an Intracellular Replication Niche. *Infection and Immunity* **74**, 6965–6972 (2006).

228. Yu, X.-J., Liu, M. & Holden, D. W. *Salmonella* Effectors SseF and SseG Interact with Mammalian Protein ACBD3 (GCP60) To Anchor Salmonella-Containing Vacuoles at the Golgi Network. *mBio* **7**, (2016).

229. Kuhle, V. & Hensel, M. SseF and SseG are translocated effectors of the type III secretion system of *Salmonella* pathogenicity island 2 that modulate aggregation of endosomal compartments. *Cell. Microbiol.* **4**, 813–824 (2002).

230. McLaughlin, L. M. *et al.* The *Salmonella* SPI2 Effector SseI Mediates Long-Term Systemic Infection by Modulating Host Cell Migration. *PLOS Pathogens* **5**, e1000671 (2009).

231. Carden, S. E. *et al.* Pseudogenization of the secreted effector gene *sseI* confers rapid systemic dissemination of *S.* Typhimurium ST313 within migratory dendritic cells. *Cell Host Microbe* **21**, 182–194 (2017).

232. Lossi, N. S., Rolhion, N., Magee, A. I., Boyle, C. & Holden, D. W. The *Salmonella* SPI-2 effector SseJ exhibits eukaryotic activator-dependent phospholipase A and

glycerophospholipid : cholesterol acyltransferase activity. *Microbiology (Reading, Engl.)* **154**, 2680–2688 (2008).

233. Trombert, A. N., Berrocal, L., Fuentes, J. A. & Mora, G. C. *S.* Typhimurium sseJ gene decreases the *S*. Typhi cytotoxicity toward cultured epithelial cells. *BMC Microbiol* **10**, 312 (2010).

234. Kujat Choy, S. L. *et al.* SseK1 and SseK2 Are Novel Translocated Proteins of *Salmonella enterica* Serovar Typhimurium. *Infection and Immunity* **72**, 5115–5125 (2004).

235. Yang, Z. *et al.* SseK3 Is a *Salmonella* Effector That Binds TRIM32 and Modulates the Host's NF-κB Signalling Activity. *PLoS One* **10**, (2015).

236. Mesquita, F. S. *et al.* The *Salmonella* Deubiquitinase SseL Inhibits Selective Autophagy of Cytosolic Aggregates. *PLOS Pathogens* **8**, e1002743 (2012).

237. Arena, E. T. *et al.* The deubiquitinase activity of the *Salmonella* pathogenicity island 2 effector, SseL, prevents accumulation of cellular lipid droplets. *Infect. Immun.* **79**, 4392–4400 (2011).

238. Rytkönen, A. *et al.* SseL, a *Salmonella* deubiquitinase required for macrophage killing and virulence. *Proc. Natl. Acad. Sci. U.S.A.* **104**, 3502–3507 (2007).

239. Haraga, A. & Miller, S. I. A *Salmonella enterica* Serovar Typhimurium Translocated Leucine-Rich Repeat Effector Protein Inhibits NF-κB-Dependent Gene Expression. *Infect Immun* **71**, 4052–4058 (2003).

240. Haraga, A. & Miller, S. I. A *Salmonella* type III secretion effector interacts with the mammalian serine/threonine protein kinase PKN1. *Cell. Microbiol.* **8**, 837–846 (2006).

241. Bhavsar, A. P. *et al.* The *Salmonella* Type III Effector SspH2 Specifically Exploits the NLR Co-chaperone Activity of SGT1 to Subvert Immunity. *PLOS Pathogens* **9**, e1003518 (2013).

242. Domingues, L., Holden, D. W. & Mota, L. J. The *Salmonella* Effector SteA Contributes to the Control of Membrane Dynamics of *Salmonella*-Containing Vacuoles. *Infection and Immunity* **82**, 2923–2934 (2014).

243. Odendall, C. *et al.* The *Salmonella* Kinase SteC Targets the MAP Kinase MEK to Regulate the Host Actin Cytoskeleton. *Cell Host Microbe* **12**, 657–668 (2012).

244. Poh, J. *et al.* SteC is a *Salmonella* kinase required for SPI-2-dependent F-actin remodelling. *Cell Microbiol* **10**, 20–30 (2008).

245. Bayer-Santos, E. *et al.* The *Salmonella* Effector SteD Mediates MARCH8-Dependent Ubiquitination of MHC II Molecules and Inhibits T Cell Activation. *Cell Host Microbe* **20**, 584–595 (2016).

246. Navarre, W. W. *et al.* Co-regulation of *Salmonella* enterica genes required for virulence and resistance to antimicrobial peptides by SlyA and PhoP/PhoQ. *Mol. Microbiol.* **56**, 492–508 (2005).

247. Jaslow, S. L. *et al. Salmonella* Activation of STAT3 Signaling by SarA Effector Promotes Intracellular Replication and Production of IL-10. *Cell Rep* **23**, 3525–3536 (2018).

248. Gibbs, K. D. *et al.* The *Salmonella* Secreted Effector SarA/SteE Mimics Cytokine Receptor Signaling to Activate STAT3. *Cell Host & Microbe* **27**, 129-139.e4 (2020).

249. Panagi, I. *et al. Salmonella* Effector SteE Converts the Mammalian Serine/Threonine Kinase GSK3 into a Tyrosine Kinase to Direct Macrophage Polarization. *Cell Host & Microbe* **27**, 41-53.e6 (2020).

250. Pham, T. H. M. *et al. Salmonella*-Driven Polarization of Granuloma Macrophages Antagonizes TNF-Mediated Pathogen Restriction during Persistent Infection. *Cell Host Microbe* **27**, 54-67.e5 (2020).

251. Lilic, M. *et al. Salmonella* SipA polymerizes actin by stapling filaments with nonglobular protein arms. *Science* **301**, 1918–1921 (2003).

252. Raffatellu, M. *et al.* SipA, SopA, SopB, SopD, and SopE2 contribute to *Salmonella enterica* serotype typhimurium invasion of epithelial cells. *Infect. Immun.* **73**, 146–154 (2005).

253. Brawn, L. C., Hayward, R. D. & Koronakis, V. *Salmonella* SPI1 effector SipA persists after entry and cooperates with a SPI2 effector to regulate phagosome maturation and intracellular replication. *Cell Host Microbe* **1**, 63–75 (2007).

254. Myeni, S. K., Wang, L. & Zhou, D. SipB-SipC complex is essential for translocon formation. *PLoS ONE* **8**, e60499 (2013).

255. Hayward, R. D. & Koronakis, V. Direct nucleation and bundling of actin by the SipC protein of invasive *Salmonella*. *EMBO J.* **18**, 4926–4934 (1999).

256. Kaniga, K., Trollinger, D. & Galán, J. E. Identification of two targets of the type III protein secretion system encoded by the *inv* and *spa* loci of *Salmonella typhimurium* that have homology to the *Shigella* IpaD and IpaA proteins. *J. Bacteriol.* **177**, 7078–7085 (1995).

257. Kamanova, J., Sun, H., Lara-Tejero, M. & Galán, J. E. The *Salmonella* Effector Protein SopA Modulates Innate Immune Responses by Targeting TRIM E3 Ligase Family Members. *PLOS Pathogens* **12**, e1005552 (2016).

258. Zhang, Y., Higashide, W. M., McCormick, B. A., Chen, J. & Zhou, D. The inflammation-associated *Salmonella* SopA is a HECT-like E3 ubiquitin ligase. *Molecular Microbiology* **62**, 786–793 (2006).

259. Valenzuela, L. M. *et al.* Pseudogenization of sopA and sopE2 is functionally linked and contributes to virulence of *Salmonella enterica* serovar Typhi. *Infect. Genet. Evol.* **33**, 131–142 (2015).

260. Finn, C. E., Chong, A., Cooper, K. G., Starr, T. & Steele-Mortimer, O. A second wave of *Salmonella* T3SS1 activity prolongs the lifespan of infected epithelial cells. *PLoS Pathog.* **13**, e1006354 (2017).

261. Knodler, L. A., Winfree, S., Drecktrah, D., Ireland, R. & Steele-Mortimer, O. Ubiquitination of the bacterial inositol phosphatase, SopB, regulates its biological activity at the plasma membrane. *Cell. Microbiol.* **11**, 1652–1670 (2009).

262. Bakowski, M. A., Cirulis, J. T., Brown, N. F., Finlay, B. B. & Brumell, J. H. SopD acts cooperatively with SopB during *Salmonella enterica* serovar Typhimurium invasion. *Cellular Microbiology* **9**, 2839–2855 (2007).

263. Friebel, A. *et al.* SopE and SopE2 from *Salmonella typhimurium* activate different sets of RhoGTPases of the host cell. *J. Biol. Chem.* **276**, 34035–34040 (2001).

264. Hardt, W. D., Chen, L. M., Schuebel, K. E., Bustelo, X. R. & Galán, J. E. *S.* typhimurium encodes an activator of Rho GTPases that induces membrane ruffling and nuclear responses in host cells. *Cell* **93**, 815–826 (1998).

265. Bulgin, R. *et al.* Bacterial guanine nucleotide exchange factors SopE-like and WxxxE effectors. *Infect. Immun.* **78**, 1417–1425 (2010).

266. Levine, M. M. & Simon, R. The Gathering Storm: Is Untreatable Typhoid Fever on the Way? *mBio* **9**, e00482-18 (2018).

267. Klemm, E. J. *et al.* Emergence of an Extensively Drug-Resistant *Salmonella enterica* Serovar Typhi Clone Harboring a Promiscuous Plasmid Encoding Resistance to Fluoroquinolones and Third-Generation Cephalosporins. *mBio* **9**, e00105-18 (2018).

268. Edsall, G. *et al.* Studies on infection and immunity in experimental typhoid fever. I. Typhoid fever in chimpanzees orally infected with Salmonella typhosa. *J. Exp. Med.* **112**, 143–166 (1960).

269. Gaines, S., Sprinz, H., Tully, J. G. & Tigertt, W. D. Studies on infection and immunity in experimental typhoid fever. VII. The distribution of *Salmonella typhi* in chimpanzee tissue following oral challenge, and the relationship between the numbers of bacilli and morphologic lesions. *J. Infect. Dis.* **118**, 293–306 (1968).

270. Langridge, G. C. *et al.* Simultaneous assay of every *Salmonella* Typhi gene using one million transposon mutants. *Genome Res* **19**, 2308–2316 (2009).

271. Barquist, L. *et al.* The TraDIS toolkit: sequencing and analysis for dense transposon mutant libraries. *Bioinformatics* **32**, 1109–1111 (2016).

272. Carver, T., Harris, S. R., Berriman, M., Parkhill, J. & McQuillan, J. A. Artemis: an integrated platform for visualization and analysis of high-throughput sequence-based experimental data. *Bioinformatics* **28**, 464–469 (2012).

273. Zhang, K. *et al.* Minimal SPI1-T3SS effector requirement for *Salmonella* enterocyte invasion and intracellular proliferation in vivo. *PLOS Pathogens* **14**, e1006925 (2018).

274. Hensel, M. *et al.* Simultaneous identification of bacterial virulence genes by negative selection. *Science* **269**, 400–403 (1995).

275. Hensel, M. *et al.* Genes encoding putative effector proteins of the type III secretion system of *Salmonella* pathogenicity island 2 are required for bacterial virulence and proliferation in macrophages. *Mol. Microbiol.* **30**, 163–174 (1998).

276. Bijlsma, J. J. E. & Groisman, E. A. The PhoP/PhoQ system controls the intramacrophage type three secretion system of *Salmonella enterica. Mol. Microbiol.* **57**, 85–96 (2005).

277. Groisman, E. A. The pleiotropic two-component regulatory system PhoP-PhoQ. *J. Bacteriol.* **183**, 1835–1842 (2001).

278. Dalebroux, Z. D. & Miller, S. I. Salmonellae PhoPQ regulation of the outer membrane to resist innate immunity. *Curr. Opin. Microbiol.* **17**, 106–113 (2014).

279. Charles, R. C. *et al.* Comparative Proteomic Analysis of the PhoP Regulon in *Salmonella enterica* Serovar Typhi Versus Typhimurium. *PLOS ONE* **4**, e6994 (2009).

280. Dougan, G. *et al.* Construction and Characterization of Vaccine Strains of *Salmonella* Harboring Mutations in Two Different *aro* Genes. *J Infect Dis* **158**, 1329–1335 (1988).

281. Hone, D. M. *et al.* Evaluation in volunteers of a candidate live oral attenuated *Salmonella typhi* vector vaccine. *J. Clin. Invest.* **90**, 412–420 (1992).

282. Felix, A. & Pitt, R. M. A new antigen of *B. typhosus*: its relation to virulence and to active and passive immunisation. *The Lancet* **224**, 186–191 (1934).

283. Wain, J. *et al.* Vi antigen expression in *Salmonella enterica* serovar Typhi clinical isolates from Pakistan. *J. Clin. Microbiol.* **43**, 1158–1165 (2005).

284. Wilson, R. P. *et al.* The Vi Capsular Polysaccharide Prevents Complement Receptor 3-Mediated Clearance of *Salmonella enterica* Serotype Typhi. *Infect. Immun.* **79**, 830–837 (2011).

285. Hart, P. J. *et al.* Differential Killing of *Salmonella enterica* Serovar Typhi by Antibodies Targeting Vi and Lipopolysaccharide O:9 Antigen. *PLOS ONE* **11**, e0145945 (2016).

286. Wilson, R. P. *et al.* The Vi-capsule prevents Toll-like receptor 4 recognition of *Salmonella*. *Cell. Microbiol.* **10**, 876–890 (2008).

287. Kintz, E. *et al. Salmonella enterica* Serovar Typhi Lipopolysaccharide O-Antigen Modification Impact on Serum Resistance and Antibody Recognition. *Infection and Immunity* **85**, e01021-16 (2017).

288. Hoare, A. *et al.* The Outer Core Lipopolysaccharide of *Salmonella enterica* Serovar Typhi Is Required for Bacterial Entry into Epithelial Cells. *Infection and Immunity* **74**, 1555–1564 (2006).

289. da Silva, P., Manieri, F. Z., Herrera, C. M., Trent, M. S. & Moreira, C. G. Novel Role of VisP and the Wzz System during O-Antigen Assembly in *Salmonella enterica* Serovar Typhimurium Pathogenesis. *Infect. Immun.* **86**, (2018).

290. Lyczak, J. B. *et al.* Epithelial cell contact-induced alterations in *Salmonella enterica* serovar Typhi lipopolysaccharide are critical for bacterial internalization. *Cellular Microbiology* **3**, 763–772 (2001).

291. Nairz, M. *et al.* Iron Regulatory Proteins Mediate Host Resistance to *Salmonella* Infection. *Cell Host Microbe* **18**, 254–261 (2015).

292. Crouch, M.-L. V., Castor, M., Karlinsey, J. E., Kalhorn, T. & Fang, F. C. Biosynthesis and IroC-dependent export of the siderophore salmochelin are essential for virulence of *Salmonella enterica* serovar Typhimurium. *Mol. Microbiol.* **67**, 971–983 (2008).

293. Fischbach, M. A. *et al.* The pathogen-associated *iroA* gene cluster mediates bacterial evasion of lipocalin 2. *Proc. Natl. Acad. Sci. U.S.A.* **103**, 16502–16507 (2006).

294. Flo, T. H. *et al.* Lipocalin 2 mediates an innate immune response to bacterial infection by sequestrating iron. *Nature* **432**, 917–921 (2004).

295. Raffatellu, M. *et al.* Lipocalin-2 resistance confers an advantage to *Salmonella enterica* serotype Typhimurium for growth and survival in the inflamed intestine. *Cell Host Microbe* **5**, 476–486 (2009).

296. Nagy, T. A., Moreland, S. M., Andrews-Polymenis, H. & Detweiler, C. S. The ferric enterobactin transporter Fep is required for persistent *Salmonella enterica* serovar Typhimurium infection. *Infect. Immun.* **81**, 4063–4070 (2013).

297. Miller, S. I., Kukral, A. M. & Mekalanos, J. J. A two-component regulatory system (phoP phoQ) controls *Salmonella typhimurium* virulence. *PNAS* **86**, 5054–5058 (1989).

298. Galán, J. E. Typhoid toxin provides a window into typhoid fever and the biology of *Salmonella* Typhi. *Proc. Natl. Acad. Sci. U.S.A.* **113**, 6338–6344 (2016).

299. Levine, M. M., Hone, D., Tacket, C., Ferreccio, C. & Cryz, S. Clinical and field trials with attenuated *Salmonella typhi* as live oral vaccines and as 'carrier' vaccines. *Res. Microbiol.* **141**, 807–816 (1990).

300. Datsenko, K. A. & Wanner, B. L. One-step inactivation of chromosomal genes in *Escherichia coli* K-12 using PCR products. *Proc. Natl. Acad. Sci. U.S.A.* **97**, 6640–6645 (2000).

301. Karlinsey, J. E. Lambda-red genetic engineering in *Salmonella enterica* serovar Typhimurium. *Meth. Enzymol.* **421**, 199–209 (2007).

302. Gallagher, L., Turner, C., Ramage, E. & Manoil, C. Creating recombination-activated genes and sequence-defined mutant libraries using transposons. *Meth. Enzymol.* **421**, 126–140 (2007).

303. Gallagher, L. A. *et al.* Resources for Genetic and Genomic Analysis of Emerging Pathogen *Acinetobacter baumannii*. *J. Bacteriol.* **197**, 2027–2035 (2015).

304. Hasgur, S., Aryee, K. E., Shultz, L. D., Greiner, D. L. & Brehm, M. A. Generation of Immunodeficient Mice Bearing Human Immune Systems by the Engraftment of Hematopoietic Stem Cells. *Methods Mol. Biol.* **1438**, 67–78 (2016).

305. Robinson, M. D., McCarthy, D. J. & Smyth, G. K. edgeR: a Bioconductor package for differential expression analysis of digital gene expression data. *Bioinformatics* **26**, 139–140 (2010).

306. Karlinsey, J. E. *et al.* Genome-wide Analysis of *Salmonella enterica* serovar Typhi in Humanized Mice Reveals Key Virulence Features. *Cell Host Microbe* **26**, 426-434.e6 (2019).

307. López, C. M., Rholl, D. A., Trunck, L. A. & Schweizer, H. P. Versatile Dual-Technology System for Markerless Allele Replacement in *Burkholderia pseudomallei*. *Appl. Environ. Microbiol.* **75**, 6496–6503 (2009).

308. Wang, R. F. & Kushner, S. R. Construction of versatile low-copy-number vectors for cloning, sequencing and gene expression in *Escherichia coli*. *Gene* **100**, 195–199 (1991).

309. Drecktrah, D. *et al.* Dynamic Behavior of *Salmonella*-Induced Membrane Tubules in Epithelial Cells. *Traffic* **9**, 2117–2129 (2008).

310. Maurice, J. A first step in bringing typhoid fever out of the closet. *The Lancet* **379**, 699–700 (2012).

311. Carter, P. B. & Collins, F. M. The route of enteric infection in normal mice. *J. Exp. Med.* **139**, 1189–1203 (1974).

312. LaRock, D. L., Chaudhary, A. & Miller, S. I. Salmonellae interactions with host processes. *Nat. Rev. Microbiol.* **13**, 191–205 (2015).

313. Parry, C. M. & Threlfall, E. J. Antimicrobial resistance in typhoidal and nontyphoidal salmonellae. *Curr. Opin. Infect. Dis.* **21**, 531–538 (2008).

314. Wain, J. *et al.* Quantitation of bacteria in bone marrow from patients with typhoid fever: relationship between counts and clinical features. *J. Clin. Microbiol.* **39**, 1571–1576 (2001).

315. Hess, J., Ladel, C., Miko, D. & Kaufmann, S. H. *Salmonella typhimurium aroA*- infection in gene-targeted immunodeficient mice: major role of CD4+ TCR-alpha beta cells and IFN-gamma in bacterial clearance independent of intracellular location. *J. Immunol.* **156**, 3321–3326 (1996).

316. Fierer, J. *et al.* Successful treatment using gentamicin liposomes of *Salmonella dublin* infections in mice. *Antimicrob. Agents Chemother.* **34**, 343–348 (1990).

317. Vassiloyanakopoulos, A. P., Okamoto, S. & Fierer, J. The crucial role of polymorphonuclear leukocytes in resistance to *Salmonella dublin* infections in genetically susceptible and resistant mice. *PNAS* **95**, 7676–7681 (1998).

318. Bergsbaken, T., Fink, S. L. & Cookson, B. T. Pyroptosis: host cell death and inflammation. *Nat. Rev. Microbiol.* **7**, 99–109 (2009).

319. Fink, S. L. & Cookson, B. T. Apoptosis, pyroptosis, and necrosis: mechanistic description of dead and dying eukaryotic cells. *Infect. Immun.* **73**, 1907–1916 (2005).

320. Kim, H. S. & Lee, M.S. STAT1 as a key modulator of cell death. *Cellular Signalling* **19**, 454–465 (2007).

321. Luo, J.-L., Kamata, H. & Karin, M. The anti-death machinery in IKK/NF-κB signaling. *J. Clin. Immunol.* **25**, 541–550 (2005).

322. Guilloteau, L. A. *et al.* The *Salmonella* virulence plasmid enhances *Salmonella*-induced lysis of macrophages and influences inflammatory responses. *Infect Immun* **64**, 3385–3393 (1996).

323. Browne, S. H., Lesnick, M. L. & Guiney, D. G. Genetic Requirements for *Salmonella*-Induced Cytopathology in Human Monocyte-Derived Macrophages. *Infect Immun* **70**, 7126–7135 (2002).

324. Mastroeni, P. Immunity to systemic *Salmonella* infections. *Curr. Mol. Med.* **2**, 393–406 (2002).

325. Ge, J. *et al.* A *Legionella* type IV effector activates the NF-κB pathway by phosphorylating the IκB family of inhibitors. *PNAS* **106**, 13725–13730 (2009).

326. Bai, X. *et al.* Inhibition of Nuclear Factor-Kappa B Activation Decreases Survival of *Mycobacterium tuberculosis* in Human Macrophages. *PLOS ONE* **8**, e61925 (2013).

327. Behar, S. M. & Briken, V. Apoptosis inhibition by intracellular bacteria and its consequence on host immunity. *Current Opinion in Immunology* **60**, 103–110 (2019).

328. Ochman, H., Soncini, F. C., Solomon, F. & Groisman, E. A. Identification of a pathogenicity island required for *Salmonella* survival in host cells. *PNAS* **93**, 7800–7804 (1996).

329. Valle, E. & Guiney, D. G. Characterization of *Salmonella*-induced cell death in human macrophage-like THP-1 cells. *Infect. Immun.* **73**, 2835–2840 (2005).

330. Pagliari, L. J., Perlman, H., Liu, H. & Pope, R. M. Macrophages Require Constitutive NF-κB Activation To Maintain A1 Expression and Mitochondrial Homeostasis. *Molecular and Cellular Biology* **20**, 8855–8865 (2000).

331. Tato, C. M. & Hunter, C. A. Host-Pathogen Interactions: Subversion and Utilization of the NF-κB Pathway during Infection. *Infect Immun* **70**, 3311–3317 (2002).

332. Hempstead, A. D. & Isberg, R. R. Host Signal Transduction and Protein Kinases Implicated in *Legionella* Infection. *Curr Top Microbiol Immunol* **376**, 249–269 (2013).

333. Rauch, I., Müller, M. & Decker, T. The regulation of inflammation by interferons and their STATs. *JAKSTAT* **2**, e23820 (2013).

334. Tugal Derin, Liao Xudong & Jain Mukesh K. Transcriptional Control of Macrophage Polarization. *Arteriosclerosis, Thrombosis, and Vascular Biology* **33**, 1135–1144 (2013).

335. de Jong, R. *et al.* Severe mycobacterial and *Salmonella* infections in interleukin-12 receptor-deficient patients. *Science* **280**, 1435–1438 (1998).

336. Cassat, J. E. & Skaar, E. P. Iron in infection and immunity. *Cell Host Microbe* **13**, 509–519 (2013).

337. Nairz, M., Haschka, D., Demetz, E. & Weiss, G. Iron at the interface of immunity and infection. *Front Pharmacol* **5**, 152 (2014).

338. Cartron, M. L., Maddocks, S., Gillingham, P., Craven, C. J. & Andrews, S. C. *Feo* transport of ferrous iron into bacteria. *Biometals* **19**, 143–157 (2006).

339. Zhou, D., Hardt, W. D. & Galán, J. E. *Salmonella typhimurium* encodes a putative iron transport system within the centisome 63 pathogenicity island. *Infect. Immun.* **67**, 1974–1981 (1999).

340. Boyer, E., Bergevin, I., Malo, D., Gros, P. & Cellier, M. F. M. Acquisition of Mn(II) in addition to Fe(II) is required for full virulence of *Salmonella enterica* serovar Typhimurium. *Infect. Immun.* **70**, 6032–6042 (2002).

341. Bleuel, C. *et al.* TolC is involved in enterobactin efflux across the outer membrane of *Escherichia coli*. *J. Bacteriol.* **187**, 6701–6707 (2005).

342. Hantke, K., Nicholson, G., Rabsch, W. & Winkelmann, G. Salmochelins, siderophores of *Salmonella enterica* and uropathogenic *Escherichia coli* strains, are recognized by the outer membrane receptor IroN. *Proc. Natl. Acad. Sci. U.S.A.* **100**, 3677–3682 (2003).

343. Fang, F. C. & Weiss, G. Iron ERRs with *Salmonella*. *Cell Host Microbe* **15**, 515–516 (2014).

344. Fritsche, G., Nairz, M., Libby, S. J., Fang, F. C. & Weiss, G. Slc11a1 (Nramp1) impairs growth of *Salmonella enterica* serovar Typhimurium in macrophages via stimulation of lipocalin-2 expression. *J. Leukoc. Biol.* **92**, 353–359 (2012).

345. Nairz, M. *et al.* Interferon-gamma limits the availability of iron for intramacrophage *Salmonella typhimurium*. *Eur. J. Immunol.* **38**, 1923–1936 (2008).

346. Nairz, M. *et al.* Absence of functional Hfe protects mice from invasive *Salmonella enterica* serovar Typhimurium infection via induction of lipocalin-2. *Blood* **114**, 3642–3651 (2009).

347. van Santen, S., de Mast, Q., Swinkels, D. W. & van der Ven, A. J. A. M. The iron link between malaria and invasive non-typhoid *Salmonella* infections. *Trends Parasitol.* **29**, 220–227 (2013).

348. Gorbacheva, V. Y., Faundez, G., Godfrey, H. P. & Cabello, F. C. Restricted growth of *ent*− and *tonB* mutants of *Salmonella enterica* serovar Typhi in human Mono Mac 6 monocytic cells. *FEMS Microbiology Letters* **196**, 7–11 (2001).

349. Zaharik, M. L. *et al.* The *Salmonella enterica* serovar typhimurium divalent cation transport systems MntH and SitABCD are essential for virulence in an Nramp1G169 murine typhoid model. *Infect. Immun.* **72**, 5522–5525 (2004).

350. Furman, M., Fica, A., Saxena, M., Di Fabio, J. L. & Cabello, F. C. *Salmonella typhi* iron uptake mutants are attenuated in mice. *Infect. Immun.* **62**, 4091–4094 (1994).

351. Tsolis, R. M., Bäumler, A. J., Heffron, F. & Stojiljkovic, I. Contribution of TonB- and Feo-mediated iron uptake to growth of *Salmonella typhimurium* in the mouse. *Infect. Immun.* **64**, 4549–4556 (1996).

352. Ozenberger, B. A., Nahlik, M. S. & McIntosh, M. A. Genetic organization of multiple *fep* genes encoding ferric enterobactin transport functions in *Escherichia coli*. *J. Bacteriol.* **169**, 3638–3646 (1987).

353. Libby, S. J. *et al.* A cytolysin encoded by *Salmonella* is required for survival within macrophages. *Proc. Natl. Acad. Sci. U.S.A.* **91**, 489–493 (1994).

354. Leclerc, J.-M., Dozois, C. M. & Daigle, F. *Salmonella enterica* serovar Typhi siderophore production is elevated and Fur inactivation causes cell filamentation and attenuation in macrophages. *FEMS Microbiol. Lett.* **364**, (2017).

355. Nemeth, E. *et al.* Hepcidin regulates cellular iron efflux by binding to ferroportin and inducing its internalization. *Science* **306**, 2090–2093 (2004).

356. Theurl, I. *et al.* Autocrine formation of hepcidin induces iron retention in human monocytes. *Blood* **111**, 2392–2399 (2008).

357. Collins, J. F., Wessling-Resnick, M. & Knutson, M. D. Hepcidin regulation of iron transport. *J. Nutr.* **138**, 2284–2288 (2008).

358. Darton, T. C. *et al.* Rapidly Escalating Hepcidin and Associated Serum Iron Starvation Are Features of the Acute Response to Typhoid Infection in Humans. *PLoS Negl Trop Dis* **9**, e0004029 (2015).

359. Hayashi, F. *et al.* The innate immune response to bacterial flagellin is mediated by Toll-like receptor 5. *Nature* **410**, 1099–1103 (2001).

360. Sheikh, A. *et al.* Interferon-γ and Proliferation Responses to *Salmonella enterica* Serotype Typhi Proteins in Patients with *S.* Typhi Bacteremia in Dhaka, Bangladesh. *PLoS Negl Trop Dis* **5**, (2011).

361. Salerno-Goncalves, R., Pasetti, M. F. & Sztein, M. B. Characterization of CD8+ Effector T Cell Responses in Volunteers Immunized with *Salmonella enterica* Serovar Typhi Strain Ty21a Typhoid Vaccine. *The Journal of Immunology* **169**, 2196–2203 (2002).

362. Buss, K. *et al.* Clustering of isochorismate synthase genes *menF* and *entC* and channeling of isochorismate in *Escherichia coli. Biochimica et Biophysica Acta (BBA) - Gene Structure and Expression* **1522**, 151–157 (2001).

363. Leclerc, J.-M., Dozois, C. M. & Daigle, F. Role of the *Salmonella enterica* serovar Typhi Fur regulator and small RNAs RfrA and RfrB in iron homeostasis and interaction with host cells. *Microbiology (Reading, Engl.)* **159**, 591–602 (2013).

364. Escolar, L., Pérez-Martín, J. & de Lorenzo, V. Opening the iron box: transcriptional metalloregulation by the Fur protein. *J. Bacteriol.* **181**, 6223–6229 (1999).

365. Oglesby-Sherrouse, A. G. & Murphy, E. R. Iron-responsive bacterial small RNAs: variations on a theme. *Metallomics* **5**, 276–286 (2013).

366. Adler, C. *et al.* The Alternative Role of Enterobactin as an Oxidative Stress Protector Allows *Escherichia coli* Colony Development. *PLoS One* **9**, (2014).

367. Carpenter, C. & Payne, S. M. Regulation of iron transport systems in Enterobacteriaceae in response to oxygen and iron availability. *J Inorg Biochem* **133**, 110–117 (2014).

368. Peng, E. D., Wyckoff, E. E., Mey, A. R., Fisher, C. R. & Payne, S. M. Nonredundant Roles of Iron Acquisition Systems in *Vibrio cholerae. Infect. Immun.* **84**, 511–523 (2016).

369. Achard, M. E. S. *et al.* An antioxidant role for catecholate siderophores in *Salmonella*. *Biochem. J.* **454**, 543–549 (2013).

370. Chaturvedi, A. K., Mishra, A., Tiwari, V. & Jha, B. Cloning and transcript analysis of type 2 metallothionein gene (SbMT-2) from extreme halophyte *Salicornia brachiata* and its heterologous expression in *E. coli. Gene* **499**, 280–287 (2012).

371. Bobrov, A. G. *et al.* The *Yersinia pestis* siderophore, yersiniabactin, and the ZnuABC system both contribute to zinc acquisition and the development of lethal septicaemic plague in mice. *Molecular Microbiology* **93**, 759–775 (2014).

372. Wright, J., Thomas, P. & Serjeant, G. R. Septicemia caused by *Salmonella* infection: an overlooked complication of sickle cell disease. *J. Pediatr.* **130**, 394–399 (1997).

373. Ortiz-Neu, C., Marr, J. S., Cherubin, C. E. & Neu, H. C. Bone and joint infections due to *Salmonella*. *J. Infect. Dis.* **138**, 820–828 (1978).

374. Holden, V. I., Breen, P., Houle, S., Dozois, C. M. & Bachman, M. A. *Klebsiella pneumoniae* Siderophores Induce Inflammation, Bacterial Dissemination, and HIF-1α Stabilization during Pneumonia. *mBio* **7**, (2016).

375. Hartmann, H. *et al.* Hypoxia-independent activation of HIF-1 by enterobacteriaceae and their siderophores. *Gastroenterology* **134**, 756–767 (2008).

376. Behnsen, J. & Raffatellu, M. Siderophores: More than Stealing Iron. *mBio* **7**, (2016).

377. Ji, C. & Miller, M. J. Siderophore-fluoroquinolone conjugates containing potential reduction-triggered linkers for drug release: synthesis and antibacterial activity. *Biometals* **28**, 541–551 (2015).

378. Švarcová, M., Krátký, M. & Vinšova, J. Investigation of potential inhibitors of chorismate-utilizing enzymes. *Curr. Med. Chem.* **22**, 1383–1399 (2015).

379. Banin, E. *et al.* The potential of desferrioxamine-gallium as an anti-*Pseudomonas* therapeutic agent. *Proc. Natl. Acad. Sci. U.S.A.* **105**, 16761–16766 (2008).

380. Bonomo, R. A. Cefiderocol: A Novel Siderophore Cephalosporin Defeating Carbapenem-resistant Pathogens. *Clin Infect Dis* **69**, S519–S520 (2019).

381. Schmittgen, T. D. & Livak, K. J. Analyzing real-time PCR data by the comparative C(T) method. *Nat Protoc* **3**, 1101–1108 (2008).

382. Berggren, R. E. *et al.* HIV gp120-specific cell-mediated immune responses in mice after oral immunization with recombinant *Salmonella*. *J. Acquir. Immune Defic. Syndr. Hum. Retrovirol.* **10**, 489–495 (1995).

383. Urbano, R. Inhibition of *Staphylococcal* Cell-To-Cell Communication and. 133.

384. Cummings, L. A., Wilkerson, W. D., Bergsbaken, T. & Cookson, B. T. In vivo, *fliC* expression by *Salmonella enterica* serovar Typhimurium is heterogeneous, regulated by ClpX, and anatomically restricted. *Mol. Microbiol.* **61**, 795–809 (2006).

385. Napolitani, G. *et al.* Clonal analysis of *Salmonella*-specific effector T cells reveals serovar-specific and cross-reactive T cell responses. *Nat. Immunol.* **19**, 742–754 (2018).

386. Alpuche-Aranda, C. M., Berthiaume, E. P., Mock, B., Swanson, J. A. & Miller, S. I. Spacious phagosome formation within mouse macrophages correlates with *Salmonella* serotype pathogenicity and host susceptibility. *Infect Immun* **63**, 4456–4462 (1995).

387. Sheppard, M. *et al.* Dynamics of bacterial growth and distribution within the liver during *Salmonella* infection. *Cell. Microbiol.* **5**, 593–600 (2003).

388. Malik-Kale, P., Winfree, S. & Steele-Mortimer, O. The Bimodal Lifestyle of Intracellular *Salmonella* in Epithelial Cells: Replication in the Cytosol Obscures Defects in Vacuolar Replication. *PLOS ONE* **7**, e38732 (2012).

389. Diard, M. *et al.* Stabilization of cooperative virulence by the expression of an avirulent phenotype. *Nature* **494**, 353–356 (2013).

390. Hiyoshi, H. *et al.* Mechanisms to Evade the Phagocyte Respiratory Burst Arose by Convergent Evolution in Typhoidal *Salmonella* Serovars. *Cell Rep* **22**, 1787–1797 (2018).

VITAE

Taylor Ann Stepien was born in Racine, WI, and attended The Prairie School from grades 6-12. She graduated with a Bachelor of Science from the University of Wisconsin - Madison in 2009 with a double major in Molecular Biology and French from the College of Letters & Sciences. During her junior year, she participated in a semester abroad in Aix-en-Provence, France to complete her French studies. Her undergraduate research examined the microbial communities of insect larval midguts in the laboratory of Dr. Jo Handelsman; she continued this work at Yale University in New Haven, CT after graduation. She joined the Pathobiology Program in the Department of Global Health at the University of Washington in 2013. While completing her dissertation work in the laboratory of Dr. Ferric Fang, she was the recipient of the Diseases of Public Health Importance Training Grant. She is a regular volunteer at the Pacific Science Center in Seattle, WA. Outside of science, she enjoys hiking and trail running in the beautiful PNW, practicing yoga, and enjoying art and live music.